AN ABSTRACT OF THE THESIS OF

Darin Rungkamol for the degree of Master of Science in Civil Engineering presented on March 15, 2001. Title: Aerobic Cometabolism of 1,1,1-Trichloroethane and Other Chlorinated Aliphatic Hydrocarbons by Indigenous and Bioaugmented Butane-Utilizers in Moffett Field Microcosms.

Abstract approved: Redacted for privacy

Lewis Semprini

This thesis has focused on developing a culture of butane-utilizing microorganics to be bioaugmented into the subsurface for the cometabolic treatment of 1,1,1-TCA, TCE and 1,1-DCE. The culture was tested in groundwater and aquifer solid microcosms that mimic conditions where a field test is to be performed. The butane mixed culture was selected from the existing microcosms (Jitnuyanont 1998) by comparing 1,1,1-TCA transformation abilities among these microcosms. Butane-utilizers that showed rapid 1,1,1-TCA transformation kinetics and long-term (10 - 44 days) 1,1,1-TCA transformation ability in the absence of butane utilization were selected. Modeling studies were performed and compared to the results of microcosm test to generate kinetic parameters for the microbial processes under conditions of the field.

Microcosms bioaugmented with the selected culture maintained effective transformation of 1,1,1-TCA, and mixtures of 1,1,1-TCA, TCE, and 1,1-DCE. Little 1,1,1-TCA transformation was found in microcosms where indigenous microorganisms were stimulated. The transformation of 1,1-DCE in the bioaugmented microcosms was the fastest, followed by 1,1,1-TCA and TCE. The limited transformation of chlorinated solvents and the cessation in butane utilization occurred after the transformation of the CAH mixtures.

The culture having the best 1,1,1-TCA transformation ability was developed for bioaugmentation studies for both the laboratory and the field tests. The culture was grown on mineral salts growth media, harvested, placed in 1 mL vials with 7%DMSO (Dimethyl Sulfoxide), and stored in –80 °C liquid nitrogen for future studies. The frozen cells were thawed, washed with growth media to rinse away DMSO and then grown in growth media. The microcosms bioaugmented with cell grown from the very frozen culture had reproducible performance, maintaining the long-term (13 days) 1,1,1-TCA transformation in the absence of butane utilization and transforming mixtures of 1,1,1-TCA, TCE, and 1,1-DCE. The transformation rates gradually decreased with continued additions of 1,1,1-TCA. The cell decay rates (b) determined with an analytical regression method were also similar to those obtained prior to using the frozen culture.

Half-saturation constants for butane and 1,1,1-TCA ($K_{s,But}$ and $K_{s,TCA}$) of bioaugmented cultures under microcosm conditions were determined using an analytical regression method that was developed. The bioaugmented microorganisms had $K_{s,But}$ and $K_{s,TCA}$ values of 0.11 mg/L and of 0.37 mg/L, respectively.

Kinetic parameters including maximum specific rate for butane utilization ($k_{max,But}$) and 1,1,1-TCA transformation ($k_{max,TCA}$), cell decay rate (b), and transformation capacity (T_c) for indigenous and bioaugmented microcosms were determined through simulations using a non-steady-state model. Reasonable fits between the model simulation and microcosm data at both low and high concentrations of both butane and 1,1,1-TCA were obtained. The values of kinetic parameters in all bioaugmented microcosms, which were inoculated with the media-culture from batches of cells grown at different times, were similar. This indicates the reproducibility of bioaugmentation process. The bioaugmented microorganisms had high transformation capacity (0.1 – 0.3 mg 1,1,1-TCA/mg cells) and achieved ratios of $k_{max,But}$ and $k_{max,TCA}$, ranging from 0.05 to 0.09. The indigenous microorganisms potentially had lower transformation capacity (T_c), higher decay rate (b), higher butane and 1,1,1-TCA half-saturation constants ($K_{s,But}$

and $K_{s,TCA}$), and lower butane and 1,1,1-TCA maximum specific rates ($k_{max,But}$ and $k_{max,TCA}$) than the bioaugmented microorganisms.

Different butane-utilizing cultures are likely present in the indigenous and bioaugmented microcosms. A slower rate of 1,1,1-TCA transformation was probably due to the indigenous microorganism being less effective towards 1,1,1-TCA transformation. Unlike the bioaugmented microcosms, the enzyme present in the indigenous microcosms was not active over long periods of time. Augmentation with proven contaminant-degrading microorganisms having consistent transformation abilities will likely lead to improved bioremediation treatment processes.

Aerobic Cometabolism of 1,1,1-Trichloroethane and Other Chlorinated Aliphatic Hydrocarbons by Indigenous and Bioaugmented Butane-Utilizers in Moffett Field Microcosms

by
Darin Rungkamol

A THESIS

submitted to

Oregon State University

in partial fulfillment of
the requirements for the
degree of

Master of Science

Presented March 15, 2001
Commencement June 2001

Master of Science thesis of Darin Rungkamol presented on March 15, 2001

APPROVED:

Redacted for privacy

Major Professor, representing Civil Engineering

Redacted for privacy

Head of Department of Civil, Construction, and Environmental Engineering

Redacted for privacy

Dean of the Graduate School

I understand that my thesis will become part of the permanent collection of Oregon State University libraries. My signature below authorizes release of my thesis to any reader upon request.

Redacted for privacy

Darin Rungkamol, Author

ACKNOWLEDGMENTS

First of all, I would like to take this opportunity to thank Dr. Lewis Semprini, my major professor, for giving me an opportunity to work with him. He has considerably provided a new valuable knowledge and guidance beyond all expectations during my pursuit of this degree. I would also like to express my sincere appreciation to Dr. Mark E. Dolan for all his help and patience during the course of this research and my stay at Oregon State University. My work would did have gone as well without his suggestions. I also appreciate the assistance of my committee members, Dr. Peter O. Nelson, and my graduated representative, Dr. James A. Coakley, Jr. I greatly appreciate all my colleagues, especially Dr. Young Kim, and Adisorn (Merf) Tovanabootr, for their laboratory assistance as I started my research. Merf, your kindheartedness will be in my memory for the rest of my life. I would also like to thank Brian Timmins for helping me review my thesis draft. I am most thankful to my parents, Kamol and Vilavan Rungkamol, who have provided endless love, support, and encouragement to my life.

TABLE OF CONTENTS

TABLE OF CONTENTS (CONTINUED)

Page

TABLE OF CONTENTS (CONTINUED)

TABLE OF CONTENTS (CONTINUED)

LIST OF FIGURES

LIST OF FIGURES (CONTINUED)

LIST OF FIGURES (CONTINUED)

LIST OF FIGURES (CONTINUED)

LIST OF FIGURES (CONTINUED)

LIST OF FIGURES (CONTINUED)

LIST OF TABLES

LIST OF TABLES (CONTINUED)

LIST OF TABLES (CONTINUED)

LIST OF APPENDICES

Page

LIST OF APPENDICES (CONTINUED)

LIST OF APPENDIX FIGURES

LIST OF APPENDIX FIGURES (CONTINUED)

LIST OF APPENDIX FIGURES (CONTINUED)

LIST OF APPENDIX FIGURES (CONTINUED)

LIST OF APPENDIX FIGURES (CONTINUED)

LIST OF APPENDIX FIGURES (CONTINUED)

LIST OF APPENDIX TABLES

LIST OF APPENDIX TABLES (CONTINUED)

LIST OF APPENDIX TABLES (CONTINUED)

LIST OF APPENDIX TABLES (CONTINUED)

Aerobic Cometabolism of 1,1,1-Trichloroethane and Other Chlorinated Aliphatic Hydrocarbons by Indigenous and Bioaugmented Butane-Utilizers in Moffett Field Microcosms

CHAPTER 1
INTRODUCTION

1.1 PROBLEM DEFINITION

Groundwater contamination is a major environmental problem encountered in the United States since groundwater is used as a source of drinking water supply. An assessment of the extent and severity of contamination is further complicated by the almost exponential growth of the synthetic organic chemistry industry in the U.S. since the early '40s (Barcelona et al., 1990). 1,1,1-trichloroethane (1,1,1-TCA), one of chlorinated aliphatic hydrocarbons (CAHs), is a synthetic organic chemical widely used as an industrial solvent, and commonly enters groundwater because of leaking storage tanks or improper disposal. As the result, it and its transformation products, such as 1,1-dichroloethane (1,1-DCA), 1,1-dichloroethene (1,1-DCE), and vinyl chloride (VC) are frequently reported contaminants in groundwater and soils.

1,1,1-TCA and other CAHs are probably the most serious groundwater contaminants today. They and their transformation products are known or suspected carcinogens. This has lead to development of treatment methods including pump-and-treat, soil vapor extraction, air stripping, and activated carbon adsorption, for their removal. These treatment processes are mostly operating at the surface, however, and cannot complete contaminant destruction, but only transfer contaminants from one medium to another. In addition, CAH persistence in the subsurface environment entails the great expense of these conventional

remediation technologies (Alvarez-Cohen and McCarty, 1991a). Biological processes occurring in situ can aerobically or anaerobically transform most CAHs, and hence have become a potentially low-cost alternative approach for the remediation of contaminated soils and groundwater. Microbial processes have now gained popularity for the transformation of CAHs in groundwater.

Moffett Naval Air Station (Moffett Field), Mountain View, California, has been used to evaluate in-situ transformation processes through aerobic cometabolism for several CAHs by indigenous microorganisms that use methane, phenol, or toluene as primary substrates. The initial concentration of target CAHs including trichloroethene (TCE), 1,1,1-TCA, 1,1-DCE, cis-1,2-dichloroethene (c-DCE), tran-1,2-dichlroethene (t-DCE) and VC ranged from 60 to 250 μg/L. The aquifer is confined and consists of silt, fine- to coarse-grained sand and gravel. The major contaminant found in site groundwater is 1,1,1-TCA present at an average concentration on the order of 100 μg/L, while the other contaminants such as 1,1-DCA and TCE are present in trace amounts (Robert et al., 1990).

In one of the field tests, methane-oxidizing bacteria, using methane as a primary substrate and cometabolically transforming CAHs with a methane monooxygenase enzyme (MMO), achieved significant transformation of VC and t-DCE, but exhibited limited transformation of 1,1,1-TCA, TCE and c-DCE (Semprini et al., 1990; Semprini et al., 1991). In other field demonstrations, Hopkins et al. (1993) and Hopkins and McCarty (1995) found that phenol- and toluene-oxidizing bacteria, having a toluene oxygenase enzyme responsible for the CAHs cometabolism, were equally effective in removing c-DCE and TCE, while t-DCE was the least transformed of the three contaminants. Hopkins and McCarty (1995) also observed great efficiency in VC removal and moderate efficiency in 1,1-DCE removal by phenol utilizers. In microcosm studies conducted by Hopkins et al. (1993) and Hopkins and McCarty (1995), none of the microcosms effectively degraded 1,1,1-TCA, when fed phenol, toluene, methane or ammonia.

The results of these tests indicated that further studies were required to explore 1,1,1-TCA degradation efficiency by microorganisms having different

oxygenase systems. Jitnuyanont (1998) found that propane- and butane-oxidizing bacteria had a very high 1,1,1-TCA transformation capacity, representing the maximum mass of CAH that can be transformed per unit mass of resting cell, and that bioaugmentation was a good strategy to reduce the long lag time required to stimulate the indigenous microorganisms in microcosms containing Moffett Field sediments and groundwater. The enrichments used for bioaugmentation were obtained from the Hanford DOE site, Washington (Kim 1996), which transformed 1,1,1-TCA effectively. The augmented propane- and butane-oxidizing bacteria also had a great efficiency for 1,1,1-TCA removal. However, both indigenous and augmented propane and butane utilizers needed further studies for 1,1,1-TCA transformation along with other CAHs including TCE, and 1,1-DCE.

1.2 OBJECTIVES

Previous work indicated the effective removal of 1,1,1-TCA by propane- and butane-oxidizing bacteria (Jitnuyanont, 1998). My study has focused on exploiting aerobic microbial metabolism in microcosms to achieve the transformation of CAHs appearing in Moffett site, including 1,1,1-TCA, TCE and 1,1-DCE. The main focus was to compare 1,1,1-TCA transformation abilities of indigenous and bioaugmented butane-utilizers in groundwater and aquifer solids microcosms. The kinetic parameters for butane utilization and 1,1,1-TCA transformation were evaluated through modeling the results of microcosm studies. The thesis is divided into three parts performed to fulfill these objectives as follows:

1.2.1 Culture development for bioaugmentation studies

Objective 1 was to develop a butane mixed culture for bioaugmentation studies. The culture for bioaugmentation was developed from the existing microcosm cultures (Jitnuyanont 1998) of butane-utilizers and propane-utilizers. The culture was selected by comparing 1,1,1-TCA transformation abilities among the microcosms.

1.2.2 Microcosm studies with groundwater and soil from the original microcosms

Objective 2 was to conduct bioaugmentation microcosm studies with groundwater and soil from the original microcosms of part 1. These studies were performed to compare the 1,1,1-TCA transformation ability between indigenous and bioaugmented butane-utilizers, and to study the long term transformation of 1,1,1-TCA as well as the transformation ability of CAH mixtures of 1,1,1-TCA, TCE, and 1,1-DCE. The culture having the best transformation ability was chosen for growing a bioaugmentation culture. The grown culture was then frozen and kept in the –196 °C liquid nitrogen for the next study.

1.2.3 Microcosm studies with the frozen butane-utilizing culture

Objective 3 was to perform bioaugmentation microcosm studies with the frozen butane-utilizing culture. Microcosm studies were conducted in order to compare the 1,1,1-TCA transformation ability between indigenous and bioaugmented butane-utilizers. The transformation of 1,1,1-TCA, TCE, and 1,1-DCE was also evaluated in bioaugmented microcosms. Studies were conducted over a range of butane and 1,1,1-TCA concentrations to determine half-saturation

constant (K_s) of indigenous and bioaugmented cultures under microcosm conditions. Additional, kinetic parameters including maximum specific rate (k_{max}) of butane and 1,1,1-TCA co-oxidation, cell decay rate (b), and/or transformation capacity (T_c) for indigenous and bioaugmented microcosms under microcosm conditions were determined through simulations of butane utilization and 1,1,1-TCA transformation, using a non-steady-state model. The equations were solved using STELLA® software (High Performance System, Inc. Hanover, NH).

CHAPTER 2
LITERATURE REVIEW

1,1,1-trichloroethane (1,1,1-TCA) is among the most frequently encountered chlorinated aliphatic compounds in contaminated groundwater resulting from its common use as industrial solvent. Its improper storage and disposal resulted in the contamination of groundwater at many federal and private facilities. It is of particular concern due to its toxicity, and potential carcinogenicity. The maximum contaminant level (MCL) of 1,1,1-TCA in drinking water is 200 μg/L (Federal Register, 1989).

2.1 PROPERTIES OF 1,1,1-TCA

1,1,1-TCA is relatively soluble in water with a solubility of 730 g/m^3 at 20 °C. It can be rapidly transported with groundwater. Thus, extensive plumes can exist in the subsurface. Due to high vapor pressure (13.2 kPa at 20 °C), 1,1,1-TCA can evaporate quickly. With a high vapor pressure, 1,1,1-TCA can be effectively removed from the vadose zone by soil vapor extraction (SVE). The Henry's coefficient of 1,1,1-TCA is 3.06 kPa m^3/mol. The formula of 1,1,1-TCA is CCl_3CH_3, having a molecular weight of 133.4 g/mole. The melting point and the boiling points of 1,1,1-TCA are –30.4 °C and 74.1 °C, respectively (Mackay and Shiu, 1982).

2.2 TRANSFORMATION OF 1,1,1-TCA

1,1,1-TCA can be abiotically transformed via dehalogenation as well as hydrolysis. 1,1,1-TCA hydrolysis produces acetic acid that can be mineralized rapidly by microorganisms, while dehalogenation produces 1,1-dichlroethene (1,1-DCE) that also can be transformed further by biological reductive dehalogenation to vinyl chloride (VC) (Vogel et al.,1987a; Vogel et al., 1987b; Vogel and McCarty, 1987). 1,1,1-TCA can also be reduced by transition metal complexes providing ethane, ethanol, ethene, chloroethene, and 1,1-dichlroethane (1,1-DCA) as products (Vogel et al., 1987a). The pathways are shown in Figures 2.1 and 2.2.

Under anaerobic conditions, 1,1,1-TCA can be biologically reduced to 1,1-DCA, an intermediate product that can be either reduced further to chloroethane (CA) and VC, or transformed abiotically by hydrolysis to ethanol. Ethanol can be mineralized easily by microorganisms (Vogel and McCarty, 1987a; Vogel and McCarty, 1987b; Vogel et al., 1987). Acetic acid and methanol are common substrates to drive the anaerobic transformation of 1,1,1-TCA. Doong and Wu (1996) found that the increase of substrate addition could enhance the transformation of 1,1,1-TCA. The growth of anaerobic microcosms was inhibited by high concentrations of 1,1,1-TCA (Galli, 1989; Doong and Wu, 1996).

1,1,1-TCA can also be biodegraded through aerobic cometabolism. The 1,1,1-TCA transformation is carried out by a non-specific oxygenase enzyme that is produced by microorganisms when oxidizing primary substrates for energy and growth. The oxygenase enzyme oxidizes 1,1,1-TCA to form 2,2,2-trichloroethanol (Oldenhuis et al., 1989; Hommes et al., 1998). However, the overall 1,1,1-TCA oxidation pathways via microbially mediated reactions under aerobic condition are still unknown. The transformation of 1,1,1-TCA can be achieved by the methane-oxidizing bacterium *Methylosinus trichosporium* OB3b (Oldenhuis et al., 1989), the ethane-oxidizing bacteria *Mycobacterium* spp. (Yagi et al., 1999), the propane-oxidizing bacteria *Rhodococcus rhodochrous and Rhodococcus sp.* Strain Sm-1

(Malachowsky et al., 1994), and the ammonia-oxidizing bacteria *Nitrosomonas europaea* (Hommes et al., 1998).

2.2.1 Cometabolism by methane-utilizers

Methane-oxidizing bacteria (Methanotrophs) utilize methane as carbon and energy source. The oxidation of methane to methanol is catalyzed by methane monooxygenase (MMO) enzyme by inserting an oxygen atom into a methane molecule and initiating the production of methanol. The reaction requires the presence of both oxygen and NADH. MMO is broadly nonspecific enzyme, and hence can catalyze a wide variety of oxidative reactions including the cometabolic transformation of CAHs including 1,1,1-TCA (Strand et al., 1990; Arvin, 1991; Broholm et al., 1990). A methane-oxidizing bacteria culture that degraded CAHs was able to grow on other primary substrates such as methanol and propane (Arvin, 1991). The MMOs can be divided into two groups, the soluble form (sMMO) and the particulate form (pMMO). Under copper limitations, some microorganisms can produce sMMO, which has a much broader substrate range and is more effective in transformation of CAHs than the pMMO form (Jansen et al., 1991; Oldenhuis et al., 1989).

Strand et al. (1990) reported that the transformation of 1,1,1-TCA by methane-oxidizing bacteria followed first-order kinetics with rate constants of 8.8 $*10^{-5}$ L/mg VSS-hr for aqueous concentration of TCA less than 7770 μg/L. Methane in excess of 0.25 mg/L aqueous concentration inhibited the transformation of 1,1,1-TCA. The transformation rate was lower when treating a mixture of 1,1,1-TCA and TCE. *Methylosinus trichosporium* OB3b incompletely transformed 1,1,1-TCA, and yielded 2,2,2-trichloroethanol as a chlorinated intermediate (Oldenhuis et al., 1989). Compared to other CAHs, the transformation rate of TCA by *Methylosinus trichosporium* OB3b was the lowest (Oldenhuis et al., 1991).

a) Hydrolysis

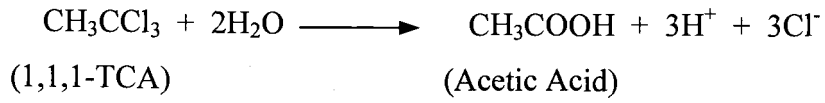

b) Dehalogenation

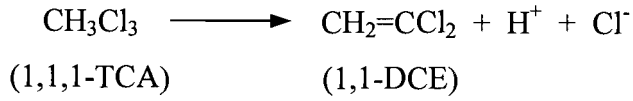

Figure 2.1 Abiotic transformation pathway of 1,1,1-TCA.

a) Anaerobic condition

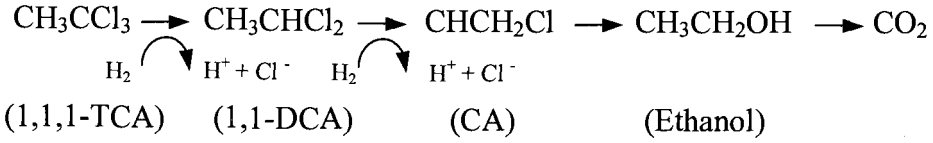

b) Aerobic condition

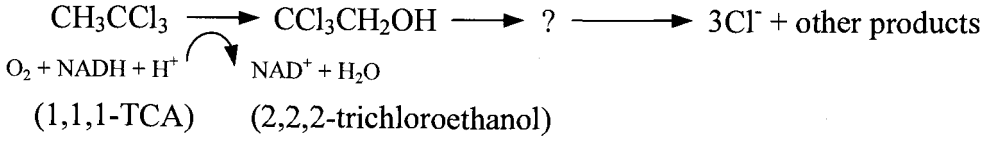

Figure 2.2 Biotic transformation pathway of 1,1,1-TCA.

Increasing concentrations of 1,1,1-TCA resulted in a decreased rate of methane consumption (Broholm et al., 1990).

There are several methane-oxidizing bacteria that were able to transform CAHs, but not 1,1,1-TCA (Speitel et al., 1993; Chang and Alvarez-Cohen, 1995a; Chang and Criddle, 1997). In Moffett field, methane-oxidizing bacteria exhibited significant cometabolic transformation of VC and trans-dichloroethene (t-DCE), and limited transformation of TCE and cis-1,2-dichloroethene (c-DCE), however 1,1,1-TCA was not transformed (Semprini et al, 1990; Semprini et al., 1991). Jitnuyanont (1998) found that propane- and butane-oxidizing bacteria had very high efficiency to transform 1,1,1-TCA. As a result, the cometabolic transformation of 1,1,1-TCA by propane- and butane-utilizing bacteria was performed in this study.

2.2.2 Cometabolism by butane-utilizers

In contrast to the significant studies with methane-utilizing bacteria, little work has been performed with butane-utilizing bacteria. Due to the relatively low solubility of methane, the production rate of biomass is limited by the transfer rate of methane to the culture. To increase the production rate of biomass, normal alkanes, such as propane and, n-butane, have been used instead since the transfer rate and solubility limits of those alkanes are higher than those of methane. Propane and butane were expected to provide 1.4 times higher biomass yield than methane (McLee et al., 1972). The advantages of using butane as a substrate have led to the isolation of several microorganisms (Davis, 1964; McLee et al., 1972; Phillips and Perry, 1979; Van-Ginkel et al., 1987).

McLee et al. (1972) found that all isolates of bacteria strains and molds grown on n-butane were able to grown on ethane, propane, isobutane, n-hexadecane, sugar, and peptides but not methane. In 1987, a nonspecific butane monooxygenase was found in *Norcadia* TB1, which could grow on butane and

several saturated straight-chain hydrocarbons but not on 1-alkenes (Van-Ginkel et al., 1987). Similar to MMO, this nonspecific enzyme driving butane oxidation might be capable of CAHs oxidation.

Kim (1996) reported the effective cometabolic transformation of chloroform induced by the oxygenase enzymes of butane-utilizing bacteria from the Hanford DOE site, Washington. In addition, these butane-utilizing microorganisms also had abilities to degrade a broad range of CAHs including 1,1,1-TCA, 1,1-DCE and their abiotic transformation products (Kim et al., 1997). The complete transformation of 1,1,1-TCA concentrations as high as 2400 μg/L in aqueous solution was observed. Resting cells were not significantly affected upon exposer to 1,1,1-TCA. Compared to 1,1-DCE and other chlorinated ethanes, the transformation of 1,1,1-TCA was relatively slow. However, the potential of 1,1,1-TCA transformation was still attractive.

As a result, the butane-utilizing enrichments from the Hanford DOE site were selected for a bioaugmentation study. The cometabolism of 1,1,1-TCA was evaluated in microcosms constructed with groundwater and aquifer solids from the Moffett site, California (Jitnuyanont, 1998). A maximum 1,1,1-TCA concentration of 8310 μg/L was completely transformed by bioaugmented butane-utilizing bacteria. The final transformation yield (the amount of cometabolic substrate degraded prior to cell inactivation divided by the amount of primary substrate consumed) obtained for the butane-utilizing bacteria was 0.04 mg 1,1,1-TCA/mg butane. Nutrient addition was also studied in order to enhance the performance of inoculated strains. The microcosms with the highest amount of mineral salt medium most effectively consumed butane and transformed 1,1,1-TCA.

2.2.3 Cometabolism by propane-utilizers

Propane-oxidizing bacteria oxidize propane for energy and growth, using a propane monooxygenase enzyme (PMO) to start the oxidation of propane (Wackett et al., 1989). PMO is nonspecific enough to oxidize short-chain alkenes and other aliphatic hydrocarbons (Hou et al., 1983; Wackett et al., 1989; Tovanabootr, 1997). Propane oxidation is carried out by inserting an oxygen molecule, converting propane to 2-propanol, which is further oxidized to acetone (Perry, 1980). Propane can also undergo terminal oxidation and be oxidized to 1-propanol (Stephens and Dalton, 1986).

Owing to the non-specification, PMO is also responsible for CAHs transformation. PMO in *Mycobacterium vaccae* JOB5 was able to transform TCE, VC, cis- and tran-DCE, but not 1,1,1-TCA and PCE (Wackett et al., 1989). Propane-oxidizing bacterium *Mycobacterium* sp. TCE28 could utilize ethane, butane, and n-butanol as well as propane, and degrade TCE, cis-1,2-DCE, 1,1-DCE, 1,2-DCA, dichloromethane, and CF cometabolically (Imano et al., 1999). The degradation of TCE, CF and 1,2-DCA by a propane-utilizing enrichment resulted in cell inactivation due to product toxicity (Imano, et al. 1999). Transformation could be enhanced by the addition of low concentration of growth substrate, presumably, due to the regeneration of reducing energy (Chang and Alvarez-Cohen, 1995b).

The cometabolic transformation of 1,1,1-TCA by propane-oxidizing enrichments was first demonstrated by Keenan et al. (1993). Propane-oxidizing bacterium *Rhodococcus* species and *R.* rhodochrous ATCC21197 was able to degrade 1,1,1-TCA but not very effectively (Malachowsky et al., 1994). Highly efficient removal of 1,1,1-TCA by propane-utilizers enriched from McClellan Air Force Base (California) aquifer material was observed in soil microcosm studies with a transformation yield of 0.088 to 0.106 g 1,1,1-TCA/g propane (Tovanabootr, 1997). 1,1,1-TCA transformation was strongly inhibited by propane (Keenan et al., 1993; Tovanabootr, 1997). Transformation was slow in the presence of high

propane concentrations and then accelerated after propane was nearly consumed (Tovanabootr, 1997). However, the presence of propane helped maintain the transformation capacity of 1,1,1-TCA in an extended study (Keenan et al., 1993, Tovanabootr, 1997). Tovanabootr (1997) also found that the high concentration of 1,1,1-TCA could slow the propane degradation rate.

Jitnuyanont (1998) evaluated the cometabolism of 1,1,1-TCA by propane- and butane-utilizing bacteria from the Moffett site, California. She found that the highest transformation yield obtained with propane-utilizers was 0.07 mg 1,1,1-TCA/mg propane. 1,1,1-TCA transformation was competitively inhibited by both butane and propane. Propane-utilizers also appeared to be more stable than butane utilizers with prolonged stimulation.

2.3 KINETICS AND MODEL DEVELOPMENT OF CAH COMETABOLIC TRANSFORMATION

The kinetics of cometabolism is an important factor for application of bioremediation. Predictive models for the cometabolic process can be useful for engineering design to plan and monitor site remediation, to conduct risk and exposure assessments and also to evaluate the project cost and duration. (Alvarez-Cohen and McCarty, 1991a; Semprini et al., 1998). However, the kinetics of cometabolic transformation is often complicated by several influencing factors. A number of different models, ranging from simple first-order reaction models to complex multi-substrate mixed models, have been developed to describe the cometabolic degradation process (Alvarez-Cohen and Speitel, in press).

Aerobic cometabolism is a biological process where microorganisms do not gain any energy or carbon for cell growth from CAH transformation (McCarty, 1997). So, the presence of a compound as energy and carbon source and oxygen is also required. The transformation rate of CAHs can be affected by many different

factors including competitive inhibition, reducing power availability, and transformation product toxicity.

Competitive inhibition can occur when the primary substrate is present along with a CAH since both primary substrate metabolism and CAH cometabolism are catalyzed by the same nonspecific oxygenase enzyme. This results in a decrease in both primary substrate and CAHs transformation rate (Broholm et al., 1990; Speitel et al., 1993; Hommes et al., 1998).

In addition to oxygen, the oxidation of primary substrate and the CAH also requires energy or reducing power in form of nicotinamide adenine dinucleotide (NADH) which can be regenerated via the oxidation pathway of primary substrate. This reducing power can be provided by internal or external sources. An internal source of reducing power can be energy reserves stored in cells in form of polyhydroxybutyrate (PHB) (Henry and Grbic-Galic, 1991). In order to increase the transformation rate and transformation capacity, but avoid competitive inhibition, an external source of reducing power can also be provided. For example, a nongrowth-inducing and noncompetitive substrate such as formate can be used (Alvarez-Cohen and McCarty, 1991a; Alvarez-Cohen and McCarty, 1991b; Alvarez-Cohen and McCarty, 1991c). However, microorganisms likely require a primary substrate to maintain the oxygenase enzyme levels. The depletion of reducing power source could be another factor that hinders the transformation of CAHs.

Transformation product toxicity is another significant factor that can cause decreased rates of CAH transformation. Toxic intermediates and products formed by the cometabolic transformation of CAHs, rather than CAHs themselves, inactivate oxygenase enzymes, as well as other cellular components (Alvarez-Cohen and McCarty, 1991b; Alvarez-Cohen and McCarty, 1991c; Oldenhuis et al., 1991; Hommes et al., 1998). Transformation product toxicity can be measured in terms of transformation yield (T_y), representing the maximum mass of CAH that can be transformed per unit mass of primary substrate consumed, or transformation

capacity (T_c), representing the maximum mass of CAH that can be transformed per unit mass of resting cell (Alvarez-Cohen and McCarty, 1991a).

The cometabolic transformation of CAHs has been modeled using Michaelis-Menten and Monod kinetics, with an active microbial concentration that is constant (Alvarez-Cohen and McCarty, 1991b) or decays over time (Galli and McCarty, 1989), or with incorporation of competitive inhibition (Broholm et al., 1990). For relatively low concentrations of chlorinated compounds, the biodegradation of chlorinated compounds could be described by pseudo first-order rate expression (Wackett and Gibson, 1988; Oldenhuis et al., 1989; Strand et al., 1990; Arvin, 1991; Speitel et al., 1993).

The transformation capacity (T_c) was introduced to incorporate the effects of product toxicity and reductant supply for the cometabolic transformation of halogenated aliphatics by resting cells of a mixed methanotrophic culture (Alvarez-Cohen and McCarty, 1991a). Alvarez-Cohen and McCarty (1991c) proposed a cometabolic transformation model incorporating competitive inhibition in addition to the transformation capacity. The reasonable fit between model predictions and experimental observations was supportive of the model formulation.

Chang and Alvarez-Cohen (1995a) proposed a mechanistic model integrating the effects of product toxicity, reducing energy limitation, and competitive inhibition, together with cell growth and decay, to describe the kinetics of the cometabolic degradation of chlorinated organics by oxygenase-expressing cultures. Various conditions were examined: resting cells, cells with reducing energy substrate, and cells with growth substrate. Assuming that cometabolic transformation rates are enhanced by reducing power obtained from oxidation of growth substrates, Chang and Criddle (1997) developed the model accounting for the effects of cell growth, endogenous cell decay, product toxicity, and competitive inhibition. The model successfully predicts TCE transformation and methane utilization for a wide range of concentrations of TCE (0.5 to 9 mg/L) and methane (0.05 to 6 mg/L).

2.4 BIOAUGMENTATION

Bioaugmentation, the introduction of microorganisms, is another strategy for enhancing the bioremediation when an immediate remediation of a chemical is required, or indigenous microorganism is unable to degrade the existing compounds (Baud-Grasset and Vogel, 1995). The inability of indigenous microorganisms to transform target compounds is probably due to the lack of the appropriate enzyme(s), low population of microorganisms (biomass), and contaminant toxicity. Augmentation with proven contaminant-degrading microorganisms leads to a higher degree of confidence in remediation success, and also eliminates long lag periods to stimulate indigenous microorganisms. This process has been practiced in various fields including soil and groundwater remediation (Mayotte et al., 1996; Munakatta-Marr et al., 1996; Duba et al., 1996; Dybas et al., 1998; Salanitro et al., 2000; Ellis et al., 2000).

The most common factors considered in bioaugmentation are pollutant characteristics (bioavailability, concentration, microbial toxicity), soil physico-chemical characteristics (humidity, organic matter content, clay content and pH), microbiology (enzyme stability and activity) and methodology (method of inoculation) (Vogel, 1996). However, a major concern with bioaugmentation is the survival of the inoculated microorganism. Nutrient limitations (P, N, and possibly other elements), suppression by predators and parasites, inability of bacteria to move appreciably through soil, concentration of organic substrate too low to support multiplication, improper pH, temperature and salinity, and toxins are factors causing bioaugmentation to fail (Martin, 1994).

Using small-column microcosms, Munakatta-Marr et al. (1996) evaluated the TCE degradation potential with bioaugmentation of both wild type and genetically altered *Burkholderia (Psedomonas) cepacia* G4 and $PR1_{301}$, phenol-utilizing microorganisms. *B. cepacia* strain $PR1_{301}$ was a nonrecombinant NTG-induced mutant of *B. cepacia* strain G4 capable of uninduced constitutive degradation of TCE in the absence of phenol or toluene. It was found that phenol-

utilizing microorganisms augmented with either *B. cepacia* strain G4 or $PR1_{301}$ transformed twice as much TCE as the indigenous phenol-utilizing microcosm stimulated from Moffett groundwater and soil. They were also able to transform TCE in the absence of phenol. In addition, immediate activity towards phenol and TCE by augmented microorganisms was observed, eliminating long startup periods.

The significant removal of CCl_4 from the aquifer solids in a bench-scale study was achieved by the inoculation with *Pseudomona* sp. strain KC accompanied by the niche adjustment with base, acetate, and phosphorus under denitrifying conditions (Mayotte et al., 1996). The in-situ remediation of CCl_4 at Schoolcraft, Michigan, was enhanced by bioaugmentation with strain KC and substrate pH adjustment (Dybas et al., 1998). There also are several bioaugmentation studies on in-situ bioremediation: TCE transformation by resting-state methane-utilizing bacteria *Methylosinus trichosporium* OB3b (Duba et al., 1996), MTBE bioremediation through bioaugmentation and oxygenation (Salanitro et al., 2000), and anaerobic TCE transformation in the aerobic aquifer prereduced by lactate addition before inoculation (Ellis et al., 2000).

The effective transformation of 1,1,1-TCA by propane-and butane-utilizing cultures and successful bioremediation enhanced by bioaugmentation have led to this study of the transformation of CAHs, including 1,1,1-TCA, TCE and 1,1-DCE, in bioaugmented microcosms constructed with Moffett Field groundwater and aquifer solids. Butane-utilizing cultures were studied in the most detail. The kinetic parameters for butane utilization and 1,1,1-TCA transformation were also evaluated by modeling the results of microcosm studies. The work was performed in support of a pilot scale field demonstration of bioaugmentation that will be conducted at the Moffett Field test site.

CHAPTER 3
MATERIALS AND METHODS

3.1 CHEMICAL SOURCES

Butane (N-butane; CP grade) was purchased from Airgas Co. (Corvallis, OR). Propane (98%) was purchased from Aldrich Chemical Co. (Milwaukee, WI). 1,1,1-trichloroethane (1,1,1-TCA; 99.9% {GC} grade), trichloroethylene (TCE; >99%), and 1,1-dichloroethylene (1,1-DCE; >99%) were also purchased from Aldrich Chemical Co (Milwaukee, WI).

3.2 MICROCOSM PREPARATION AND OPERATION

Microcosms were set up in either 125 mL amber serum bottles with PTFE/ red rubber aluminum seal or 125 mL media bottles with gray butyl rubber septa (Wheaton Glass Co., Millville, NJ). They were constructed under a laminar flow hood (The Baker Company, Sanford, MA) to avoid microbial contamination. All tools for microcosm fabrication were autoclaved. The microcosms were constructed with aquifer material and groundwater from the Stanford Test Facility at Moffett field, or, in some studies, containing mineral salt growth media. The remaining was air filled headspace. The composition of mineral salt growth media is given in Appendix A.3. Various ratios of groundwater and aquifer material were used, as will be described for specific microcosm tests. The core materials and groundwater were kept in cold storage prior to use. The background aqueous concentrations of 1,1,1-TCA in the Moffett groundwater ranged from 2.51 to 3.73 μg/L. The nitrate concentration ranged from 40 to 43 mg/L as NO_3^-. The core samples consisted of particles sizes ranging from silts to large cobbles. The core

materials were unpacked under a laminar flow hood and wet sieved through a no. 8 sieve (2.38 mm opening) to remove the large particles. The core materials used in the microcosm fabrication are listed in Appendix A.1.

3.2.1 Preparation of CAH saturated aqueous stock solution

1,1,1-TCA, TCE or 1,1-DCE was added to a 125 mL serum bottle filled with demineralized water to achieve concentrations at the solubility limit in water. The bottle was crimped sealed, and, prior to use, shaken vigorously, and allowed to settle overnight.

3.2.2 Utilization of butane and propane

Butane or propane gas was added into each microcosm as a substrate, using a 100 μL gas tight syringe (Hamilton, NEV). The bottles were vigorously shaken by hand for 10 s to allow the equilibration of substrate before initial headspace samples were taken. During the course of the experiments, the microcosms were incubated at 20 °C temperature on a shaker table at 200 rpm. Gas samples, 100 μL, were withdrawn periodically for analysis. Vacuums created by the consumption of butane or propane were re-equilibrated by injecting air or pure oxygen into the headspace.

3.2.3 Transformation of 1,1,1-TCA

The 1,1,1-TCA experiments were conducted on microcosms stimulated on butane or propane through successive additions of 1,1,1-TCA in order to test the

continuity of transformation of 1,1,1-TCA in the absence of butane utilization. The experiments were performed similarly to the butane and propane experiments. The saturated 1,1,1-TCA solution was injected by a 100 μL liquid microsyringe (Hamilton, NEV) into the microcosms through the rubber septa to obtain an aqueous concentration of around 350 μg/L. A control bottle contained the same amount of 1,1,1-TCA as the microcosms. The concentration of 1,1,1-TCA in microcosm headspace was monitored periodically.

3.2.4 Transformation of CAH mixture

A mixture of saturated 1,1,1-TCA, TCE, and 1,1-DCE stock solutions was added into microcosms stimulated on butane to study the transformation ability of this mixture of compounds. Similar to the TCA experiments, the saturated aqueous stock solution of CAHs was added by a 100 μL liquid microsyringe into the microcosms through the rubber septa to obtain the desired concentration. The aqueous concentration of 1,1,1-TCA, TCE, and 1,1-DCE ranged from 300 to 600 μg/L, 500 to 900 μg/L, and 100 to 500 μg/L, respectively. The concentration of CAHs in the microcosm headspace was monitored periodically.

3.2.5 Rate measurement of 1,1,1-TCA transformation

Transformation rate of 1,1,1-TCA was measured in microcosms stimulated on butane, through successive additions of 1,1,1-TCA. The 1,1,1-TCA-saturated aqueous stock solution was injected by a 100 μL liquid microsyringe into the microcosms through the rubber septa to obtain the aqueous concentration of around 350 μg/L. The concentration of 1,1,1-TCA in the microcosm headspace was monitored to obtain at least 3 data points for a rate determination. During the

course of the experiments, the microcosms were incubated at 20°C temperature on a shaker table at 200 rpm. The derivation of the equations and the calculation method to determine the transformation rate of 1,1,1-TCA are shown in Appendix D.

3.2.6 Butane and 1,1,1-TCA kinetic experiments

The kinetic experiments were conducted similarly to the above butane and TCA experiments. Butane and 1,1,1-TCA-saturated aqueous stock solution were added into microcosms, using a 100 μL gas tight syringe and a 100 μL liquid microsyringe, respectively. The microcosms were incubated at 20°C temperature on a shaker table at 200 rpm. The headspace gaseous concentration was monitored during the experiment. The amounts of gaseous butane or saturated solution of 1,1,1-TCA added resulted in aqueous concentration much more than the value of the half-saturation constant (K_s). This provided concentrations that covered both zero-order rates for the high concentration range and first-order rates for the low concentration range. In the case of the butane kinetic experiments, the increase of biomass from butane utilization in each test was less than 5% of total biomass so that the biomass can be assumed to be constant. The derivation of the rate equations and the calculation method to evaluate butane and 1,1,1-TCA K_s values are shown in Appendix E.

3.2.7 Groundwater amendment

The microcosms were maintained for a long period of time, with periodic exchanges of groundwater and with growth substrate readdition. Prior to adding the growth substrate and chlorinated solvents, the groundwater was exchanged to

resupply nutrients and prevent the accumulation of transformation by-products. The microcosms were centrifuged for 20 minutes at 1000 rpm to settle and keep the microorganisms in the microcosms. The caps were then removed under a laminar flow hood. Sixty percent of the groundwater was replaced with new groundwater and the microcosms were then resealed. When nitrogen was found to be limiting, the groundwater was amended with nitrate to 30 mg/L.

3.3 GROWTH REACTORS

3.3.1 Growth reactor inoculated with groundwater/soil slurry

To create the mixed culture for bioaugmentation studies, a batch growth reactor was set up in a 500 mL bottle sealed with a Teflon fluorocarbon resin-lined cap. One mL of suspended liquid taken from the soil microcosms (Jitnuyanont 1998) was added to inoculate the growth reactor, which was filled with 250 mL mineral salt growth media (Appendix A.3). Butane or propane was added by gaseous addition to each bottle to yield 10% vol/vol in the headspace. The growth reactor was placed on a shaker table at 200 rpm in a 20 °C constant temperature room. Pressures were equilibrated daily with pure oxygen or air. After about 90% of the butane was consumed, all liquid from each bottle was combined and centrifuged to concentrate the biomass. The concentrated biomass was either used for bioaugmentation, or placed in 1 mL vials with 7%DMSO (Dimethyl Sulfoxide) and stored in –196 °C liquid nitrogen for future studies.

3.3.2 Growth reactor inoculated with frozen culture

To create a bioaugmentation culture, a second growth reactor with low headspace was set up in a 2000 mL flask filled with 1800 mL of mineral salt growth media at room temperature. The reactor is shown in Figure 3.1.

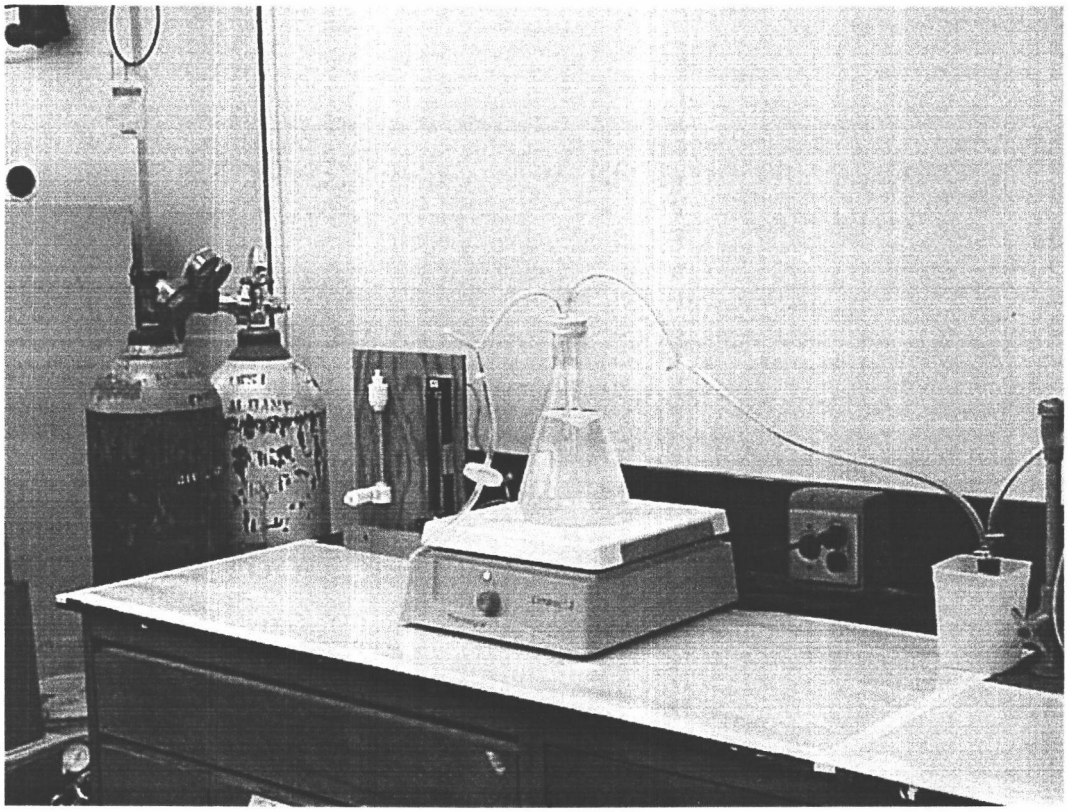

Figure 3.1 Continuously fed 2-L growth reactor.

The reactor was completely mixed, using a star-shaped stirring bar that was rotated at 600 rpm to facilitate butane and oxygen transfer. To provide for continuous feed of substrate and oxygen, butane and air gas tanks were connected to the reactor through a flowmeter equipped with an inline filter device and glass

dispersion tubes with fritted cylinders. The air flowrate was approximately 50 mL/min and the butane flowrate was adjusted to achieve the headspace partial pressure ranging from 2 % to 4%. The vent gas was exhausted to a fume hood. To inoculate the growth reactor, one mL of the frozen culture (–196 °C) was left in the freezer overnight and then at room temperature until it was completely thawed. The culture was washed with mineral salt growth media to rinse away the DMSO prior to inoculation into the growth reactor. The optical density (OD_{600}) and dry mass density were measured periodically.

Figure 3.2 shows the growth curve, presenting the optical density and dry density of biomass of one of the culture growth tests. Both OD_{600} and dry density are in the lag phase during the first 3 days and then increase with time, resulting from the microbial growth in the exponential phase. The percentage of butane and oxygen in the inlet and outlet were measured in the growth reactor, and are shown in Figure 3.3. The measured percentage of inlet and outlet gases was similar, indicating neither oxygen and butane became limited.

The growth curves for other tests are shown in Figure 3.4. All growth tests provided similar results. The lag phase for microbial growth was around 3 days. The enrichment was harvested from the growth reactor in the exponential phase, between day 4 and 5. The measured optical density and dry mass density ranged from 0.2 to 0.3 and from 0.09 to 0.12 g/L, respectively. After day 5, the color of culture changed from milky to yellow.

3.4 BIOAUGMENTATION

Bioaugmentation microcosm studies were conducted to compare the 1,1,1-TCA transformation ability between indigenous and bioaugmented butane-utilizers, and to study the long term transformation of 1,1,1-TCA. The transformation of CAH mixtures of 1,1,1-TCA, TCE, and 1,1-DCE was also studied.

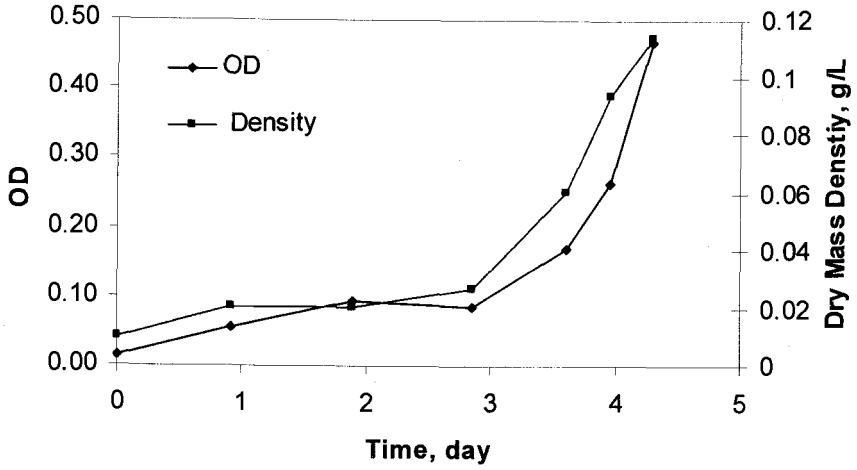

Figure 3.2 Growth curve of the continuously fed batch reactor preparing the culture for inoculation.

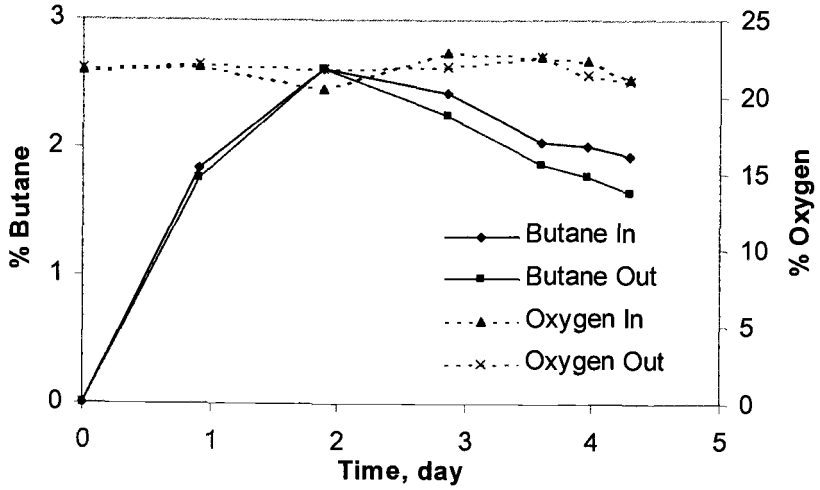

Figure 3.3 Percentage of butane and oxygen in the inlet and outlet measured in the continuously fed batch reactor.

a) Growth Reactor 1

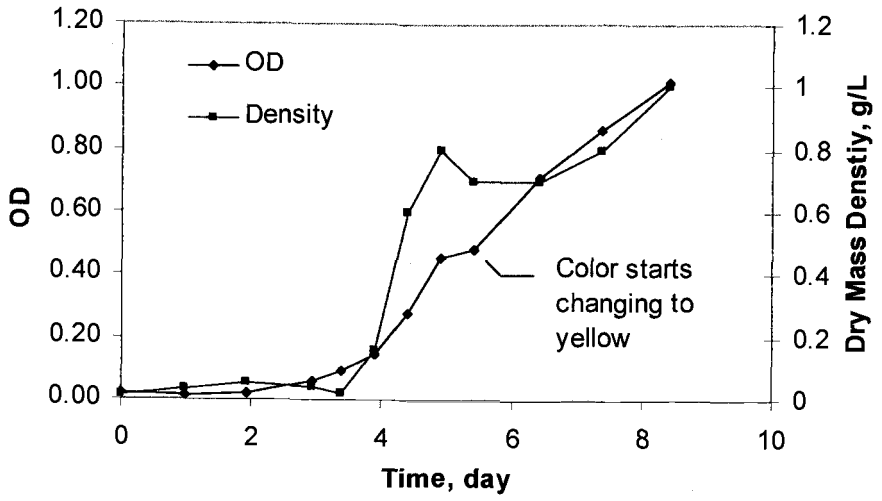

b) Growth Reactor 2

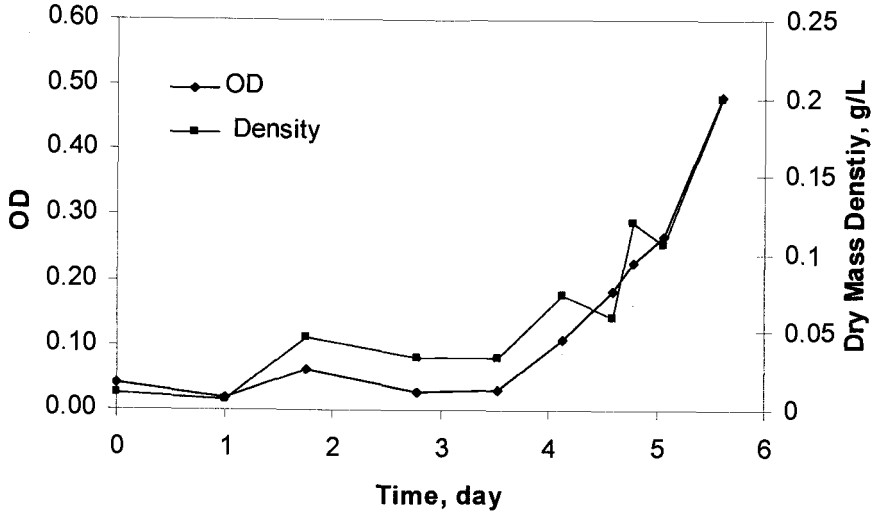

Figure 3.4 Growth curve of the other continuously fed batch reactors preparing the culture for inoculation.

3.4.1 Bioaugmentation with groundwater/soil slurry

To conduct initial bioaugmentation microcosm studies, one mL of suspended liquid was taken from selected soil microcosms (Jitnuyanont 1998) and added to inoculate the microcosm. The suspended liquid was composed of groundwater and aquifer material.

3.4.2 Bioaugmentation with media-culture

The bacterial culture for bioaugmentation was acquired from the enrichment obtained from the growth reactor grown in the mineral salts growth medium. In an earlier study, the culture was obtained from the growth reactor inoculated with groundwater/soil slurry and was washed with groundwater to rinse away the media before adding to microcosms. In this case the culture was obtained from the continuously fed 2 L growth reactor and was directly added to microcosms without washing.

3.5 ANALYTICAL PROCEDURES

1,1,1-TCA, TCE and 1,1-DCE were measured by taking a 100 μL headspace sample and injecting it into Hewlett Packard (Wilmington, DE) 5890 gas chromatograph equipped with a ^{63}Ni electron capture detector (ECD). Separation was obtained by an HP-624 30 m x 0.25 mm x 1.4 mm film thickness stainless steel packed column (Hewlett Packard, Wilmington, DE). The column was operated isothermally at 80 °C. An argon/methane (95%:5%) mixture at a head pressure of 80 psi was used as the carrier gas (60 mL/min). The gaseous concentrations were

determined by comparing peak areas of samples with those of external standards curves as shown in Appendix B.

Butane and propane sampling was also measured by taking a 100 μL headspace sample and injecting it into Hewlett Packard (Wilmington, DE) 5890 gas chromatograph equipped with a flame ionization detector (FID) and a GS-Q 30 m x 0.53 mm stainless steel packed column (J&W Scientific, Folsom, CA). The column was operated isothermally at 100 °C. Nitrogen gas at a head pressure of 60 psi was used as the carrier gas (25 mL/min). The method was calibrated using an external standard (Appendix C).

Oxygen was analyzed by taking a 100 μL headspace sample and injecting it into a gas chromatograph on an HP 5890 Series II GC equipped with a thermal conductivity detector (TCD) and a Supelco 15 ft x 1/8 inch 60/80 Cardoxen^{TM} 1000 packed column (Supelco, Bellefonte, PA). Argon gas at a head pressure of 40 psi was used as the carrier gas. The method was calibrated using an external standard.

The culture dry mass density was measured as a total suspended solid (TSS) analysis (American Public Health Association, 1985). The density was determined by filtering a specific volume of suspended culture through a 0.1-μL-membrane filter (Micro Separation Inc., Westboro, MA), drying overnight at 60 °C, cooling in desiccator for 30 min and weighing. Before being used, the filter was kept in the desiccator overnight and weighed. The dry mass density was determined from the weight change of the filter. The optical density (OD_{600}) of the culture was measured at 600 nm using an HP 8453 UV-Visible spectrophotometer.

3.6 MODEL DEVELOPMENT

Predictive models for the cometabolic process are useful for engineering design to plan and monitor site remediation, to conduct risk and exposure assessments and also to evaluate the project cost and duration (Alvarez-Cohen and

McCarty, 1991a; Semprini et al., 1998). In this study, the kinetic parameters for indigenous and bioaugmented microcosms under microcosm conditions were determined through modeling the results of the microcosm studies. The simulation of butane utilization and 1,1,1-TCA transformation was conducted, using partial differential equations that were solved using STELLA® software (High Performance System, Inc. Hanover, NH).

The rates of butane utilization and 1,1,1-TCA transformation were described by Monod kinetics that relates the transformation rate to concentration in aqueous phase. To simplify the kinetics expressions, the experiments were designed to avoid the effects of competitive inhibition. The effect of reducing power limitation was also assumed to be negligible. Since the experiments were conducted for long periods of time, equilibrium two-phase (air and liquid) partition was assumed based on Henry's Law. The dimensionless Henry partition coefficient (H_{cc}) was used to describe the distribution of butane and 1,1,1-TCA between phases. Equations 3.1 and 3.2 expressed the rates of butane utilization and 1,1,1-TCA transformation in terms of total mass of butane or 1,1,1-TCA transformed in the microcosms. Both equations assume oxygen does not limit butane utilization or 1,1,1-TCA reaction rates, and all transformations occur only in the liquid phase.

$$\frac{dM_{But}}{dt} = -\frac{k_{\max,But} X V_l}{K_{s,But} + \left(\frac{M_{But}}{V_\ell + H_{cc,But} V_g}\right)} \left(\frac{M_{But}}{V_\ell + H_{cc,But} V_g}\right) \tag{3.1}$$

$$\frac{dM_{TCA}}{dt} = -\frac{k_{\max,TCA} X V_\ell}{K_{s,TCA} + \left(\frac{M_{TCA}}{V_\ell + H_{cc,TCA} V_g}\right)} \left(\frac{M_{TCA}}{V_\ell + H_{cc,TCA} V_g}\right) \tag{3.2}$$

where,

M_{But}	=	Total mass of butane, mg
M_{TCA}	=	Total mass of 1,1,1-TCA, mg
$k_{max,But}$	=	Maximum specific rate of butane, mg/mg-day
$k_{max,TCA}$	=	Maximum specific rate of butane or 1,1,1-TCA, mg/mg-day
$K_{s,But}$	=	Half-saturation constant for butane, mg/L
$K_{s,TCA}$	=	Half-saturation constant for butane or 1,1,1-TCA, mg/L
$H_{cc,But}$	=	Henry partition coefficient of butane, mg/L/mg/L
$H_{cc,TCA}$	=	Henry partition coefficient of 1,1,1-TCA, mg/L/mg/L
V_g	=	Gas volume, L
V_l	=	Liquid volume, L
X	=	Active microbial concentration in the aqueous phase, mg/L
t	=	Time, day

Similar to the rate of butane utilization and 1,1,1-TCA transformation, Monod kinetics was also used to express the rate of microbial growth as a function of growth and cell decay:

$$\frac{dX}{dt} = Y \frac{k_{\max,But} X}{K_{s,But} + \left(\frac{M_{But}}{V_\ell + H_{cc,But} V_g} \right)} \left(\frac{M_{But}}{V_\ell + H_{cc,But} V_g} \right) - bX \qquad (3.3)$$

where,

μ	=	Net specific cellular growth rate, day^{-1}
Y	=	Cellular yield of butane, mg cell/ mg butane
b	=	Cell decay rate, day^{-1}

Since the transformation product toxicity is another factor effecting cell decay, it was also incorporated into the model. The transformation capacity term

(T_c) was incorporated into the model to include the effect of transformation product toxicity on cell activity:

$$\frac{dX}{dt} = Y \frac{k_{\max,But} X}{K_{s,But} + \left(\frac{M_{But}}{V_\ell + H_{cc,But} V_g} \right)} \left(\frac{M_{But}}{V_\ell + H_{cc,But} V_g} \right)$$
$$- \frac{1}{T_c} \frac{-k_{\max,TCA} X}{K_{s,TCA} + \left(\frac{M_{TCA}}{V_\ell + H_{cc,TCA} V_g} \right)} \left(\frac{M_{TCA}}{V_\ell + H_{cc,TCA} V_g} \right) - bX \qquad (3.4)$$

where,

T_c = Transformation capacity for 1,1,1-TCA, mg TCA / mg cells

To develop the model, all parameters were introduced into the above equations. The known parameters, including initial biomass (X_0) in bioaugmented microcosms, butane and 1,1,1-TCA mass added to the microcosms (M_{But} and M_{TCA}), butane and 1,1,1-TCA half-saturation constant ($K_{s,But}$, $K_{s,TCA}$), and cellular yield (Y), were fixed in the equations. The remaining $k_{max,But}$, $k_{max,TCA}$, b or/and T_c values were varied in a heuristic approach to obtain a good fit between model predictions and the experimental observations. The errors of unknown parameters were expressed in terms of standard deviation based on modeling of the five replicate microcosms. The differential equations 3.1, 3.2, and 3.3 or 3.4 were solved in STELLA®. Numerical integration in time was performed in STELLA® using a fourth-order Runge-Kutta method. The derivation of equations 3.1 to 3.4 is illustrated in Appendix F.

CHAPTER 4
RESULTS AND DISCUSSION

4.1 CULTURE DEVELOPMENT FOR BIOAUGMENTATION STUDIES

The objective of this work was to develop a mixed culture for bioaugmentation. The culture for bioaugmentation was obtained from the existing microcosms of butane-utilizers and propane-utilizers (Jitnuyanont, 1998). The existing microcosms were constructed in 125 mL amber serum bottles with PTFE/ red rubber aluminum seals. The bottles contained 65 mL of groundwater and aquifer material from Moffett field, leaving 60 mL of headspace. The conditions of all microcosms are presented in Table 4.1.

Table 4.1 Conditions of the existing microcosms (Jitnuyanont, 1998).

Microcosm	Contents	Substrate	Description
P1	GW/Soil	Propane	Indigenous Moffett field microcosm
P2	GW/Soil	Propane	Inoculated with the enrichments obtained from the Hanford DOE site.
P6	GW/Soil	Propane	Microcosm augmented with propane culture
P7	GW/Soil	Propane	Microcosm augmented with propane culture
B1	GW/Soil	Butane	Indigenous Moffett field microcosm
B2	GW/Soil	Butane	Inoculated with the enrichments obtained from the Hanford DOE site.
B6	GW/Soil	Butane	Microcosm augmented with butane culture
B7	GW/Soil	Butane	Microcosm augmented with butane culture

All microcosms had been previous operated, but were inactive for about 1 year before being re-stimulated by adding 4-5 mg of gaseous propane or butane. After the microcosms were stimulated through substrate addition, 1,1,1-TCA tests were performed to determine the long-term transformation ability of 1,1,1-TCA. The aqueous concentration of 1,1,1-TCA ranged from 200 to 1300 μg/L. To resupply nutrients and prevent the accumulation of transformation by-products, groundwater exchange was performed before each new 1,1,1-TCA experiment.

No 1,1,1-TCA transformation was observed in the controls, as shown in Figure 4.1. The control bottles contained 65 mL of demineralized water and 1,1,1-TCA at the same concentration as the microcosms.

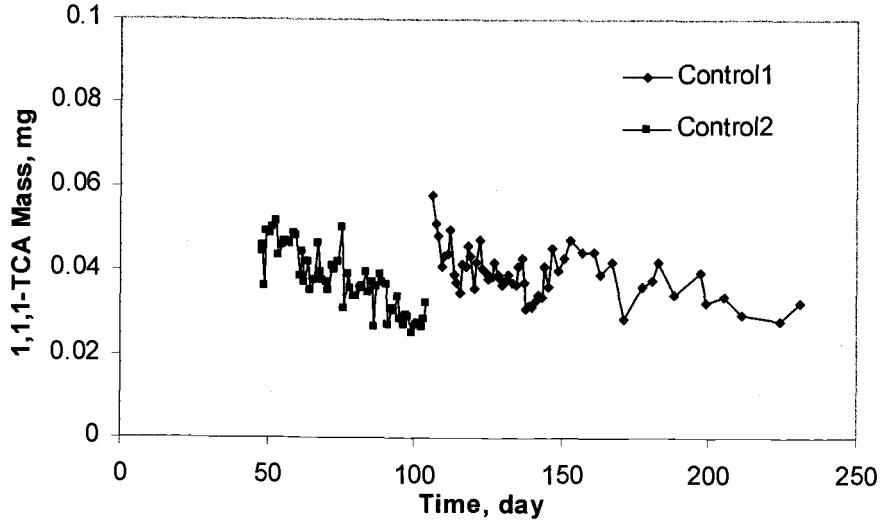

Figure 4.1 Control bottles for all the microcosms.

Figure 4.2 presents butane utilization and 1,1,1-TCA transformation by indigenous butane-utilizers in microcosm B1. The first addition of butane was consumed within 7 days. On day 19, more butane and 1,1,1-TCA (1300 μg/L) were added. The rates of butane utilization and TCA transformation were very slow. Butane was consumed in 11 days and only 50% of the TCA was

transformed. On day 48, the microcosm was purged under a laminar flow hood to remove 1,1,1-TCA. More butane and 1,1,1-TCA at lower concentration (500 μg/L) were added to repeat the experiment. TCA transformation ceased after 40% of the TCA was transformed. On day 70, butane was added to enhance TCA transformation. The transformation of successive 1,1,1-TCA additions was maintained for 12 days in the absence of butane utilization. The transformation rate decreased with continued addition of 1,1,1-TCA. The total mass of TCA transformed was 0.11 mg. On day 92, the experiment was repeated with the addition of a lower butane mass (1.42 mg). The transformation of 1,1,1-TCA ceased after 0.04 mg of TCA was transformed. As a result, 5.5 mg of butane was added on day 131 to increase the transformation ability. More 1,1,1-TCA (0.09 mg) was transformed.

Butane utilization and 1,1,1-TCA transformation by butane-utilizers in microcosm B6 are shown in Figure 4.3. Successive 1,1,1-TCA additions of 200 to 600 μg/L were started after eight additions of butane, and were rapidly transformed. The transformation rate of 1,1,1-TCA decreased with continued additions of 1,1,1-TCA. Microcosm B6 showed long-term transformation ability of 1,1,1-TCA in the absence of butane utilization. For example, on day 70, 1,1,1-TCA transformation ability was maintained for 44 days after butane was consumed. The total amount of 1,1,1-TCA transformed was 0.44 mg. The successive additions of 1,1,1-TCA were also transformed after butane additions on days 115, 131 and 144. The transformation continued from 10 to 42 days in the absence of butane utilization. The amount of 1,1,1-TCA transformed ranged from 0.12 to 0.18 mg, which was less than that occurred during the first transformation period.

Figure 4.4 presents the butane utilization and 1,1,1-TCA transformation by the butane-utilizers in microcosm B7. Five additions of butane were made to the microcosm in order to re-stimulate the butane-utilizers. On day 51, 1,1,1-TCA was then added along with another addition of butane. The transformation of 1,1,1-TCA was much slower than that in microcosm B6. Approximately 90% of 1,1,1-TCA was transformed in 9 days. More butane and TCA were added on day 67.

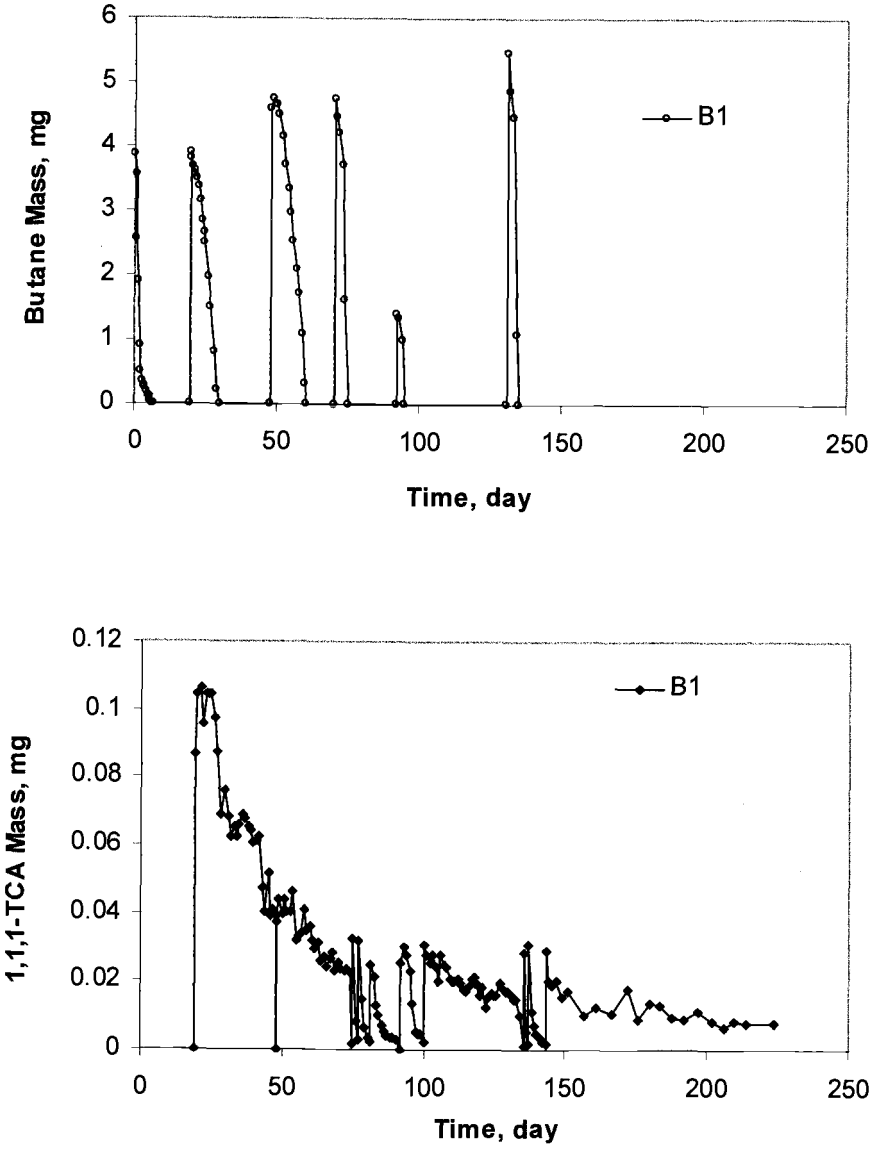

Figure 4.2 Butane utilization and 1,1,1-TCA transformation achieved in indigenous microcosm B1.

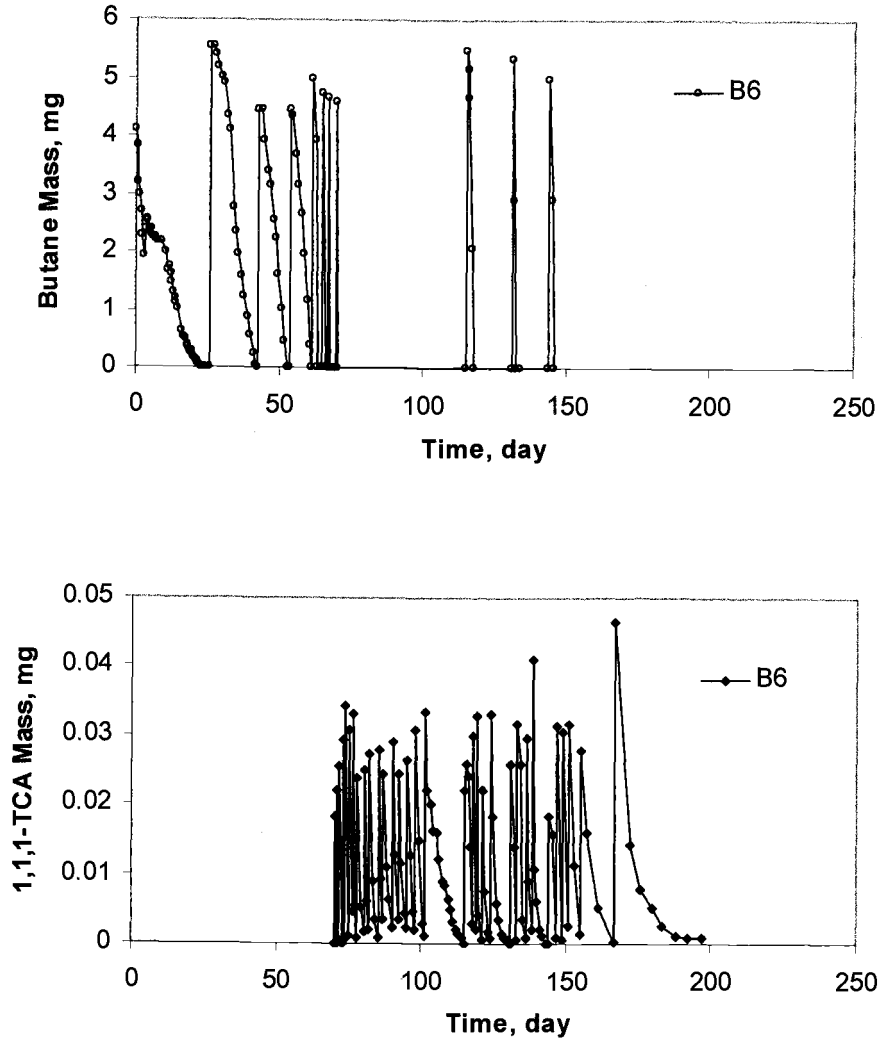

Figure 4.3 Butane utilization and 1,1,1-TCA transformation achieved in bioaugmented microcosm B6 .

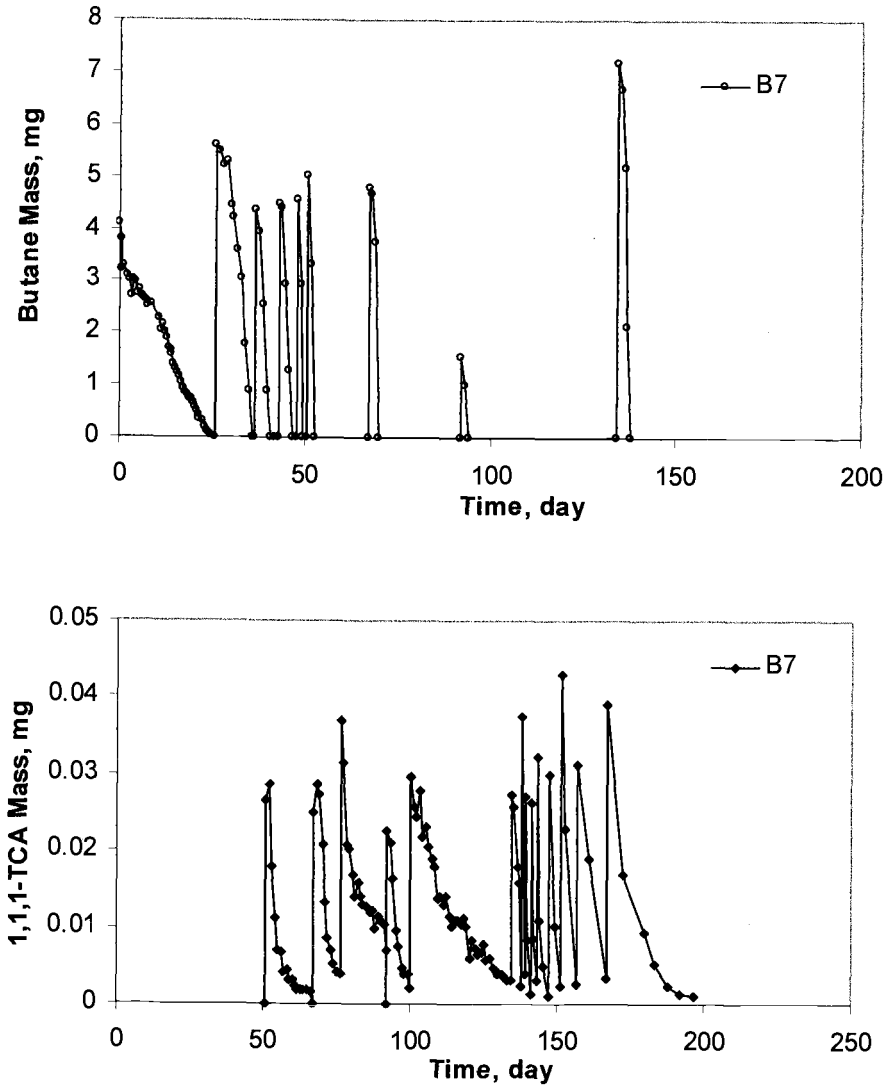

Figure 4.4 Butane utilization and 1,1,1-TCA transformation achieved in bioaugmented microcosm B7.

TCA transformation was still slow and by day 92 only 0.05 mg of 1,1,1-TCA was transformed. Before starting another experiment, the microcosm was purged under a laminar flow hood to remove 1,1,1-TCA. After the addition of 2 mg butane, slow long-term TCA transformation was observed. Approximately 0.05 mg of 1,1,1-TCA was transformed in 42 days. On day 134, successive additions of 1,1,1-TCA were conducted after the addition of 7.5 mg/L butane. TCA transformation rates increased and transformation continued 59 days in the absence of butane. The total mass of 1,1,1-TCA transformed was 0.25 mg. The improvement of transformation ability in microcosm B7 was possibly due to an increase of organisms responsible for the transformation of 1,1,1-TCA. This implies that the microbial community of the mixed butane-utilizing culture probably changed over time.

Figure 4.5 presents propane utilization and 1,1,1-TCA transformation by propane-utilizers in microcosm P6. 1,1,1-TCA at a concentration of 1000 μg/L was added after two additions of propane, and was transformed within 12 days. Competitive inhibition between propane and 1,1,1-TCA was observed. Successive additions of 1,1,1-TCA at lower concentration were performed on days 35, 51, 92, 115 and 131. The concentrations ranged from 400 to 750 μg/L. The transformation rate decreased with continued additions of 1,1,1-TCA. Similar to butane-utilizers in microcosm B6, propane-utilizers in microcosm P6 were able to transform 1,1,1-TCA over long periods. The transformation continued from 13 to 22 days after propane was consumed. The amount of 1,1,1-TCA transformed ranged from 0.07 to 0.45 mg. After 130 days of incubation, propane utilization became slower, even in the absence of 1,1,1-TCA. This probably resulted from the transformation product toxicity of 1,1,1-TCA.

The substrate utilization and 1,1,1-TCA transformation achieved in the other propane and butane-utilizers in microcosms P1, P2, P7, and B2 are shown in appendix Figures G.1 to G.4. All microorganisms were capable of transforming 1,1,1-TCA. The indigenous propane and butane-utilizers in microcosm P1 and B1 transformed 1,1,1-TCA more slowly and had a lower transformation capacity of 1,1,1-TCA than the bioaugmented microorganisms. Similar to microcosms B6 and

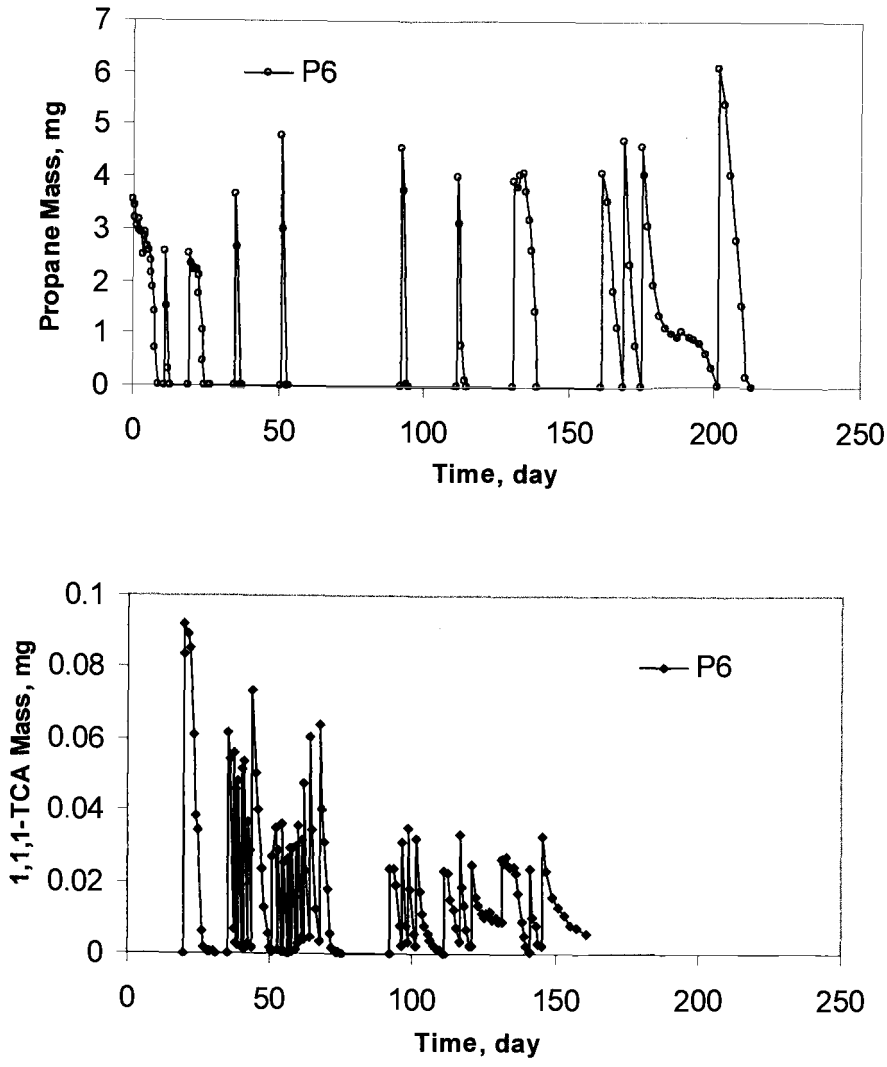

Figure 4.5 Propane utilization and 1,1,1-TCA transformation achieved in bioaugmented microcosm P6.

P6, the bioaugmented microcosms P2, P7, B2 and B7 had long-term transformation ability of 1,1,1-TCA in the absence of substrate utilization. The maximum transformation periods in the absence of substrate utilization are shown in Table 4.2 along with the transformation yields. The bioaugmented butane-utilizers showed longer transformation periods than the propane-utilizers. This may have resulted from a greater amount of substrate addition. The long-term transformation ability of 1,1,1-TCA observed in the microcosms indicates that the enzyme responsible for transformation was present and active long after the substrate was utilized.

Table 4.2 The maximum transformation period in the absence of substrate utilization, the average and final 1,1,1-TCA transformation yield achieved in the microcosms.

Microcosm	Maximum period (day)	Transformation yield (mg 1,1,1-TCA/mg substrate)	
		Average	On day 200
P1	22	0.014 ± 0.011	0.007
P2	27	0.031 ± 0.022	0.019
P6	22	0.046 ± 0.044	0.019
P7	28	0.029 ± 0.023	0.003
B1	14	0.013 ± 0.006	0.019
B2	43	0.021 ± 0.015	0.031
B6	44	0.024 ± 0.010	0.036
B7	50	0.019 ± 0.016	0.035

The transformation yield for 1,1,1-TCA at aqueous concentrations ranging from 220 to 530 μg/L was determined by dividing the total amount of 1,1,1-TCA transformed by the amount of butane utilized. The comparison of 1,1,1-TCA transformation yield among the microcosms is shown in Figure 4.6. The microcosms containing only indigenous microorganisms (P1 and B1) had lower transformation yields than the inoculated microcosms P2, P6, P7, B2, B6 and B7. The microcosms that were fed propane (P2, P6 and P7) had much high

transformation yields during the period of 25 – 50 days; however, the yield decreased considerably at later time. Unlike propane-utilizers, butane fed microcosms B2, B6 and B7 had lower transformation yields, but maintained higher yield values over the study period. The transformation yield for 1,1,1-TCA relates to the amount of active biomass in the microcosms and energy reserves to drive the transformation. Similar to the transformation rate of 1,1,1-TCA, the transformation yield decreases with the additions of 1,1,1-TCA. This probably results from the transformation product toxicity of 1,1,1-TCA, decreasing the amount of active microbial cells and/or oxygenase enzyme responsible for the 1,1,1-TCA transformation.

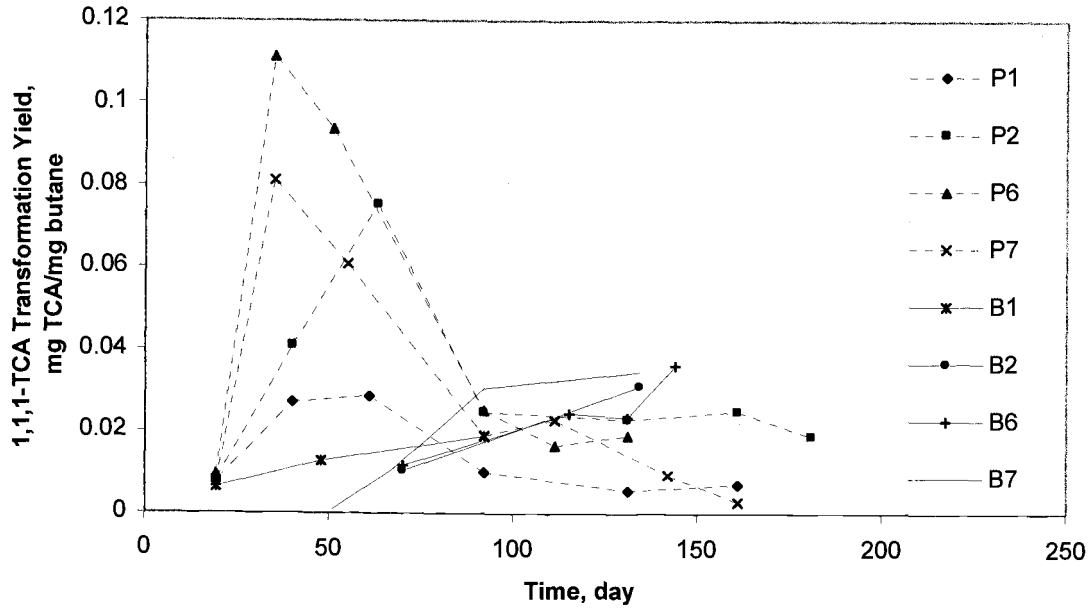

Figure 4.6 1,1,1-TCA transformation yield achieved in the microcosms.

As shown in Table 4.2, the average and final (on day 200) transformation yields achieved in indigenous microcosms P1 and B1 were lower than those in the other inoculated microcosms except microcosm P7, which had the lowest final

yield. The final transformation yields of inoculated propane-utilizers were lower than the average yields. The average and final yields of inoculated butane-utilizers were similar. Propane-utilizers had higher average transformation yields, but lower final transformation than butane-utilizers. To ensure that there was a sufficient amount of active biomass, the final yield was used to determine which microcosm was suitable for the bioaugmentation of additional microcosms. As a result, butane fed microcosm B6 was chosen to be the parent microcosm for bioaugmentation studies. Microorganisms in microcosm B6 also exhibited very rapid transformation of 1,1,1-TCA, which was also a desirable characteristic for the bioaugmentation culture.

4.2 MICROCOSM STUDIES WITH GROUNDWATER AND SOIL FROM MICROCOSM B6

4.2.1 Transformation of 1,1,1-TCA

Microcosm studies were conducted to compare the 1,1,1-TCA transformation ability between indigenous and bioaugmented butane-utilizers, and to study long-term 1,1,1-TCA transformation. Microcosms were constructed in 125 mL media bottles sealed with Teflon fluorocarbon resin-lined caps. They were filled with either 75 mL of Moffett groundwater and aquifer material or 75 mL of mineral salt growth media. Each microcosm was constructed in triplicate. Since microcosm B6 showed the best 1,1,1-TCA transformation performance, it was selected to be the parent culture for bioaugmentation. A slurry, composed of groundwater and aquifer material, was taken from microcosm B6 on day 141 (Figure 4.3) and used to inoculate microcosms. The microcosm conditions are shown in Table 4.3. Butane gas was added as the primary substrate for each microcosm. Successive additions of saturated 1,1,1-TCA solution were made to

achieve an aqueous concentration of 350 μg/L. Control microcosms contained the same amount of TCA (appendix Figure G.5). Before starting the new 1,1,1-TCA experiment, groundwater was exchanged to resupply nutrients and prevent the accumulation of transformation by-products.

Table 4.3 Microcosms used for the experiment of 1,1,1-TCA transformation.

Microcosm	Contents	Substrate	CAHs	Description
B1-1 to B1-3	GW/Soil	Butane	1,1,1-TCA	Indigenous microcosm
B2-1 to B2-3	GW/Soil	Butane	1,1,1-TCA	Inoculated with 1 ml of GW/soil slurry transferred from microcosm B6
B3-1 to B3-3	Growth media	Butane	1,1,1-TCA	Inoculated with 1 ml of GW/soil slurry transferred from microcosm B6
B4-1 to B4-3	GW/Soil	Butane	1,1,1-TCA	Inoculated with 100 μl of washed media-culture harvested from the growth reactor having 1 mL of GW/soil slurry transferred from microcosm B6 as a culture seed.

The butane utilization and 1,1,1-TCA transformation achieved in the triplicate indigenous microcosms (no bioaugmentation) B1-1, B1-2 and B1-3 are shown in Figure 4.7. The first addition of butane was completely consumed on day 35, 25, and 45, respectively. 1,1,1-TCA was then added to microcosms along with the second addition of butane. All indigenous microorganisms utilized butane, but little 1,1,1-TCA transformation occurred.

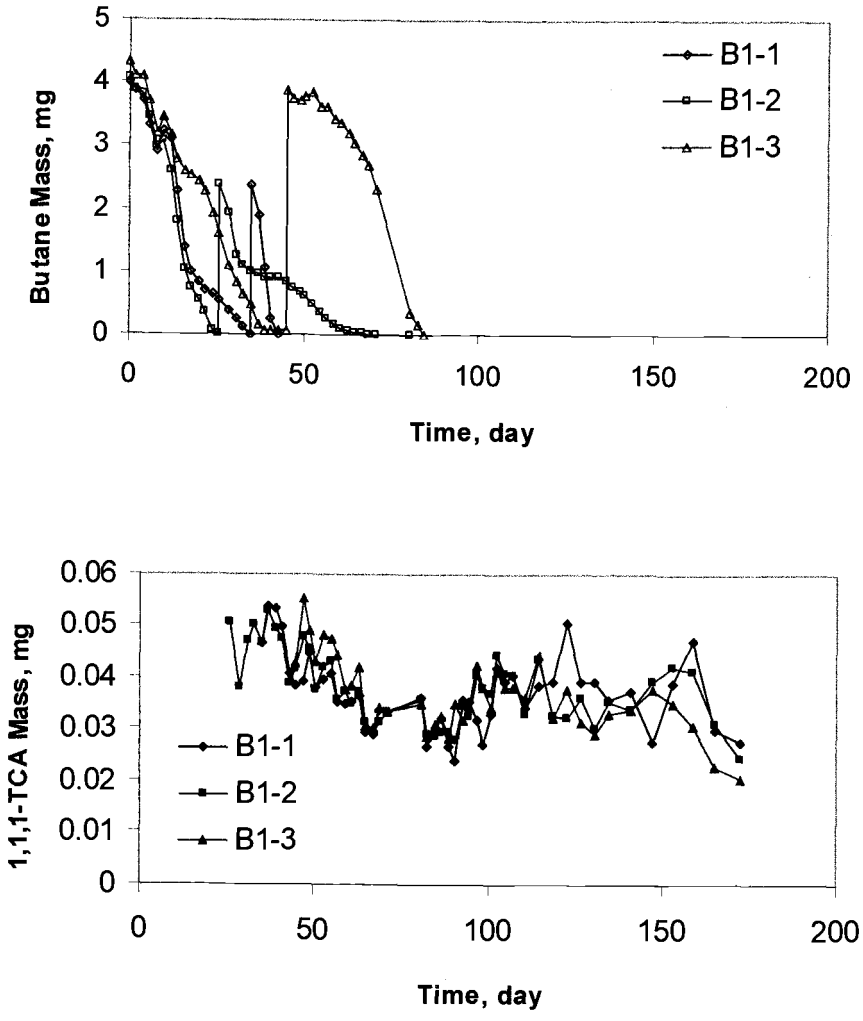

Figure 4.7 Butane utilization and 1,1,1-TCA transformation achieved in the indigenous microcosms constructed with groundwater and aquifer solids.

Figure 4.8 presents butane utilization and 1,1,1-TCA transformation achieved in slurry, transferred from microcosm B6, inoculated microcosms B2-1, B2-2, and B2-3 during the first 50 days of incubation. The microcosms were constructed with Moffett field groundwater and aquifer solids. Butane was completely consumed within 10 days of incubation. With the second addition of butane, 1,1,1-TCA was rapidly consumed. Repeated additions of 1,1,1-TCA (350 μg/L) were transformed in the absence of butane, although the transformation rate decreased after each addition. Butane was again added on day 29 and was rapidly consumed, and 1,1,1-TCA transformation accelerated as butane concentration was reduced, as shown in Figure 4.9. This indicates the competitive inhibition of 1,1,1-TCA transformation by butane. The high concentration of 1,1,1-TCA (2 mg/L) that microcosms experienced on day 40 (Figure 4.8) was also rapidly transformed. The triplicate microcosms all showed similar results. The bioaugmented microcosms, thus, had very reproducible performance towards butane utilization and 1,1,1-TCA transformation. The average transformation yield achieved in the B2 microcosm set during the first 50 days of incubation was 0.079 ± 0.005 mg 1,1,1-TCA/mg butane.

The butane utilization and 1,1,1-TCA transformation achieved in the media-grown culture bioaugmented microcosms are presented in Figure 4.10. Butane in microcosms B4-1, B4-2 and B4-3 was completely consumed within 6 to 8 days. Similar to the B2 microcosm set, the second addition of butane and 1,1,1-TCA was rapidly consumed. The competitive inhibition of butane on 1,1,1-TCA transformation was also observed, as shown in Figure 4.11. Successive additions of 1,1,1-TCA (350 μg/L) were also transformed in the absence of butane, and the transformation rate decreased after each addition. While 1,1,1-TCA in microcosms B4-1 and B4-3 was completely transformed, microcosm B4-2 behaved differently. The transformation of 1,1,1-TCA in microcosm B4-2 began to slow down at day 34. The limited transformation of 1,1,1-TCA in microcosm B4-2 appears to be correlated with a slower rate of butane uptake. The average transformation yield

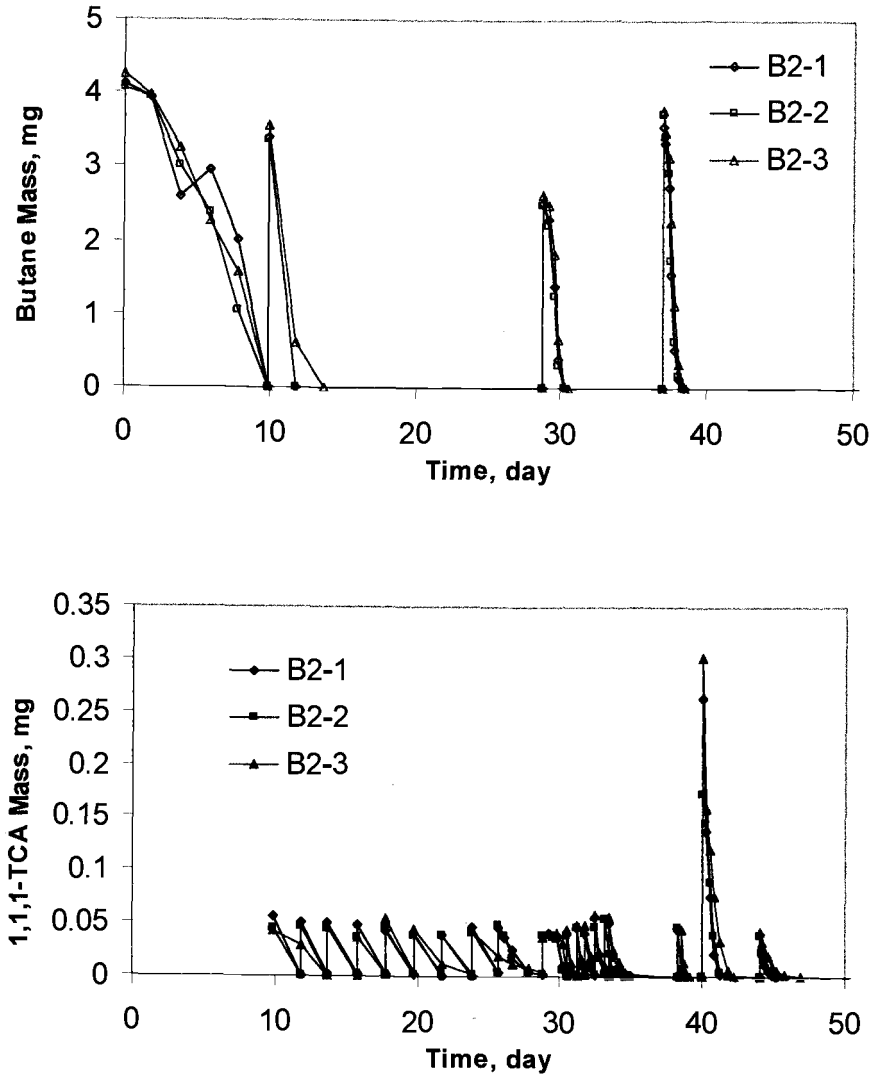

Figure 4.8 Butane utilization and 1,1,1-TCA transformation achieved in the slurry (microcosm B6) inoculated microcosms constructed with groundwater and aquifer solids.

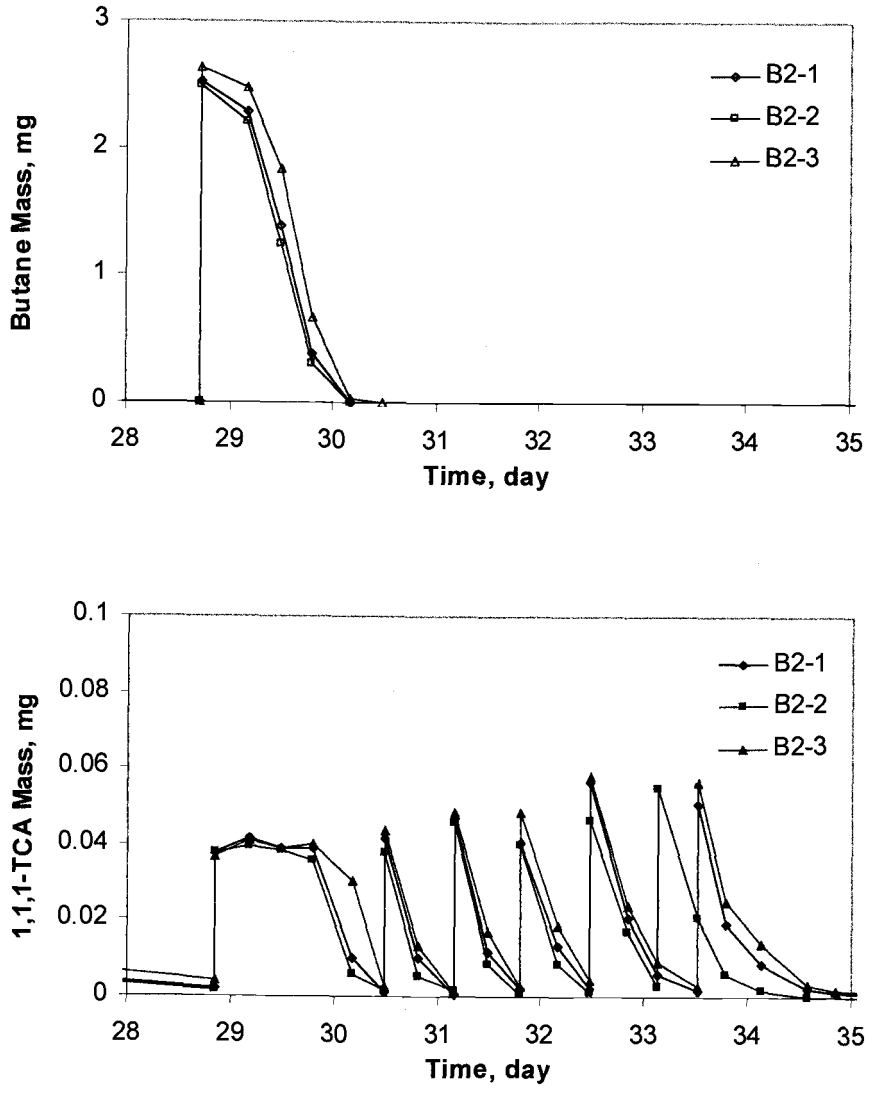

Figure 4.9 The competitive inhibition (day 29 to 31) of 1,1,1-TCA transformation by butane in the slurry (microcosm B6) inoculated microcosms constructed with groundwater and aquifer solids.

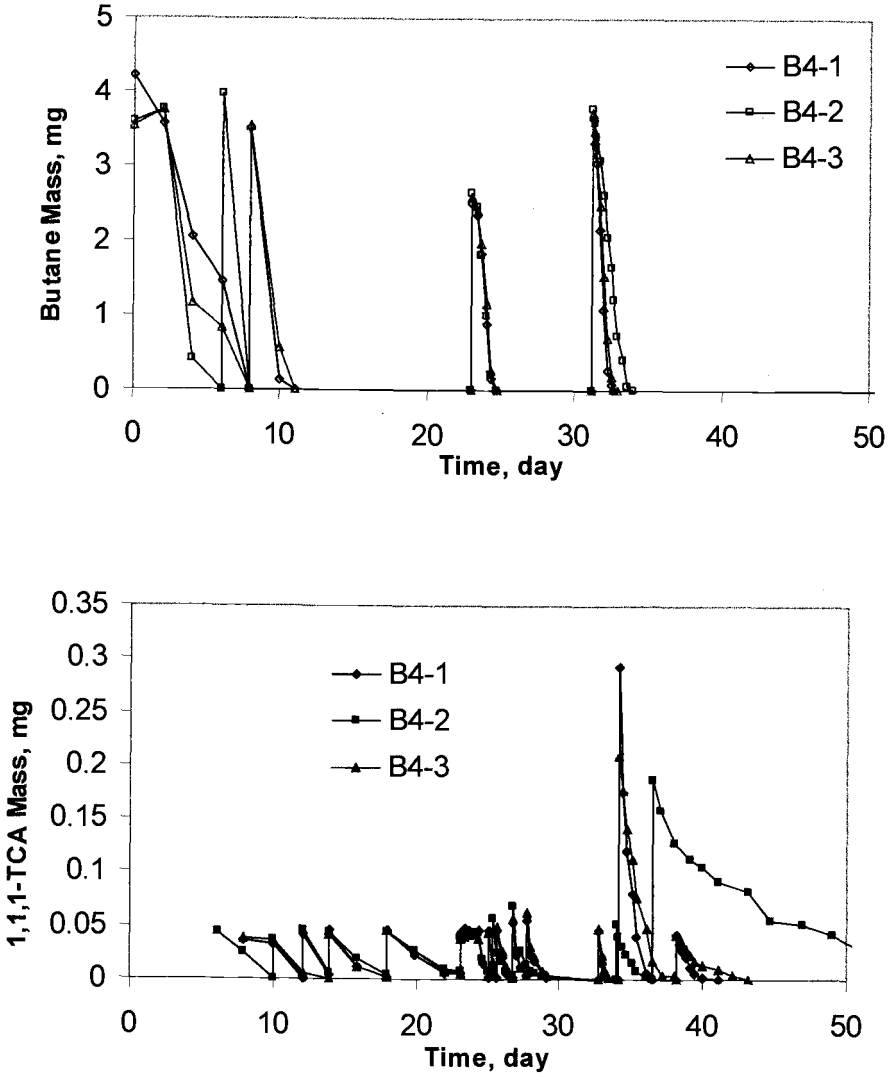

Figure 4.10 Butane utilization and 1,1,1-TCA transformation achieved in the media-culture inoculated microcosms constructed with groundwater and aquifer solids.

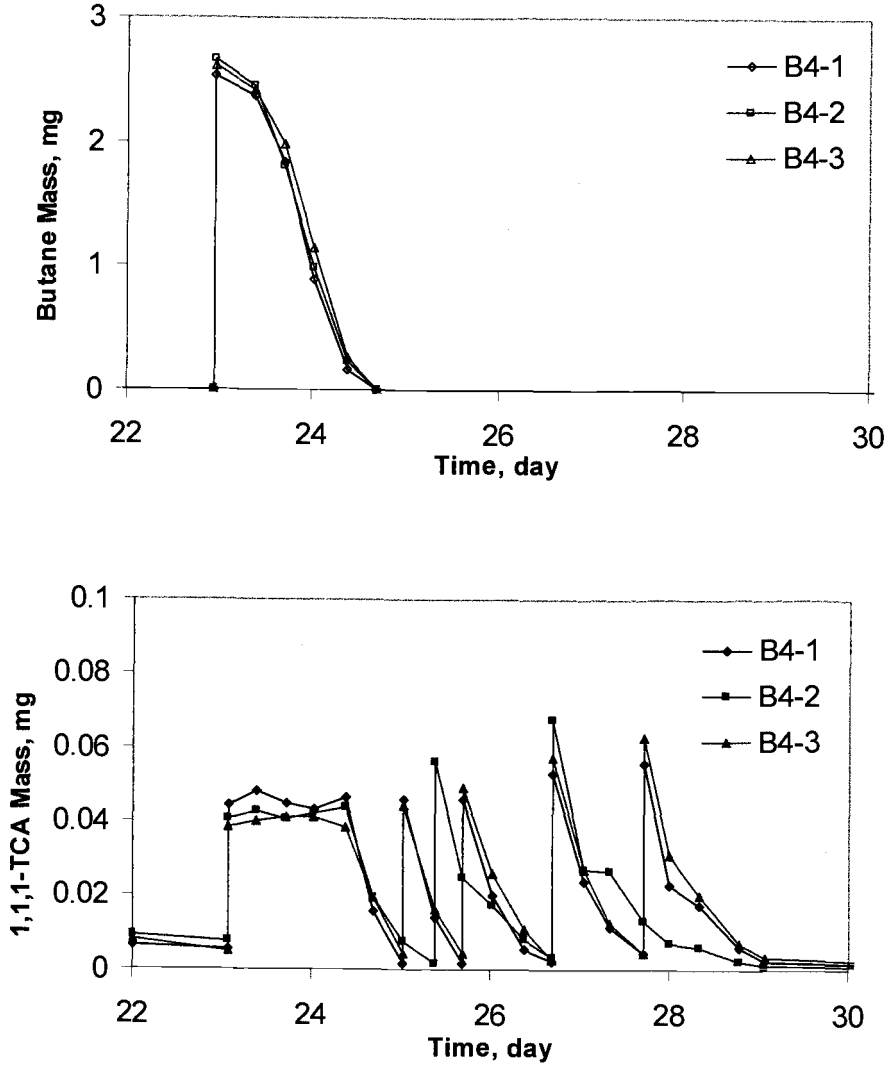

Figure 4.11 The competitive inhibition (day 23 to 25) of 1,1,1-TCA transformation by butane in the media-culture inoculated microcosms constructed with groundwater and aquifer solids.

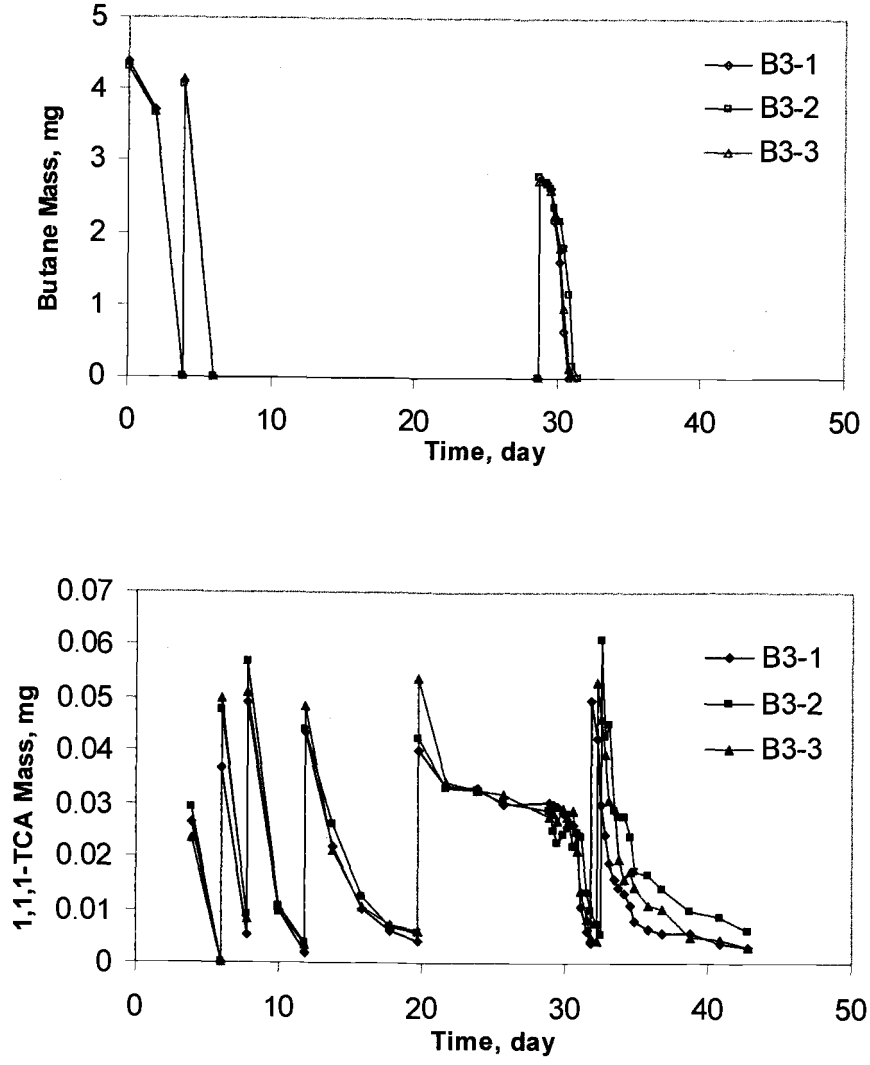

Figure 4.12 Butane utilization and 1,1,1-TCA transformation achieved in the slurry (microcosm B6) inoculated microcosms containing mineral salts growth media.

for the B4 microcosm set during the first 50 days of incubation was 0.061 ± 0.012 mg 1,1,1-TCA/mg butane, which was slightly lower than that achieved in the B2 microcosm set.

Figure 4.12 presents the butane utilization and 1,1,1-TCA transformation in microcosms B3-1, B3-2, and B3-3. The microcosms were constructed with mineral salts growth media and bioaugmented with slurry from microcosm B6. The first addition of butane was consumed by day four. Transformation of 1,1,1-TCA achieved in the B3 microcosm set was lower than that achieved in the B2 and B4 microcosm sets. By day 28, 1,1,1-TCA transformation had essentially ceased after 24 days of active transformation. More butane was then added, and with its utilization 1,1,1-TCA was again transformed. The average transformation yield in the B3 microcosm set during the first 50 days of incubation was 0.024 ± 0.001 mg 1,1,1-TCA/mg butane.

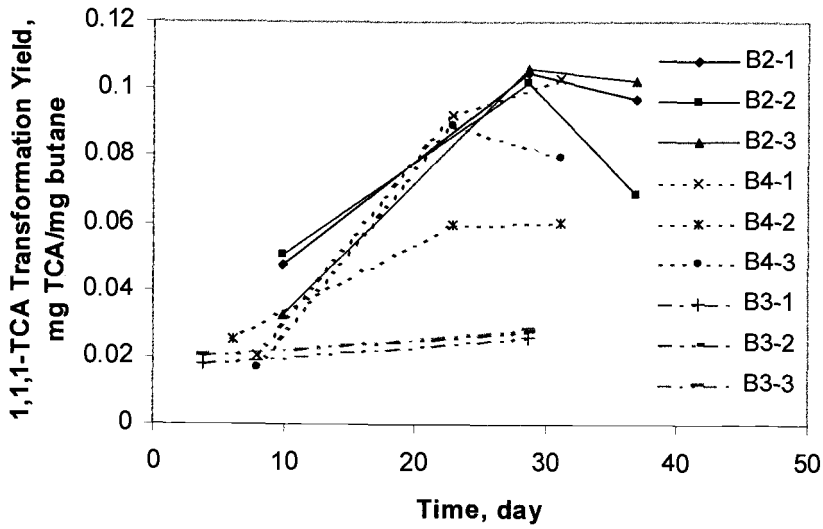

Figure 4.13 Transformation yield for 1,1,1-TCA achieved in the inoculated microcosms during the first 50 days of incubation

The transformation yields achieved in the microcosms during the first 50 days of incubation are presented in Figure 4.13 and Table 4.4. The measured amount of TCA in the indigenous microcosms fluctuated, yet little decrease in concentration was observed; thus, the transformation yield could not be accurately determined. Transformation yields in the B2 and B4 bioaugmented microcosm sets were similar to each other. Jitnuyanont (1998) reported a similar transformation yield of butane-utilizers (0.07 mg 1,1,1-TCA/mg butane), which was determined during the first 190 days of incubation. In this study, the transformation yield increased with time. This is likely due to more frequent additions of TCA and exposure to higher TCA concentrations. Although all bioaugmented microcosms behaved similarly during the first 10 days of incubation, the B3 bioaugmented microcosm set, which contained mineral salts growth media, showed significantly lower transformation ability. The transformation yield for the B3 microcosm set was two to three times lower than the other microcosm sets. The culture characteristics in the B3 microcosm set may have changed when grown in mineral salts growth media for longer than 20 days.

Table 4.4 Transformation yield for 1,1,1-TCA achieved in the microcosms during the first 50 days of incubation.

Microcosm	Transformation yield (mg 1,1,1-TCA/mg butane)
B1 set: indigenous microcosms constructed with groundwater and aquifer solids	0
B2 set: slurry-inoculated microcosms constructed with groundwater and aquifer solids	0.079 ± 0.005
B3 set: slurry-inoculated microcosms constructed with mineral salts growth media	0.024 ± 0.001
B4 set: media-culture inoculated microcosms constructed with groundwater and aquifer solids	0.061 ± 0.012

The rates of 1,1,1-TCA transformation in the B2 and B4 microcosm sets were measured during day 30 - 35, and day 38 - 45. To exclude competitive inhibition effects between butane and 1,1,1-TCA, the rates were measured in the absence of butane. Thus, these represent resting cell transformation rate values.

Figure 4.14 presents the 1,1,1-TCA transformation rate data for microcosm B2-1 during day 30 – 35. A gradual slowing in the transformation rate is shown. The experimental data was plotted on a semi-logarithmic scale to test for first-order transformation, as shown in Figure 4.15. The slope of the linear regression line in each graph represented the pseudo-first-order rate coefficient (P), the combination term of kinetic parameters and biomass and equilibrium distribution of 1,1,1-TCA, which is illustrated in equation D.5, Appendix D. The values of pseudo-first-order rate coefficient (P) obtained from the rate tests in all microcosms are presented in appendix Tables G.1 to G.6.

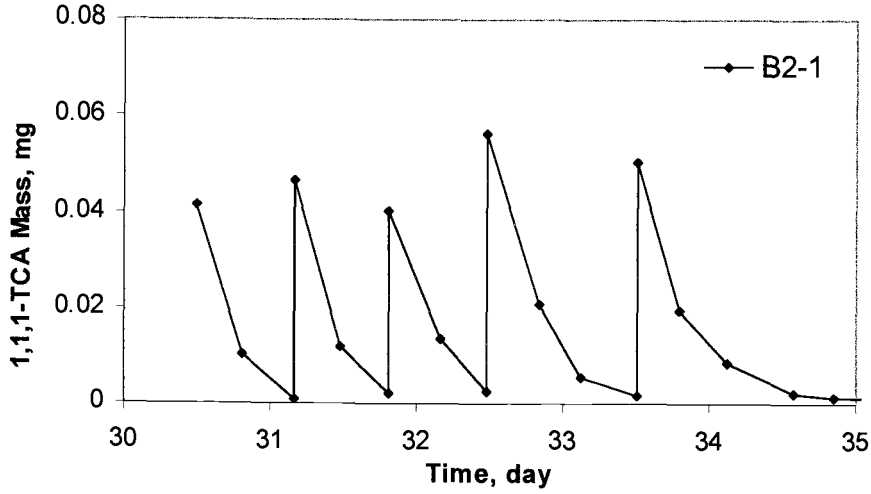

Figure 4.14 1,1,1-TCA transformation rate data for microcosm B2-1 during day 30 – 35.

a) The 1st addition of 1,1,1-TCA

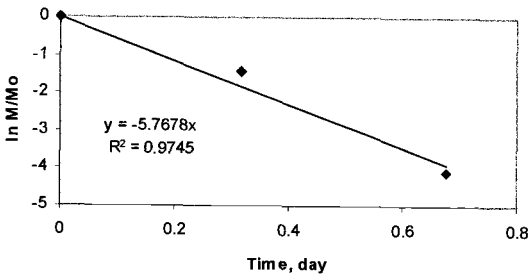

b) The 2nd addition of 1,1,1-TCA

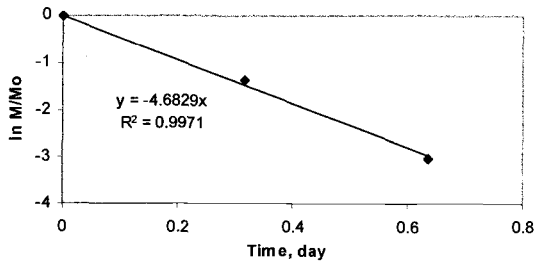

c) The 3rd addition of 1,1,1-TCA

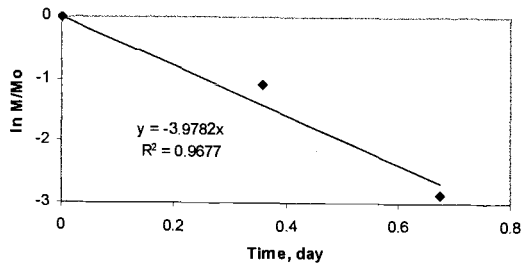

d) The 4th addition of 1,1,1-TCA

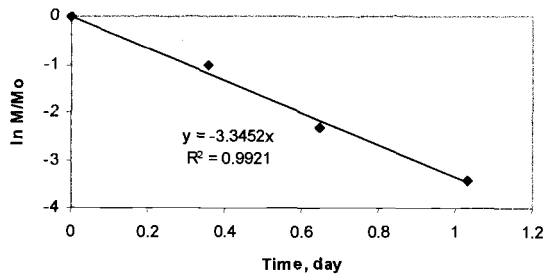

e) The 5th addition of 1,1,1-TCA

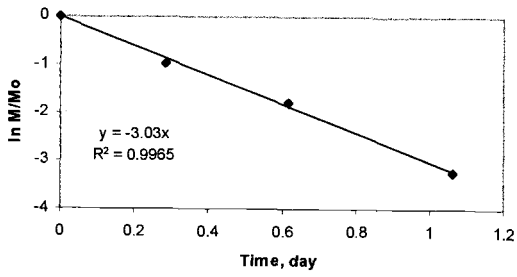

Figure 4.15 1,1,1-TCA transformation rate data for microcosm B2-1 during day 30 - 35 plotted on a semi-logarithmic scale.

Values of the pseudo-first-order rate coefficient (P) from each graph in Figure 4.15 are plotted against time, as shown in Figure 4.16. The exponential regression line in the graph was obtained from Microsoft Excel 2000. The slope and the power of the exponential regression line provided the values of the pseudo first-order rate parameter ($k_{max}X_0/K_s$) and cell decay rate (b), respectively. The calculation of these two values is based on equation D.8, as illustrated in Appendix D. The pseudo-first-order rate coefficient (P) decreased with time. This is probably due to a decreased amount of active biomass or the gradual inactivation of oxygenase enzyme or a loss in energy, or the combination of all three processes.

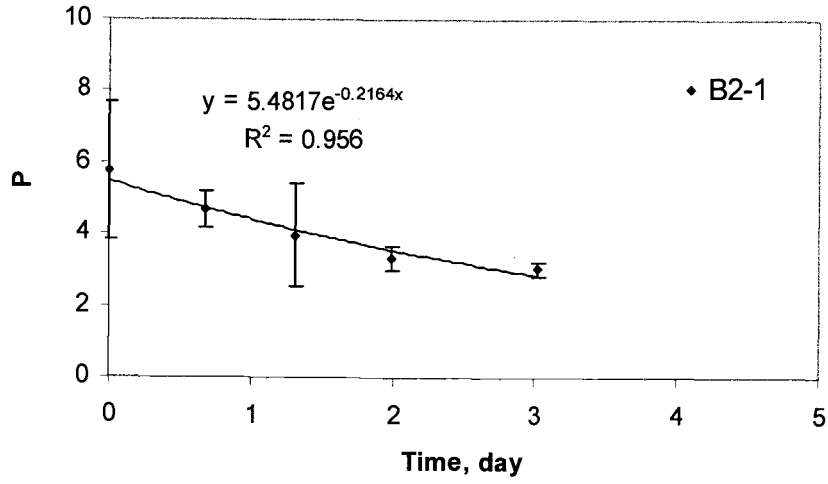

Figure 4.16 The decrease in pseudo-first-order rate coefficient (P) as a function of time during day 30 – 35.

Table 4.5 presents the values of pseudo-first-order rate parameters ($k_{max}X_0/K_s$) and cell decay rates (b) obtained from the rate tests for all the microcosms. The average decay rates of both microcosm sets were similar, ranging from 0.15 to 0.28 day^{-1}. These values are in the range for cell decay by aerobic microorganisms. Similar values of the decay rates between both microcosm sets

indicate that growing the culture on growth media before bioaugmentation may not change the microbial community. The pseudo-first-order rate parameters ($k_{max}X_0/K_s$) were within a factor of two of each other. This possibly resulted from the different amount of active biomass in the microcosms.

Table 4.5 The pseudo-first-order rate parameter ($k_{max}X_0/K_s$) and cell decay rate (b) for the B2 and B4 microcosm sets during day 30 – 35.

Microcosm	$k_{max}X_0/K_s$ (day^{-1})	b (day^{-1})
B2-1	8.77	0.22
B2-2	10.66	0.23
B2-3	10.49	0.21
Average	9.97 ± 1.04	0.22 ± 0.013
B4-1	6.62	0.28
B4-2	3.38	0.20
B4-3	4.99	0.15
Average	4.99 ± 1.62	0.21 ± 0.064

Experimental data for microcosm B2-1 during day 38 – 45 are shown in Figure 4.17. Similar to the former rate test, the data are plotted on a semi-logarithmic scale, as shown in Figure 4.18, in order to determine the value of pseudo-first-order rate coefficient (P) from the slope of the linear regression line in each graph. Figure 4.19 presents the decrease in pseudo-first-order rate coefficient (P) as a function of time. The data did not fit the exponential decay model well. The high 1,1,1-TCA concentration in the second TCA addition data maybe out of the pseudo-first-order range and may partly be causing the poor fit.

The pseudo-first-order rate coefficients (P) from the experimental data during both day 30 - 35 and day 38 – 45 were plotted against the accumulation mass of 1,1,1-TCA transformed, to examine if there was a correlation. As shown in Figure 4.20, the transformation rate decreases with the increasing mass of 1,1,1-TCA transformed. Similar values of the coefficient of determination (R^2) indicate

that the data at low concentration during day 30 – 35 are fit equally well by time (Figure 4.16) or mass (Figure 4.20a) regression lines. When in a high concentration range, during day 38 – 45, the coefficient of determination (R^2) is smaller for the time fit than the mass fit as shown in Figures 4.19 and 4.20b. Thus the decrease in pseudo-first-order coefficients (P) tends to be more strongly correlated with the transformed mass of 1,1,1-TCA rather than time.

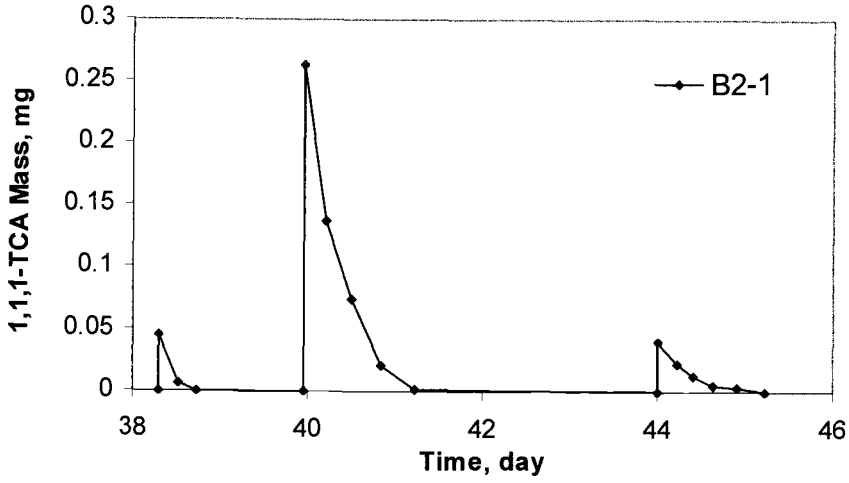

Figure 4.17 1,1,1-TCA transformation rate data for microcosm B2-1 during day 38 – 45.

Similar to the microorganisms in parent microcosm B6, the microorganisms in all bioaugmented microcosms were able to transform 1,1,1-TCA over long periods in the absence of butane utilization. The indigenous microorganisms in the B1 microcosm set showed less ability to transform 1,1,1-TCA than those in Figure 4.2. Thus the bioaugmented microcosms had more reproducible performance than the non-augmented microcosms. Growing the culture on growth media before bioaugmentation did not change 1,1,1-TCA transformation abilities. However, the mixed cultures probably changed when growing in mineral salts growth media for longer than 20 days, as indicated by the differences in transformation yields (Figure 4.13).

a) The 1st addition of 1,1,1-TCA

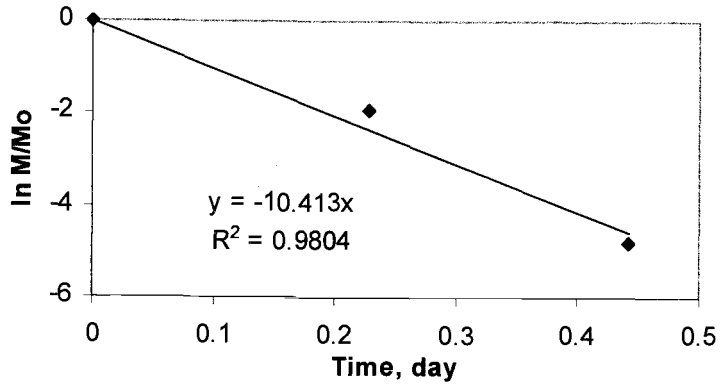

b) The 2nd addition of 1,1,1-TCA

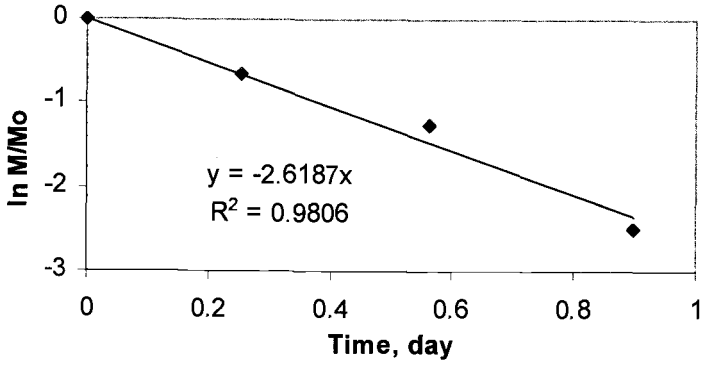

c) The 3rd addition of 1,1,1-TCA

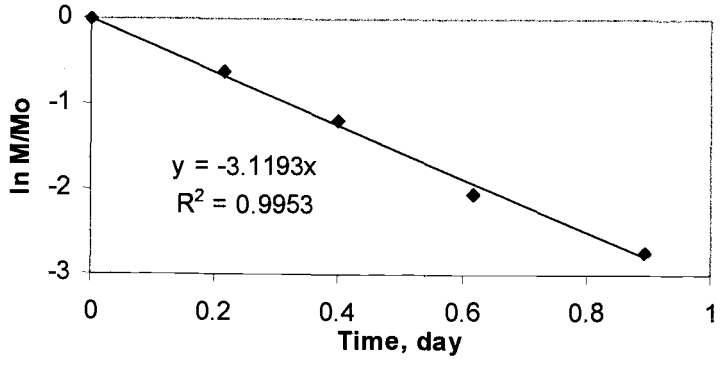

Figure 4.18 1,1,1-TCA transformation rate data for microcosm B2-1 during day 38 - 45 plotted on a semi-logarithmic scale

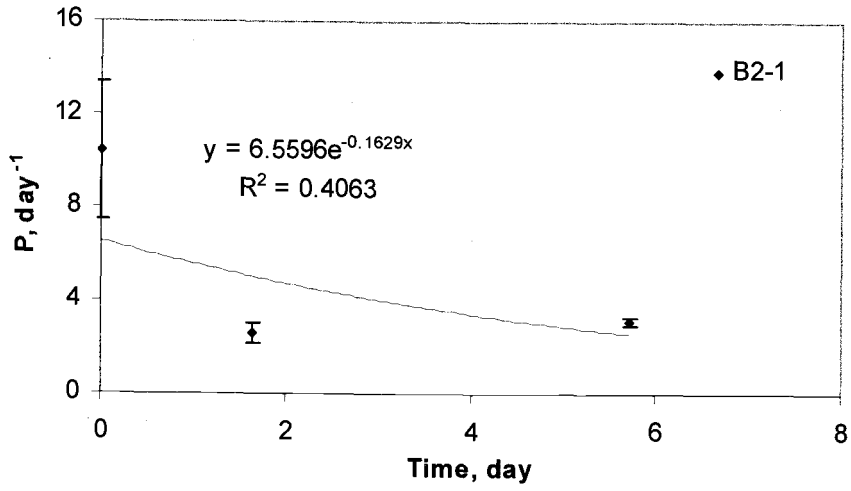

Figure 4.19 The decrease in pseudo-first-order rate coefficient (P) as a function of time during day 38 – 45

The long-term transformation ability of 1,1,1-TCA observed in the microcosms indicates that the enzyme responsible for transformation was present and active long after butane was utilized. The decrease in transformation rate at high TCA concentration tends to correlate better with the mass of 1,1,1-TCA transformed than with time, while that at low concentration transformation rate decreases correlate with both time and mass transformed. It may be that repeated transformation of low amounts of 1,1,1-TCA did not significantly affect the microorganisms, but served to induce enzyme activity. Limited and slow transformation of 1,1,1-TCA appeared to be correlated with a slow rate of butane uptake. 1,1,1-TCA transformation product toxicity, a drain of energy reserves and cell decay may all be contributing to a loss in activity.

a) During day 30 – 35

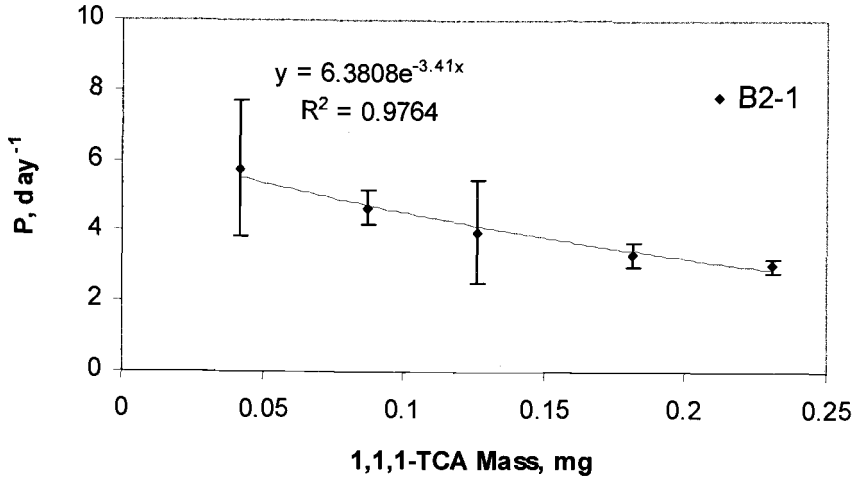

b) During day 38 - 45

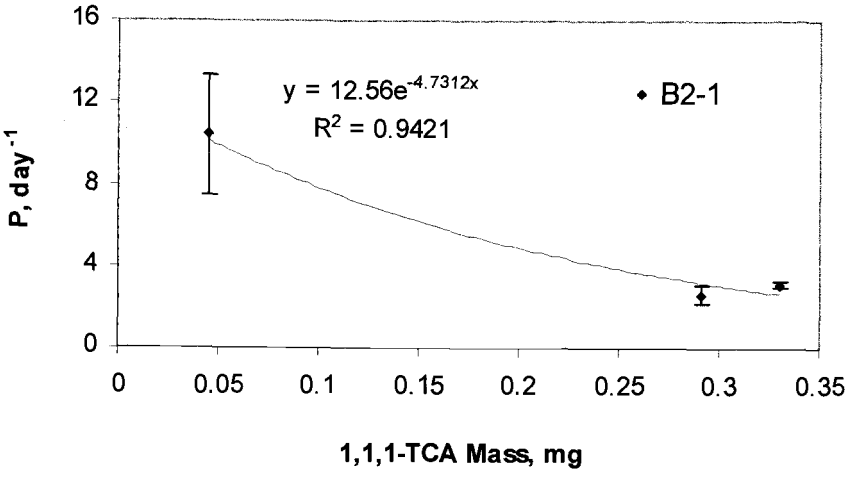

Figure 4.20 The decrease in pseudo-first-order rate coefficient (P) as a function of transformed 1,1,1-TCA mass during day 30 - 35 and day 38 – 45.

4.2.2 Transformation of CAH mixture

The transformation of CAH mixtures of 1,1,1-TCA, TCE, and 1,1-DCE was also studied in microcosms stimulated on butane. The microcosms were constructed in the same fashion as in the previous experiment. Microcosms B2-1 and B2-2 were used in the past study of 1,1,1-TCA transformation. The BM microcosm set was stimulated by one addition of butane, and was inactive for about 80 days before starting this experiment. The microcosm conditions are presented in Table 4.6.

Table 4.6 Microcosms used for the experiment of CAH mixture transformation

Microcosm	Contents	Substrate	CAHs	Description
B2-1 B2-2	GW/Soil	Butane	1,1,1-TCA, 1,1-DCE, TCE	Inoculated with 1 ml of GW/soil slurry transferring from microcosm B6
BM1-2 BM2-2 BM3-2	Growth media	Butane	1,1,1-TCA, 1,1-DCE, TCE	Inoculated with 100 µl of washed media-culture harvested from the growth reactor having 1 mL of groundwater/soil slurry transferring from microcosm B6 as a culture seed

Figure 4.21 presents the utilization of butane and the transformation of the CAH mixture in microcosm B2-1. Microcosm B2-1 was inactive for 43 days after the previous experiment of 1,1,1-TCA transformation. On day 97, butane was added to re-stimulate the microcosm and was consumed within three days. After the second addition of butane was consumed, 390 µg/L of 1,1,1-TCA, 540 µg/L of

TCE, and 280 μg/L of 1,1-DCE were added to the microcosm. The transformation rate of 1,1-DCE was so fast that all 1,1-DCE was transformed within 4 hours, while 1,1,1-TCA, butane and TCE were transformed within 20 hours, 1 day, and 5 days, respectively. The experiment was repeated on day 105 but at a higher concentration of the CAHs. Butane utilization occurred within 2 days. Approximately 730 μg/L of 1,1-DCE, and 590 μg/L of 1,1,1-TCA were transformed within 3 hours and 7 days, respectively. However, the transformation of TCE (1400 μg/L) ceased after 80% of TCE was transformed. The re-addition of butane on day 123 enhanced TCE transformation. On day 139, the experiment was repeated. However, the transformation capacity decreased dramatically. Only 6% of butane, 13 % of TCA, 17% of TCE, and 72% of 1,1-DCE were transformed.

The utilization of butane and the transformation of a CAH mixture in microcosm BM2-2 are presented in Figure 4.22. Microcosm BM2-2 was stimulated once by one addition of butane, and was inactive for about 78 days. On day 81, the microcosm was re-stimulated by two additions of butane. After butane was consumed, 1,1,1-TCA, TCE and 1,1-DCE were added to the microcosm. 1,1-DCE (100 μg/l), 1,1,1-TCA (550 μg/l) and TCE (630 μg/l) were transformed within 1 day, 6 days, and 8 days, respectively. The inhibition of 1,1,1-TCA and TCE transformation by 1,1-DCE was observed. The transformation rates of all compounds including butane decreased in the second experiment on day 92 and 95. 1,1-DCE (420 μg/l) was completely transformed within 3 days, while only 36% of 1,1,1-TCA (550 μg/l) and 12% of TCE (840 μg/l) were transformed. More butane was then added to enhance 1,1,1-TCA and TCE transformation on day 102. With the third addition of CAH mixture, no butane utilization and limited chlorinated solvent transformation occurred. The utilization of butane and the transformation of mixtures of 1,1,1-TCA, TCE and 1,1-DCE in the other microcosms were similar, as shown in appendix Figures G.6 to G.8.

In addition to 1,1,1-TCA, the bioaugmented butane-utilizers were able to transform other chlorinated solvents such as 1,1-DCE and TCE. The

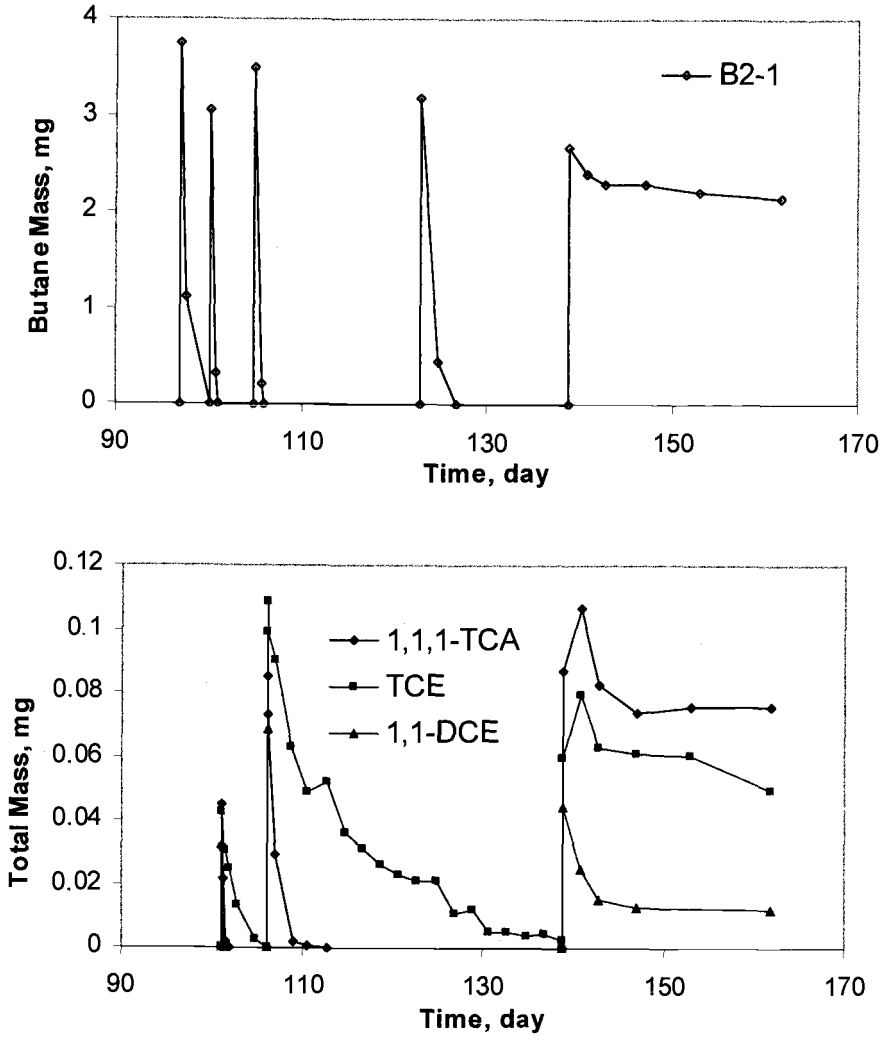

Figure 4.21 Butane utilization and chlorinated compound transformation achieved in slurry-inoculated microcosm B2-1.

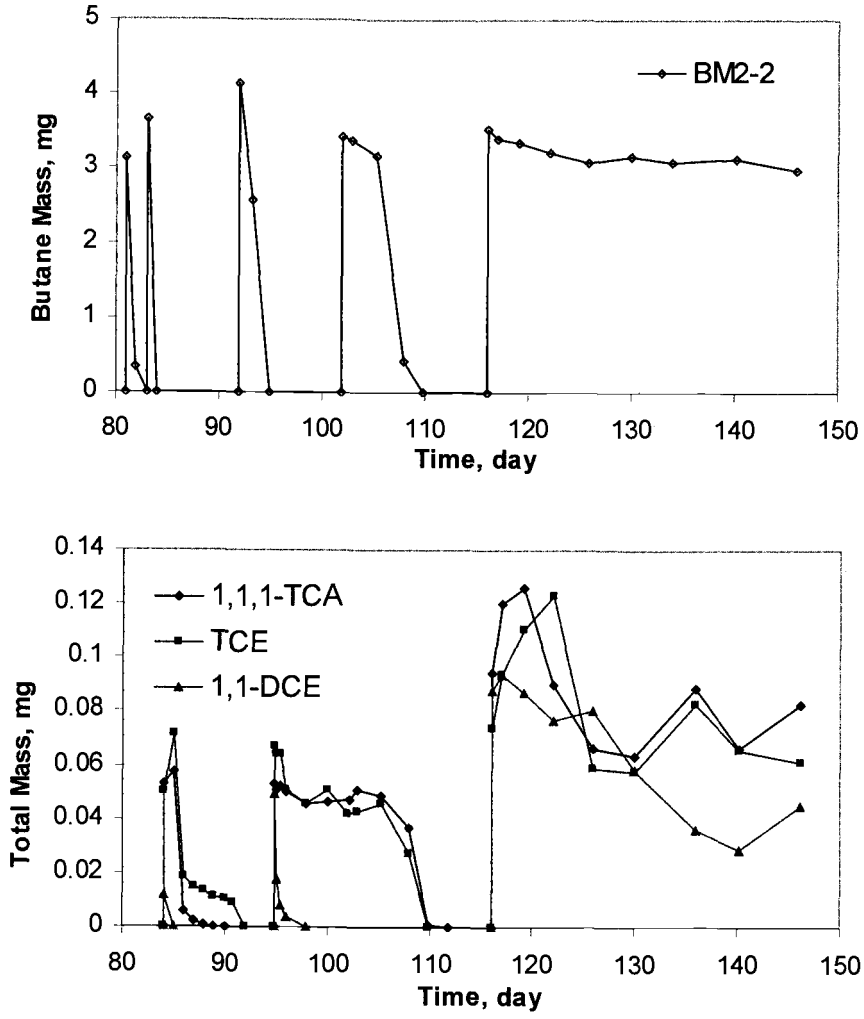

Figure 4.22 Butane utilization and chlorinated compound transformation achieved in the media-culture inoculated microcosm BM2-2.

transformation of 1,1-DCE was very fast, while the transformation rate of 1,1,1-TCA and TCE were slower. The transformation product toxicity from chlorinated solvents, especially from 1,1-DCE and possibly TCE at high concentrations, was suspected to be the major cause of the limited transformation of CAHs and the cessation in butane utilization.

4.2.3 Selecting microcosm for bioaugmentation studies

Based on the good performance of 1,1,1-TCA transformation, microcosm B2-1 was chosen to be the culture seed to obtain a uniform culture for bioaugmentaion studies both in the laboratory and the field tests. After the experiment of 1,1,1-TCA transformation (Figure 4.8), on day 53, butane was added to enrich the culture before transferring one milliliter of the groundwater/soil slurry for growth in each of ten batch reactors. A batch growth reactor was set up in a 500 mL bottle sealed with a grey butyl rubber lined cap, and filled with 250 mL mineral salt growth media (Appendix A.3). Butane was added by gaseous addition to each bottle to yield a 10% vol/vol in the headspace. The growth reactor was placed on a shaker table at 200 rpm in a 20°C constant temperature room. Pressures were equilibrated daily with pure oxygen or air. The butane mass and the optical density were monitored during the incubation. Figure 4.23 presents the growth curve of one of the batch reactors. The lag phase of the culture was around 4-5 days. The culture was harvested on day 7, at an OD_{600} of approximate 0.36. The liquids from all the bottles were combined and centrifuged to concentrate the biomass. The concentrated biomass was placed in 1 mL vials with 7%DMSO (Dimethyl Sulfoxide) and stored in –196 °C liquid nitrogen for future studies. The calculated yield was around 0.7 mg cell / mg butane, and the density of the frozen culture was 2500 mg TSS /L.

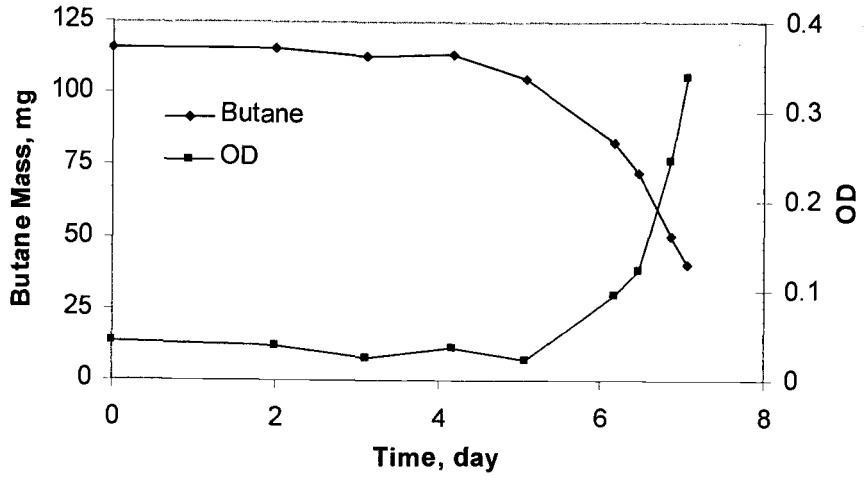

Figure 4.23 Growth curve of one of the batch reactors providing the culture for bioaugmentation study.

4.3 MICROCOSM STUDIES WITH FROZEN BUTANE-UTILIZING CULTURE

4.3.1 Transformation of chlorinated solvents

The objective of these experiments was to compare the 1,1,1-TCA transformation ability between indigenous microorganisms from Moffett test site and butane-utilizers bioaugmented to Moffett Field microcosms. The transformation of CAH mixtures of 1,1,1-TCA, TCE, and 1,1-DCE was also evaluated in bioaugmented microcosms. Microcosms were constructed in 125 mL media bottles sealed with grey butyl rubber lined caps. They were filled with 100 mL of Moffett groundwater and aquifer material. The conditions of the microcosms are shown in Table 4.7. A media-culture for bioaugmentation was obtained from a growth reactor inoculated with the frozen butane-utilizing culture. The enrichment was harvested from the batch growth reactor at the measured optical density (OD_{600}) of 0.25 and density of 120 mg TSS /L. The cells were not

washed before bioaugmentation. Successive additions of saturated 1,1,1-TCA solution were made to the microcosms stimulated on butane. The aqueous 1,1,1-TCA concentrations ranged from 350 to 1000 μg/L. In the CAH mixture study, 1,1,1-TCA (350 μg/L), TCE (440 μg/L), and 1,1-DCE (340 μg/L) were added to the bioaugmented microcosms.

Table 4.7 Microcosms used for the experiment of CAH transformation.

Microcosm	Contents	Substrate	CAHs	Description
BR2-C3	GW/Soil	Butane	1,1,1-TCA	Indigenous microcosm
BR2-2	GW/Soil	Butane	1,1,1-TCA, 1,1-DCE, TCE	Inoculated with 100 μl of media-culture
BR2-3	GW/Soil	Butane	1,1,1-TCA, 1,1-DCE, TCE	Inoculated with 500 μl of media-culture

Figure 4.24 presents the butane utilization and 1,1,1-TCA transformation achieved in non bioaugmented microcosm BR2-C3. No 1,1,1-TCA transformation was observed even after four additions of butane. With long-term exposure to 1,1,1-TCA, the rate of butane utilization slowed.

The butane utilization and 1,1,1-TCA transformation achieved in microcosm BR2-2 is presented in Figure 4.25. 1,1,1-TCA was added to the microcosm along with butane. Butane was consumed in 5 days, and 1,1,1-TCA transformation was then observed. On day 18, 1,1,1-TCA transformation ceased after 0.2 mg of 1,1,1-TCA was transformed. More butane was then added to enhance the transformation. On day 26 and 44, the successive additions of TCA were repeated. The total mass of TCA transformed was 0.36 and 0.25 mg, respectively. On day 28, after butane was consumed, 1,1,1-TCA transformation accelerated. This is most likely due to butane competitive inhibitory effect on

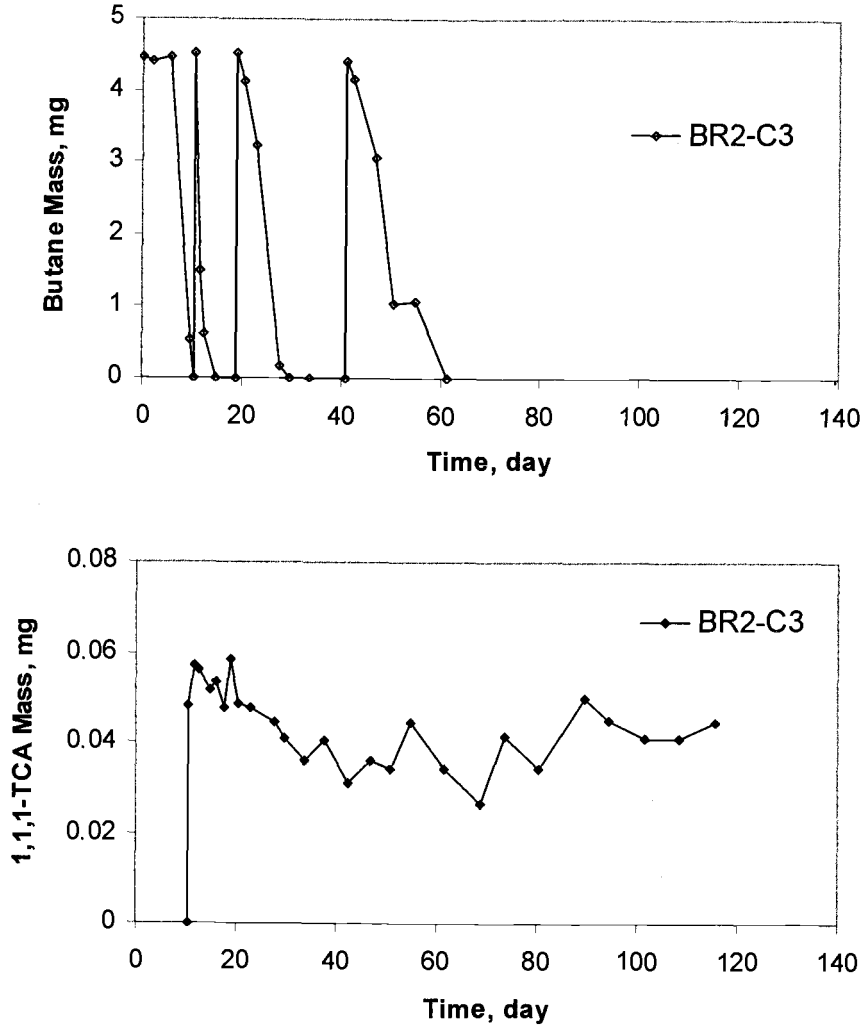

Figure 4.24 Butane utilization and 1,1,1-TCA transformation achieved in indigenous microcosm BR2-C3

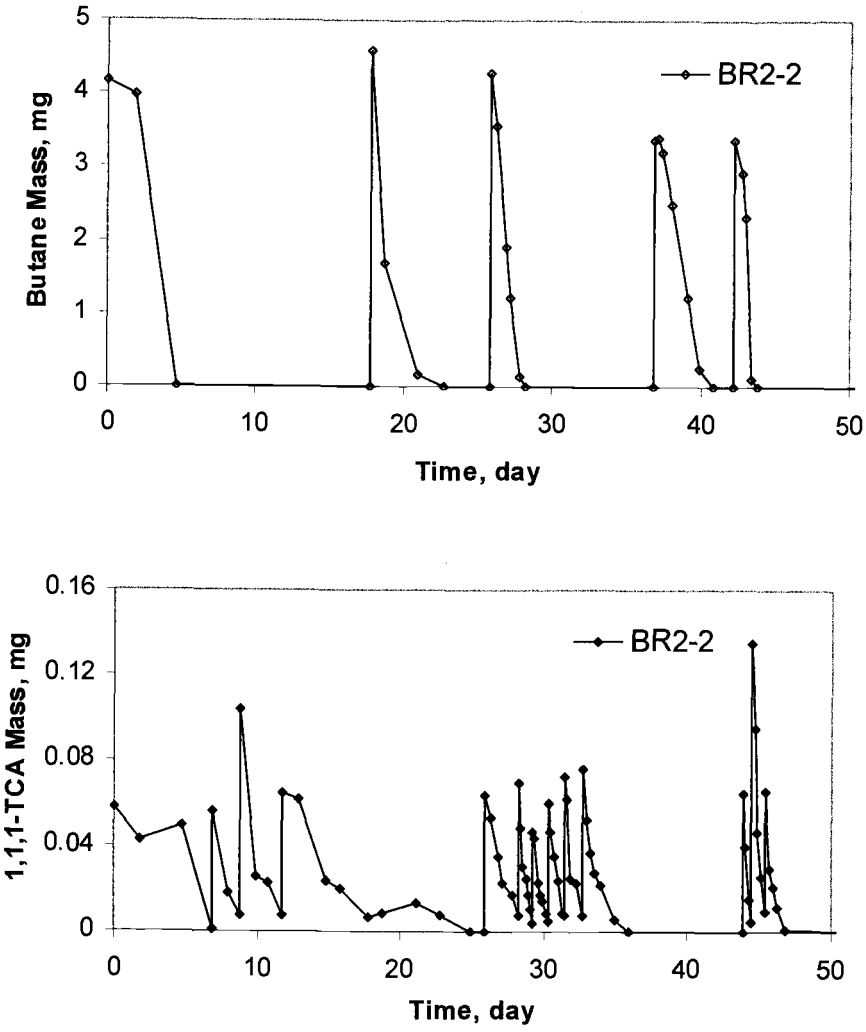

Figure 4.25 Butane utilization and 1,1,1-TCA transformation achieved in media-culture inoculated microcosm BR2-2

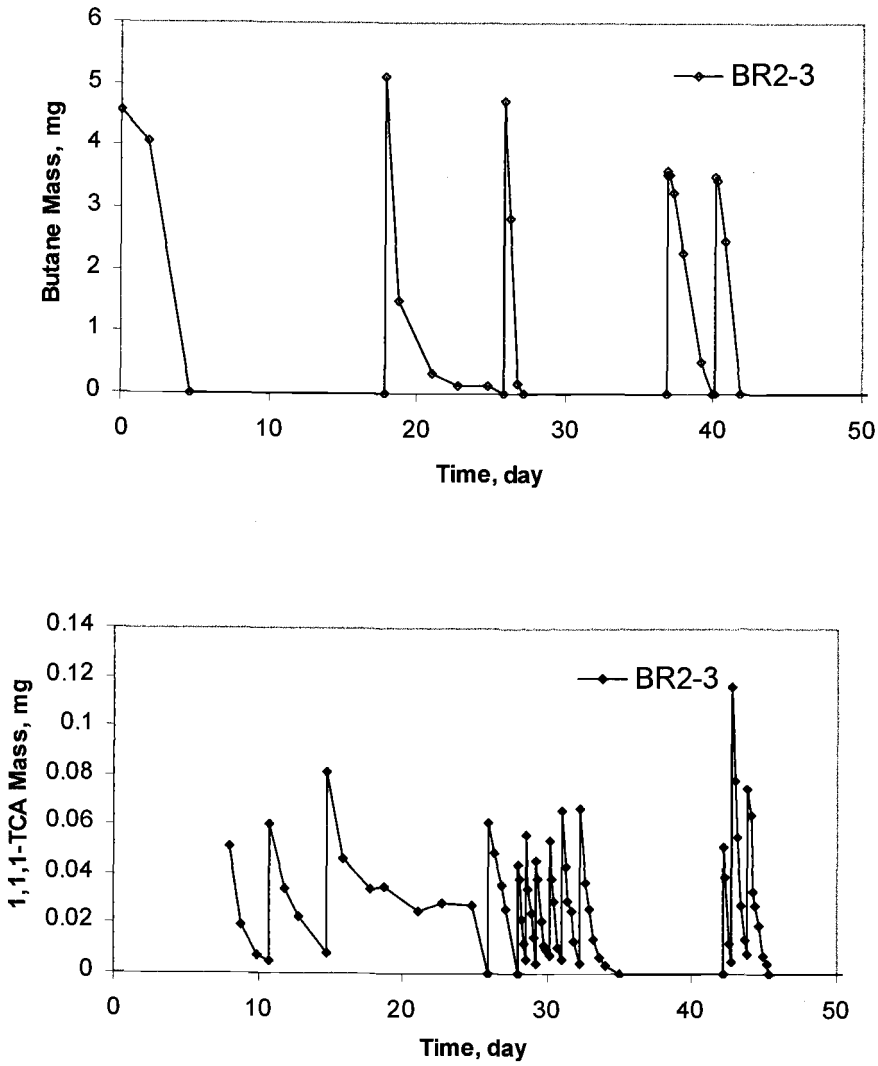

Figure 4.26 Butane utilization and 1,1,1-TCA transformation achieved in media-culture inoculated microcosm BR2-3

1,1,1-TCA transformation. The transformation rate decreased gradually with continued additions of 1,1,1-TCA. The butane utilization also slowed down around day 37 after continued 1,1,1-TCA.transformation.

Figure 4.26 presents the butane utilization and 1,1,1-TCA transformation achieved in microcosm BR2-3. Microcosm BR2-3 had the five times amount of inoculation as microcosm BR2-2. Unlike microcosm BR2-2, only butane was initially added to microcosm BR2-3, and it was consumed in 5 days, the same as microcosm BR2-2. After the butane was consumed, 1,1,1-TCA was added to the microcosm. Similar to microcosm BR2-2, 1,1,1-TCA transformation ceased on day 18. The mass of transformed 1,1,1-TCA was 0.15 mg. The re-addition of butane was conducted to enhance the transformation. The 1,1,1-TCA experiments were repeated day 26, and 42. The total mass of TCA transformed was 0.3 and 0.23 mg, respectively. After day 37, the butane uptake rate had slowed down. Similar to microcosm BR2-2, the competitive inhibition of 1,1,1-TCA transformation by butane and a decrease in transformation rate with continued addition of 1,1,1-TCA were also observed in microcosm BR2-3.

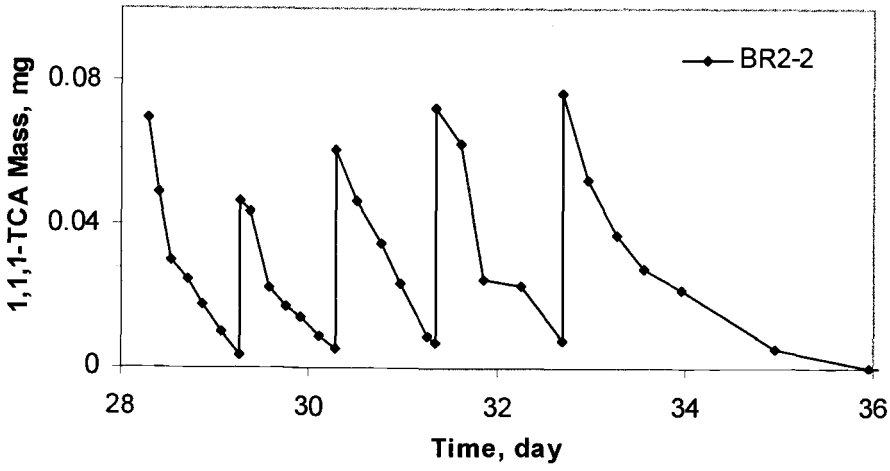

Figure 4.27 1,1,1-TCA transformation rate data for microcosm BR2-2 during day 28 - 37

a) The 1st addition of 1,1,1-TCA

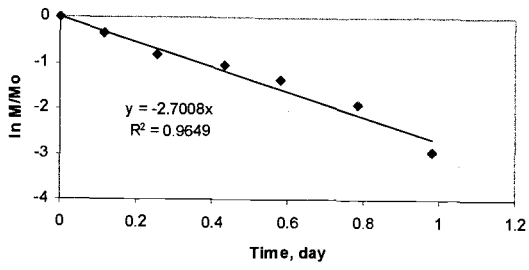

b) The 2nd addition of 1,1,1-TCA

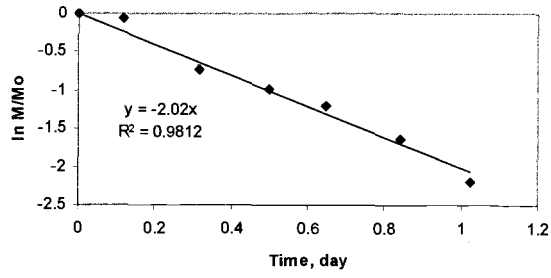

c) The 3rd addition of 1,1,1-TCA

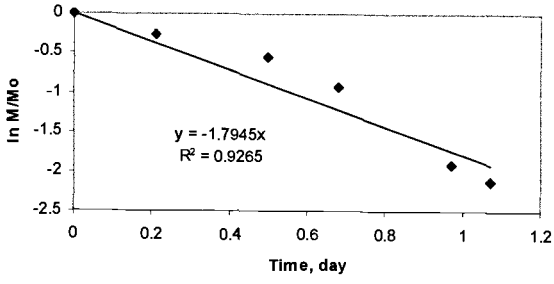

d) The 4th addition of 1,1,1-TCA

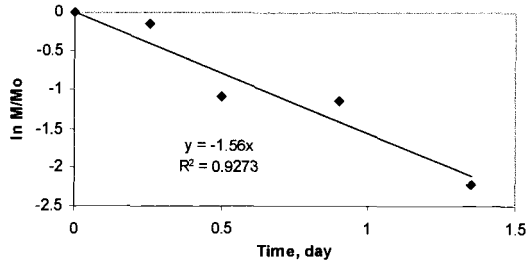

e) The 5th addition of 1,1,1-TCA

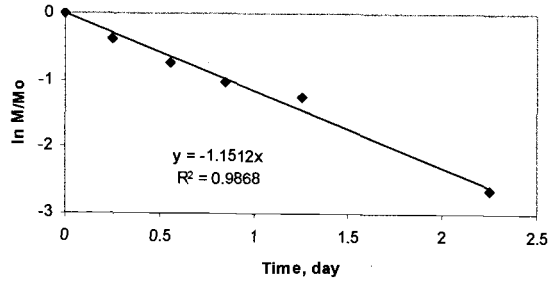

Figure 4.28 1,1,1-TCA transformation rate data for microcosm BR2-2 during day 28 - 37 plotted on a logarithmic scale

Figure 4.27 presents the experimental data during on day 28 to 37 for microcosm BR2-2. The gradual slowing in 1,1,1-TCA transformation rates can be seen. These data were plotted on a logarithmic scale to test for first-order transformation behavior, and to determine the pseudo-first-order rate coefficient (P) from the slope of regression line, as shown in Figure 4.28. The pseudo-first-order rate coefficient (P) is a combination term including kinetic parameters and biomass as illustrated in equation D.5. The values of this term (P) obtained from the rate tests in both microcosms are shown in appendix Tables G.7 and G.8.

The values of the pseudo-first-order rate coefficient (P) from each graph in Figure 4.28 are plotted against time, as shown in Figure 4.29. The values of pseudo first-order rate parameter ($k_{max}X_0/K_s$) and cell decay rate (b) were determined from the slope and the power of an exponential regression line, respectively. An example calculation is shown in Appendix D. A good fit to the exponential decay model was observed.

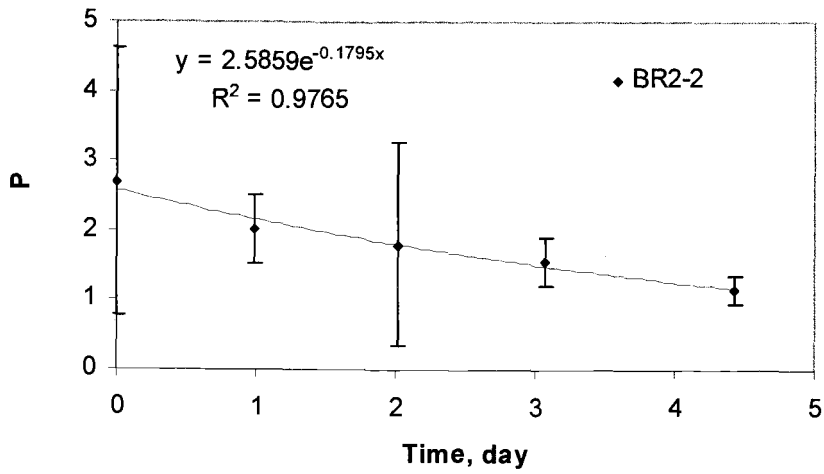

Figure 4.29 The decrease in pseudo-first-order rate coefficient (P) as a function of time during day 28 – 37.

The results from all microcosm rate tests are presented in Table 4.8. The pseudo first-order rate parameter ($k_{max}X_0/K_s$) for microcosm BR2-3 was slightly greater than that of BR2-2. The initial inoculated biomass of BR2-3 was five times greater than that of BR2-2. The result is consistent with the more rapid uptake of the third addition of butane. The cell decay rates (b) in both microcosms were similar to those in microcosms inoculated with either slurry or media-culture (Table 4.5). The similarities in 1,1,1-TCA transformation indicates the mixed cultures in the slurry survive growth in media and freezing at –196 °C.

Table 4.8 The pseudo-first-order rate parameter ($k_{max}X_0/K_s$) and cell decay rate (b) for the B2 and B4 microcosm sets during day 28 – 37.

Microcosm	Initial inoculum (mg/L)	$k_{max}X_0/K_s$ (day^{-1})	b (day^{-1})
BR2-2	0.12	3.4	0.18
BR2-3	0.6	4.3	0.16

Figure 4.30 presents the utilization of butane and transformation of chlorinated solvent mixtures of 1,1,1-TCA, TCE and 1,1-DCE achieved in microcosm BR2-2 after 52 days of incubation. On day 53, butane was added along with 1,1,1-TCA, TCE, and 1,1-DCE. Butane utilization occurred within 3 days. 1,1-DCE, and 1,1,1-TCA were transformed within 2 and 4 days, respectively. However, the TCE transformation ceased after 90% of the TCE was transformed. On day 58, the microcosm was purged under a laminar flow hood to remove TCE, and more butane was added to increase the amount of biomass. The experiment was repeated on day 60. Butane was consumed within 2 days. 1,1-DCE, 1,1,1-TCA and 70% of TCE were transformed within 13 hours, 3 days and 6 days, respectively. After 66 days of incubation, the utilization of butane and the transformation of chlorinated solvents slowed down. Butane utilization and 1,1-DCE transformation occurred within 4 days. 1,1,1-TCA and 87% of TCE was

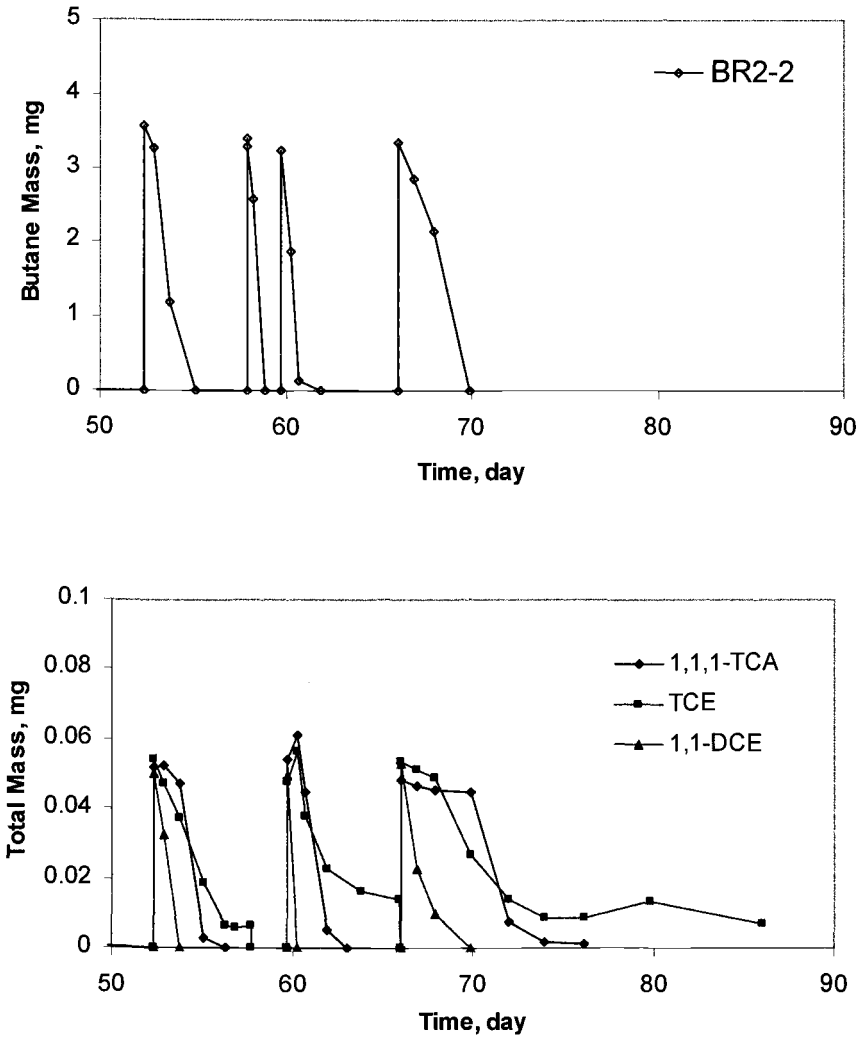

Figure 4.30 Butane utilization and chlorinated compound transformation achieved in the media-culture inoculated microcosm BR2-2.

transformed within 10 days. Inhibition of 1,1,1-TCA and TCE transformation by butane and 1,1-DCE was observed. The behavior of microcosm BR2-3 was similar, as shown in appendix Figure G.9.

The microcosms bioaugmented with the frozen butane-utilizing culture showed the same performance as the microcosms inoculated with slurry. Long-term transformation of 1,1,1-TCA in the absence of butane utilization was achieved at rapid rates. The transformation of a mixture of 1,1,1-TCA, 1,1-DCE and TCE also showed similar trends. The transformation rate of 1,1-DCE was the fastest, while the transformation rate of 1,1,1-TCA and TCE were slower. After transforming the mixture of these chlorinated solvents, the rates of butane utilization and chlorinated solvent transformation slowed down. This is probably due to the transformation product toxicity, especially that of 1,1-DCE.

4.3.2 Butane and 1,1,1-TCA kinetic experiments

Table 4.9 Microcosms used for the kinetic experiments

Microcosm	Contents	Substrate	CAHs	Description
BRC-1 to BRC5	GW/Soil	Butane	1,1,1-TCA	Indigenous microcosm
BR3-1 to BR3-5	GW/Soil	Butane	1,1,1-TCA	Inoculated with 500 µl of media-culture, and having initial biomass of 0.47 mg/L
BR4-1 to BR4-5	GW/Soil	Butane	1,1,1-TCA	Inoculated with 500 µl of media-culture, and having initial biomass of 0.45 mg/L
BR4-M	Growth media	Butane	1,1,1-TCA	Inoculated with 500 µl of media-culture, and having initial biomass of 0.45 mg/L

Studies were conducted over a range of butane and 1,1,1-TCA concentrations to determine the half-saturation constants (K_s) of indigenous and bioaugmented butane-utilizers under microcosm conditions. The microcosms constructed for this experiment are presented Table 4.9. The microcosm fabrication was the same as for the previous experiment. The bioaugmented cultures of the BR3 and BR4 microcosm sets, and microcosm BR4-M were obtained from reactors inoculated with the frozen butane-utilizing culture but at different times. These studies help demonstrate the reproducibility of the bioaugmentation process.

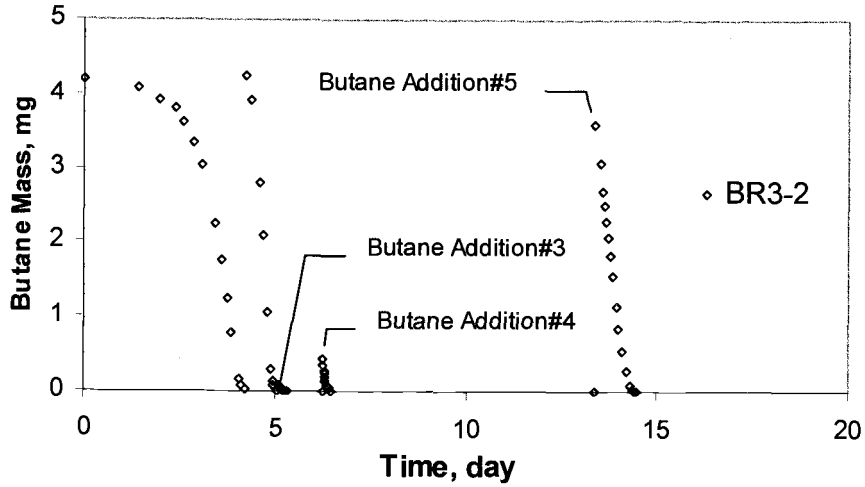

Figure 4.31 Overall results from the butane kinetic experiments conducted in the bioaugmented microcosm, BR3-2

Figure 4.31 presents the overall results from the butane kinetic experiments conducted in inoculated microcosm BR3-2. Two additions of butane (4 mg) were added to each microcosm to stimulate the microbial population. To determine a butane K_s value, a kinetic experiment was conducted on day 5, starting at an aqueous concentration of 40 μg/L. Butane utilization followed first-order kinetics

a) The third addition of butane

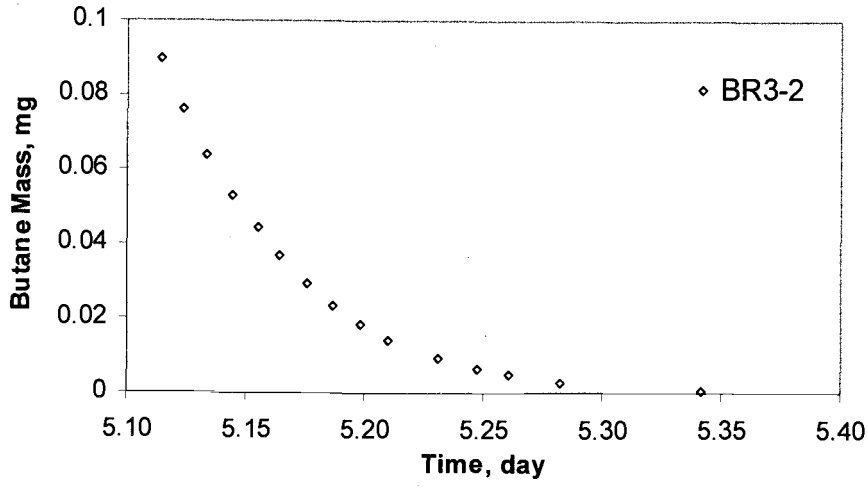

b) Butane utilization following first-order kinetics

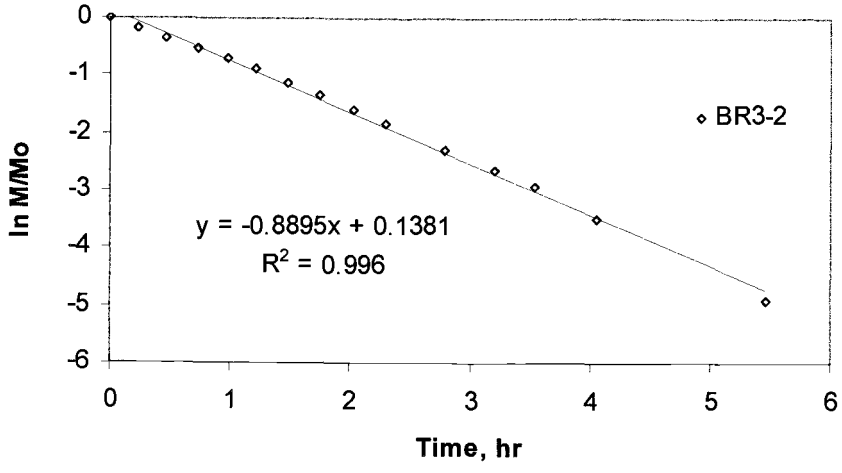

Figure 4.32 Experimental data from the butane kinetic experiment conducted in microcosm BR3-2 on day 5

a) The fourth addition of butane

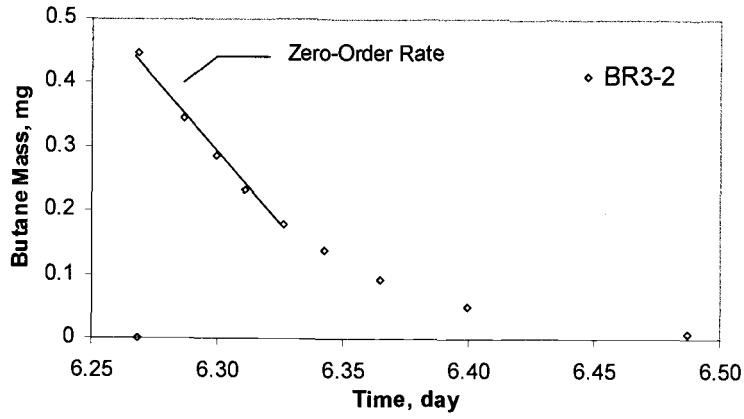

b) Initial butane utilization following zero-order kinetics

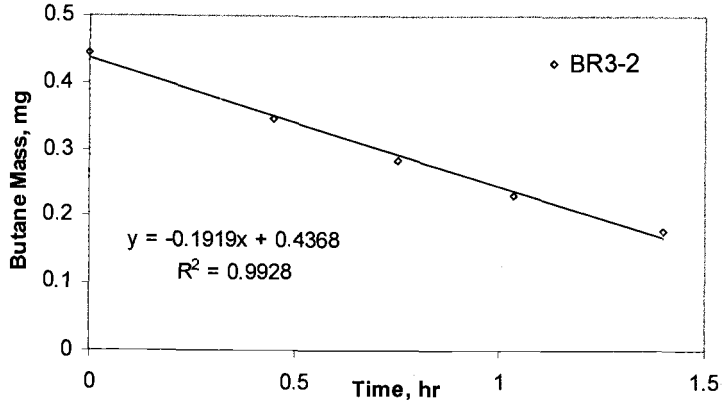

c) Butane utilization following first-order kinetics

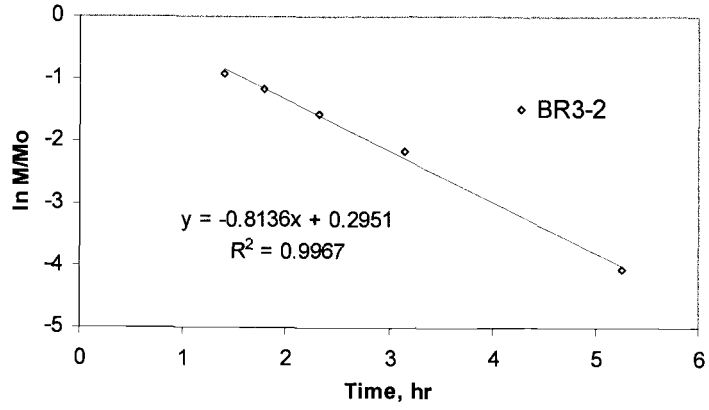

Figure 4.33 Experimental data from the butane kinetic experiment conducted in microcosm BR3-2 on day 6

a) The fifth addition of butane

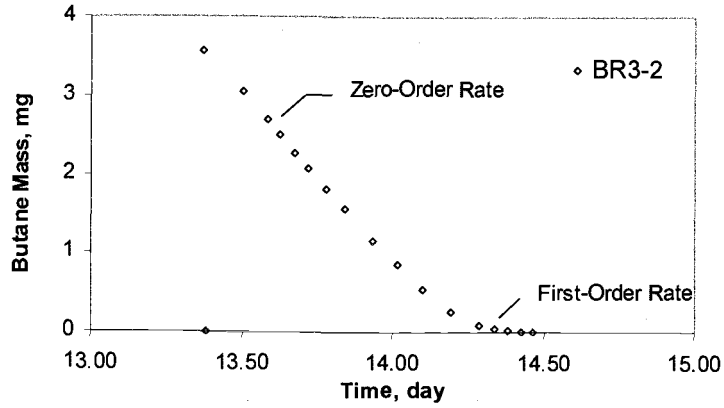

b) Initial butane utilization following zero-order kinetics

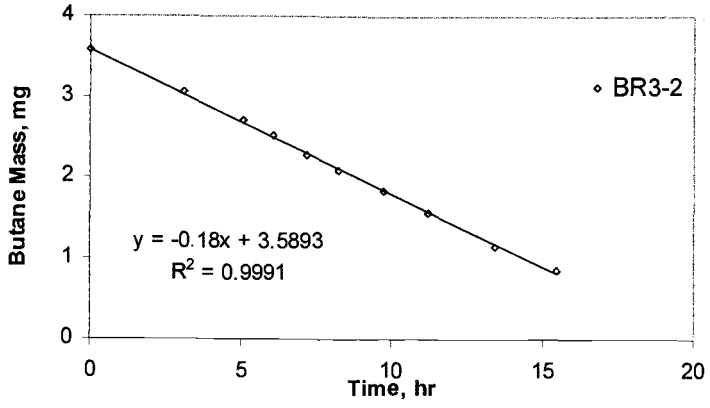

c) Butane utilization following first-order kinetics

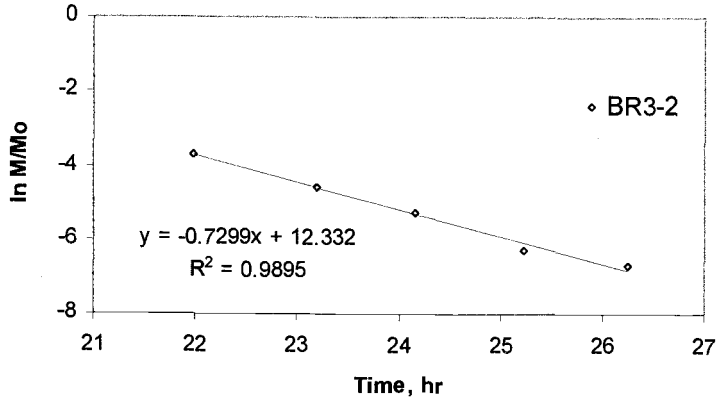

Figure 4.34 Experimental data from the butane kinetic experiment conducted in microcosm BR3-2 from day 13 to 14

as shown in Figure 4.32. Another kinetic experiment was then conducted on day 6 at a higher butane concentration (200 μg/L). As shown in Figure 4.33, the first five data points tend to follow zero-order kinetics and the remaining seem to follow first-order kinetics. On day 13, another kinetic test was performed at an aqueous concentration of 1800 μg/L. Butane transformation rates covered both zero-order and first-order ranges, as shown in Figure 4.34. All microcosms behaved similarly as shown in appendix Figures G.10 to G.13. As shown in appendix Table G.9, the butane K_s values of the BR3 microcosm set were determined from the results of the fourth and fifth additions of butane, following the procedure described in Appendix E. Table 4.10 presents the K_s values for butane and the initial aqueous concentration of butane. The K_s values obtained from both experiments were similar. The average value for the BR3 microcosm set is 0.11 ± 0.014 mg/L.

Table 4.10 Butane half-saturation constant (K_s) achieved in the BR3 microcosm set.

Microcosm	The 4th addition of butane		The 5th addition of butane	
	C_l (μg/L)	K_s (mg/L)	C_l (μg/L)	K_s (mg/L)
BR3-1	196	0.119	1514	0.077
BR3-2	196	0.104	1577	0.109
BR3-3	196	0.109	1711	0.102
BR3-4	193	0.11	1711	0.113
BR3-5	175	0.12	1709	0.132
Average		0.11 ± 0.007		0.11 ± 0.02

After the fifth addition of butane was completely consumed, a 1,1,1-TCA kinetic test was started on day 15. The 1,1,1-TCA kinetic experiments were conducted in a similar manner as the butane experiments. Figure 4.35 presents the overall results from the 1,1,1-TCA kinetic experiments conducted in microcosm BR3-2. 1,1,1-TCA transformation at an initial concentration of 100 μg/L followed

first-order kinetics, as shown in Figure 4.36. Thus the K_s value could not be determined from this 1,1,1-TCA addition. Another kinetic experiment was performed at a higher aqueous concentration. As shown in Figure 4.37, the transformation of 1,1,1-TCA at 700 μg/L followed zero-order kinetics initially, and then followed first-order kinetic after the 1,1,1-TCA was lower than 250 μg/L. This indicates that the K_s value is between 250 and 700 μg/L. Results from the other microcosms were similar, as shown in appendix Figures G.14 to G.17. The K_s values for 1,1,1-TCA achieved in the BR3 microcosm set are determined from the results of the second 1,1,1-TCA addition, as shown in appendix Table G.10. Table 4.11 presents the K_s values along with the initial aqueous concentration of 1,1,1-TCA. All microcosms had similar K_s values. The average K_s value is 0.37 ± 0.051 mg/L. The results show that the bioaugmentation process is very consistent.

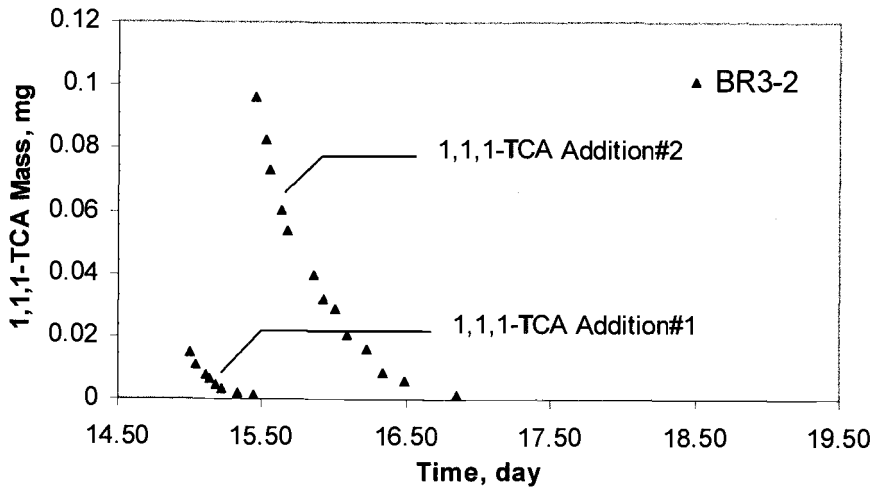

Figure 4.35 Overall results from the 1,1,1-TCA kinetic experiment conducted in bioaugmented microcosm, BR3-2

a) The first addition of 1,1,1-TCA

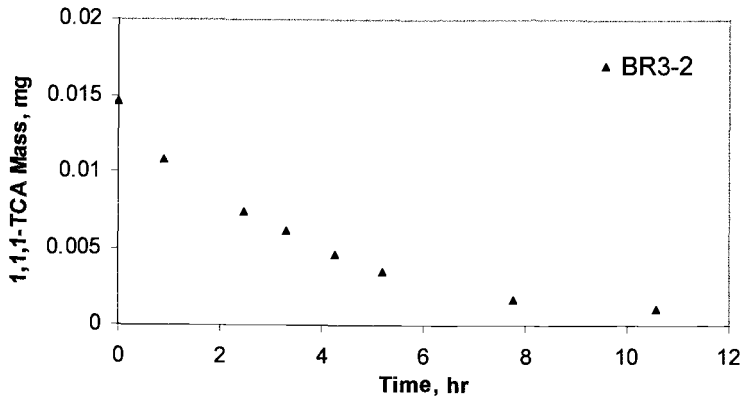

b) 1,1,1-TCA transformation following first-order kinetics

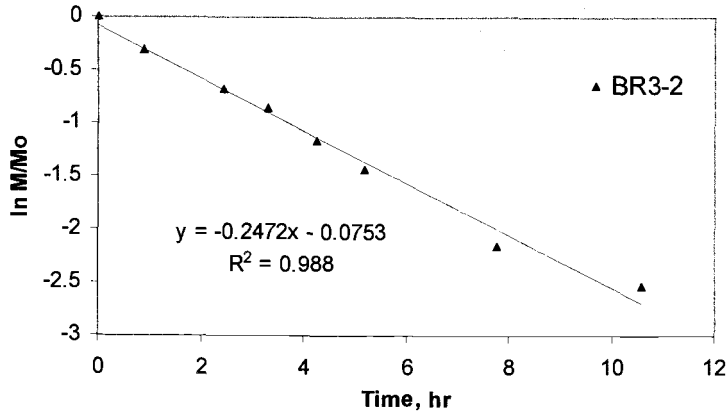

Figure 4.36 Experimental data from the 1,1,1-TCA kinetic experiment conducted in microcosm BR3-2 on day 15 .

a) The second addition of 1,1,1-TCA

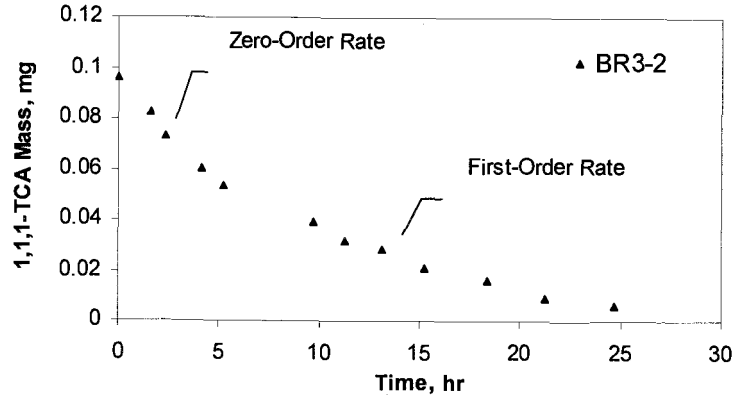

b) Initial 1,1,1-TCA transformation following zero-order kinetics

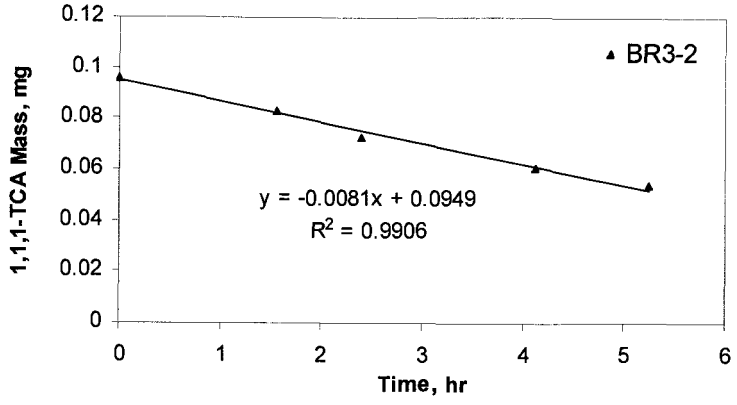

c) 1,1,1-TCA transformation following first-order kinetics

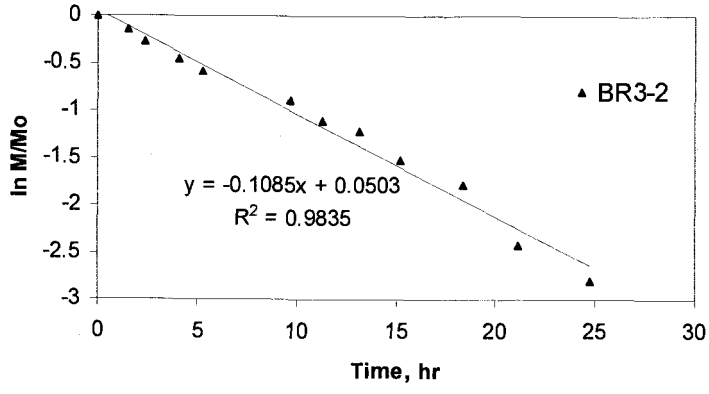

Figure 4.37 Experimental data from the 1,1,1-TCA kinetic experiment conducted in microcosm BR3-2 from day 15 to 16

Table 4.11 1,1,1-TCA half-saturation constant (K_s) achieved in the BR3 microcosm set.

Microcosm	The 2nd addition of 1,1,1-TCA	
	C_I (μg/L)	K_s (mg/L)
BR3-1	680	0.400
BR3-2	731	0.443
BR3-3	698	0.324
BR3-4	720	0.335
BR3-5	711	0.345
Average		0.37 ± 0.051

Kinetic experiments were also conducted in the BR4 microcosm set. The overall results from the kinetic experiments for both butane and 1,1,1-TCA in microcosm BR4-5 are presented in Figure 4.38. The first two additions of butane were performed to stimulate the microbial population. The butane kinetic experiments were conducted with the third and fifth additions of butane. As shown in Figure 4.39 and 4.40, the data from both experiments followed zero-order kinetics initially and then first-order kinetics. The initial concentration ranged from 230 to 330 μg/L. The results from the kinetic experiments in all microcosms were similar as shown in appendix Figures G.18 to G.22 and appendix Table G.11. Table 4.12 presents the K_s values for butane from the BR4 microcosm set and the initial concentrations of butane. The similar results from all microcosms indicate the reproducibility of bioaugmentation process. The average K_s value for the BR4 microcosm set is 0.11 ± 0.012 mg/L. Microcosm BR4-M, which contained growth media, had a slightly lower K_s value than the other microcosms.

After the third and fifth additions of butane were consumed, kinetic experiments with 1,1,1-TCA were performed on day 5 and 13. As shown in Figures 4.41 and 4.42, 1,1,1-TCA transformation at low concentrations followed first-order kinetics while transformation at high concentrations was approximated by zero-order kinetics. On day 5, after six data points were collected, 1,1,1-TCA in

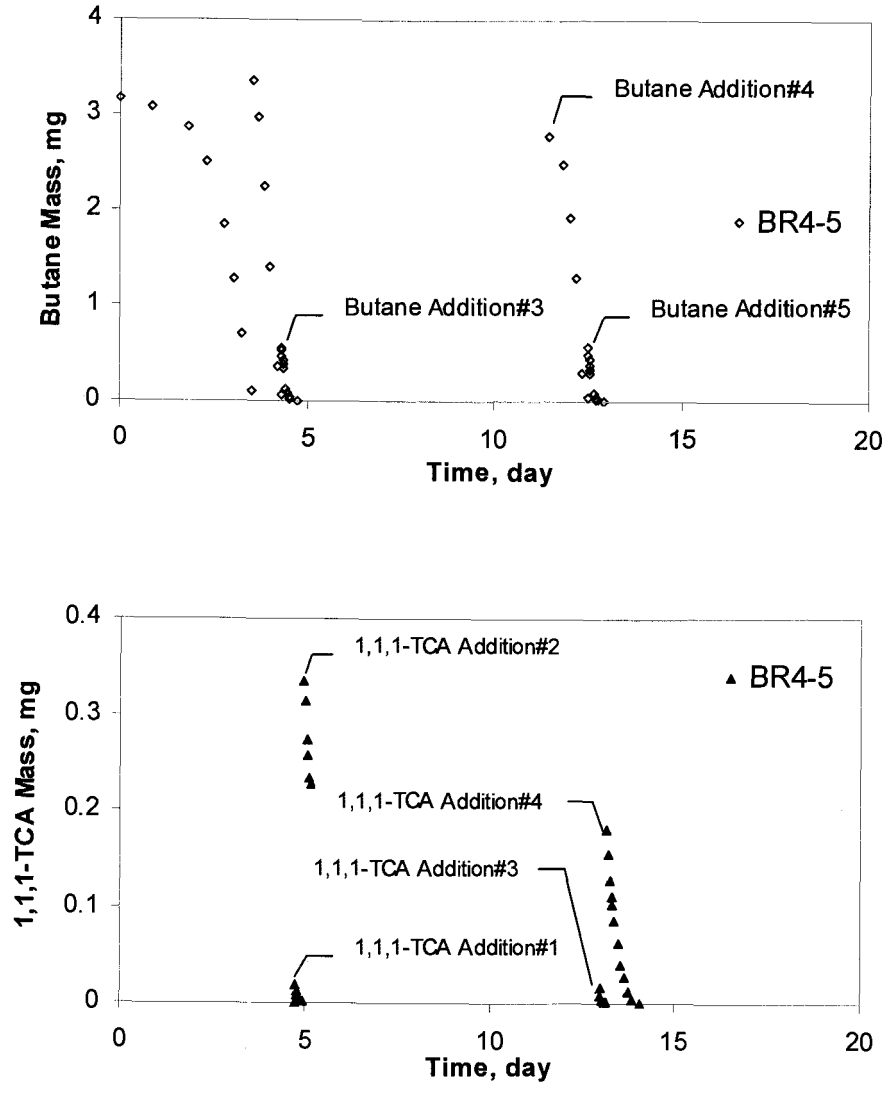

Figure 4.38 Overall results from the butane and 1,1,1-TCA kinetic experiments conducted in bioaugmented microcosm BR4-5

a) The third addition of butane

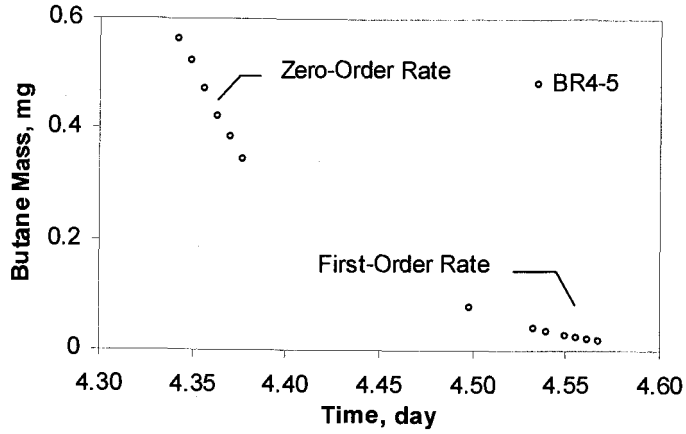

b) Initial butane utilization following zero-order kinetics

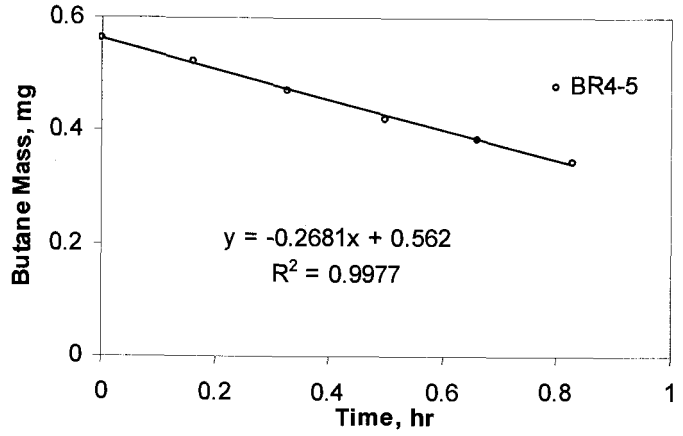

c) Butane utilization following first-order kinetics

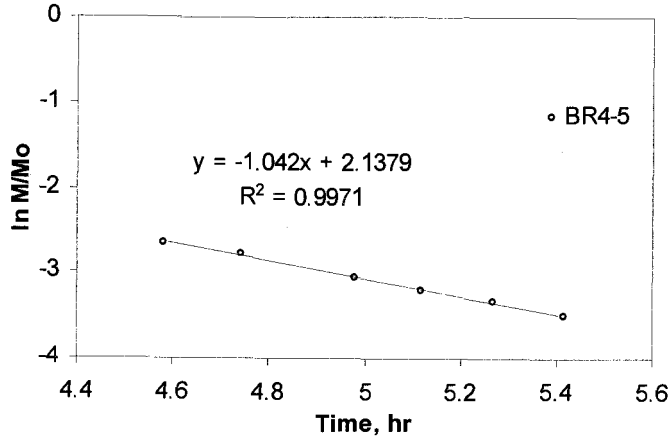

Figure 4.39 Experimental data from the butane kinetic experiment conducted in microcosm BR4-5 on day 4

a) The fifth addition of butane

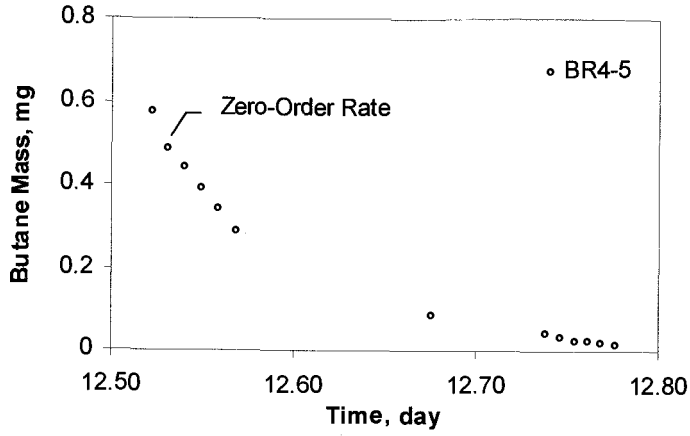

b) Initial butane utilization following zero-order kinetics

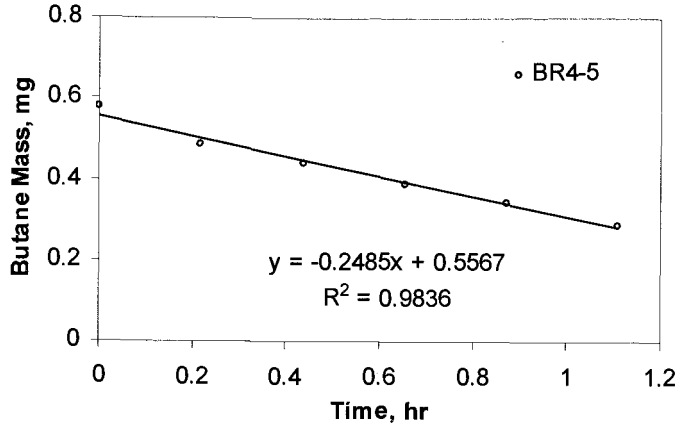

c) Butane utilization following first-order kinetics

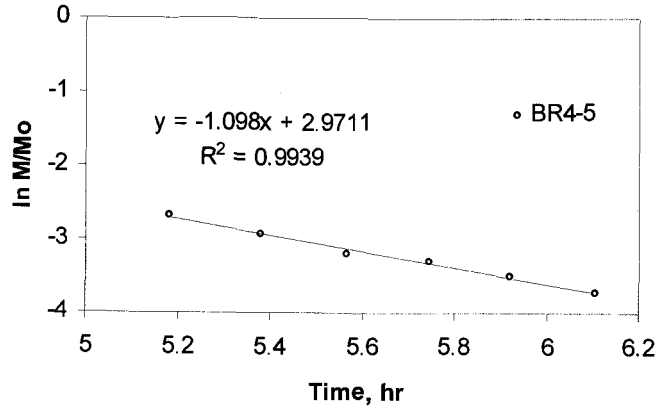

Figure 4.40 Experimental data from the butane kinetic experiment conducted in microcosm BR4-5 on day 13

the microcosms was purged. The results from the experiments in all microcosms were similar, as presented in appendix Table G.12. The 1,1,1-TCA K_s values obtained from the BR4 microcosm set are presented in Table 4.13. The average K_s value for the BR4 microcosm set is 0.35 ± 0.114 mg/L. Very reproducible bioaugmentation was achieved in all the microcosms.

Table 4.12 Butane half-saturation constant (K_s) achieved in the BR4 microcosm set.

Microcosm	The 3rd addition of butane		The 5th addition of butane	
	C_l (μg/L)	K_s (mg/L)	C_l (μg/L)	K_s (mg/L)
BR4-M	326	0.061	242	0.071
BR4-1	271	0.095	267	0.105
BR4-2	253	0.108	233	0.093
BR4-3	264	0.129	232	0.116
BR4-4	284	0.127	248	0.117
BR4-5	248	0.113	254	0.100
Average		0.12 ± 0.014		0.11 ± 0.01

Table 4.14 presents the average butane and 1,1,1-TCA K_s values achieved in the BR3 and BR4 microcosm sets and microcosm BR4-M. The microcosms were all bioaugmented with the same frozen culture, but from batches of cells grown at different time and with different frozen cells. They all had the similar K_s values for butane and 1,1,1-TCA. The results indicate a very reproducibility of the bioaugmentation process, using the procedures that were established.

a) The first and second additions of 1,1,1-TCA

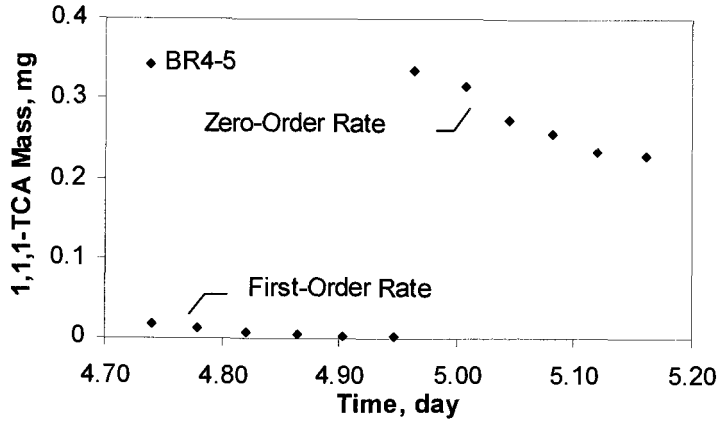

b) 1,1,1-TCA transformation following first-order kinetics

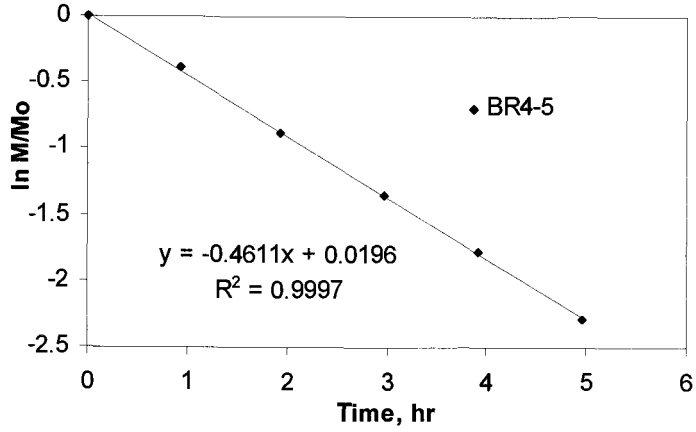

c) 1,1,1-TCA transformation following zero-order kinetics

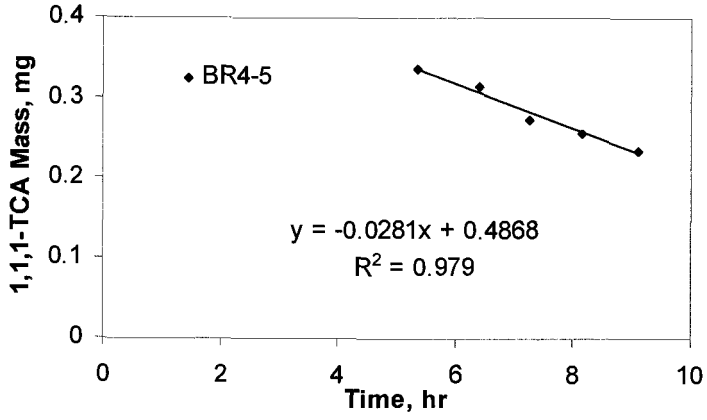

Figure 4.41 Experimental data from the 1,1,1-TCA kinetic experiment conducted in microcosm BR4-5 on day 5

a) The third and fourth additions of 1,1,1-TCA

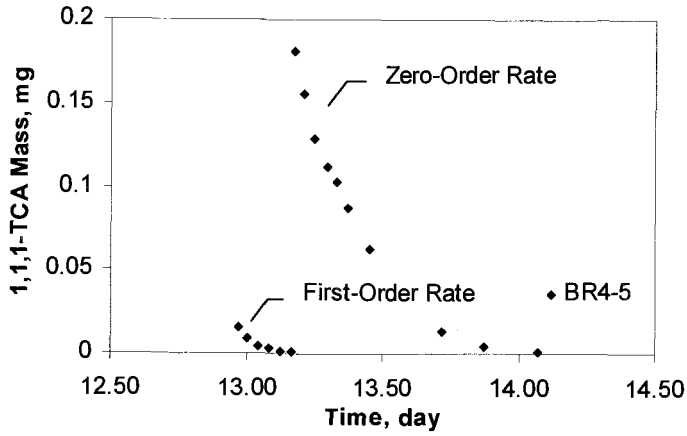

b) 1,1,1-TCA transformation following first-order kinetics

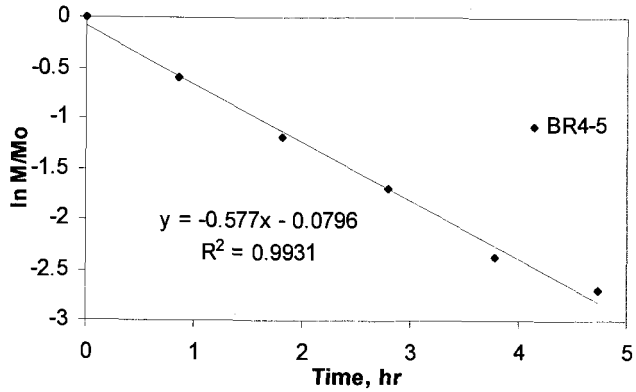

c) 1,1,1-TCA transformation following zero-order kinetics

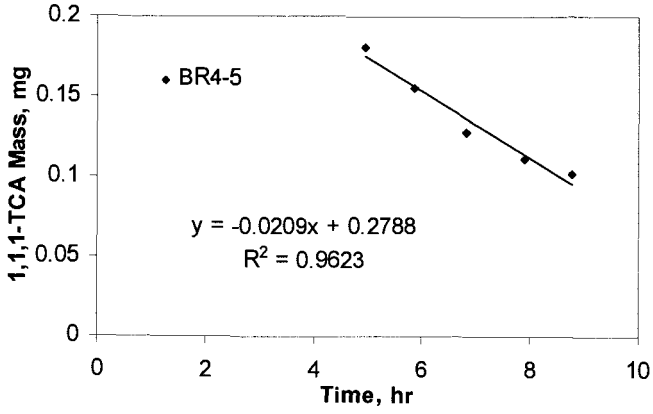

Figure 4.42 Experimental data from the 1,1,1-TCA kinetic experiment conducted in microcosm BR4-5 from day 13 to 14

Table 4.13 1,1,1-TCA half-saturation constant (K_s) achieved in the BR4 microcosm set.

a) The first and second additions of 1,1,1-TCA

Microcosm	Low C_l (μg/L)	High C_l (μg/L)	K_s (mg/L)
BR4-M	112	2394	0.306
BR4-1	110	2633	0.519
BR4-2	154	2615	0.480
BR4-3	120	2399	0.259
BR4-4	136	2543	0.464
BR4-5	139	2557	0.427
Average			0.430 ± 0.101

b) The third and fourth additions of 1,1,1-TCA

Microcosm	Low C_l (μg/L)	High C_l (μg/L)	K_s (mg/L)
BR4-M	89	1386	0.206
BR4-1	88	1663	0.365
BR4-2	102	1297	0.263
BR4-3	106	1326	0.186
BR4-4	58	1467	0.289
BR4-5	121	1381	0.276
Average			0.28 ± 0.064

Table 4.14 Average values of butane and 1,1,1-TCA half-saturation constant achieved in all microcosms

Microcosm	Butane K_s (mg/L)	1,1,1-TCA K_s (mg/L)
BR3 set	0.11 ± 0.014	0.37 ± 0.051
BR4 set	0.11 ± 0.012	0.35 ± 0114
BR4-M	0.07 ± 0.007	0.26 ± 0.07

4.3.3 Model development

Kinetic parameters including the maximum specific rate of butane utilization ($k_{max,But}$) and 1,1,1-TCA transformation ($k_{max,TCA}$), cell decay rate (b), and/or transformation capacity (T_c) for non-augmented and bioaugmented microcosms for microcosm test were determined through simulations of butane utilization and 1,1,1-TCA transformation, using the non-steady-state model described in Chapter 3. The results of microcosm studies in the BR3, BR4 and B4 bioaugmented microcosm sets and the BRC indigenous microcosm set were selected to conduct these simulations (Table 4.3 and 4.9).

Table 4.15 Measured parameters for model development

Parameter	Microcosm			
	BR3 set	BR4 set	B4 set	BRC set
X_0, mg/L	0.47	0.45	unknown	unknown
Y, mg/mg	0.7	0.7	0.7	0.7
$K_{s,But}$, mg/L	0.11	0.11	0.11	0.11
$K_{s,TCA}$, mg/L	0.37	0.37	0.37	0.37
V_L, L	0.1	0.1	0.075	0.1
V_g, L	0.057	0.057	0.082	0.057
$H_{cc,But}$, mg-L/mg-L	38.05	38.05	38.05	38.05
$H_{cc,TCA}$, mg-L/mg-L	0.55	0.55	0.55	0.55

To run the model, all the parameters in equations 3.1, 3.2, and 3.3 or 3.4 need to be supplied. Measured parameters including initial biomass (X_0) in the bioaugmented microcosms, the mass of butane and 1,1,1-TCA added, butane and 1,1,1-TCA half-saturation constants ($K_{s,But}$ and $K_{s,TCA}$), cellular yield (Y), volume in liquid and gas phases (V_L and V_g), and Henry partition coefficient for butane and 1,1,1-TCA ($H_{cc,But}$ and $H_{cc,TCA}$) were not varied in the fitting proceed. These values are presented in Table 4.15. The values of $K_{s,But}$ and $K_{s,TCA}$ were obtained from the kinetic experiments previously described, while the value of Y was determined from growth studies with the frozen butane-utilizing culture. The unknown

parameter values for the maximum specific rate of butane utilization ($k_{max,But}$) and 1,1,1-TCA transformation ($k_{max,TCA}$), cell decay rate (b), and/or transformation capacity (T_c) were varied in a heuristic approach to obtain a good fit between model predictions and experimental observations. The errors of unknown parameters were expressed in terms of standard deviation based on modeling of the five replicate microcosms. Equations 3.1, 3.2, 3.3 and 3.4 were solved in STELLA®. Numerical integration in time was performed in STELLA® using a fourth-order Runge-Kutta method.

4.3.3.1 The simulation of butane utilization and 1,1,1-TCA transformation in the BR3 microcosm set

Figure 4.43 presents the butane utilization data from microcosm BR3-5 and model simulations. The data was divided into 4 sections (A, B, C, and D). The A section presented the data from the first and second additions of butane, while the B, C, and D sections included the data from the third, fourth, and fifth additions of butane, respectively. The values of $k_{max,But}$ and b were varied to obtain a good fit between model predictions and experimental data shown in section A. The data of the other sections were then modeled using these values, once they were fixed.

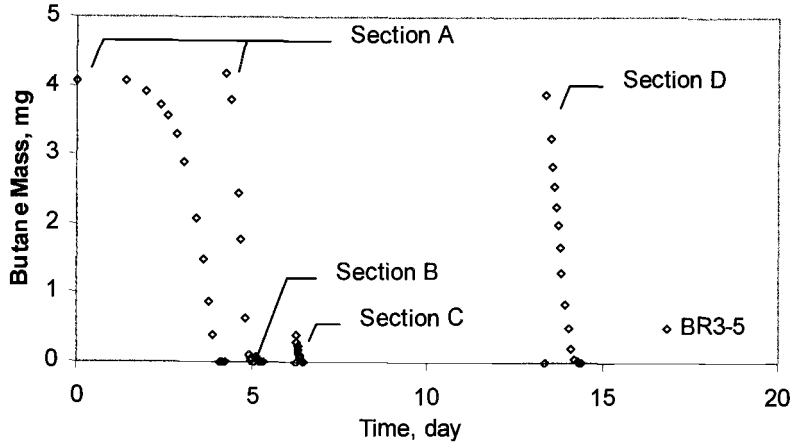

Figure 4.43 Butane utilization data from microcosm BR3-5

Complete simulation of butane utilization for microcosm BR3-5

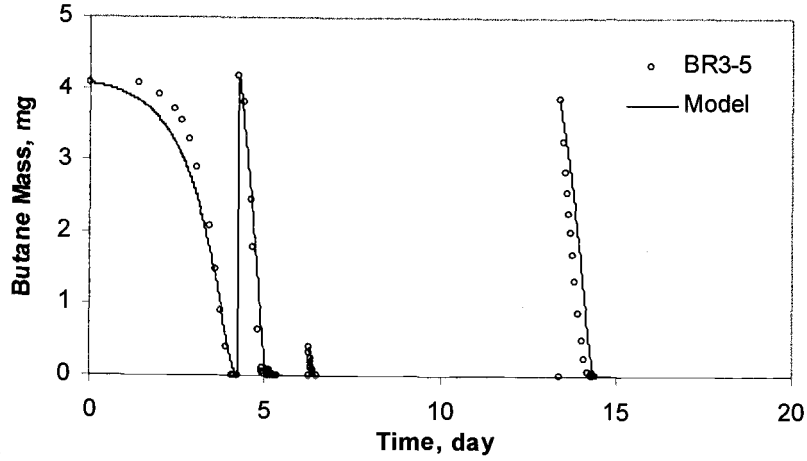

Section A: The first and second additions of butane from day 0 to 5

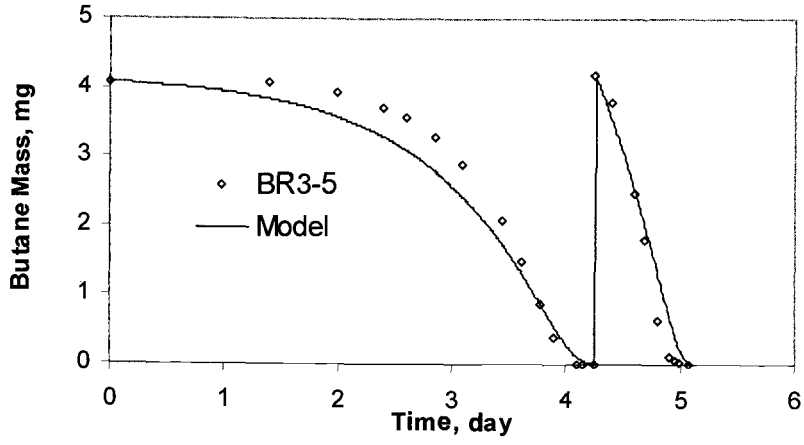

Section B: The third addition of butane on day 5

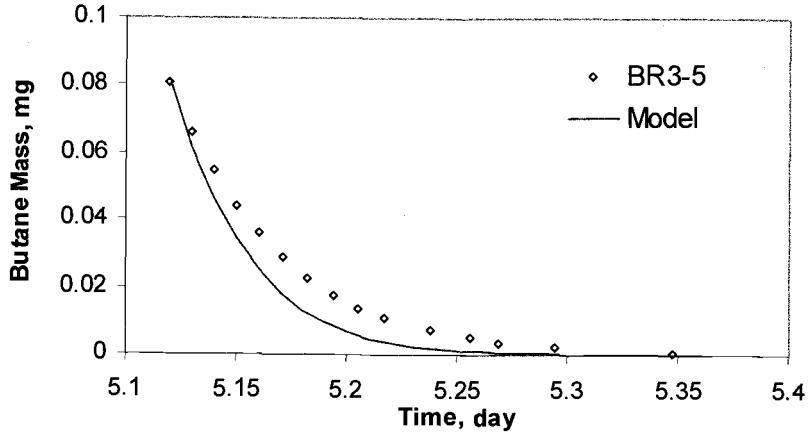

Figure 4.44 Simulation of butane utilization for microcosm BR3-5

Section C: The fourth addition of butane on day 6

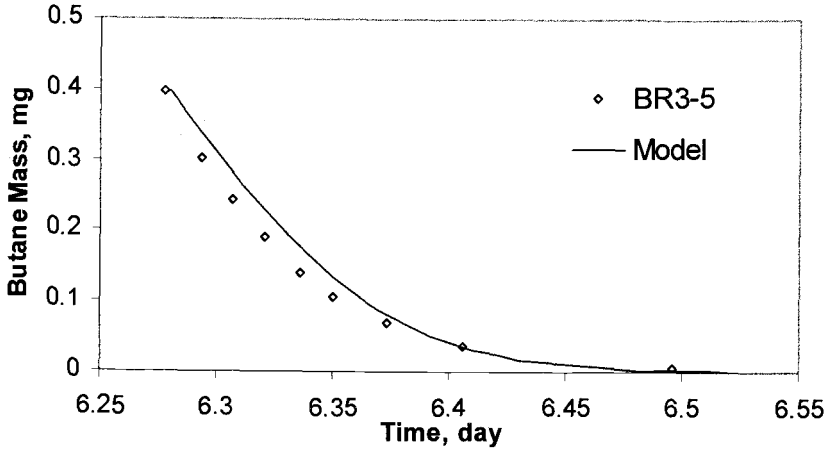

Section D: The fifth addition of butane from day 13.38 to 14.44

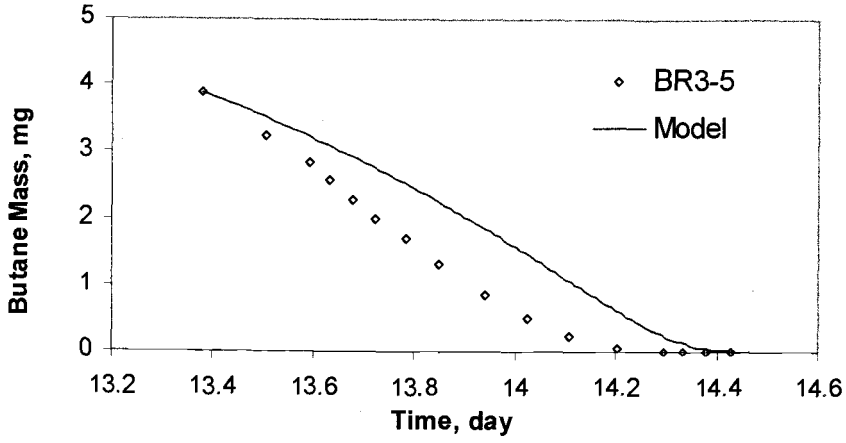

Figure 4.44, Continued

The simulation of butane utilization for microcosm BR3-5 is presented in Figure 4.44. The model fit data well at low concentration as well as high concentration. The initial concentration ranged from 35 to 1800 μg/L. The $K_{s,But}$ values obtained from the kinetic experiments provided good matches of the simulation to the microcosm results, as presented in section C. The model started deviating from the experimental data in section D. This probably results from fitting cell decay rate (b) with only early time data. Thus the value of cell decay rate (b) may have been in error by a small amount. The results from the model simulation for the other microcosms were similar, as presented in Figure 4.48 to 4.51. The values for the butane maximum specific rate ($k_{max,But}$) and cell decay rate (b) of the BR3 bioaugmented microcosm set are shown in Table 4.16. Both values obtained from all microcosms were similar. This indicates the reproducibility of the bioaugmentation process. The average values for the butane maximum specific utilization rate ($k_{max,But}$) and cell decay rate (b) were 1.76 ± 0.023 mg/mg-day and 0.15 ± 0.006 day^{-1}, respectively.

Table 4.16 Butane maximum specific rate ($k_{max,But}$) and cell decay rate (b) achieved in the BR3 microcosm set.

Microcosm	$k_{max,But}$ (mg/mg-day)	b (day^{-1})
BR3-1	1.79	0.15
BR3-2	1.74	0.15
BR3-3	1.76	0.15
BR3-4	1.73	0.14
BR3-5	1.76	0.14
Average	1.76 ± 0.023	0.15 ± 0.006

The 1,1,1-TCA transformation data from microcosm BR3-5 presented in Figure 4.45 was also simulated. To simplify the modeling, the effect of transformation product toxicity was not considered. Similar to butane utilization

modeling, the data were divided into 2 sections (E and F). The E and F sections presented the data from the first and second additions of 1,1,1-TCA. All parameters previously determined for butane were used in the simulation. The only unknown parameter was $k_{max,TCA}$. The variation of $k_{max,TCA}$ values was performed until the model best fit the data in section E. This value was then used to model in section F.

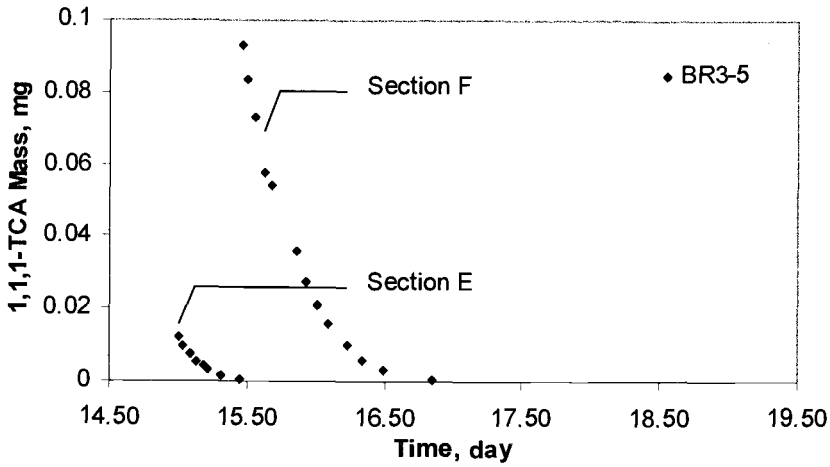

Figure 4.45 1,1,1-TCA transformation data from microcosm BR3-5

Figure 4.46 presents the simulation of 1,1,1-TCA transformation for microcosm BR3-5. A good fit between the model simulation and data is achieved in both sections of low and high concentrations. The initial concentration of data ranged from 90 to 750 μg/L. The 1,1,1-TCA maximum specific rate ($k_{max,TCA}$) values for microcosm set BR3 are shown in Table 4.17. All microcosms had similar values, except microcosm BR3-1, which had the lowest 1,1,1-TCA k_{max}. The $k_{max,TCA}$ values of microcosm set BR3 varied more than the $k_{max,But}$ values. The value of 1,1,1-TCA maximum specific rate ($k_{max,TCA}$) ranged from 0.05 to 0.12 mg/mg-day.

Complete simulation of 1,1,1-TCA transformation for microcosm BR3-5

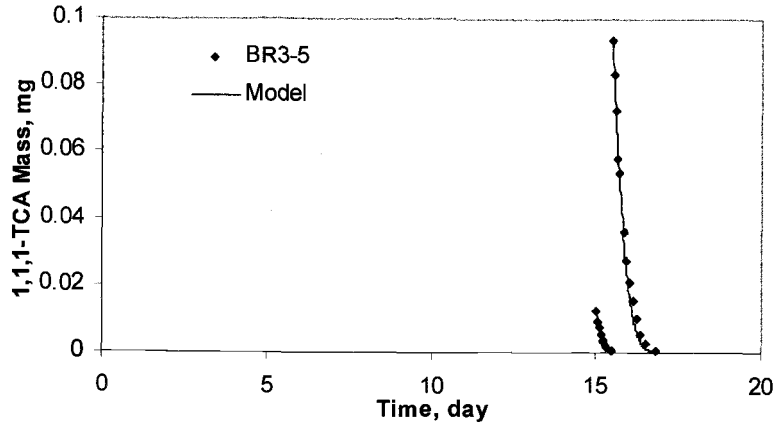

Section E: The first addition of 1,1,1-TCA on day 15

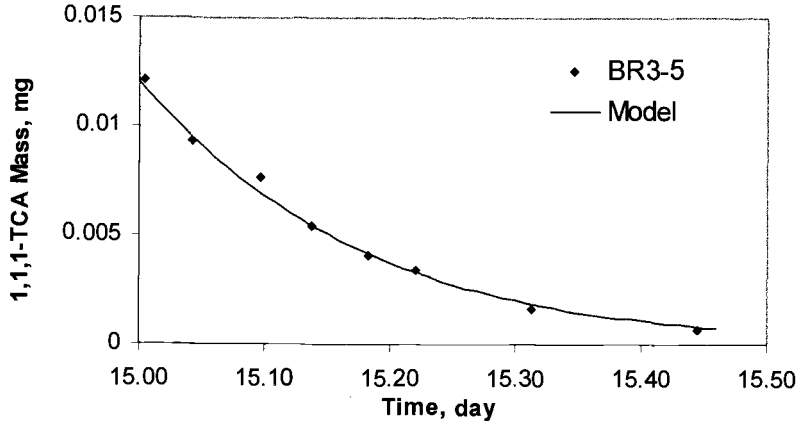

Section F: The second addition of 1,1,1-TCA from day 15 to 16

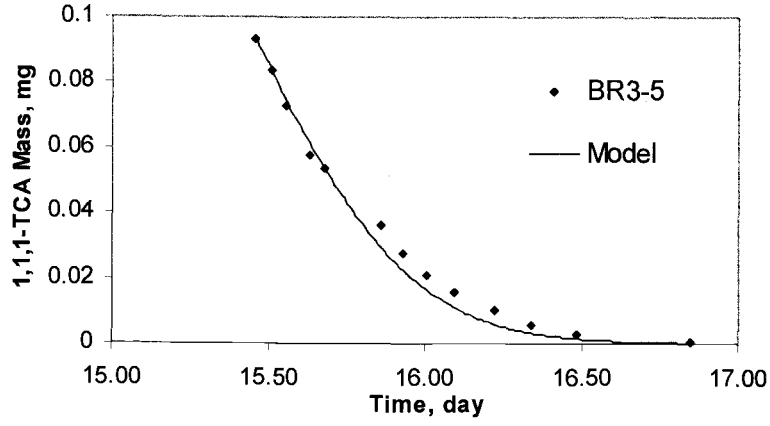

Figure 4.46 Simulation of 1,1,1-TCA transformation for microcosm BR3-5

Table 4.17 1,1,1-TCA maximum specific rate ($k_{max,TCA}$) achieved in the BR3 microcosm set.

Microcosm	$k_{max,TCA}$ (mg/mg-day)
BR3-1	0.05
BR3-2	0.12
BR3-3	0.11
BR3-4	0.09
BR3-5	0.09
Average	0.09 ± 0.027

The simulations of butane utilization and 1,1,1-TCA transformation for microcosms BR3-1 to BR3-5 are presented in Figure 4.47 to 4.51. A good fit between model simulation and data at both low and high concentrations was achieved in all microcosms. The deviation of model from the data occurred at late time. This is probably due to the error is the cell decay rate (b) that were obtained from fitting the data at early time. However, the reasonable fit between the model and experimental data from all microcosms was still obtained. This supports the model assumption that the effect of product transformation toxicity was negligible, and the enzyme for 1,1,1-TCA transformation remained active for long time periods.

Simulations of 1,1,1-TCA transformation were also conducted to determine if inclusion of transformation capacity value (T_c) improved results. Instead of equation 3.3, equation 3.4 was used to include the effect of a transformation product toxicity in terms of a transformation capacity (T_c). The other values of parameter values in equation 3.4 were maintained constant from the previous model simulation. Values of T_c were varied to see if better fits were obtained.

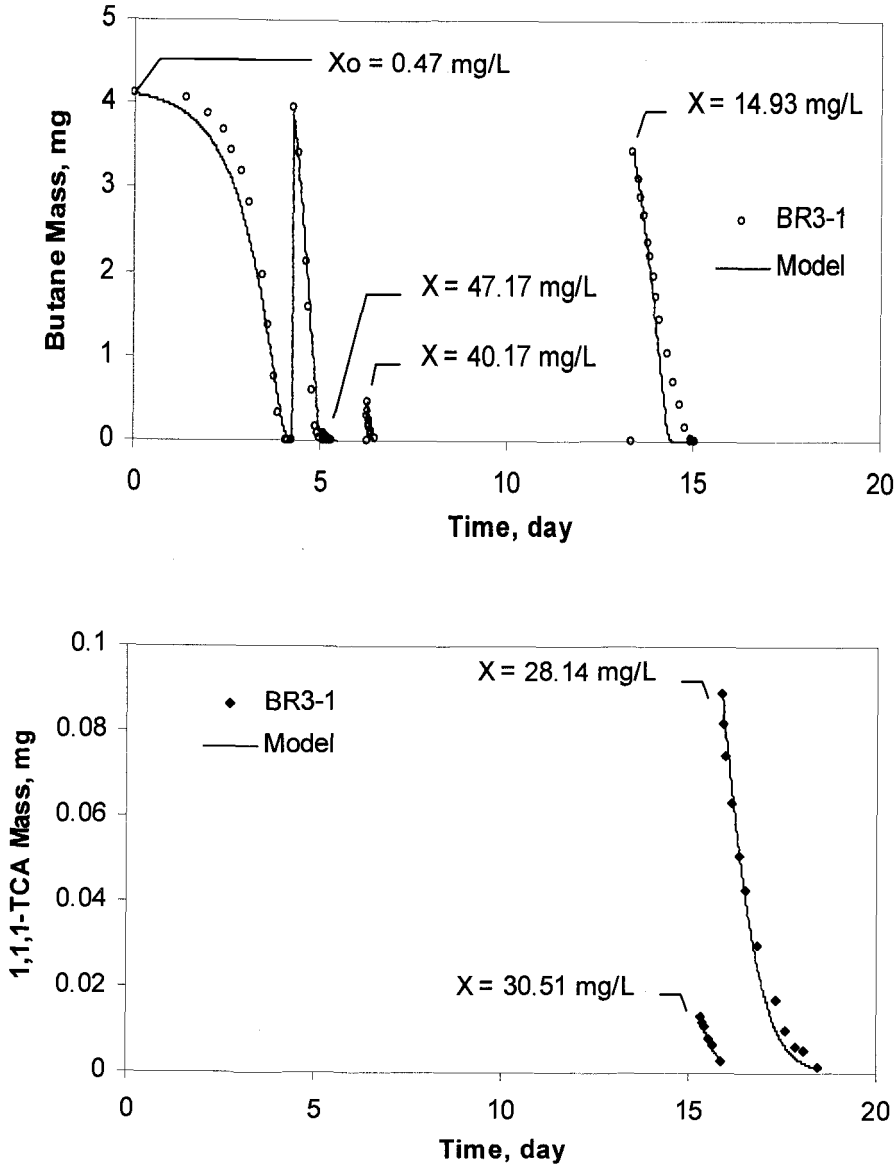

Figure 4.47 Simulations of butane utilization and 1,1,1-TCA transformation for microcosm BR3-1 without the term for transformation capacity

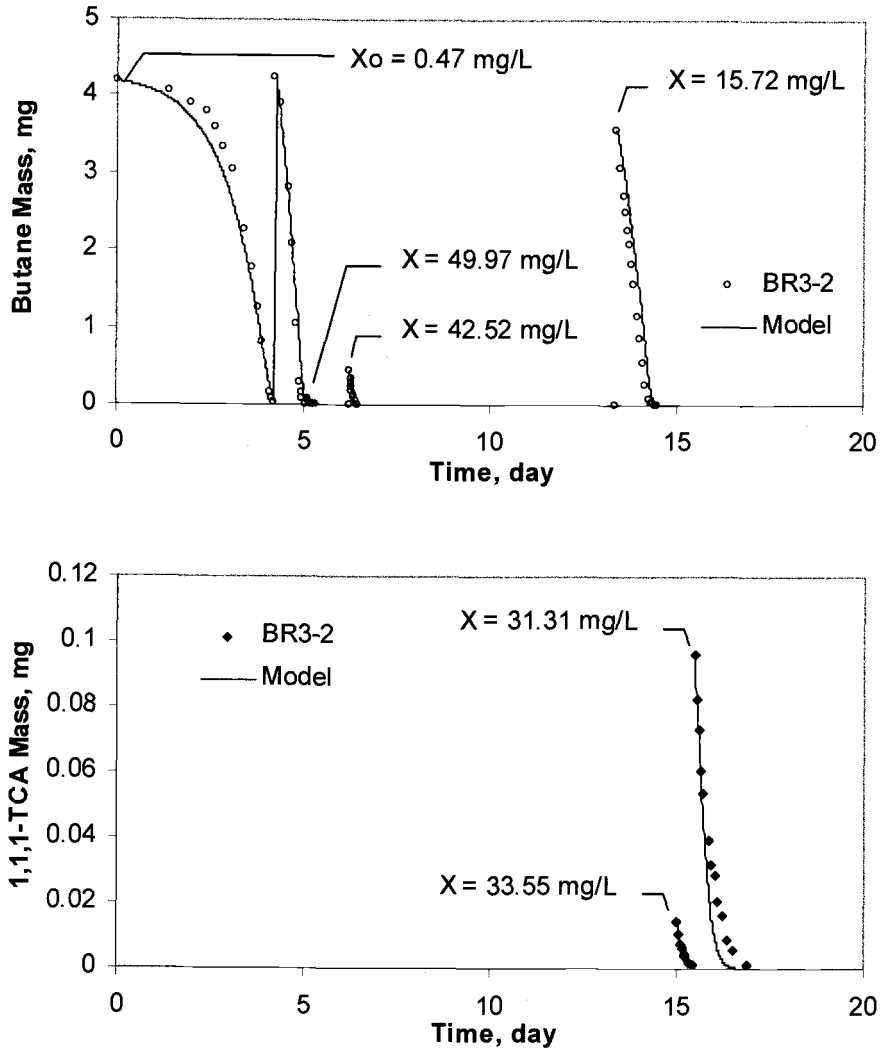

Figure 4.48 Simulations of butane utilization and 1,1,1-TCA transformation for microcosm BR3-2 without the term for transformation capacity

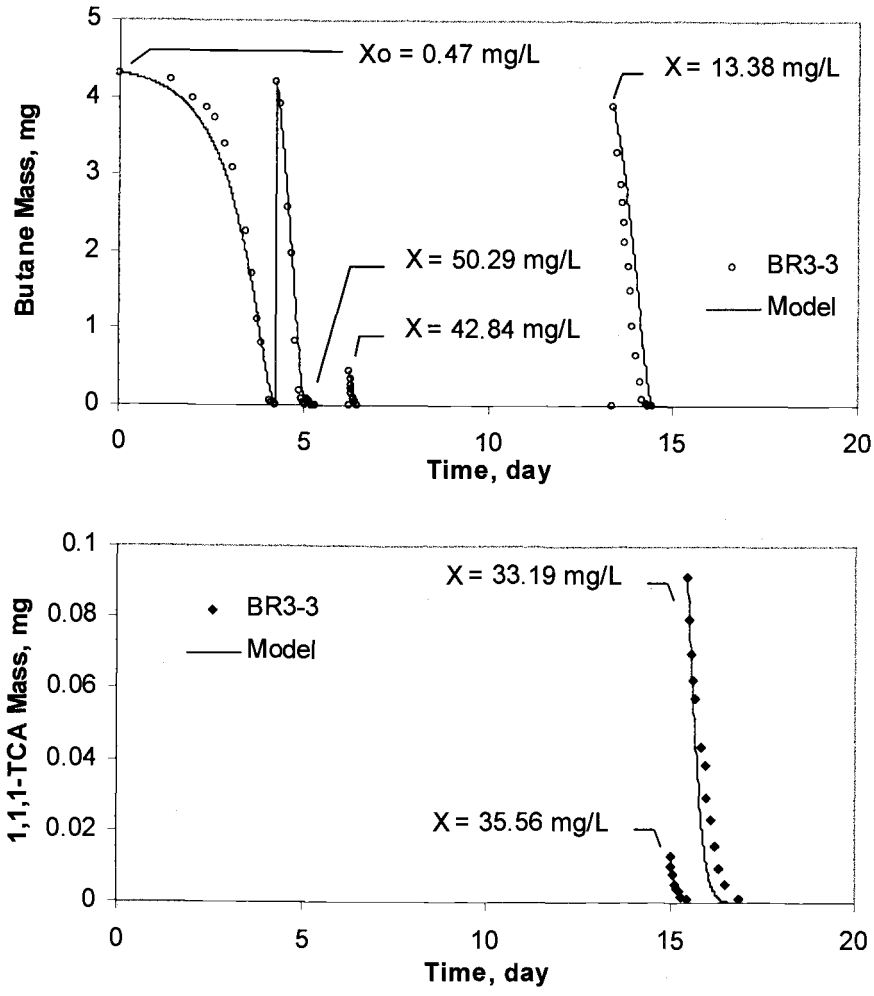

Figure 4.49 Simulations of butane utilization and 1,1,1-TCA transformation for microcosm BR3-3 without the term for transformation capacity

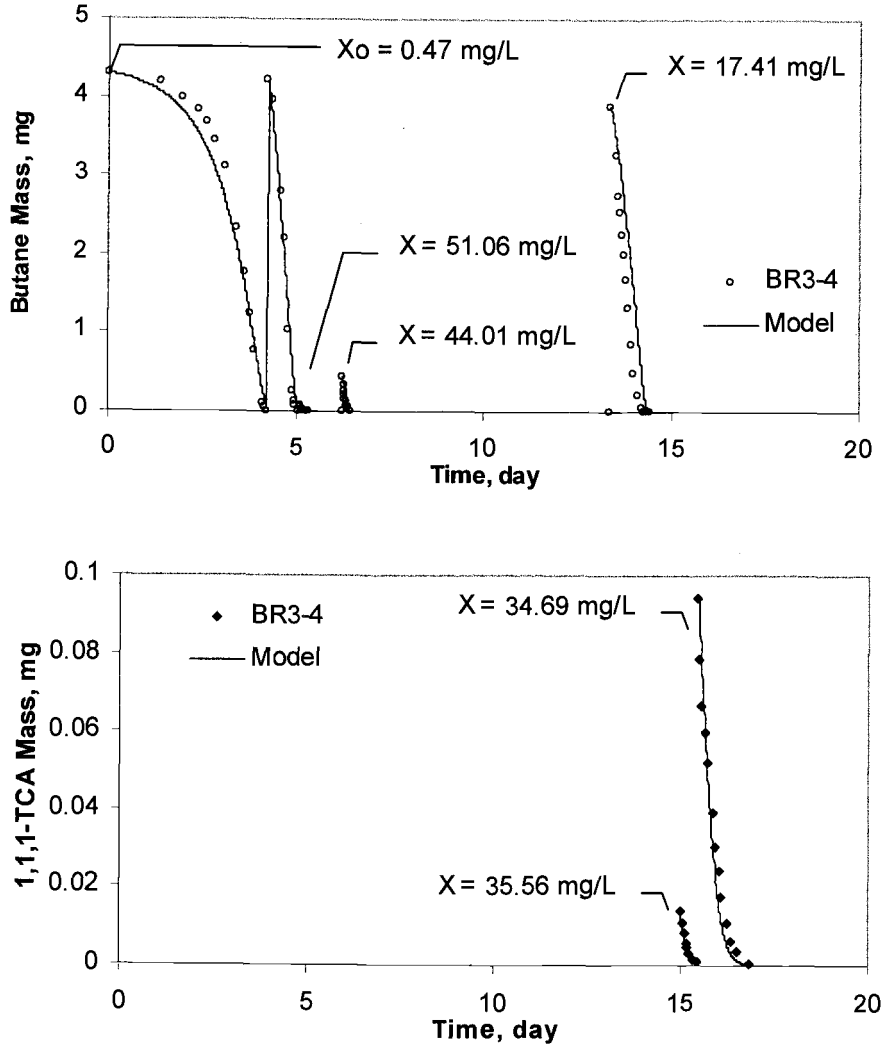

Figure 4.50 Simulations of butane utilization and 1,1,1-TCA transformation for microcosm BR3-4 without the term for transformation capacity

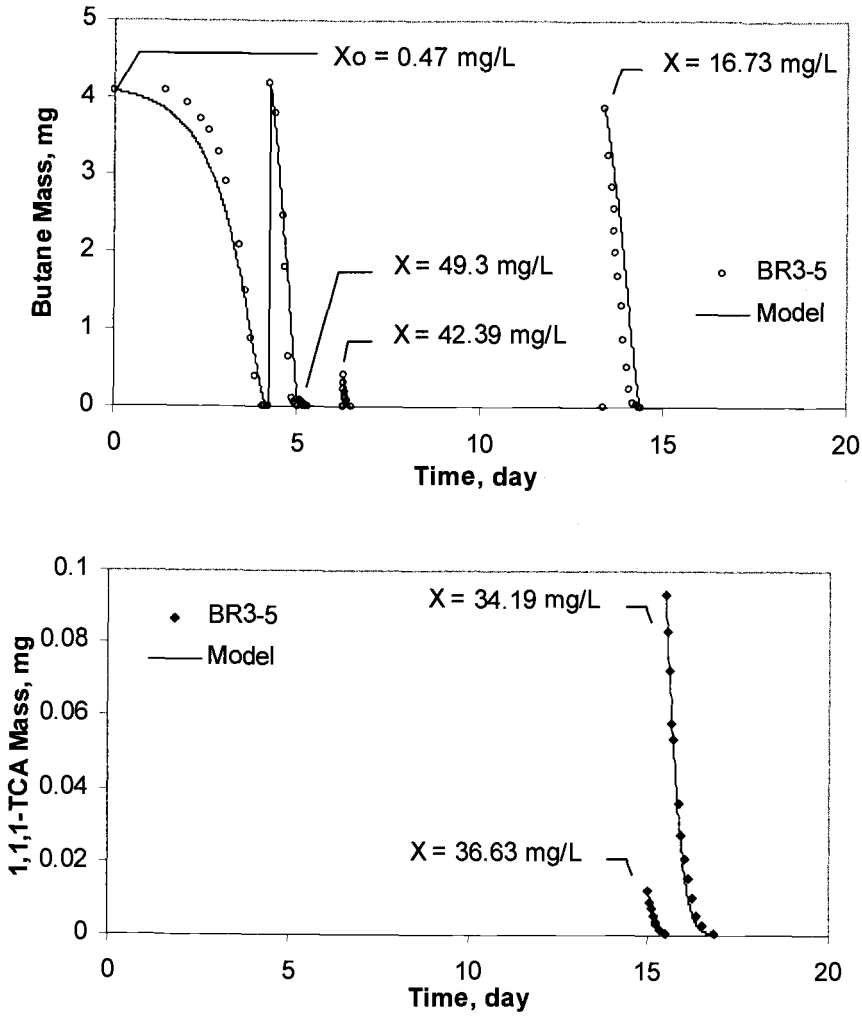

Figure 4.51 Simulations of butane utilization and 1,1,1-TCA transformation for microcosm BR3-5 without the term for transformation capacity

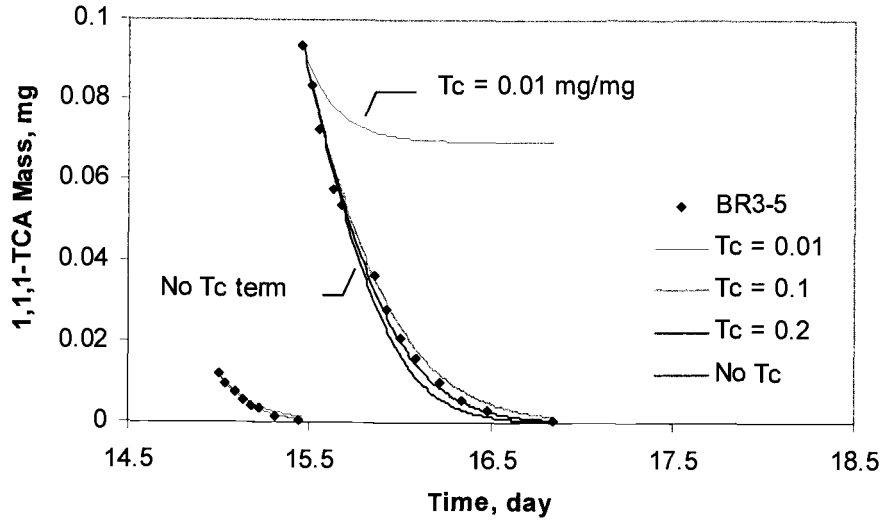

Section	Biomass (X) at starting of model simulation (mg/L)			
	$T_c = 0.01$	$T_c = 0.1$	$T_c = 0.2$	No T_c term
E	36.63	36.63	36.63	36.63
F	24.02	33.12	33.65	34.19

Figure 4.52 Simulations of 1,1,1-TCA transformation for microcosm BR3-5 over a range of transformation capacities

Figure 4.52 presents the results of model simulation over a range of transformation capacities along with the biomass (X) at starting of model simulation for microcosm BR3-5. The low T_c value of 0.01 mg 1,1,1- TCA/mg cell caused a significant decrease in biomass. Similar biomass values were obtained from simulations with $T_c \geq 0.1$ and those without a T_c term ($T_c = \infty$). Little improvement was obtained by including the transformation capacity term. The results from the data at low concentration were not sensitive to the transformation capacity term. Thus fits to transformation capacity model were obtained from the data at high concentration. The maximum concentration of tested 1,1,1-TCA was approximately 700 μg/L. Even at these high concentrations there was little sensitivity to transformation capacity. Little sensitivity to transformation capacity

was also due to the amount of biomass available, as illustrated in following calculations:

Initial biomass $= X_0 * V_l$
$= (36 \text{ mg/L})(0.1 \text{ L})$
$= 3.6 \text{ mg cells}$

Mass of transformed 1,1,1-TCA $= C_l * V_l$
$= (0.7 \text{ mg/L})(0.1 \text{ L})$
$= 0.07 \text{ mg TCA}$

Destroyed cells $=$ Mass of transformed 1,1,1-TCA / T_c
$= (0.07 \text{ mg TCA})/(0.1 \text{ mg TCA/mg cells})$
$= 0.7 \text{ mg cells} << 3.9 \text{ mg cells}$

Compared to the initial biomass, the amount of destroyed cells was small. As a result, the simulation was not very sensitivity to the transformation capacity. The results from the other microcosms were similar, as shown in appendix Figures G.23 to G.26. A range of transformation capacity (T_c) values obtained from microcosm BR3 set are presented in Table 4.18 since there is little sensitivity to the transformation capacity. The average value of transformation capacity was 0.11 ± 0.064 mg 1,1,1-TCA/mg cell. All parameters used in the model simulation for microcosm set BR3 are presented in Table 4.19.

Table 4.18 Transformation capacity ranges (T_c) achieved in the BR3 microcosm set.

Microcosm	Maximum $C_{l,TCA}$ tested (μg/L)	T_c (mg TCA/mg cells)
BR3-1	680	0.1 - 0.2
BR3-2	731	0.05 - 0.07
BR3-3	690	0.04 - 0.06
BR3-4	720	0.1 - 0.2
BR3-5	711	0.1 - 0.2
Average		0.11 ± 0.064

Table 4.19 Parameters for model development in the BR3 microcosm set

Parameter	Microcosm set BR3
X_0, mg/L	0.47
Y, mg/mg	0.7
b, day^{-1}	0.15 ± 0.006
$K_{s,But}$, mg/L	0.11
$k_{max,But}$, mg/mg-day	1.76 ± 0.023
$K_{s,TCA}$, mg/L	0.37
$k_{max,TCA}$, mg/mg-day	0.09 ± 0.027
T_c, mg /mg	0.11 ± 0.064

4.3.3.2 The simulation of butane utilization and 1,1,1-TCA transformation in the BR4 microcosm set

The experimental data of butane utilization and 1,1,1-TCA transformation in microcosm set BR4 were modeled by using the same butane and 1,1,1-TCA half-saturation constant ($K_{s,But}$ and $K_{s,TCA}$), cellular yield (Y), and cell decay rate (b) values as were used in simulations of microcosm set BR3 (Table 4.19). Similar to microcosm set BR3, the values of butane and 1,1,1-TCA maximum specific rates ($k_{max,But}$ and $k_{max,TCA}$) were varied to obtain a good fit between the model and experimental data. The model assumed that the effect of transformation product

toxicity was negligible. The simulation of butane utilization and 1,1,1-TCA transformation for microcosms BR4-M and BR4-4 are presented in Figure 4.53, and Figure 4.54, respectively. Microcosm BR4-M contained growth media while microcosm BR4-4 was constructed with groundwater and aquifer material. Reasonable fits between the model and experimental data were obtained for both sets of microcosm results. The model fit data well at low concentration as well as high concentration. The initial concentration of tested butane and 1,1,1-TCA ranged from 230 to 2,600 μg/L and 60 to 1,500 μg/L, respectively. The model simulations for the other microcosms are shown in appendix Figures G.27 to G.30. A good fit was achieved in all microcosms. However, in some cases the simulation deviated from the data. For example on day 12, as shown in appendix Figure G.27, the model seems to overestimate the rate of butane utilization. The slower rate of butane utilization may be due to the effect of transformation product toxicity, resulting from the effect of the high concentration of TCA transformed at 7 days.

Model simulations including a transformation capacity (T_c) term were evaluated using the same procedure as the microcosm BR3set. Figure 4.55 presents the results of model simulation for microcosm BR4-5 over a range of transformation capacities. The simulations for the other microcosms are presented in appendix Figures G.31 to G.35. Although the effect of the transformation product toxicity was included in the simulation, the simulations did not fit the data better. Figures 4.55a and 4.55b present the transformation of the first and second additions of 1,1,1-TCA. A good fit was obtained from the data at low concentration. However, the transformation at high concentration was a little faster than the model prediction. The reason for this is not known. The model overestimated the utilization rate of the fourth addition of butane, as shown in Figure 4.55c. The model with a lower transformation capacity fit the data better, but it underestimated the butane utilization and 1,1,1-TCA transformation in later time. As shown in Figures 4.55e and 4.55f, the third and fourth additions of 1,1,1-TCA were transformed faster than the model prediction. The reason for the faster transformation at both low and high concentration is not known. The effects of

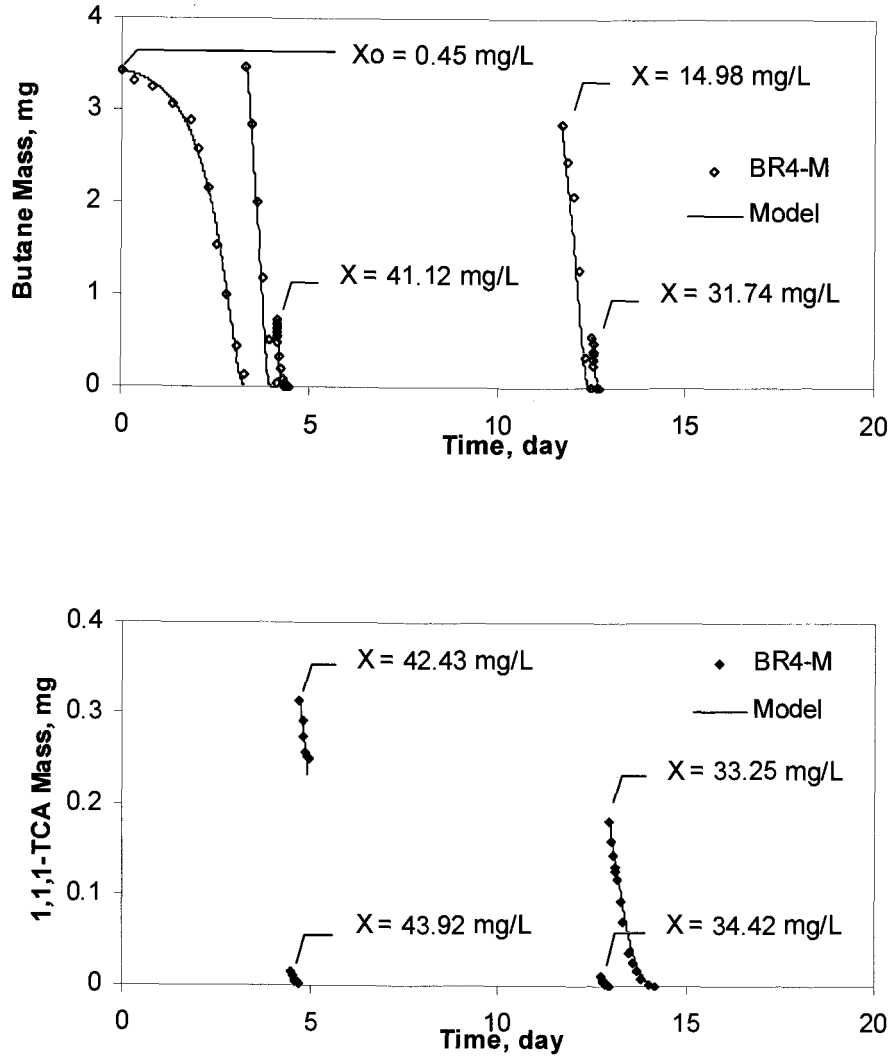

Figure 4.53 Simulations of butane utilization and 1,1,1-TCA transformation for microcosm BR4-M without the term for transformation capacity

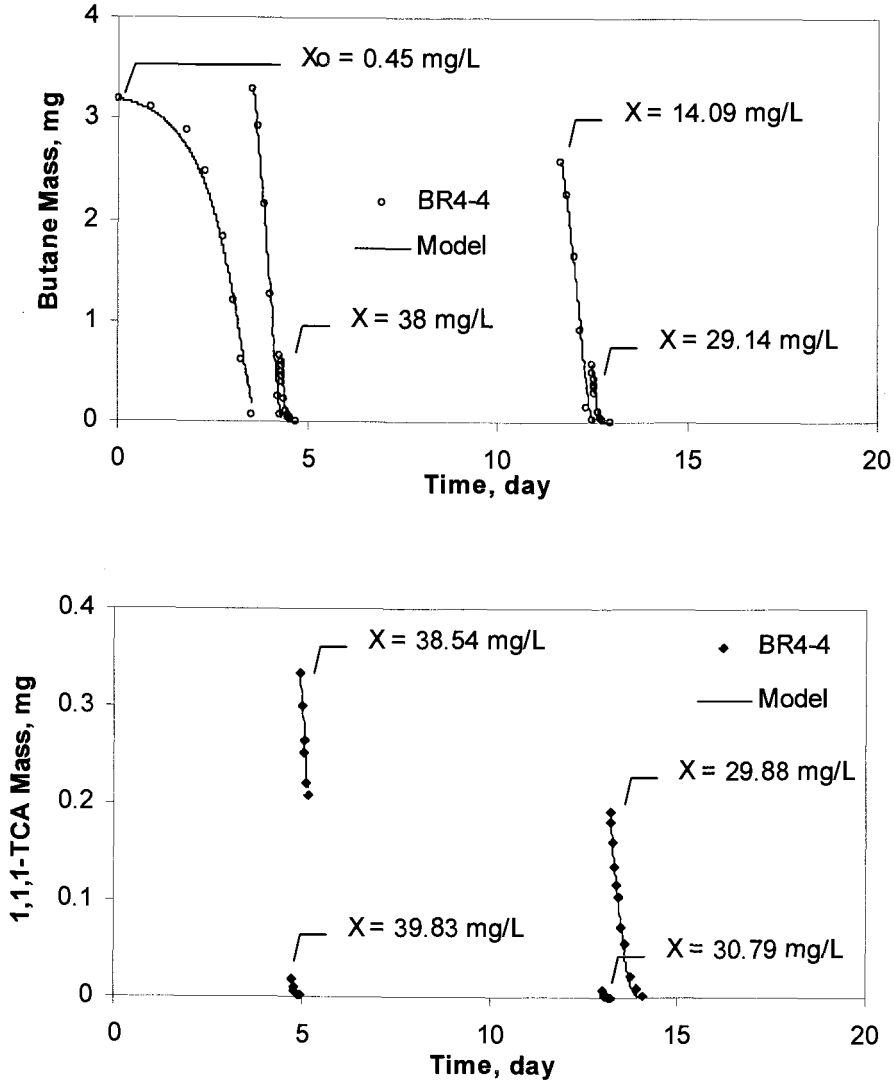

Figure 4.54 Simulations of butane utilization and 1,1,1-TCA transformation for microcosm BR4-4 without the term for transformation capacity

a) The first addition of 1,1,1-TCA on day 4

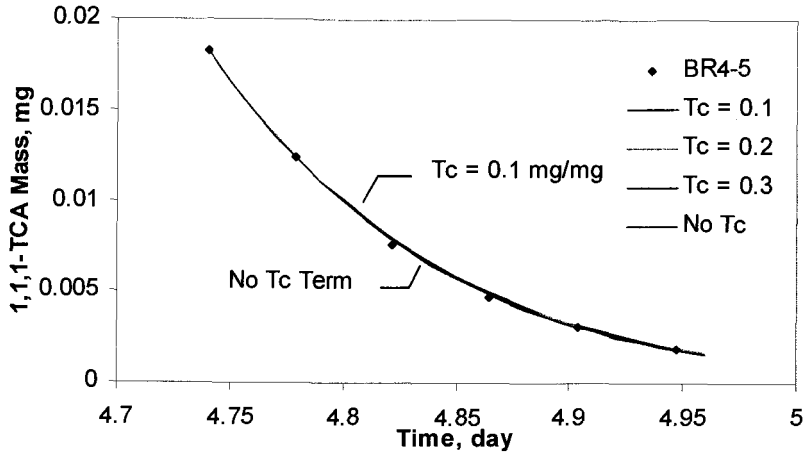

Biomass (X) at starting of model simulation (mg/L)			
$T_c = 0.1$	$T_c = 0.2$	$T_c = 0.3$	No T_c term
39.45	39.45	39.45	39.45

b) The second addition of 1,1,1-TCA on day 4

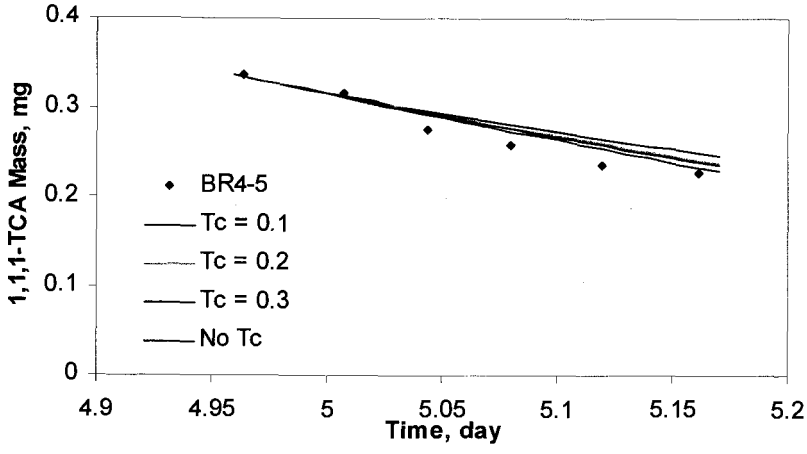

Biomass (X) at starting of model simulation (mg/L)			
$T_c = 0.1$	$T_c = 0.2$	$T_c = 0.3$	No T_c term
36.55	37.36	37.63	38.17

Figure 4.55 Simulations of butane utilization and 1,1,1-TCA transformation for microcosm BR4-5 over a range transformation capacities capacity

c) The fourth addition of butane on day 11

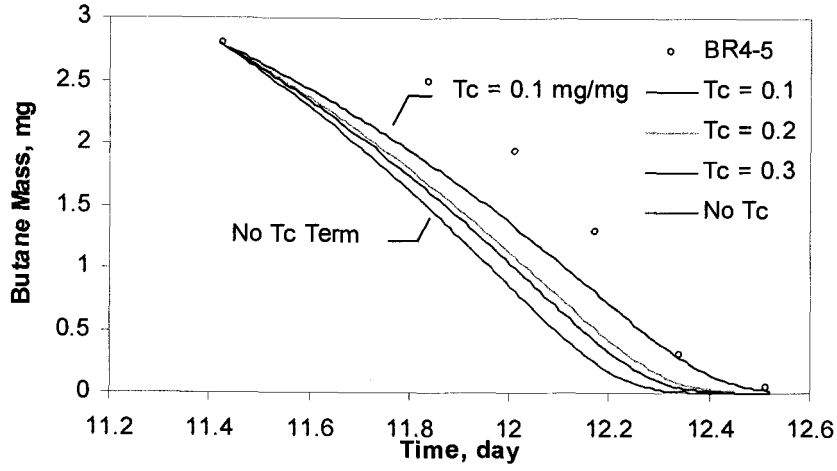

Biomass (X) at starting of model simulation (mg/L)			
$T_c = 0.1$	$T_c = 0.2$	$T_c = 0.3$	No T_c term
10.40	12.28	12.97	14.48

d) The fifth addition of butane on day 12

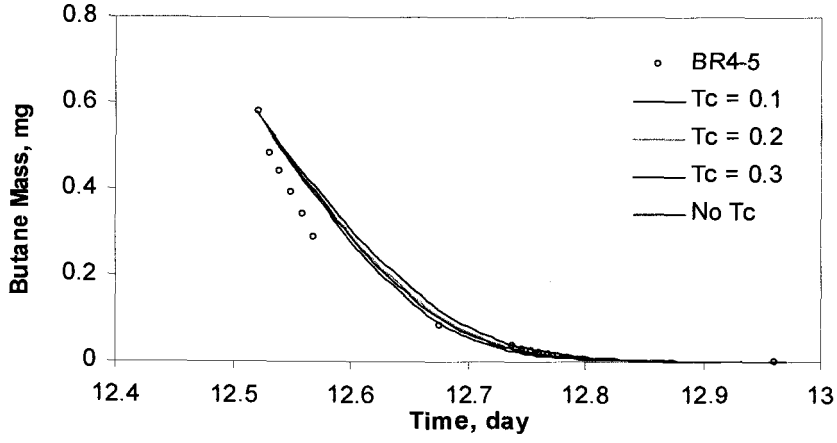

Biomass (X) at starting of model simulation (mg/L)			
$T_c = 0.1$	$T_c = 0.2$	$T_c = 0.3$	No T_c term
26.71	28.26	28.80	29.99

Figure 4.55, Continued

e) The third addition of 1,1,1-TCA on day 12

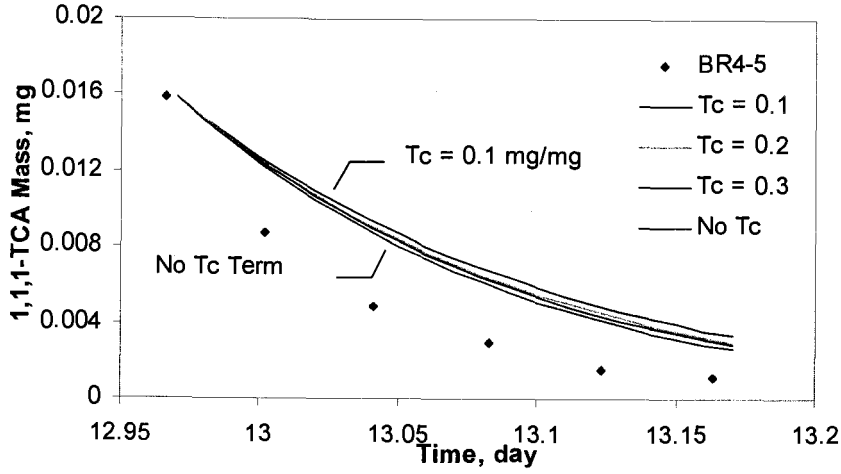

Biomass (X) at starting of model simulation (mg/L)			
$T_c = 0.1$	$T_c = 0.2$	$T_c = 0.3$	No T_c term
28.80	30.24	30.78	31.86

f) The fourth addition of 1,1,1-TCA on day 13

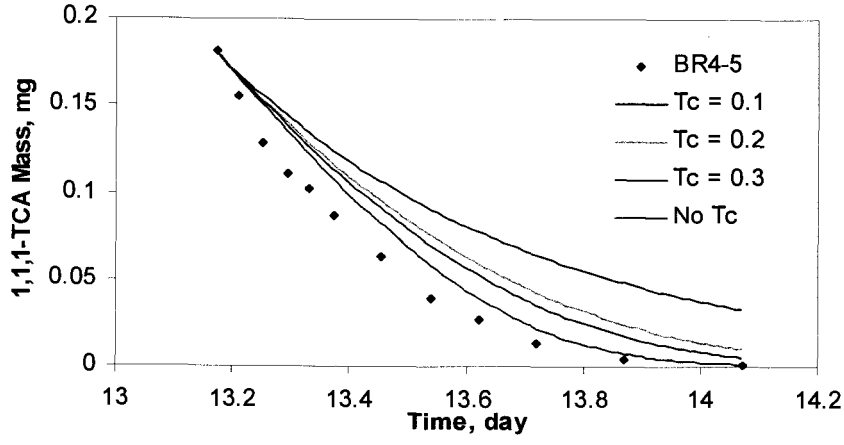

Biomass (X) at starting of model simulation (mg/L)			
$T_c = 0.1$	$T_c = 0.2$	$T_c = 0.3$	No T_c term
26.72	28.72	29.45	30.92

Figure 4.55, Continued

enzyme induction or possible changes in microbial community that were not included in the model simulations are possible factors resulting in the higher transformation rates.

The results from the first and second additions of 1,1,1-TCA were not sensitive to the transformation capacity term, as shown in Figures 4.55a and 4.55b. As a result, the tests should have been performed for longer periods of time. The simulation of 1,1,1-TCA transformation in later time still had low sensitivity at low concentration, but became more sensitivity at higher concentration, as shown in Figures 4.55e and 4.55f. This is probably due to the high transformation capacity of 1,1,1-TCA.

As shown in Figure 4.55c, the simulation of the fourth addition of butane showed more sensitivity to transformation capacity values than that of 1,1,1-TCA transformation. A different result was observed in the simulation of the fifth addition of butane, as shown in Figure 4.55d. No 1,1,1-TCA was transformed between these two additions of butane. The biomass in the microcosm was low before the fourth addition of butane. Thus the high biomass at the fifth addition of butane probably made the simulation less sensitive to the transformation capacity values.

Table 4.20 Butane and 1,1,1-TCA maximum specific rate ($k_{max,But}$ and $k_{max,TCA}$) and transformation capacity (T_c) values achieved in the BR4 microcosm set

Microcosm	$k_{max,But}$ (mg/mg-day)	$k_{max,TCA}$ (mg/mg-day)	T_c (mg TCA/mg cells)
BR4-M	2.2	0.11	0.3
BR4-1	1.58	0.1	0.3
BR4-2	1.74	0.19	0.3
BR4-3	1.74	0.14	0.3
BR4-4	1.95	019	0.3
BR4-5	1.93	0.16	0.3
Average	1.79 ± 0.154	0.16 ± 0.038	0.3 ± 0

The estimated values of butane and 1,1,1-TCA maximum specific rates ($k_{max,But}$ and $k_{max,TCA}$) and transformation capacity (T_c) for microcosm BR4-M and the BR4 microcosm set are shown in Table 4.20. All microcosms, either constructed with groundwater and aquifer material or contained growth media, had similar parameter values. This indicates the reproducibility of the bioaugmentation process, and indicates a similar butane-utilizing microbial community was present in both media and groundwater microcosms. Estimates of transformation capacity were obtained through the simulation of 1,1,1-TCA transformation at the fourth addition, which showed the most sensitivity to the transformation capacity term. All microcosms had a very high value of transformation capacity (0.3 mg/mg). The results from the model simulation at the tested concentration showed little difference between having no transformation term ($T_c = \infty$) and a T_c value of 0.3 mg/mg. Table 4.21 presents all parameters used in the model simulation for microcosm BR4-M and the BR4 microcosm set. The use of the same parameters with only small differences in k_{max} values also demonstrate the reproducibility of the bioaugmentation process.

Table 4.21 Parameters for model development in microcosm BR4-M and the BR4 microcosm set

Parameter	Microcosm BR4-M	Microcosm set BR4
X_0, mg/L	0.45	0.45
Y, mg/mg	0.7	0.7
b, day^{-1}	0.15	0.15
$K_{s,But}$, mg/L	0.11	0.11
$k_{max,But}$, mg/mg-day	2.2	1.79 ± 0.154
$K_{s,TCA}$, mg/L	0.37	0.37
$k_{max,TCA}$, mg/mg-day	0.11	0.16 ± 0.378
T_c, mg/mg	0.3	0.3 ± 0

4.3.3.3 The simulation of butane utilization and 1,1,1-TCA transformation in the B4 microcosm set

The culture bioaugmented in the BR3 and BR4 microcosm sets was not washed with groundwater to rinse away the mineral salts media prior to inoculation. The nutrients were suspected to have an effect on the growth of the culture and the values of the estimated kinetic parameters. For comparison purposes, model simulations of butane utilization and 1,1,1-TCA transformation achieved in the B4 microcosm set, where cells were washed to remove the mineral salts media was conducted. Estimates of butane and 1,1,1-TCA maximum specific rates ($k_{max,But}$ and $k_{max,TCA}$) and the transformation capacity (T_c) were obtained through model simulations and compared with BR3 and BR4 microcosm results. The values of cellular yield (0.7 mg/mg), cell decay rate (0.15 day^{-1}), butane half-saturation constant (0.11 mg/L) and 1,1,1-TCA half-saturation constant (0.37 mg/L) were the same as used in simulating the BR3 and BR4 microcosm sets.

Figure 4.56 presents the experimental data of butane utilization and 1,1,1-TCA transformation for microcosm B4-3. The simulation of butane utilization was performed by modeling the butane observations during the first 33 days of incubation. The inhibition effect of 1,1,1-TCA on butane utilization was ignored since the concentration of 1,1,1-TCA was much lower than the concentration of butane. The augmented biomass of the B4 microcosm set was unknown, so initial biomass of 0.5 mg/L was assumed in the simulation. The value of $k_{max,But}$ was varied until a good model fit was obtained. However, it was difficult to obtain a good fit to all of the experimental data. As a result, the model simulation was conducted by considering the data after day 20 since more data were collected during this time, and initial conditions at early time were uncertain.

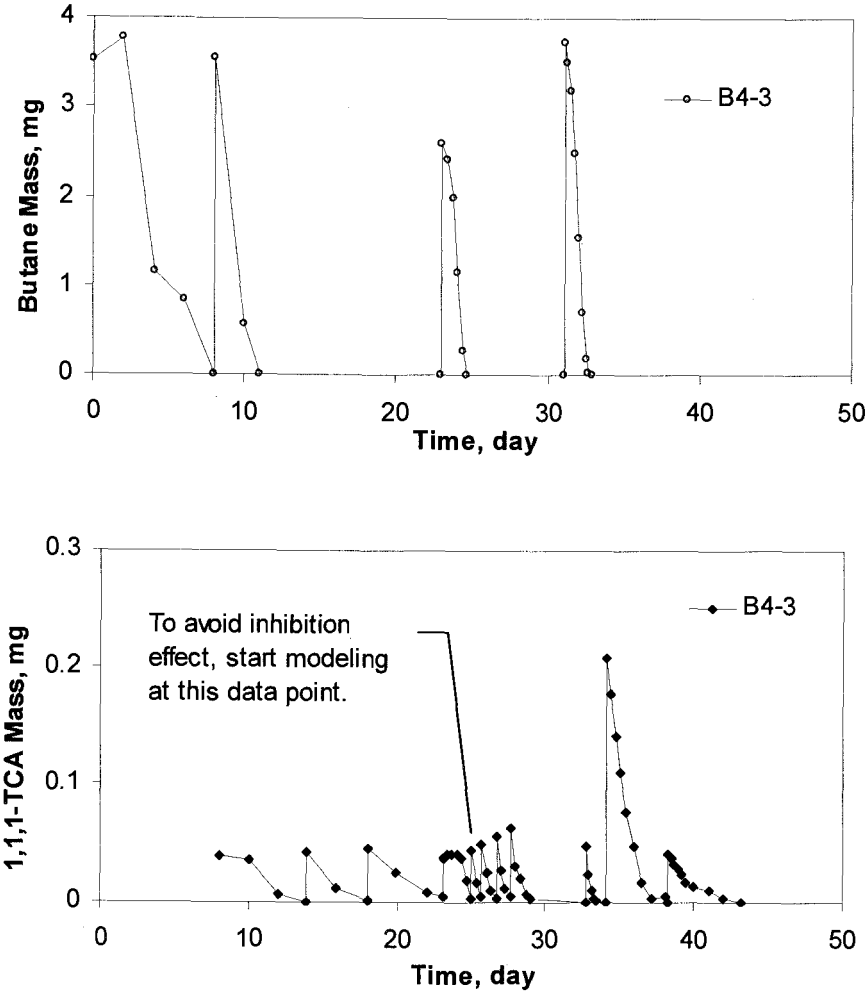

Figure 4.56 Butane utilization and 1,1,1-TCA transformation achieved in microcosm B4-3

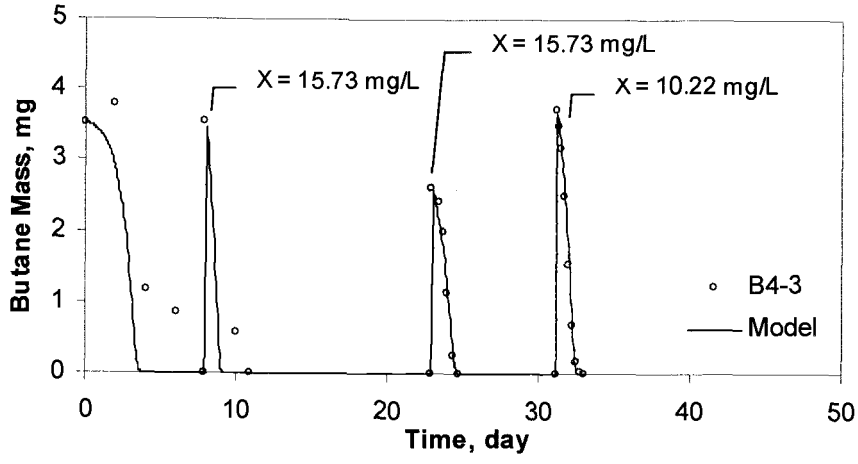

Figure 4.57 Simulations of butane utilization for microcosm B4-3 without the term for transformation capacity

The model simulation of butane utilization for microcosm B4-3 is presented in Figure 4.57. A good fit between the model and data was obtained after day 20. The model did not fit the data well during the first 10 days of incubation. The rate of butane utilization was slower than the model prediction. This implies that the values of $k_{max,But}$ between two periods of time are different. Additionally, the slower utilization rate of the second addition of butane was probably due to the inhibition of 1,1,1-TCA, which was not considered in the model. The results from the simulations of butane utilization for the other microcosms B4-1 and B4-2 were similar, as shown in appendix Figures G.36 and G.39, respectively. Table 4.22 presents the values of butane maximum specific rate ($k_{max,But}$) for the B4 microcosm set. All microcosms had the same values (2.2 mg/mg-day). The $k_{max,But}$ values of all microcosms were the same, and also similar to those of microcosm sets BR3 and BR4 (Tables 4.19 and 4.21). The results indicate a similar butane utilization rate with and without minor nutrient amendments over a 1-month test period.

Table 4.22 Butane maximum specific rate ($k_{max,But}$) values achieved in the B4 microcosm set

Microcosm	$k_{max,But}$ (mg/mg-day)
B4-1	2.2
B4-2	2.2
B4-3	2.2
Average	2.2 ± 0

Simulations of 1,1,1-TCA transformation in the B4 microcosm set were also conducted to evaluate the 1,1,1-TCA maximum specific rate ($k_{max,TCA}$). Data obtained in the absence of butane utilization were selected for simulation comparisons, in order to avoid the effects of inhibition of butane on 1,1,1-TCA transformation. 1,1,1-TCA data that was simulated is shown in Figure 4.56. For initial simulations, the transformation product toxicity was assumed to be negligible. Similar to the simulations for the BR3 and BR4 microcosm sets, a heuristic fitting of $k_{max,TCA}$ values was performed. Figure 4.58 presents the simulation of 1,1,1-TCA transformation for microcosm B4-3. Although the model fit the data at early time well, it overestimated the 1,1,1-TCA transformation at later time. The slower transformation may have resulted from transformation product toxicity or energy limitations or higher cell decay rates. The results from the simulations for the other microcosms were similar, as shown in appendix Figures G.37 and G.40, respectively.

Additional simulations were conducted to incorporate the transformation capacity (T_c) term. Figure 4.59 presents the simulation of butane utilization and 1,1,1-TCA transformation for microcosm BR3-5 over a range of transformation capacities. The inclusion of transformation capacity term did not improve the model fit of 1,1,1-TCA transformation and butane utilization at early time, as shown in Figures 4.59a and 4.59b. The model with high transformation capacity (T_c = 0.4 mg 1,1,1-TCA/mg cells) fit the 1,1,1-TCA transformation data in early

time. The deviation between model and data increased with time. The model underpredicted 1,1,1-TCA transformation rates. The model with no transformation capacity term ($T_c = \infty$) better simulated butane utilization also after low concentration level 1,1,1-TCA additions. However, a lower transformation capacity fit the 1,1,1-TCA transformation data at later time, as shown in Figure 4.59c, but it under predicted both butane utilization and 1,1,1-TCA transformation in early time. The slower transformation of 1,1,1-TCA at later time could not be completely explained by incorporating the transformation capacity term. The slow deactivation of enzyme might be another factor, resulting in a decrease of $k_{max,TCA}$ as a function of the 1,1,1-TCA mass transformed. Other factors such as a change of microbial community, or nutrient limitations cannot be ruled out.

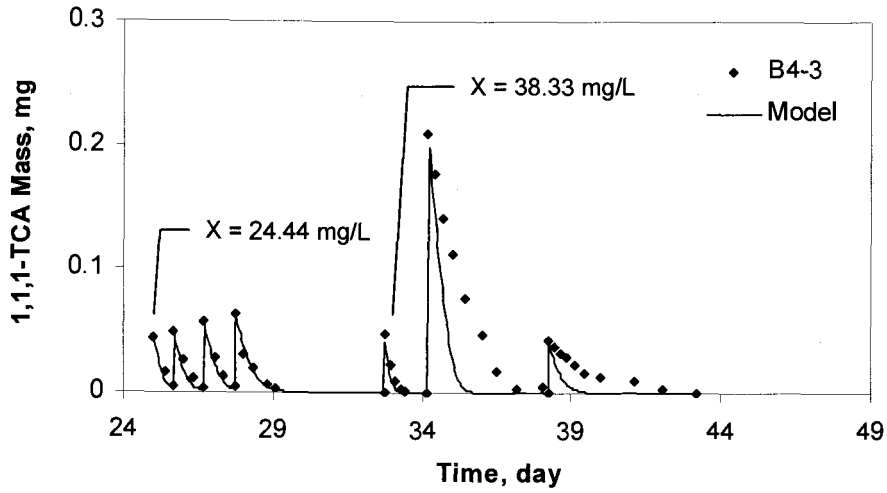

Figure 4.58 Simulations of 1,1,1-TCA transformation for microcosm B4-3 without the term for transformation capacity

a) 1,1,1-TCA transformation from day 25 to 32

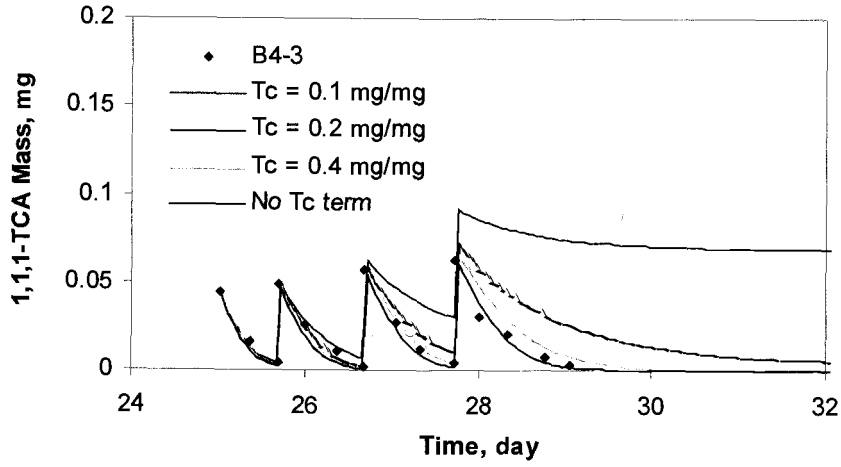

Biomass (X) at starting of model simulation (mg/L)			
$T_c = 0.1$	$T_c = 0.2$	$T_c = 0.4$	No T_c term
24.44	24.44	24.44	24.44

b) Butane utilization from day 31 to 33

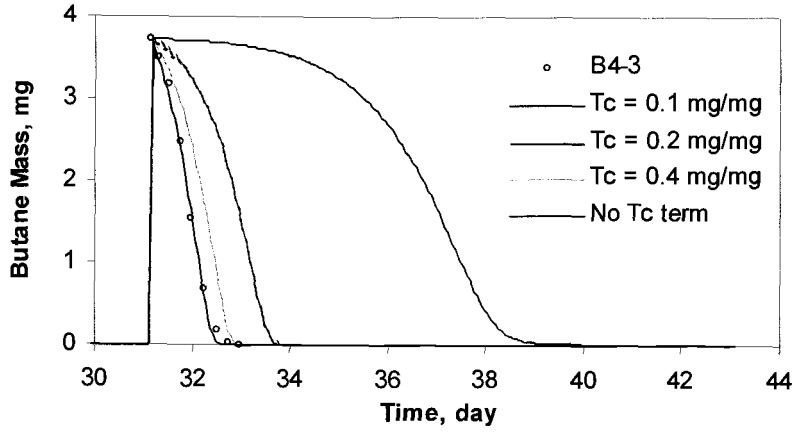

Biomass (X) at starting of model simulation (mg/L)			
$T_c = 0.1$	$T_c = 0.2$	$T_c = 0.4$	No T_c term
0.09	2.37	6.26	10.26

Figure 4.59 Simulations of butane utilization and 1,1,1-TCA transformation for microcosm B4-3 over a range transformation capacities

c) 1,1,1-TCA transformation from day 33 to 43

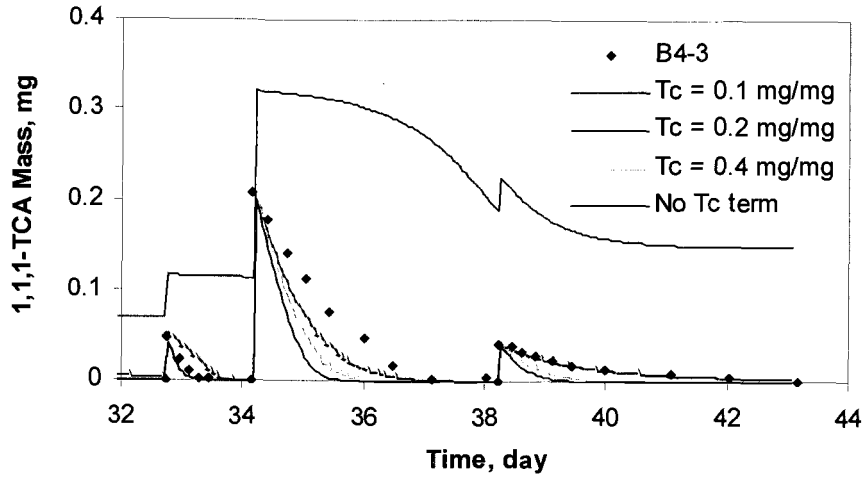

Biomass (X) at starting of model simulation (mg/L)			
$T_c = 0.1$	$T_c = 0.2$	$T_c = 0.4$	No T_c term
0.41	15.24	34.19	38.33

Figure 4.59, Continued

The results from the simulations for microcosms B4-1 and B4-2 are presented in appendix Figures G.38 and G.41, respectively. The model with no or high transformation capacity term ($T_c = \infty$ or $T_c = 0.4$ mg/mg) better fit the data at early time, while the model with lower transformation capacity better fit the data at later time. For microcosms B4-2 and B4-3, it is difficult to point out the value of transformation capacity since the model with only one value of transformation capacity could not provide a good fit for all microcosm data. The values of 1,1,1-TCA maximum specific rate ($k_{max,TCA}$) and transformation capacity (T_c) for the B4 microcosm set are presented in Table 4.23. Values for all microcosms were similar and also in the range obtained from the BR3 and BR4 microcosm sets (Tables 4.19 and 4.21).

Table 4.23 1,1,1-TCA maximum specific rate ($k_{max,TCA}$) and transformation capacity (T_c) values achieved in the B4 microcosm set

Microcosm	$k_{max,TCA}$ (mg/mg-day)	T_c (mg TCA /mg cells)
B4-1	0.15	0.4
B4-2	0.10	0.2 - 0.4
B4-3	0.15	0.2 - 0.4
Average	0.13 ± 0.024	0.33 ± 0.103

The results obtained from the model simulations and the rate measurements were compared to evaluate if the simplified analysis in the rate measurement could provide reliable values of kinetic parameters. Table 4.24 presents the values of pseudo-first-order rate parameter ($k_{max}X_0/K_s$) and cell decay rate (b) for microcosm set B4 based on the rate measurements during day 30 – 35 and the model simulations. The values of cell decay rate obtained from the rate measurement of 1,1,1-TCA transformation (0.21 day^{-1}) were higher than those from the simulation of butane utilization (0.15 day^{-1}). The higher b value probably represents both cell and enzyme decay rate. The values of pseudo-first-order rate parameter ($k_{max}X_0/K_s$) obtained from the rate measurements and the model simulations ranged from 3.4 to 6.6 day^{-1}, and 6.6 to 10.6 day^{-1}, respectively. The higher values of the parameters obtained from the model simulation were probably due to the higher value of initial biomass (X_0) since the value of cell decay rate (b) from the model simulation was lower than that obtained from the rate regression measurement. The rate regression method provided fairly reasonable values for the pseudo-first-order rate parameter ($k_{max}X_0/K_s$), within factor of 2. A good agreement between the values of pseudo-first-order rate parameter ($k_{max}X_0/K_s$) and cell decay rate (b) was also obtained. This indicates the practicality of the simplified analysis in the rate regression measurement.

Table 4.24 The pseudo-first-order rate parameter ($k_{max}X_0/K_s$) and cell decay rate (b) for the B4 microcosm set from the rate measurement during day 28 – 37 and from the model simulation

Microcosm	Rate measurement		Model simulation	
	$k_{max}X_0/K_s$ (day^{-1})	b (day^{-1})	$k_{max}X_0/K_s$ (day^{-1})	b (day^{-1})
B4-1	6.6	0.28	9.7	0.15
B4-2	3.2	0.20	6.3	0.15
B4-3	5.0	0.15	9.9	0.15
Average	5.0 ± 1.62	0.21 ± 0.064	8.6 ± 2.01	0.15

All parameters used in the model simulation for the B4 microcosm set are presented in Table 4.25. In the B4 microcosm set the cells were washed to remove the mineral salts media. Similar kinetic parameters including butane maximum specific rate ($k_{max,But}$), 1,1,1-TCA maximum specific rate ($k_{max,TCA}$) and transformation capacity (T_c) were obtained as in the BR3 and BR4 microcosm sets. This indicates that these parameters, including the transformation ability of bioaugmented microcosms, are not influenced by the addition of nutrients.

Table 4.25 Parameters for model development in the B4 microcosm set

Parameter	Microcosm set B4
X_0, mg/L	0.5 (assumed number)
Y, mg/mg	0.7
b, day^{-1}	0.15
$K_{s,But}$, mg/L	0.11
$k_{max,But}$, mg/mg-day	2.2 ± 0
$K_{s,TCA}$, mg/L	0.37
$k_{max,TCA}$, mg/mg-day	0.13 ± 0.024
T_c, mg /mg	0.33 ± 0.103

4.3.3.4 The simulation of butane utilization and 1,1,1-TCA transformation in the BRC microcosm set

Butane utilization and 1,1,1-TCA transformation data for indigenous microorganisms in the BRC microcosm set (Table 4.9) were also modeled to determine kinetic parameters. All kinetic parameters for butane utilization and 1,1,1-TCA transformation in the indigenous microcosms were unknown. The value of butane and 1,1,1-TCA half-saturation constant ($K_{s,But}$ and $K_{s,TCA}$) could not be determined from the kinetic experiments since butane utilization and 1,1,1-TCA transformation were slow, and 1,1,1-TCA transformation stopped after the microcosms were exposed to the second addition of 1,1,1-TCA (800 μg/L). The kinetic parameters of bioaugmented butane-utilizers in the BR3 microcosm set including butane and 1,1,1-TCA half-saturation constant ($K_{s,But}$ and $K_{s,TCA}$), butane and 1,1,1-TCA maximum specific rate ($k_{max,But}$ and $k_{max,TCA}$), cellular yield (Y), and cell decay rate (b) were therefore used to simulate butane utilization and 1,1,1-TCA transformation in the BRC microcosm set (Table 4.19).

Initially the simulation of butane utilization and 1,1,1-TCA transformation occurring in the indigenous microcosms was conducted by not considering the effect of transformation product toxicity. Figure 4.60 presents the simulation of butane utilization and 1,1,1-TCA transformation for microcosm BRC-1. The microcosm data were divided into 7 sections (A, B, C, D, E and F). Each section represented the data from each addition of butane and 1,1,1-TCA, and was modeled separately, as shown in Figure 4.61. The initial biomass in the indigenous microcosm was unknown. So the values of biomass were varied to achieve a reasonable fit between the model and the microcosm data in section A. The estimated initial biomass for all microcosms is presented in Table 4.26.

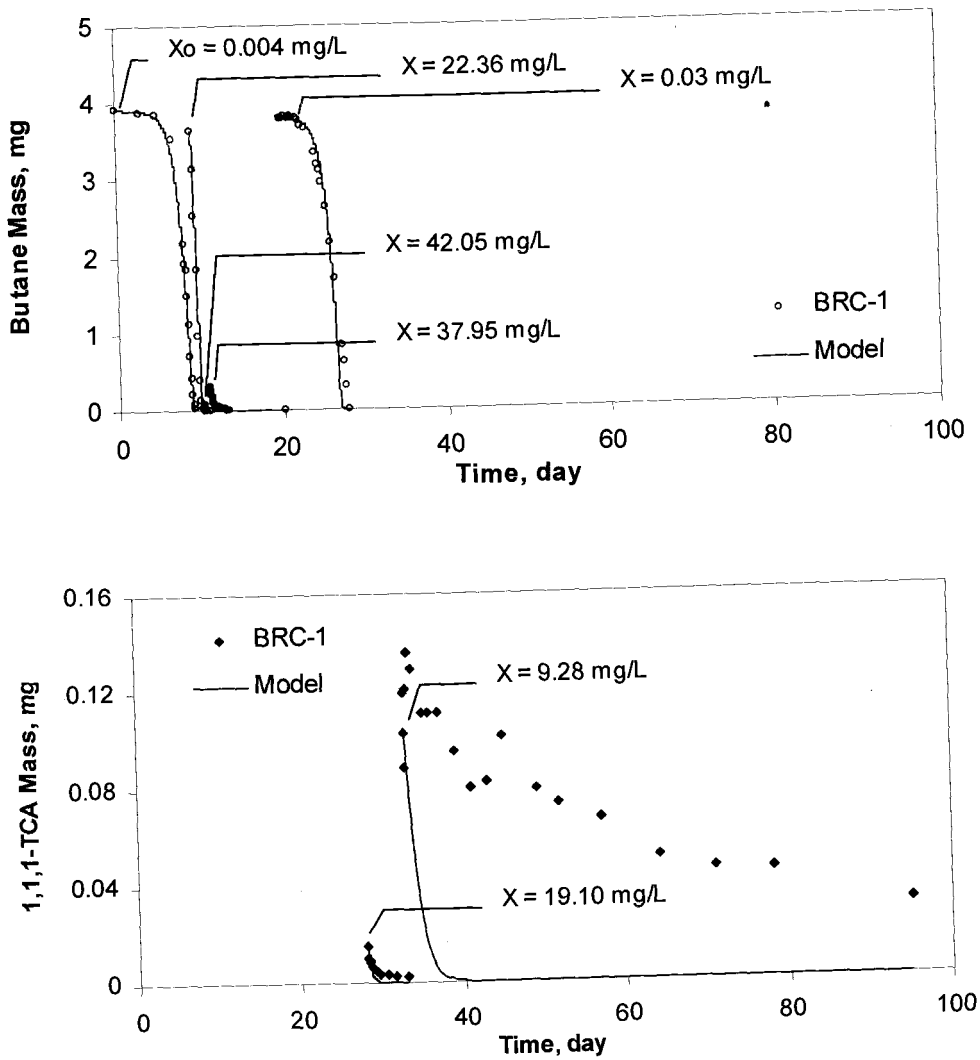

Figure 4.60 Simulations of butane utilization and 1,1,1-TCA transformation for microcosm BRC-1 without the term for transformation capacity

Section A: The first addition of butane on day 0

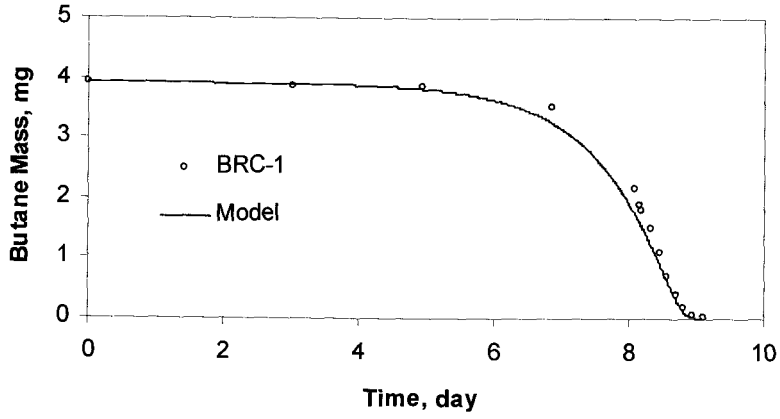

Section B: The second addition of butane on day 9

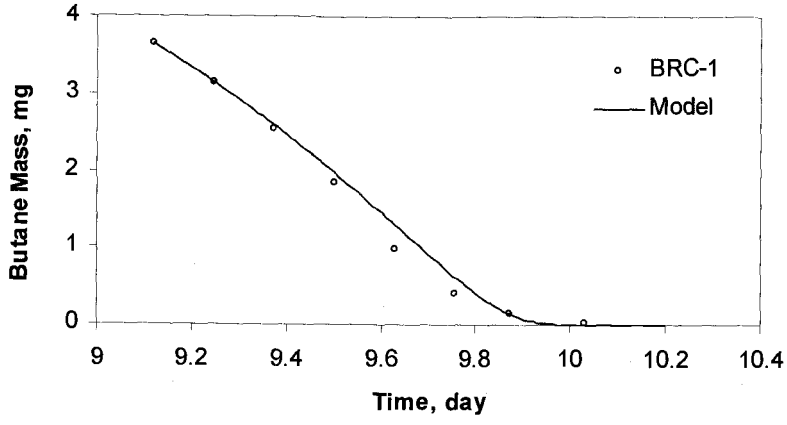

Section C: The third addition of butane on day 10

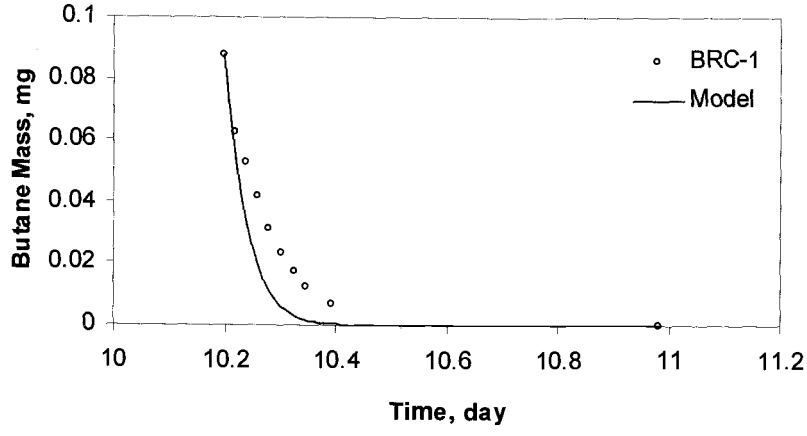

Figure 4.61 Simulations of butane utilization and 1,1,1-TCA transformation in each section for microcosm BRC-1 without the term for transformation capacity

Section D: The fourth addition of butane on day 10

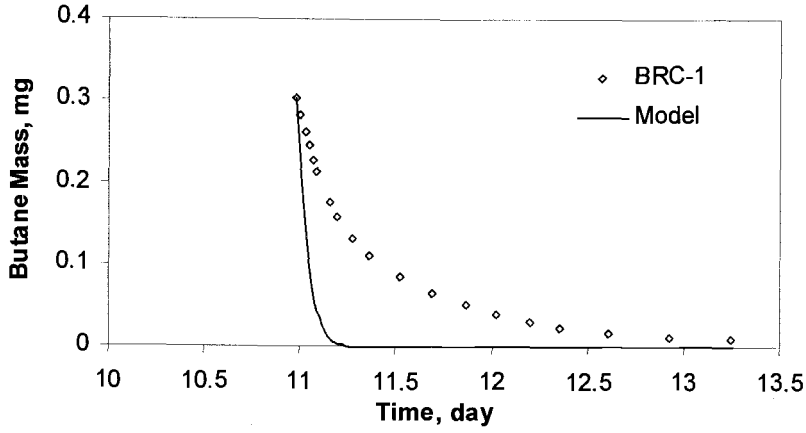

Section E: The fifth addition of butane on day 20

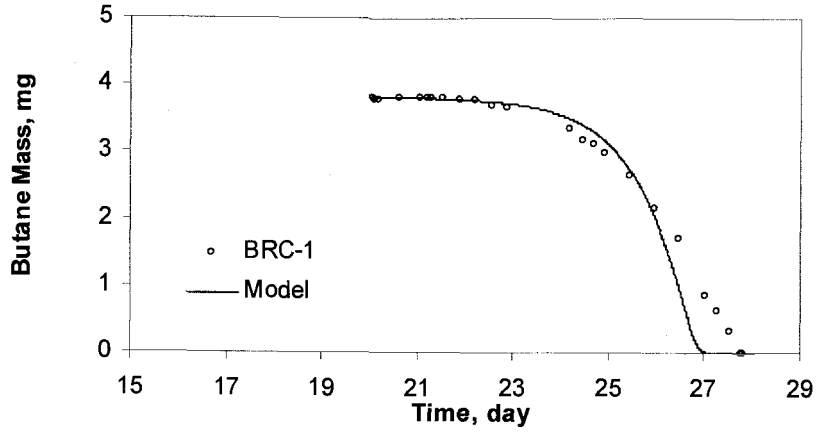

Section F: The first addition of 1,1,1-TCA on day 28

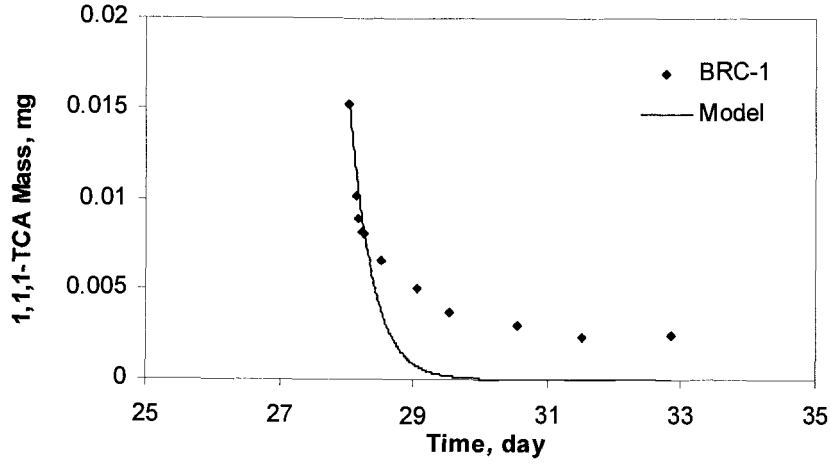

Figure 4.61, Continued

Section G: The second addition of 1,1,1-TCA on day 32

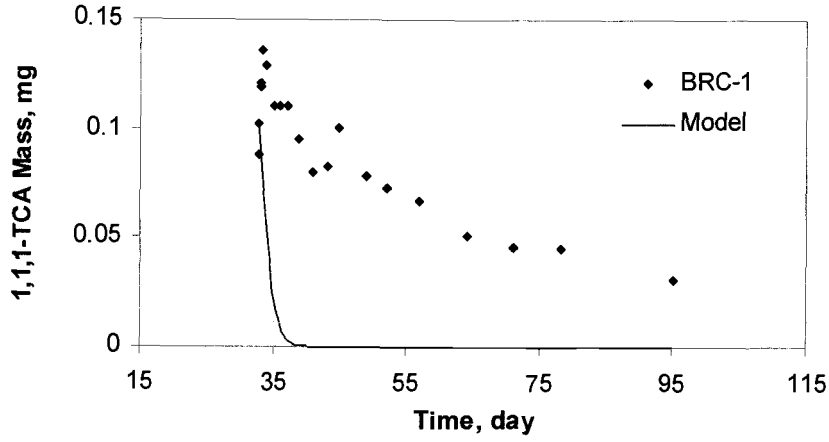

Figure 4.61, Continued

The model fit the data well during the first 10 days of incubation, as shown in section A and B, but started deviating from the data on day 10, as shown in section C and D (Figure 4.61). This indicates that the kinetic parameters of bioaugmented microcosm do not fit the non-augmented data well. As shown in section D (Figure 4.61), the initial rates of butane utilization at moderate concentrations of butane were slower than the model prediction. One possibility is that the indigenous microorganisms have a lower butane maximum specific rate ($k_{max,But}$) than the bioaugmented microorganisms. The rate of butane utilization followed first-order kinetics when the concentration was below 100 μg/L, as shown in section D (Figure 4.61). Thus the butane half-saturation constant ($K_{s,But}$) of the indigenous microorganisms should be higher than that of bioaugmented microorganisms. The deviation of model from the microcosm data increased with time, especially after day 20 or section E (data not shown). Thus the biomass was adjusted in section E to make the model fit the data. Table 4.27 presents the initial biomass in section E that was obtained from model simulations and adjusted biomass. The estimated biomass resulting from model simulations was much higher than that obtained from the adjusted values. Based on the cell decay rate

equation (equation D.7), the indigenous microorganisms had four to ten times the cell decay rate (b) of the bioaugmented microorganisms. As shown in section E (Figure 4.61), the initial rate of butane utilization at moderate concentrations of butane, after the lag phase, was slower than the model prediction. This corroborates the results from section D indicating that the indigenous microorganisms have a lower butane maximum specific rate ($k_{max,But}$) than the bioaugmented microorganisms. However, the slower rate of butane utilization might be due to nutrient limitations that were not included in the model simulations. The results from the simulation of other indigenous microcosms were similar as shown in appendix Figures G.42 to G.45.

Table 4.26 Initial biomass (X_0) for the BRC microcosm set.

Microcosm	X_0 (mg/L)
BRC-1	0.004
BRC-2	0.006
BRC-3	0.001
BRC-4	0.004
BRC-5	0.005
Average	0.004 ± 0.002

Table 4.27 Initial biomass (X_0) in section E for the BRC microcosm set obtained from the adjustment and the model simulation.

Microcosm	Starting day	X_0 (mg/L)	
		Adjusted	Modeled
BRC-1	28	0.03	10.27
BRC-2	26	0.2	10.79
BRC-3	25	1	14
BRC-4	32	0.001	10.92
BRC-5	25	0.7	10.82

The simulations of 1,1,1-TCA transformation were performed by using the same kinetic parameters as the bioaugmented microorganisms in the BR3 microcosm set. The initial biomass (X = 19.10 mg/L) was obtained from the previous simulations using the revised biomass. The model overestimated the transformation rate of 1,1,1-TCA, as shown in section F and G (Figure 4.61). Similar to butane utilization, the initial rate of 1,1,1-TCA transformation at high concentration was slower than the model prediction, as shown in section G. This shows that the 1,1,1-TCA maximum specific rate ($k_{max,TCA}$) of the bioaugmented microorganisms is higher than that of the indigenous microorganisms. The fluctuation of data points and also the slow transformation rate in section G provided a difficulty in estimating the value of 1,1,1-TCA half-saturation constant ($K_{s,TCA}$). The slow disappearance of 1,1,1-TCA after day 50 was possibly due to microcosm leakage rather than the microbial transformation. As shown in appendix Figure G.45, there was no 1,1,1-TCA transformation in microcosm BRC-5, but slow disappearance of 1,1,1-TCA was observed after day 50. Thus the results from the simulations were performed using the microcosm data before day 50.

Another simulation of 1,1,1-TCA transformation was performed to evaluate the effect of transformation product toxicity. Figure 4.62 presents the simulation of 1,1,1-TCA transformation for microcosm BRC-1 over a range of transformation capacities. The values of all kinetic parameters except the transformation capacity (T_c) were maintained constant (Table 4.19). The initial biomass (X = 19.10 mg/L) was also the same as the previous simulation of 1,1,1-TCA transformation which used the revised biomass. Unlike the bioaugmented microorganisms, the simulations of 1,1,1-TCA transformation at both high and low concentrations for indigenous microorganisms were sensitive to the transformation capacity. As shown in section F, the model with a low transformation capacity (T_c = 0.01 mg 1,1,1-TCA/mg cells) fit the microcosm data at low concentration well although it slightly under predicted the initial rate of 1,1,1-TCA transformation. The results from section G show that the inclusion of transformation capacity did not help to

Section F: The first addition of 1,1,1-TCA on day 28

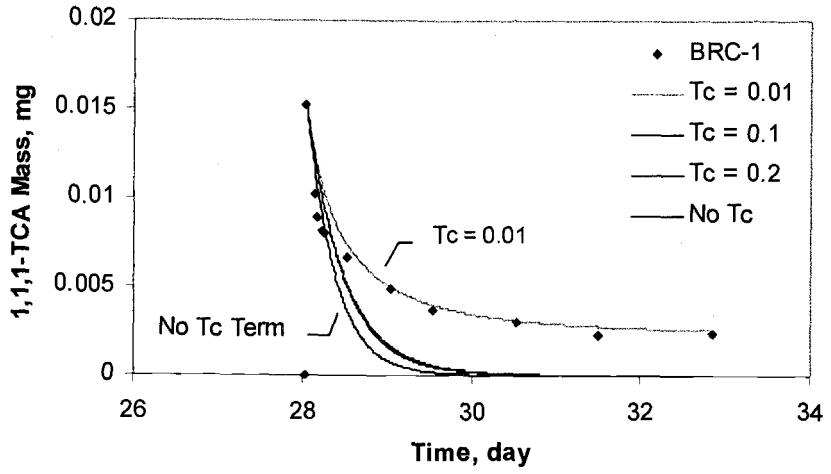

Biomass (X) at starting of model simulation (mg/L)			
$T_c = 0.01$	$T_c = 0.1$	$T_c = 0.2$	No T_c term
19.10	19.10	19.10	19.10

Section G: The second addition of 1,1,1-TCA on day 32

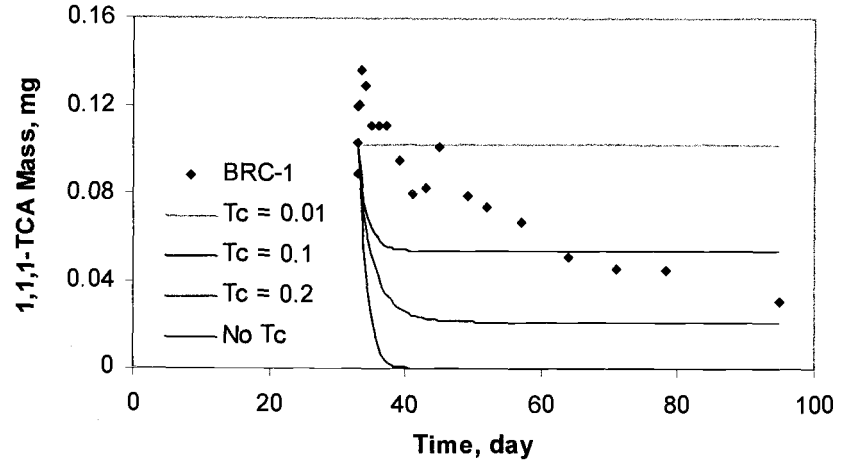

Biomass (X) at starting of model simulation (mg/L)			
$T_c = 0.01$	$T_c = 0.1$	$T_c = 0.2$	No T_c term
0.24	8.23	8.76	9.28

Figure 4.62 Simulations of 1,1,1-TCA transformation for microcosm BRC-1 over a range of transformation capacities

achieve a better fit to the microcosm data. The slow transformation occurring over a long period of time could not be explained. The results from the simulations for the other microcosms are similar as shown in appendix Figures G.46 to G.48. The simulation for microcosm BRC-5 was not performed since no transformation of 1,1,1-TCA occurred. Table 4.28 presents the values of transformation capacity (T_c) for the indigenous microorganisms. The values were obtained from the simulation at low concentration (section F). It is likely that the indigenous microorganisms had a lower transformation capacity than the bioaugmented microorganisms.

Table 4.28 Transformation capacity (T_c) values achieved in the BRC microcosm set

Microcosm	T_c (mg 1,1,1-TCA/mg cells)
BRC-1	0.01
BRC-2	0.01
BRC-3	0.02
BRC-4	0.01
Average	0.01 ± 0.005

Although the model with low transformation capacity fit the microcosm data at low concentrations well, it could not fit the microcosm data at the higher concentrations at later time. One of hypotheses is that the indigenous microorganisms had a different decay rate from the bioaugmented microorganisms. Figure 4.63 presents the simulation of 1,1,1-TCA for microcosm BRC-1 over a range of decay rates (b). In this simulation, the indigenous microorganisms were assumed to have high transformation capacity, as presented in Table 4.29. These values were estimated from the previous simulation of 1,1,1-TCA transformation at high concentrations in section G, Figure 4.62. The values of initial biomass (X = 19.10 mg/L) and the other kinetic parameters including the maximum specific rate of butane utilization ($k_{max,But}$) and 1,1,1-TCA transformation ($k_{max,TCA}$), cell decay rate (b), butane and 1,1,1-TCA half-saturation constants ($K_{s,But}$ and $K_{s,TCA}$), and

cellular yield (Y) were maintained constant from the previous model simulation (Table 4.19). The simulation was sensitive to decay rates at both low and high concentrations. As shown in Figure 4.63, the high decay rate model (b = 1.3 day^{-1}) better fit the microcosm data at low concentrations (section F), but it did not fit the microcosm data at high concentrations (section G). The reason for the slow 1,1,1-TCA transformation in section G was not known. The variation of decay rates did not achieve a good model fit to the microcosm data. This indicates that other kinetic parameters for the indigenous microorganisms are most likely different from those for the bioaugmented microorganisms. The results from the simulations for other microcosms are similar, as shown in appendix Figures G.49 to G.51. Table 4.30 presents the values of decay rate for the indigenous microorganisms. These values were estimated from the simulation at low concentrations (section F). The decay rates ranged from 1.2 to 1.5 day^{-1}. In this case, the high decay rate represented the enzyme decay rate resulting from the 1,1,1-TCA transformation rather than the cell decay rate. Unlike the bioaugmented microcosms, long-term 1,1,1-TCA transformation did not occur in indigenous microcosms.

Table 4.29 Transformation capacity (T_c) values used in the simulation of 1,1,1-TCA transformation for the BRC microcosm set

Microcosm	T_c (mg 1,1,1-TCA/mg cells)
BRC-1	0.1
BRC-2	0.4
BRC-3	0.3
BRC-4	0.6

Section F: The first addition of 1,1,1-TCA on day 28

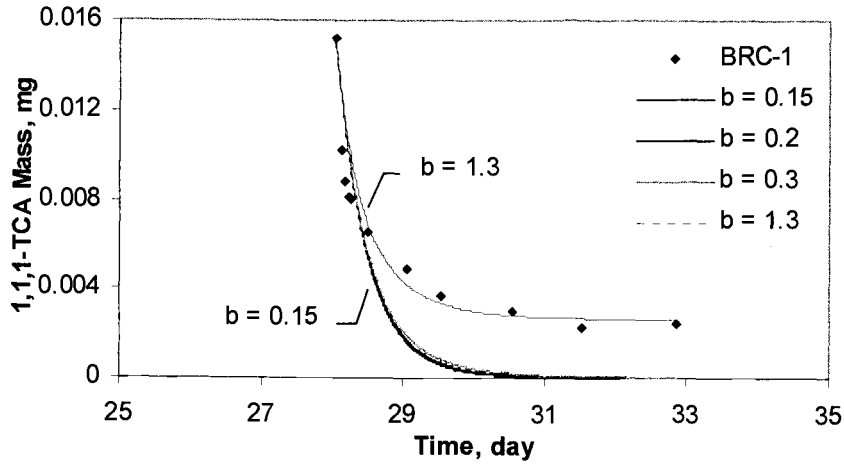

Biomass (X) at starting of model simulation (mg/L)			
b = 0.15	b = 0.2	b = 0.3	b = 1.3
19.10	19.10	19.10	19.10

Section G: The second addition of 1,1,1-TCA on day 32

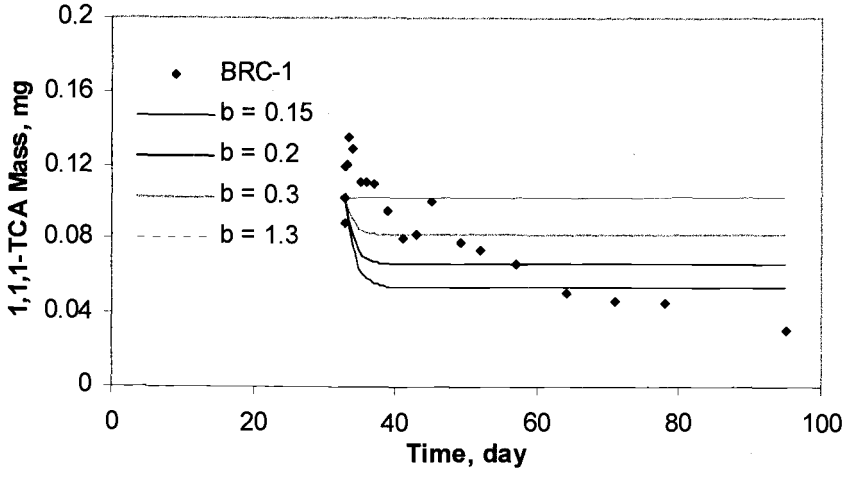

Biomass (X) at starting of model simulation (mg/L)			
b = 0.15	b = 0.2	b = 0.3	b = 1.3
8.23	6.45	3.95	0.026

Figure 4.63 Simulations of 1,1,1-TCA transformation for microcosm BRC-1 over a range of decay rates.

Table 4.30 Decay rate (b) values achieved in the BRC microcosm set

Microcosm	b (day^{-1})
BRC-1	1.3
BRC-2	1.3
BRC-3	1.2
BRC-4	1.5
Average	1.33 ± 0.13

The simulation of 1,1,1-TCA for microcosm BRC-1 over a range of 1,1,1-TCA maximum specific rates ($k_{max,TCA}$) is presented in Figure 4.64. Similar to the previous simulation, the indigenous microorganisms were assumed to have high transformation capacity, as presented in Table 4.29. The values of initial biomass (X = 19.10 mg/L) and the other kinetic parameters including the maximum specific rate of butane utilization ($k_{max,But}$), cell decay rate (b), butane and 1,1,1-TCA half-saturation constants ($K_{s,But}$ and $K_{s,TCA}$), and cellular yield (Y) were also maintained constant from the previous model simulation (Table 4.19). The simulation was sensitive to the $k_{max,TCA}$ values at both low and high concentrations. However, changing only the $k_{max,TCA}$ value did not achieve a good model fit to the microcosm data at both low and high concentrations. The value of 1,1,1-TCA half-saturation constant ($K_{s,TCA}$) is possibly another factor controlling the shape of the model fit at the low concentrations (section F). However, the microcosm data at low concentrations (section F) presented between the models having $k_{max,TCA}$ values ranging from 0.02 to 0.12 mg/mg-day. The slow transformation of 1,1,1-TCA at high concentrations in section G was not greatly explained by the $k_{max,TCA}$. The simulations for other microcosms are similar, as presented in appendix Figures G.52 to G.54. Table 4.31 presents a range of 1,1,1-TCA maximum specific rates ($k_{max,TCA}$) estimated from the simulation at low concentrations (section F). It is impossible to indicate the exact $k_{max,TCA}$ values for the indigenous microorganisms since a good model fit was not obtained. The indigenous microorganisms were likely to have lower $k_{max,TCA}$ values than the bioaugmented microorganisms.

Section F: The first addition of 1,1,1-TCA on day 28

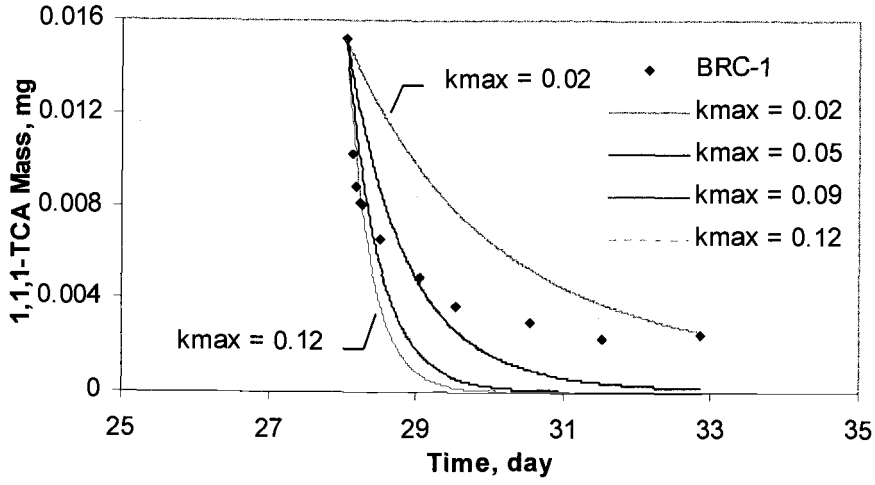

Biomass (X) at starting of model simulation (mg/L)			
$k_{max,TCA}$ = 0.02	$k_{max,TCA}$ = 0.05	$k_{max,TCA}$ = 0.09	$k_{max,TCA}$ = 0.12
19.10	19.10	19.10	19.10

Section G: The second addition of 1,1,1-TCA on day 32

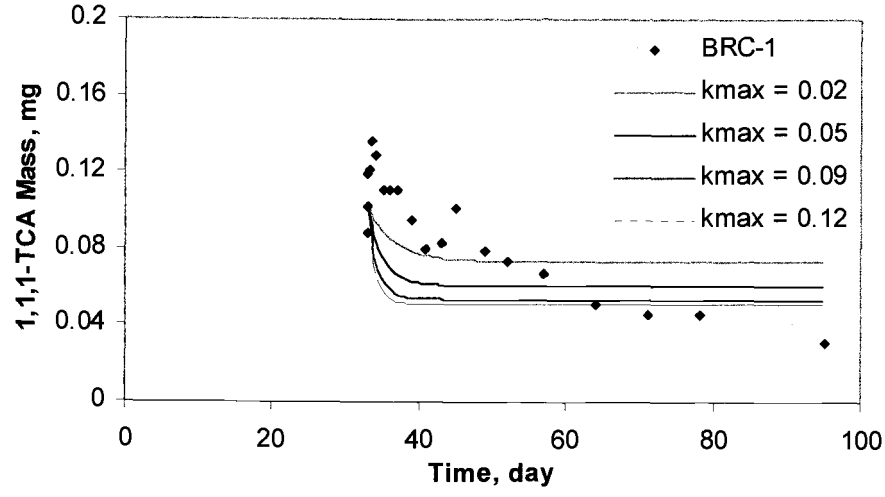

Biomass (X) at starting of model simulation (mg/L)			
$k_{max,TCA}$ = 0.02	$k_{max,TCA}$ = 0.05	$k_{max,TCA}$ = 0.09	$k_{max,TCA}$ = 0.12
8.24	8.17	8.23	8.25

Figure 4.64 Simulations of 1,1,1-TCA transformation for microcosm BRC-1 over a range of 1,1,1-TCA maximum specific rates

Table 4.31 1,1,1-TCA maximum specific rates ($k_{max,TCA}$) values achieved in the BRC microcosm set.

Microcosm	$k_{max,TCA}$ (mg/mg-day)
BRC-1	0.02 – 0.12
BRC-2	0.02 – 0.09
BRC-3	0.02 – 0.05
BRC-4	0.02 – 0.12
Average	0.06 ± 0.046

Figure 4.65 presents the simulation of 1,1,1-TCA for microcosm BRC-1 over a range of 1,1,1-TCA half-saturation constants ($K_{s,TCA}$). The values of initial biomass and all kinetic parameters except $K_{s,TCA}$ were maintained constant from the previous simulations. Good model fits were not achieved by changing only the $K_{s,TCA}$ values. The simulation was sensitive to the $K_{s,TCA}$ values at low concentrations (section F) rather than at high concentrations (section G) since the simulation of initial transformation at high concentrations followed zero-order kinetics. Furthermore, the high K_s values could not explain the slow transformation of 1,1,1-TCA in section G. The results from the simulations for other microcosms are similar as shown in appendix Figures G.55 to G.57. The models with $K_{s,TCA}$ higher than 0.37 mg/L were likely to provide better fit to the microcosm data at low concentrations (section F). Estimates of $K_{s,TCA}$ values for the indigenous microcosms are presented in Table 4.32. The indigenous microorganisms seem to have higher $K_{s,TCA}$ values than the bioaugmented microorganisms.

Section F: The first addition of 1,1,1-TCA on day 28

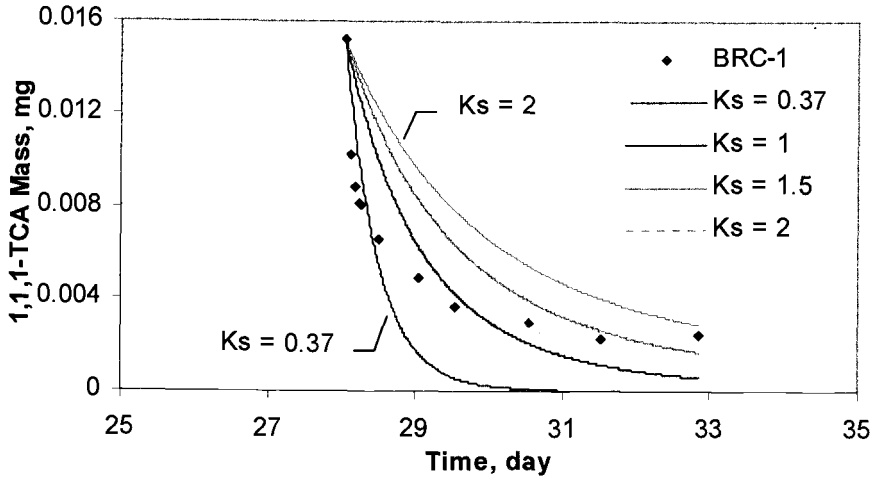

Biomass (X) at starting of model simulation (mg/L)			
$K_{s,TCA}$ = 0.37	$K_{s,TCA}$ = 1	$K_{s,TCA}$ = 1.5	$K_{s,TCA}$ = 2
19.10	19.10	19.10	19.10

Section G: The second addition of 1,1,1-TCA on day 32

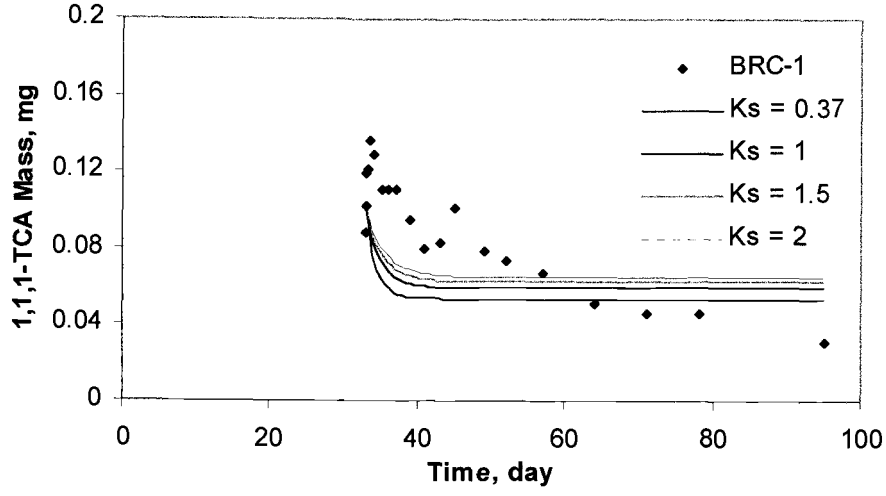

Biomass (X) at starting of model simulation (mg/L)			
$K_{s,TCA}$ = 0.37	$K_{s,TCA}$ = 1	$K_{s,TCA}$ = 1.5	$K_{s,TCA}$ = 2
8.23	8.16	8.20	8.27

Figure 4.65 Simulations of 1,1,1-TCA transformation for microcosm BRC-1 over a range of 1,1,1-TCA half-saturation constants

Table 4.32 1,1,1-TCA half-saturation constant ($K_{s,TCA}$) values achieved in the BRC microcosm set.

Microcosm	$K_{s,TCA}$ (mg/L)
BRC-1	0.37 – 1.5
BRC-2	0.37 – 1.5
BRC-3	0.37 – 2
BRC-4	0.37 – 2
Average	1.06 ± 0.761

Table 4.33 presents the kinetic parameters used for the model development for indigenous microcosms. The model simulations for the indigenous microcosms were conducted by using all kinetic parameters for the BR3 bioaugmented microcosms. The initial biomass in the indigenous microcosms was the average value obtained from the variation in the simulations (Table 4.27). The kinetic parameters in parentheses, including cell decay rate (b), 1,1,1-TCA half-saturation constant ($K_{s,TCA}$) and 1,1,1-TCA maximum specific rate ($k_{max,TCA}$), were estimated from the variation of single kinetic parameter at a time in the simulations using high transformtation capacity.

Table 4.33 Parameters for model development in the BRC microcosm set.

Parameter	Microcosm set B4
X_0, mg/L	0.004 ± 0.002[a]
Y, mg/mg	0.7
b, day^{-1}	0.15 (1.33 ± 0.13)[b]
$K_{s,But}$, mg/L	0.11
$k_{max,But}$, mg/mg-day	2.2
$K_{s,TCA}$, mg/L	0.37 (1.06 ± 0.761)[b]
$k_{max,TCA}$, mg/mg-day	0.09 (0.06 ± 0.046)[b]
T_c, mg /mg	0.01 ± 0.005

Note a = Average value from Table 4.27
b = Obtained from a variation of single kinetic parameter at a time in model simulation using high transformation capacity

Table 4.34 Parameters used in the simulation of butane utilization and 1,1,1-TCA transformation

Parameter	Augmented Microcosm without cell washing			Augmented Microcosm with cell washing	Indigenous Microcosm
	GW/Soil BR3 set	GW/Soil BR4 set	Medium BR4-M	GW/Soil B4 set	GW/Soil BRC set
X_0, mg/L	0.47	0.45	0.45	0.5[a]	0.004 ± 0.002[b]
Y, mg/mg	0.7	0.7	0.7	0.7	0.7
b, day^{-1}	0.15 ± 0.006	0.15	0.15	0.15	0.15 (1.33 ± 0.13)[c]
$K_{s,But}$, mg/L	0.11 ± 0.014	0.11	0.11	0.11	0.11
$k_{max,But}$, mg/mg-day	1.76 ± 0.023	1.79 ± 0.15	2.2	2.2 ± 0	1.76
$K_{s,TCA}$, mg/L	0.37 ± 0.05	0.37	0.37	0.37	0.37 (1.06 ± 0.761)[c]
$k_{max,TCA}$, mg/mg-day	0.09 ± 0.027	0.16 ± 0.038	0.11	0.13 ± 0.0236	0.09 (0.06 ± 0.046)[c]
T_c, mg/mg	0.11 ± 0.064	0.3 ± 0	0.3	0.33 ± 0.103	0.01 ± 0.005
V_L, L	0.1	0.1	0.1	0.075	0.1
V_g, L	0.057	0.057	0.057	0.082	0.057
$H_{cc,But}$, mg-L/mg-L	38.05	38.05	38.05	38.05	38.05
$H_{cc,TCA}$, mg-L/mg-L	0.55	0.55	0.55	0.55	0.55

Note a = Assumed number

b = Obtained from the variation in model simulation (Table 4.27)

c = Estimated from a variation of single kinetic parameter at a time in model simulation using high transformation capacity

Table 4.34 presents the values of parameters for the simulation of butane utilization and 1,1,1-TCA transformation for the BR3, BR4 and B4 bioaugmented microcosm sets, the BR4-M bioaugmented microcosm, and the BRC indigenous microcosm set. The butane and 1,1,1-TCA half-saturation constants ($K_{s,But}$ and $K_{s,TCA}$) and cell decay rate (b) values of the bioaugmented microcosms were obtained from the model simulations in the BR3 microcosm set. The butane and 1,1,1-TCA maximum specific rates ($k_{max,But}$ and $k_{max,TCA}$) and transformation capacity (T_c) values achieved in all bioaugmented microcosms were similar. These microcosms were inoculated with the same culture that was grown at different times. This indicates that the bioaugmented microcosms have a reproducible performance. Additionally, the kinetic parameters obtained from the simulations were not influenced by the addition of nutrients. The consistency of the transformation ability of bioaugmented microorganisms will be required to insure success in field bioaugmentation applications.

Since the kinetic parameters for the BRC indigenous microcosm set could not be determined, the parameters for the BR3 bioaugmented microcosm set were used in the model simulation. The model fit the butane utilization well in early time, but overestimated the butane utilization and 1,1,1-TCA transformation after 10 days of incubation. The results from the simulations showed that the indigenous microorganisms likely had higher values of butane half-saturation constant ($K_{s,But}$) and cell decay rate (b), and lower values of butane and 1,1,1-TCA maximum specific rate ($k_{max,But}$ and $k_{max,TCA}$) than the bioaugmented microorganisms. However, the slower butane utilization could have been caused by the other factors, possibly nutrient limitation. The results also indicated that the indigenous microorganisms had lower transformation capacity than the bioaugmented microorganisms.

The values of decay rate (b), 1,1,1-TCA maximum specific rate ($k_{max,TCA}$), and 1,1,1-TCA half-saturation constant ($K_{s,TCA}$) in parentheses were estimated from the variation of a single kinetic parameter at a time. In these simulations, the indigenous microorganisms were assumed to have high transformation capacity. It

was difficult to determine how the values differed for the indigenous microorganisms compared to the bioaugmented microorganisms. The indigenous microorganisms potentially had higher decay rates, higher 1,1,1-TCA half-saturation constants and lower 1,1,1-TCA maximum specific rates than the bioaugmented microorganisms. The estimated value of high decay rate possibly represented the enzyme decay rate resulting from the 1,1,1-TCA transformation rather than the cell decay rate.

Different butane-utilizing cultures are likely present in the indigenous and bioaugmented microcosms. A slower rate of 1,1,1-TCA transformation was probably due to the indigenous microorganisms being less effective towards 1,1,1-TCA transformation. Unlike the bioaugmented microcosms, TCA transformation in the indigenous microcosms was not active over long periods of time. However, the model construct that was used could not accurately model the results obtained in the indigenous microcosms. The model did a much better job simulating the results obtained in the bioaugmented microcosms. This was partly due to better estimations of vital model parameters.

CHAPTER 5
SUMMARY AND ENGINEERING SIGNIFICANCE

5.1 SUMMARY

Microcosm studies were conducted to develop a culture to be bioaugmented into the subsurface for the cometabolic treatment of 1,1,1-TCA, TCE and 1,1-DCE. The culture was tested in groundwater and aquifer solid microcosms that mimic conditions where a field test was to be performed. The culture was originally acquired from existing microcosms (Jitnuyanont 1998) used for the 1,1,1-TCA transformation tests.

The results presented in these studies demonstrated that all propane- and butane-utilizers in the existing microcosms could cometabolically transform 1,1,1-TCA. The indigenous propane and butane-utilizers transformed TCA more slowly and had lower transformation yields than bioaugmented microorganisms (Table 4.2). The bioaugmented propane- and butane-utilizers showed long-term transformation ability for 1,1,1-TCA in the absence of butane utilization, indicating that the enzyme system responsible for transformation was present and active long after the substrate was utilized. After prolonged treatment, transformation efficiency in bioaugmented propane-utilizing microcosms decreased. The final transformation yields of bioaugmented propane-utilizers were lower than the average transformation yields. Unlike bioaugmented propane-utilizers, bioaugmented butane-utilizers maintained transformation yield values over the study period. The bioaugmented butane-utilizers also showed longer 1,1,1-TCA transformation periods in the absence of butane utilization than the bioaugmented propane-utilizers. To ensure that there was sufficient active biomass, the final transformation yield was used to determine which microcosm was suitable for the bioaugmentation of additional microcosms. The maximum final transformation

yields in bioaugmented propane- and butane-utilizers were 0.019 and 0.036 mg TCA/mg substrate. Thus bioaugmented butane-utilizers in microcosm B6 were chosen to be the parent microcosm for bioaugmentation studies.

Similar to the butane-utilizers in parent microcosm B6, the butane-utilizers in all bioaugmented microcosms were able to transform 1,1,1-TCA over long periods in the absence of butane utilization. The indigenous butane-utilizers showed less ability to transform 1,1,1-TCA than those in the existing microcosms (Jitnuyanont, 1998). Thus the bioaugmented microcosms had more reproducible performance than the non-augmented microcosms.

The slurry-inoculated and media-culture inoculated microcosms (B2 and B4 sets) had similar values of average transformation yield, 0.079 ± 0.005 and 0.061 ± 0.012 mg TCA/mg butane, respectively. Jitnuyanont (1998) reported a similar transformation yield for butane-utilizers, which was determined during the first 190 days of incubation (0.07 mg TCA/mg butane). Although all bioaugmented butane-utilizers behaved similarly during the first 10 days of incubation, slurry-inoculated microcosms (B3 set), which contained no aquifer solids but only mineral salts growth media, showed much lower transformation ability. The transformation yield for the B3 microcosm set was 0.024 ± 0.001 mg TCA/mg butane, which was two to three times less than the other microcosm sets.

The transformation rates of 1,1,1-TCA in the slurry-inoculated and media-culture inoculated microcosms (B2 and B4 sets) were also measured in the absence of butane. The values of the pseudo first-order rate parameter ($k_{max}X_0/K_s$) and cell decay rate (b) for these microcosms were determined through the rate regression method. The transformation rates were assumed to follow first-order kinetics. The average cell decay rates in both slurry-inoculated and media-culture inoculated microcosms (B2 and B4 sets) were similar (Table 4.5). The pseudo-first-order rate parameters ($k_{max}X_0/K_s$) were within a factor of two of each other (Table 4.5). This could have resulted from the different amounts of microbial cells in two inoculums, and indicates kinetic factors did not change significantly.

The similarity of transformation yields and cell decay rates between the slurry-inoculated and media-culture inoculated microcosms (B2 and B4 sets) suggest that growing the culture on growth media before bioaugmentation might not change the activity of the microbial community. However, the mixed cultures probably changed when growing in mineral salts growth media for longer than 20 days, as indicated by the differences in transformation yields.

Competitive inhibition of 1,1,1-TCA transformation by butane was observed. The results from rate measurements demonstrated that the decrease in transformation rate at high concentration, ranging from 1,500 to 2,600 μg/L, tends to correlate with the mass of transformed 1,1,1-TCA rather than with time, while at low concentration, ranging from 300 to 500 μg/L, the decrease in rate tends to correlate with either time or the amount of 1,1,1-TCA transformed. It may be that repeated transformation of low amounts of 1,1,1-TCA did not drain energy reserves, but served to induce enzyme activity. Additionally, limited and slow transformation of 1,1,1-TCA appears to be correlated with a slow rate of butane uptake. 1,1,1-TCA transformation product toxicity, a drain in energy reserves, and cell decay might all be contributing to this loss in activity.

In addition to 1,1,1-TCA, the bioaugmented butane-utilizers were able to transform other chlorinated solvents such as 1,1-DCE and TCE. Initial aqueous concentrations of 1,1,1-TCA, TCE, and 1,1-DCE ranged from 390 to 590 μg/L, 540 to 1400 μg/L, and 100 to 730 μg/L, respectively. The transformation of 1,1-DCE was very fast, while the transformation rate of 1,1,1-TCA and TCE were slower. The inhibition of 1,1,1-TCA and TCE transformation by 1,1-DCE was also observed. The transformation efficiency decreased with mass of chlorinated solvent mixture transformed. Transformation product toxicity from chlorinated solvents, especially from 1,1-DCE, and possibly TCE at high concentrations, was suspected to be the major cause of the limited transformation of chlorinated solvents and the cessation in butane utilization.

Based on the good performance of 1,1,1-TCA transformation, bioaugmented butane-utilizers in microcosm B2-1 was chosen to be the culture seed to obtain a uniform culture for use in bioaugmentaion studies both in the laboratory and in field tests. The culture was grown in mineral salt media, harvested, placed in 1 ml vials with 7%DMSO (Dimethyl Sulfoxide), and stored in −196 °C liquid nitrogen for future studies. When the cultures were harvested, the measured OD_{600} was approximate 0.36. The calculated yield was around 0.7 mg cell / mg butane, and the density of the frozen culture was 2500 mg TSS /L.

Microcosm studies using the frozen butane-utilizing culture were conducted to compare 1,1,1-TCA transformation ability between indigenous and bioaugmented butane-utilizers. No 1,1,1-TCA transformation was observed in the indigenous microcosms. With long-term exposure to 1,1,1-TCA, the rate of butane utilization in the indigenous microcosms slowed. The microcosms bioaugmented with the frozen butane-utilizing culture showed the same performance as the microcosms bioaugmented with slurry. Long-term transformation of 1,1,1-TCA in the absence of butane utilization was achieved at rapid rates. The values of cell decay rate in the frozen-culture inoculated microcosms were determined through the rate regression method (Table 4.8). These values were similar to those in the slurry-inoculated and media-culture inoculated microcosms. This indicates that the mixed cultures are likely similar after being kept in the frozen condition and then grown in media before bioaugmentation. The transformation of a mixture of chlorinated solvents, 1,1,1-TCA, 1,1-DCE and TCE, also shows similar trends. The transformation rate of 1,1-DCE was the fastest, while the transformation rate of 1,1,1-TCA and TCE were slower. The competitive inhibition of 1,1,1-TCA and TCE transformation by butane and 1,1-DCE was observed. After transforming the mixture of these chlorinated solvents, the rates of butane utilization and chlorinated solvent transformation slowed down.

Results from the kinetic experiments demonstrated that the butane and 1,1,1-TCA half-saturation constants ($K_{s,But}$ and $K_{s,TCA}$) in the frozen-culture bioaugmented microcosms (BR3 and BR4 sets) were similar (Table 4.14). These

microcosms were bioaugmented with frozen butane-utilizing cultures after one growth step in mineral media, but from batches of cells grown at different times. This illustrates the very reproducibility of the bioaugmentation process. The values of butane and 1,1,1-TCA half-saturation constant ($K_{s,But}$ and $K_{s,TCA}$) for the indigenous microcosms could not be determined from kinetic experiments since the butane utilization and 1,1,1-TCA transformation was slow, and 1,1,1-TCA transformation stopped after the microcosms were exposed to the second addition of TCA (800 μg/L).

The results of microcosm studies in the BR3, BR4 and B4 bioaugmented microcosm sets, and the BRC non-augmented microcosm set were selected to conduct a model simulation of butane utilization and 1,1,1-TCA transformation. Values of kinetic parameters were determined including the maximum specific rate of butane utilization ($k_{max,But}$) and 1,1,1-TCA transformation ($k_{max,TCA}$), cell decay rate (b), and transformation capacity (T_c). The bioaugmented microcosms were inoculated with the media-culture from batches of cells grown at different times. The bioaugmented cultures in the BR3 and BR4 microcosm sets were not washed with groundwater to rinse away the mineral salts media prior to inoculation, while the cultures bioaugmented in the B4 microcosm set were washed.

The results from the simulation of butane utilization and 1,1,1-TCA transformation for the BR3 bioaugmented microcosm set showed that the model fit data well at both and high TCA concentrations (Figure 4.47). The butane and 1,1,1-TCA half-saturation constants ($K_{s,But}$ and $K_{s,TCA}$) obtained from the kinetic experiment provided good matches between the simulation and the microcosm results. The model started to deviate from the microcosm data at later time. Little improvement was obtained by including a transformation capacity term. The results from the data at low concentrations were not sensitive to the transformation capacity term, since the mass of TCA transformed was much less than the transformation capacity term (Figure 4.52). The lack of sensitivity to transformation capacity was also due to the high amount of biomass available. Fits to the transformation capacity model were obtained from microcosm data at high

concentrations. The values of kinetic parameters including maximum specific rate of butane utilization ($k_{max,But}$) and 1,1,1-TCA transformation ($k_{max,TCA}$), cell decay rate (b), and transformation capacity (T_c) were similar among the microorganisms in the BR3 bioaugmented microcosm set (Tables 4.16 to 4.18). Again, this indicates the reproducibility of bioaugmentation process.

The microcosm data of butane utilization and 1,1,1-TCA transformation in the BR4 bioaugmented microcosm set and the BR4-M bioaugmented microcosm were modeled by using the same butane and 1,1,1-TCA half-saturation constant ($K_{s,But}$ and $K_{s,TCA}$), cellular yield (Y), and cell decay rate (b) values as the BR3 microcosm set (Figures 4.53 to 4.54). Reasonable fits between the model simulation and data were obtained. The results from the 1,1,1-TCA transformation at early time were not sensitive to the transformation capacity term (Figures 4.55a and 4.55b). This was possibly due to the high transformation capacity of 1,1,1-TCA. The simulation of 1,1,1-TCA transformation at later time still had low sensitivity at low concentrations, but became more sensitive at higher concentrations (Figures 4.55e and 4.55f). The high biomass also made the simulation less sensitive to the transformation capacity values. The bioaugmented microorganisms had high transformation capacity (0.3 mg 1,1,1-TCA/mg cells). The results from the model simulation at the tested concentration showed little difference between having no transformation term ($T_c = \infty$) and a T_c value of 0.3 mg/mg. Although the effect of the transformation product toxicity was included in the simulation, it did not improve the model fit to the data. The slower butane uptake rate at later time may be caused by nutrient limitations. Effects of enzyme induction or a change of microbial community that were not included in the model simulations are possible factors resulting in the higher transformation rates. All bioaugmented microcosms, either constructed with groundwater and aquifer material (BR4 set) or containing only growth media (BR4-M), had similar kinetic parameter values (Table 4.20). This indicates the reproducibility of bioaugmentation process, and indicates the same butane-utilizing microbial activity is present in both media and groundwater microcosms.

The results from the model simulation for the B4 bioaugmented microcosm set demonstrated that the model fit the data well after day 20 (Figures 4.57 to 4.58). The rate of butane utilization during the 10 days of incubation was slower than the model prediction. This implies that the values of $k_{max,But}$ between the two periods are possible different. Additionally, the slower butane utilization rate was probably due to the inhibition of 1,1,1-TCA, which was not considered in the model. The model also overestimated butane utilization and 1,1,1-TCA transformation at later time. The inclusion of a transformation capacity term did not help to achieve a better fit to the data (Figure 4.59). The model with no or high transformation capacity term ($T_c = \infty$ or $T_c = 0.4$ mg/mg) better fit the data at early time, while it under predicted the transformation of 1,1,1-TCA at later time. The slower transformation of 1,1,1-TCA at later time could not be completely explained by incorporating the transformation capacity term. Slow deactivation of enzyme might be another factor, resulting in a decrease of $k_{max,TCA}$ as a function of the mass of 1,1,1-TCA transformed. Other factors, such as the change of microbial community, cannot be ruled out. The cell decay rate obtained from the rate measurement of 1,1,1-TCA transformation was higher than that from the simulation of butane utilization (Table 4.24). The higher b value probably represents both cell and enzyme decay rate. The values of pseudo-first-order rate parameter ($k_{max}X_0/K_s$) obtained from the model simulation were higher than that from the rate regression method (Table 4.24). This was possibly due to the higher value of initial biomass (X_0) in the model simulation since the value of cell decay rate (b) from the model simulation was lower than that obtained from the rate regression measurement. The results obtained from the model simulations and the rate measurements indicate the practicality of the simplified analysis in the rate regression measurement. The rate regression method provided fairly reasonable values of the pseudo-first-order rate parameter ($k_{max}X_0/K_s$), within factor of 2. A good agreement between the values of pseudo-first-order rate parameter ($k_{max}X_0/K_s$) and cell decay rate (b) was also obtained.

The values of butane maximum specific utilization rate ($k_{max,But}$), TCA maximum specific transformation rate ($k_{max,TCA}$) and transformation capacity (T_c) in the B4 bioaugmented microcosm set were similar and also similar to those of the BR3 and BR4 bioaugmented microcosm sets (Table 4.34). This indicates that the bioaugmented microorganisms have very reproducible performance. Additionally, the kinetic parameters obtained from the simulations were not influenced by the addition of nutrients over a one-month period of operation.

The simulations of butane utilization and TCA transformation for the indigenous microcosms were conducted by using the same kinetic parameters as the BR3 bioaugmented microcosm set (Figure 4.60). The model fit the butane utilization well in early time, but it overestimated the butane utilization and 1,1,1-TCA transformation after 10 days of incubation. The results from these simulations showed that the indigenous microorganisms potentially had higher values of butane half-saturation constant ($K_{s,But}$) and cell decay rate (b), and lower values of butane and TCA maximum specific rate ($k_{max,But}$ and $k_{max,TCA}$) than the bioaugmented microorganisms. However, the slower rate of butane utilization may have been caused by the other factors such as nutrient limitations. The indigenous microorganisms had ten to thirty times lower transformation capacity (T_c) values than the bioaugmented microorganisms (Table 4.28). However, the inclusion of transformation capacity could not explain the slow transformation of 1,1,1-TCA at later time (Figure 4.62). Additionally, changing the value of only one kinetic parameter at a time could not achieve a good fit between model and microcosm data. Results from the sensitivity analysis of the simulation using high transformation capacity show that the indigenous microorganisms seem to have either higher values of decay rate (b) and TCA half-saturation constant ($K_{s,TCA}$), or lower values of 1,1,1-TCA maximum specific rate ($k_{max,TCA}$) than the bioaugmented microorganisms (Table 4.34). A best combination of these values was not determined. The very high value of decay rate possibly represented the rapid enzyme decay rate resulting from the TCA transformation rather than the cell decay rate.

Different butane-utilizing cultures are likely present in the indigenous and bioaugmented microcosms. A slower rate of TCA transformation was probably due to the indigenous microorganisms being less effective towards TCA transformation. Unlike the bioaugmented microcosms, TCA transformation in the indigenous microcosms was not active over long periods of time without butane present.

5.2 ENGINEERING SIGNIFICANCE

The transformation of chlorinated solvents including TCE, t-DCE, c-DCE and VC through aerobic cometabolism by indigenous methane-, phenol-, and toluene-utilizing cultures has been found in the Moffett field (Mountain View, CA) (Semprini et al., 1990; Semprini et al., 1991; Hopkins et al., 1993; Hopkins et al., 1995). However, the transformation of 1,1,1-TCA, the major contaminant in th native groundwater, was not observed. Jitnuyanont (1998) found that propane- and butane-oxidizing bacteria were more effective in 1,1,1-TCA transformation, and that bioaugmentation was a good strategy to reduce the long lag time required to stimulate the indigenous microorganisms. The transformation of 1,1,1-TCA and other CAHs, including TCE, and 1,1-DCE, by both indigenous and bioaugmented propane-and butane-utilizers was further studied in order to develop the appropriate cultures for bioaugmentation studies both in the laboratory and the field tests.

In this study, both propane- and butane-utilizers in the existing microcosms (Jitnuyanont, 1998) could cometabolically transform 1,1,1-TCA. However, the transformation efficiency in bioaugmented propane-utilizers decreased after prolong treatment, while bioaugmented butane-utilizers maintained transformation yield values over the study period. As a result, the mixed butane-utilizing culture was developed for bioaugmentation studies.

The bioaugmented microcosms had reproducible performance, maintaining the transformation ability. The indigenous butane-utilizers transformed 1,1,1-TCA

less effectively, and their transformation abilities were inconsistent. Thus bioaugmentation will likely be required to insure success in the field demonstration. The transformation efficiency of bioaugmented butane-utilizers decreased with continued transformation of 1,1,1-TCA. After the transformation of a mixture of 1,1,1-TCA, TCE and 1,1-DCE, a limitation of butane utilization and chlorinated transformation was also observed. This probably resulted from transformation product toxicity, especially from 1,1-DCE. Reinoculating the cultures could be another strategy to maintain the transformation performance.

Bioaugmentation is a good strategy for enhancing bioremediation when indigenous microorganisms are unable to degrade the existing contaminants. The inability of indigenous microorganisms to degrade existing contaminants is probably due to the lack of the appropriate enzyme(s), low population of microorganisms, and contaminant toxicity. Augmentation with proven contaminant-degrading microorganisms can lead to a higher degree of confidence in remediation success, and can also eliminate long lag periods required to stimulate indigenous microorganisms.

To produce reliable bioaugmentation cultures, the developed cultures were stored with 7%DMSO (Dimethyl Sulfoxide) in –196 °C liquid nitrogen. Prior to use, the frozen cultures were thawed, washed with growth media to rinse away DMSO and then grown in mineral salts growth media. The growth media used for culture development is presented in appendix A.3.

The kinetic parameters for butane utilization and 1,1,1-TCA transformation were also evaluated by modeling the results of microcosm studies. The kinetics of cometabolism is an important factor for application of bioremediation. Predictive models for the cometabolic process will be useful for engineering design to plan and monitor site remediation, to conduct risk and exposure assessments and also to evaluate the project cost and duration. (Alvarez-Cohen and McCarty, 1991a; Semprini et al., 1998). The kinetic parameters obtained from these microcosm studies can now be used in modeling the field demonstration.

BIBLIOGRAPHY

Alvarez-Cohen, L. and P.L. McCarty. 1991a. A cometabolic biotransformation model for halogenated aliphatic compounds exhibition product toxicity. *Appl. Environ. Microbiol.* 25: 1381-1387.

Alvarez-Cohen, L. and P.L. McCarty. 1991b. Effects of toxicity, aeration, and reductant supply on trichloroethylene transformation by a mixed methanotrophic culture. *Appl. Environ. Microbiol.* 57: 228-235.

Alvarez-Cohen, L. and P.L. McCarty. 1991c. Product toxicity and cometabolic competitive inhibition modeling of chloroform and trichloroethylene transformation by methanotrophic resting cells. *Appl. Environ. Microbiol.* 57: 1031-1037.

Alvarez-Cohen L. and Jr. G.E Speitel. Kinetics of aerobic cometabolism of chlorinated solvents biodegradation. Submitted in *Biodegradation.* In press.

American Public Health Association. 1985. Standard methods for the examination of water and wastewater. 16th edition. APHA, New York, NY.

Arvin, E. 1991. Biodegradation kinetics of chlorinated aliphatic hydrocarbons with methane oxidizing bacteria in an aerobic fixed biofilm reactor. *Wat. Res.* 25: 873-881.

Barcelona, M., Wehrmann, J.F. Keely and W.A. Pettyjojn. 1990. *Contamination of ground water preventation, assessment, restoration.* Noyes Data Corporation, Park Ridge, NJ.

Baud-Grasset, F. and T.M.Vogel. 1995. Bioaugmentaion: Biotreatment of Contaminated Soil by Adding Adapted Bacteria. In *Bioaugmentation for site Remediation*; Hinchee, R.E., Fredrickson, J., Alleman, B.C., Eds.; Battlle Press, Columbus, OH; pp 39-56.

Broholm, K., B.K. Jensen, T.H. Christensen and L. Olsen. 1990. Toxicity of 1,1,1-trichroloethane and trichloroethene on a mixed culture of methane-oxidizing bacteria. *Appl. Environ. Microbiol.* 56: 2488-2493.

Chang, H.L. and L. Alvarez-Cohen. 1995a. Model for the cometabolic biodegradation of chlorinated organics. *Environ. Sci. Technol.* 29: 2357-2367.

Chang, H.L. and Alvarez-Cohen. 1995b. Transformation capacities of chlorinated organics by mixed cultures enriched on methane, propane, toluene, or phenol. *Biotechnology and Bioengineering.* 45: 440-449.

Chang, W. and C.S. Criddle. 1997. Experimental evaluation of a model for cometabolism: prediction of simulataneous degradation of trichloroethylene and methane by a methanotrophic mixed culture. *Biotechnology and Bioengineering.* 56: 1492-501.

Davis, J.B. 1964. Cellular lipids of a *Nocardia* grown on propane and n-butane. *Appl. Environ. Microbiol.* 12: 301-304.

Doong, R. and S. Wu. 1996. Effect of substrate concentration on the biotransformation of carbon tetrachloride and 1,1,1-trichloroethane under anaerobic condition. *Wat. Res.* 30: 577-586.

Duba, A.G., K.J. Jackson, M.C. Jovanovich, R.B. Knapp and R.T. Taylor. 1996. TCE remediation using in situ, resting-state bioaugmentation. *Environ. Sci. Technol.* 30: 1982-1989.

Dybas, J.M., M. Barcelona, S. Bezborodnikov, S. Davies, L. Forney, H. Hewer, O. Kaaka, T. Mayotte, L. Sepulveda-Torres, K. Smalla, M. Sneathen, J. Tiedje, T. Voice, D.C. Wiggert, M.E. Witt and C.S. Criddle. 1998. Pilot-scale evaluation of bioaugmentation for in-situ remediation of a carbon tetrachloride-contaminated aquifer. *Environ. Sci. Technol.* 32: 3598-3611.

Ellis D.E., E.J. Lutz, J.M. Odom, R.J. Buchanan, JR., C.L. Bartlett, M.R. Harkness and K.A. Deweerd. 2000. Bioaugmentation for accelerated in situ anaerobic bioremediation. *Environ. Sci. Technol.* 34: 2254-2260.

Federal Register. 1989. National primary and secondary drinking water regulations; proposed rule *Fed. Regist.* 54: 22062-22160.

Galli, R. and P.L. McCarty. 1989. Kinetics of Biotransformation of 1,1,1-Trichloroethane by Clostridium sp. Strain TCAIIB. *Appl. Environ. Microbiol.* 55: 845-851.

Henry, S.M. and D. Grbic-Galic. 1991. Influence of endogenous and exogenous electron donors and trichloroethylene oxidation toxicity on trichloroethylene oxidation by methanotrophic cultures from a groundwater aquifer. *Appl. Environ. Microbiol.* 57: 236-244.

Hommes, N.G., S.A Russell, P.J. Bottomley and D.J. Arp. 1998. Effects of soil on ammonia, ethylene, chloroethane, and 1,1,1-trichloroethane oxidation by *Nitrosomonas europaea. Appl. Environ. Microbiol.* 64: 1372-1378.

Hopkins, G.D., L. Semprini and P.L. McCarty. 1993. Microcosm and in situ field studies of enhanced biotransformation of trichloroethylene by phenol-utilizing microorganisms. *Appl. Environ. Microbiol.* 59: 2277-2285.

Hopkins, G.D. and P.L. McCarty. 1995. Field evaluation of in situ aerobic cometabolism of trichloroethylene and three dichloroethylene isomers using phenol and toluene as the primary substrates. *Environ. Sci. Technol.* 29: 1628-1637.

Hou, C.T., R. Patel, E.I. Lanskin, N. Barnabe and I. Barist. 1983. Epoxidation of short-chain alkenes by resting-cell suspensions of propane-grown bacteria. *Appl. Environ. Microbiol.* 46: 171-177.

Imano S., T. Ohashi, K. Iwasaki and O. Yagi. 1999. Biodegradation of trichloroethylene by propane-utilizing bacterium *Mycobacterium* sp. TCE28. In *Engineered Approaches for In Situ Bioremediation of Chlorinated Solvent Contamination*; Leeson, A., Allenman, B.C., Eds.; Battelle Press, Columbus, OH; pp 95-100.

Janssen, D.B., A.J.v.d. Wijingaard, J.J.v.d. Waarde and R. Oldenhuis. 1991. Biochemistry and kinetics of aerobic degradation of chlorinated aliphatic hydrocarbons. In *On-site Bioreclamation Process for Xenobiotic and Hydrocarbon Treatement*; Hinchee, R.E., Olfenbuttel, R.F., Eds.; Butterworth-Heinemann, Stonehame, MA; pp 92-113.

Jitnuyanont, P. 1998. Comparison of indigenous and bioaugmented butane and propane-utilizers for transforming of 1,1,1-trichloroethane in Moffett Field microcosms. M.S. Thesis. Oregon State University, Corvallis, OR.

Keenan, J.M., S.E. Strand, and H.D. Stensel. 1994. Degradation kinetics of chlorinated solvents by a propane-oxidzing enrichment culture. In *Bioremediation of Chlorinated and Polycyclic Aromatic Hydrocarbon Compounds*; Hinchee, R.E., Leeson, A., Semprini, L., Kong, S., Eds.; Lewis Publishers, Boca Ratan, FL; pp 1-13.

Kim, Y. 1996. Aerobic cometabolism of chloroform by butane-and propane grown microorganisms from the Hanford subsurface. M.S. Thesis. Oregon State University, Corvallis, OR.

Kim, Y., L. Semprini and D.J. Arp. 1997. Aerobic cometabolism of chloroform and 1,1,1-trichloroethane by butane-grown microorganisms. *Journal of Bioremediation.* 1: 135-148.

Malachowsky, K.J., T.J. Phelps, A.B. Teboli, D.E. Minnikin and D.C. White. 1994. Aerobic mineralization of trichloroethylene, vinyl chloride, and aromatic compounds by *Rhodococcus species. Appl. Environ. Microbiol.* 60: 542-548.

Martin, A. 1994. *Biodegradation and bioremediation.* Academic Press, Inc., Sandiego, CA.

Mayotte, T.J., M.J. Dybas and C.S. Criddle. 1996. Bench-scale evaluation of bioaugmetation to remediate carbon tetrachloride contaminated aquifer materials. *Ground Water.* 34: 358-367.

Mackay, D. and W.Y. Shiu. 1982. Critical review of Henry's law constants for chemicals of environment interest. *J. Phys. Chem. Ref. Data.* 10: 1175-1199.

McCarty P.L. 1997 Aerobic Cometabolism of chlorinated aliphatic hydrocarbons. In *Subsurface Restoration*; Ward, C.H., Cherry, J.A., Scalf, M.R., Eds.; Ann Arbor Press, Inc., Chelsea, MI; pp 373-395.

McLee, A.G., A.C. Kormendy and M. Wayman. 1972. Isolation and characterization of n-butane-utilizing microorganisms. *Canadian Journal of Microbiology.* 18: 1191-1195.

Munakata-Marr, J., P.L. McCarty, M.S. Shields, M. Reagina nd S.C. Francesconi. 1996. Enhancement of trichloroethylene degradation in aquifer microcosms bioaugmented with wild Type and genetically altered *Burkholderia (Pseudomonas) cepacia* G4 and PR1. *Environ. Sci Technol.* 30: 2045-2052.

Oldenhuis, R., R.J.M. Vink, D.B. Janssen and B. Witholt. 1989. Degradation of chlorinated aliphatic hydrocarbons by *Methylosinus trichosporium* OB3 expressing soluble methane monooxygenase *Appl. Environ. Microbiol.* 55: 2819-2826.

Oldenhuis, R., J.Y. Oedzes, J.J. Waarade and D.B. Janssen. 1991. Kinetics of chlorinated hydrocarbon degradation by *Methylosinus trichosporium* OB3b and toxicity of trichloroethylene. *Appl. Environ. Microbiol.* 57: 7-14.

Perry, J.J. 1980. Propane utilization by microorganism. *Adv. Appl. Microbiol.* 26: 89-115.

Philips, W.E. and J.J. Perry. 1974. Metabolism of n-butane and 2-butanol by *Mycobacterium vaccae. Journal of Bacteriology.* 120: 987-989.

Robert, P.V., G.D. Hopkins, D.M. Mackay and L. Semprini. 1990. A field evaluation of in-situ biodegradation of chlorinated ethenes: part 1, methodology and field site characterization. *Ground Water.* 28: 591-604.

Salanitro, J.P., P.C. Johnson, G.E. Spinnler, P.M. Maner, H.L. Wisniewski and C. Bruce. 2000. Field-scale demonstration of enhanced MTBE bioremediation through aquifer bioaugmentation and oxygenation. *Environ. Sci. Technol.* 34: 4152-4162.

Semprini, L., G.D. Hopkins, P.V. Roberts, D. Grbic-Galic and P.L. McCarty. 1991. A field evaluation of in-situ biodegradation of chlorinated ethenes: part 3, studies of competitive inhibition. *Ground Water.* 29: 239-250.

Semprini, L., P.V. Roberts, G.D. Hopkins and P.L. McCarty. 1990. A field evaluation of in-situ biodegradation of chlorinated ethenes: part 2, cometabolic transformations. *Ground Water.* 28: 715-727.

Semprini, L., R.L Ely and M.M. Lang. 1998. Modeling of cometabolism for the in situ biodegradation of trichloroethylene and other chlorinated aliphatic hydrocarbons. *Bioremediation.* 1: 89-134.

Speitel JR. G.E., R.C. Thomson and D. Weissman. 1993. Biodegradation kinetics of *Methylosinus Trichosporium* OB3b at low concentrations of chloroform in the presence and absence of enzyme competition by methane. *Wat. Res.* 27: 15-24.

Stephens, G.M. and H. Dalton. 1986. The role of the terminal and subterminal oxidation pathways in propane metabolism by bacteria. *Journal of General Microbiology* 132: 2453-2462.

Strand, S.E., M.D. Bjelland, and H.D. Stensel. 1990. Kinetics of chlorinated hydrocarbon degradation by suspended cultures of methane-oxidizing bacteria. *Research Journal WPCF.* 62: 124-129.

Tovanabootr, A. 1997. Aerobic cometabolism of chlorinated aliphatic hydrocarbons by subsurface microbes grown on methane, propane, and butane from McClellan Air Force Base. M.S. Thesis. Oregon State University, Corvallis, OR.

Van-Ginkel, C.G., H.G.J. Welten, S. Hartmans, and J.A.M.D. Bont. 1987. Metabolism of trans-2-butane and butane in *Novardia* TB1. *Journal of General Microbiology.* 133: 1713-1720.

Vogel, T.M. 1996. Bioaugmentation as a soil bioremediation approach. *Biotechnology.* 7: 311-316.

Vogel, T.M. and P.L. McCarty. 1987. Rate of abiotic formation of 1,1-dichloroethylene from 1,1,1-trichloroethane in groundwater. *Journal of Contaminant Hydrology.* 1: 299-308.

Vogel, T.M., C.S. Criddle and P.L McCarty. 1987.Transformations of halogenated aliphatic compounds. *Environ. Sci. Technol.* 21: 722-736.

Vogel, T.M. and P.L. McCarty. 1987. Abiotic and biotic transformations of 1,1,1-trichloroethane under methanogenic conditions. *Environ. Sci. Technol.* 21: 1208-1213.

Wackett, L.P. and D.T. Gibson. 1988. Degradation of trichloroethylene by toluene dioxygenase in whole-cell studies with *Pseudomonas putida* F1. *Appl. Environ. Microbiol.* 54: 1703-1708.

Wackett, L.P., G.A. Brusseau, S.R. Householder, and R.S. Hanson. 1989. Survey of microbial oxygenase: trichloroethylene degradation by propane oxidizing bacteria. *Appl. Environ. Microbiol.* 55: 2960-2964

Yagi, O., A. Hashimoto, K. Iwasaki and M. Nakajima. 1999. Aerobic degradation of 1,1,1-trichloroethane by *Mycobacterium* spp. isolated from soil. *Appl. Environ. Microbiol.* 65: 4693-1696.

APPENDICES

APPENDIX A
MICROCOSM PREPARATION AND OPERATION

A.1 AQUIFER MATERIAL

The core material was taken from the Moffett Field site in California. It was kept in cold storage before unpacking. The aquifer material consisted of particle sizes ranging from silts to large cobbles. All cores were unpacked and blended together, under a laminar flow hood, prior to transferring them into the microcosms. They were unpacked under a laminar flow hood and wet sieved through a no. 8 sieve (2.38 mm opening) to remove the large particles. The core materials used in microcosm fabrication are listed in Table A.1

A.2 GROUNDWATER

Groundwater was collected from the Moffett Field site in California and kept in cold storage prior to use. The background aqueous concentrations of 1,1,1-TCA in the Moffett groundwater ranged from 2.51 to 3.73 μg/L. The nitrate concentration was in the range of 40 mg/L as nitrate.

Table A.1 List of core material used in microcosm fabrication.

a) Microcosm studies with groundwater and soil from the original microcosms (Jitnuyanont 1998)

Location	Depth (ft)
SU 39-14	18

Table A.1, Continued.

b) Microcosm studies with the frozen culture

Location	Depth (ft)
SU39-PP1	16-16.5
SU39-PP2	14.5-15
SU39-PP3	16-16.5
SU39-PP4	15-15.5
SU39-PP5	15-15.5
SU39-PP6	15.5-16
SU39-FP1	14.5-15
SU39-FP2	16-16.5
SU39-FP3	15.5-16
SU39-17	16-16.5
SU39-18	14.5-15
SU39-19	16-16.5
SU39-20	18.5-19

A.3 MINERAL SALT GROWTH MEDIUM

The mineral salt growth media was prepared in demineralized water and autoclaved prior to use. The composition was as follows:

1. Phosphate Buffer		
- $K_2HPO_4*3H_2O$	2030.9	mg/L
- $NaH_2PO_4*H_2O$	739.0	mg/L
2. $MgSO_4$	60.2	mg/L
3. $CaCl_2$	11.1	mg/L
4. $NaNO_3$	153.0	mg/L

5. Trace Element Solution

- $FeSO_4*7H_2O$	6283.0	µg/L
- $MnCl_2*4H_2O$	300.8	µg/L
- $ZnSO_4*7H_2O$	146.6	µg/L
- H_3BO_3	61.8	µg/L
- $Na_2MoO_4*2H_2O$	108.9	µg/L
- $NiCl_2*6H_2O$	23.8	µg/L
- $CuCl_2*2H_2O$	17.0	µg/L
- $CoCl_2*6H_2O$	23.8	µg/L

APPENDIX B
CAH ANAYSIS

To quantify the concentration of 1,1,1-TCA, TCE and 1,1-DCE, a 100 μL headspace sample was injected into a Hewlett Packard (Wilmington, DE) 5890 gas chromatograph equipped with a ^{63}Ni electron capture detector (ECD). Separation was obtained by an HP-624 30 m x 0.25 mm x 1.4 mm film thickness stainless steel packed column (Hewlett Packard, Wilmington, DE) operated isothermally at 80 °C. A flow rate of 60 mL/min of argon/methane (95%:5%) mixture at a head pressure of 80 psi was used as the carrier gas. A Hewlett Packard 3393 integrator was connected to the gas chromatograph, providing the peak area for gaseous concentration analysis by comparing with a standard curve prepared with external standards.

B.1 PREPARATION OF CAH STOCK SOTLUTION

A 10 mL volumetric flask was filled with methanol nearly to the meniscus and placed on a balance. One drop of 1,1,1-TCA, TCE or 1,1-DCE solvents from a 10 μL microsyringe was then added in the flask without touching the sides of the flask. After the added weight was recorded, the flask was capped, shaken vigorously, and stored in refrigerator for later use.

B.2 STANDARD CURVE PREPARATION

A 125 ml amber serum bottle was filled with 15 mL of demineralized water and then a given amount of the stock solution of water saturated with 1,1,1-TCA, TCE or 1,1-DCE was added. The bottle was shaken for 20 to 30 minutes to allow

equilibration. Various volumes of headspace sample were taken with a 100 μL gas tight syringe (Hamilton 1701N), diluted to 100 μL, and injected into gas chromatography to achieve different concentrations. Standard curves were generated by plotting the peak area versus gas concentration. The chromatograms of various concentrations of CAHs are shown in Figure B.1.

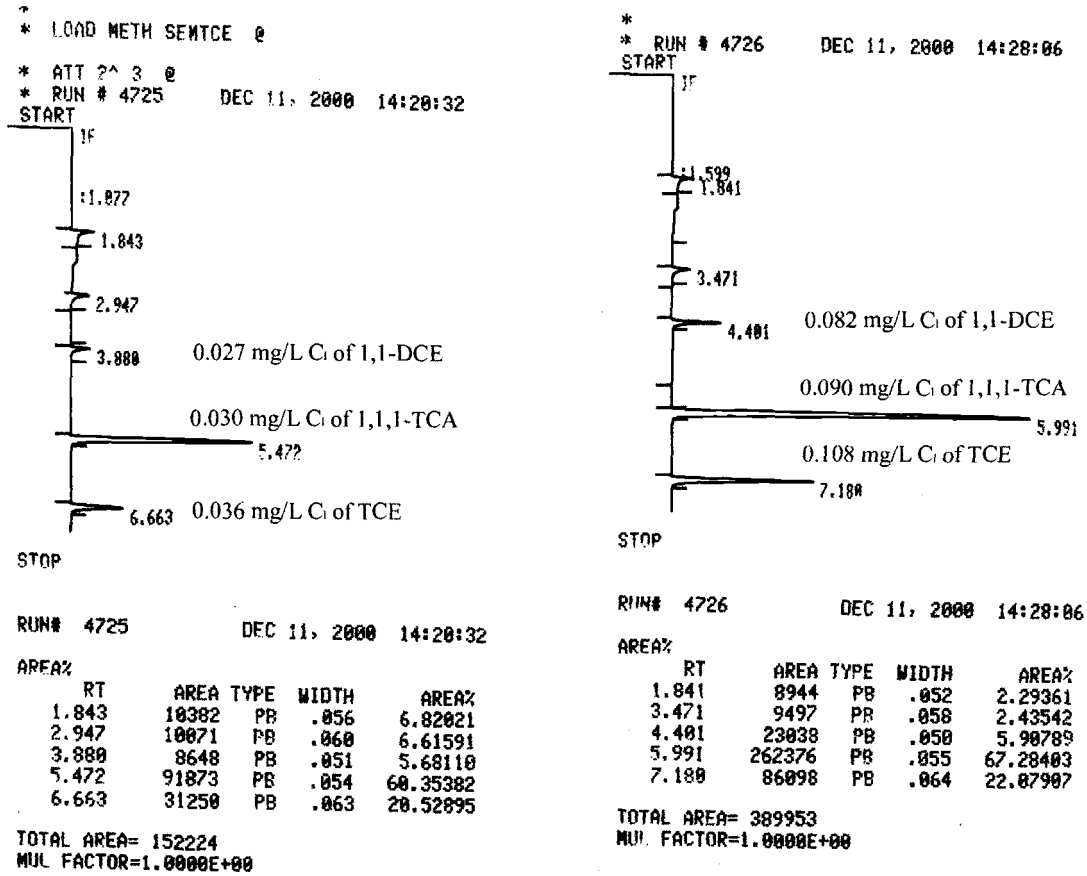

Figure B.1 Chromatograms for 1,1-DCE, 1,1,1-TCA and TCE.

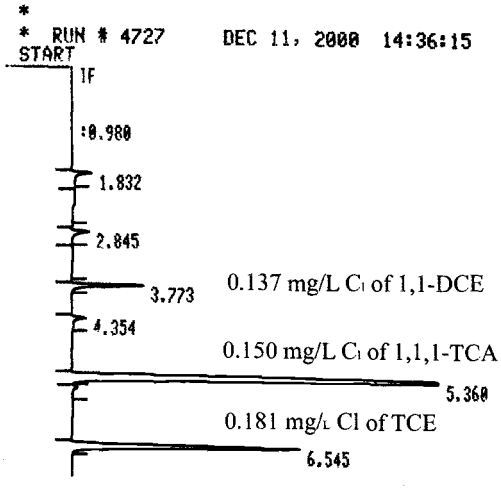

RUN# 4727 DEC 11, 2000 14:36:15

AREA%

RT	AREA	TYPE	WIDTH	AREA%
1.832	8637	PB	.050	1.46999
2.845	8958	BB	.058	1.52462
3.773	30202	PB	.045	5.14028
4.354	7236	PB	.057	1.23154
5.360	398397	PB	.055	67.80592
6.545	134125	PB	.063	22.82765

TOTAL AREA= 587555
MUL FACTOR=1.0000E+00

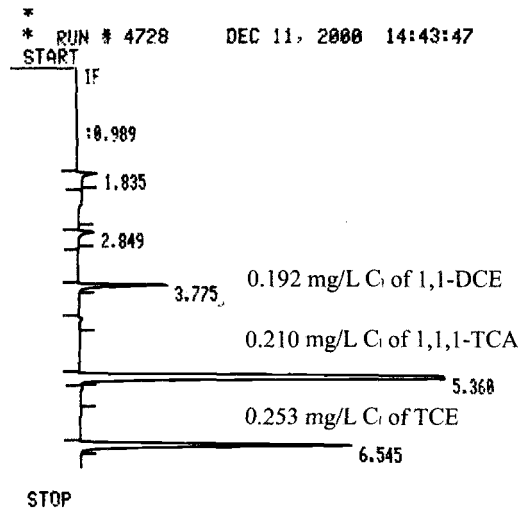

RUN# 4728 DEC 11, 2000 14:43:47

AREA%

RT	AREA	TYPE	WIDTH	AREA%
1.835	8036	PB	.051	1.15318
2.849	7742	BB	.055	1.11099
3.775	35716	PB	.043	5.12529
5.360	485344	PB	.055	69.64749
6.545	160020	PB	.063	22.96307

TOTAL AREA= 696858
MUL FACTOR=1.0000E+00

Figure B.1, Continued.

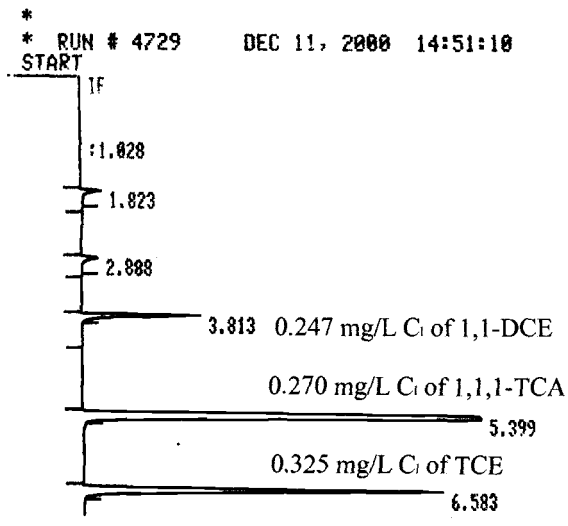

RUN# 4729 DEC 11, 2000 14:51:10

AREA%

RT	AREA	TYPE	WIDTH	AREA%
1.823	8535	PB	.052	.99325
2.888	7982	PB	.056	.92889
3.813	43821	PB	.043	5.09960
5.399	602575	PB	.056	70.12368
6.583	196390	PB	.063	22.85457

TOTAL AREA= 859303
MUL FACTOR=1.0000E+00

Figure B.1, Continued.

APPENDIX C
PROPANE AND BUTANE ANAYSIS

To quantify the concentration of butane and propane, a 100 μL headspace sample was injected into a Hewlett Packard 5890 gas chromatograph equipped with a flame ionization detector (FID), coupled with a GS-Q 30 m x 0.53 mm stainless steel packed column (J&W Scientific, Folsom, CA). A flowrate of 25 mL/min of nitrogen gas at a head pressure of 60 psi was used as the carrier gas. A Hewlett Packard 3393 integrator was connected to the gas chromatograph, providing the peak area for gaseous concentration analysis by comparing with a standard curve prepared with external standards.

C.1 STANDARD CURVE PREPARATION

A gas container was filled up with demineralized water and then closed with a rubber cap without creating any headspace. Various amounts of butane or propane and air were added into the gas container to achieve different concentrations. A headspace sample was taken with a 100 μL gas tight syringe (Hamilton 1701N) and injected into the gas chromatograph. Standard curves were generated by plotting the peak area versus gas concentration. The chromatograms of various concentrations of butane are shown in Figure C.1.

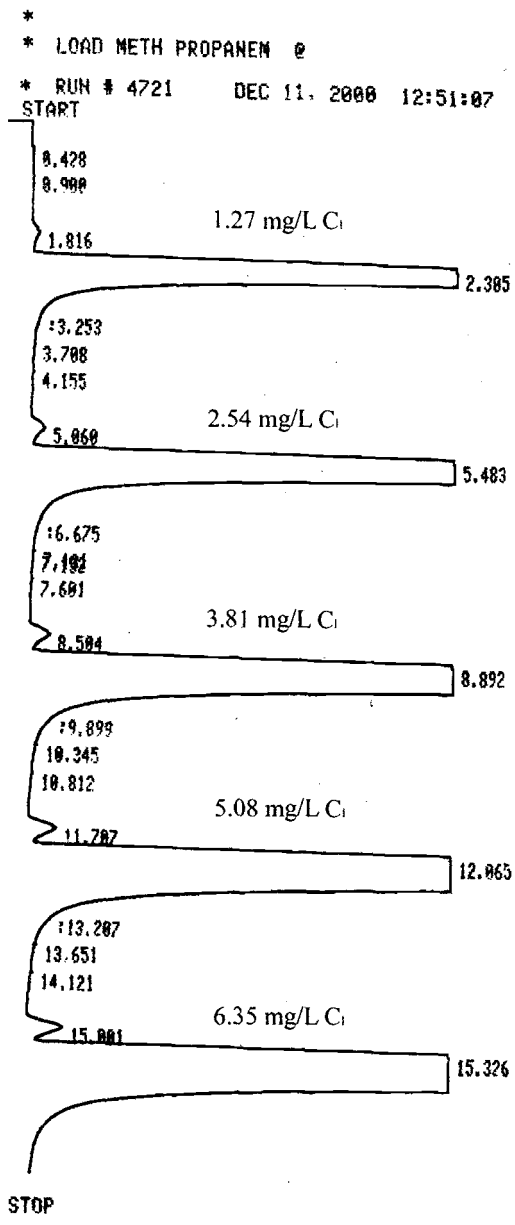

RUN# 4721 DEC 11, 2000 12:51:07

METHOD NAME: M:PROPANEM.MET

AREA%

RT	AREA	TYPE	WIDTH	AREA%
.428	1865	PB	.017	.00061
.900	657	PB	.042	.00022
1.816	55634	PP	.242	.01831
2.305	21218128	PB	.194	6.98483
3.708	883	BB	.009	.00029
4.155	908	BB	.030	.00030
5.060	105026	PP	.231	.03457
5.483	40424032	PB	.209	13.30726
7.131	472	BP	.007	.00016
7.152	1197	PB	.015	.00039
7.601	1403	BB	.035	.00046
8.504	148727	PP	.226	.04896
8.892	59722304	PB	.238	19.66009
10.345	892	BB	.016	.00029
10.812	1709	BB	.034	.00056
11.707	190956	PP	.217	.06286
12.065	80811392	PB	.259	26.60243
13.651	872	I BB	.013	.00029
14.121	1874	BB	.029	.00062
15.001	233488	PP	.206	.07686
15.326	100852080	PB	.269	33.19966

TOTAL AREA=3.0377E+08
MUL FACTOR=1.0000E+00

Figure C.1: Chromatograms for butane.

APPENDIX D
THE TRANSFORMATION RATE OF 1,1,1-TCA

D.1 DERIVATION OF MONOD KINETICS

The transformation rate of 1,1,1-TCA was described by Monod kinetics. The experiments were designed to avoid competitive inhibition. The effects of product toxicity and reducing power limitation were also assumed to be negligible. The transformation rate is provided by equation D.1, relating the transformation rate to the aqueous phase concentration.

$$\frac{\partial M}{\partial t} = -\frac{k_{max} X C_l}{K_s + C_l} \cdot V_l \qquad \text{(D.1)}$$

where,

M	=	Total mass of 1,1,1-TCA at time t, mg
C_l	=	1,1,1-TCA concentration in aqueous phase, mg/L
K_s	=	Half-saturation constant for 1,1,1-TCA, mg/L
k_{max}	=	Maximum specific rate of 1,1,1-TCA, mg/mg-day
X	=	Active microbial concentration, mg/L
t	=	Time, day

Since the aqueous concentration of 1,1,1-TCA was relatively low (assuming $C_l << K_s$), the transformation rate (equation D.1) was simplified to follow a pseudo first order model.

$$\frac{\partial M}{\partial t} = -\frac{k_{max} X C_l}{K_s} \cdot V_l \qquad \text{(D.2)}$$

The mass balance on 1,1,1-TCA in the microcosms can be written as

$$M = C_l V_l + C_g V_g \tag{D.3}$$

where,

C_g = 1,1,1-TCA concentration in gas phase, mg/L

V_l = Liquid volume, L

V_g = Gas volume, L

The equilibrium two-phase (air and liquid) partitioning was assumed based on Henry's Law. The dimensionless Henry partition coefficient (H_{cc}) was used to describe the distribution of 1,1,1-TCA between phases. Equation D.3 was rearranged and expressed in terms of the aqueous concentration.

$$C_l = \frac{M}{V_l + H_{cc} V_g} \tag{D.4}$$

Substituting equation D.4 into D.2,

$$\frac{\partial M}{\partial t} = -\frac{k_{\max} X}{K_s}\left(\frac{M}{V_l + H_{cc} V_g}\right) \cdot V_l$$

$$= -\frac{k_{\max} XM}{K_s}\left(\frac{V_l}{V_l + H_{cc} V_g}\right)$$

Letting $P = \frac{k_{\max} X}{K_s}\left(\frac{V_l}{V_l + H_{cc} V_g}\right)$,

$$\frac{\partial M}{\partial t} = -PM \tag{D.5}$$

Integrating equation D.5,

$$\int_{M_0}^{M} \frac{\partial M}{M} = -P \int_{0}^{t} \partial t$$

$$\ln \frac{M}{M_0} = -Pt \qquad \text{(D.6)}$$

where,

M_0 = Initial total mass of 1,1,1-TCA, mg

Equation D.6 represents the linear equation y = mx + b, allowing the y-axis to be ln M/M_0, and the x-axis to be time. The regression line of experimental data plotted in the graph should follow this linear equation, providing the value of pseudo first-order rate coefficient (P) from the slope of the regression line.

The cell decay rate equation was also modified from Monod kinetics, expressed as

$$X = X_0 e^{-bt} \qquad \text{(D.7)}$$

where,

X_0 = Initial total cell mass, mg/L

b = Cell decay rate, day^{-1}

Substituting equation D.7 into the P term,

$$P = \frac{k_{\max} X_0}{K_s} \left(\frac{V_\ell}{V_\ell + H_{CC} V_g} \right) e^{-bt} \qquad \text{(D.8)}$$

Equation D.8 can symbolize $y = me^{-nx}$. The value of pseudo first-order rate coefficient (P) will be plotted against time. The values of $k_{max}X_0/K_s$ and b will be obtained from the exponential regression line.

D.2 EXAMPLE OF CALCULATION

Figure D.1 presents the experimental data of 1,1,1-TCA obtained from the transformation rate measurement for microcosm B2-1. The experimental data are plotted on a semi-logarithmic scale to test for first-order transformation, as shown in Figure D.2. The slope of the regression line in each graph presents the pseudo first-order rate coefficient (P), the combination term of kinetic parameters and biomass as illustrated in equation D.5.

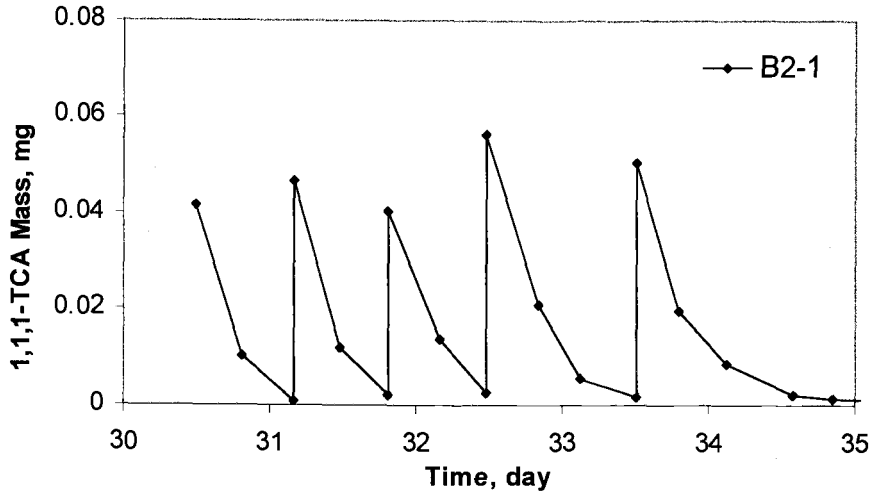

Figure D.1 1,1,1-TCA transformation data for microcosm B2-1.

a) The 1st addition of 1,1,1-TCA

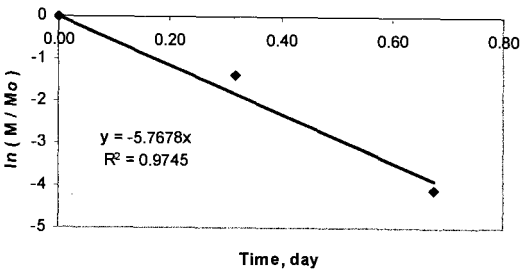

b) The 2nd addition of 1,1,1-TCA

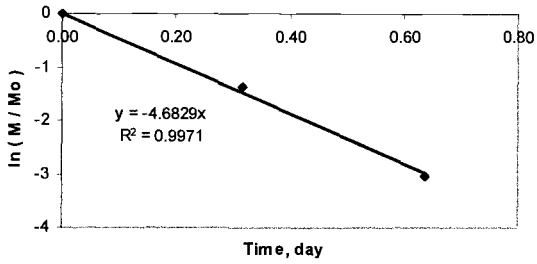

c) The 3rd addition of 1,1,1-TCA

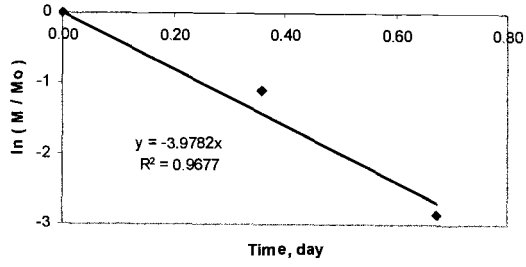

d) The 4th addition of 1,1,1-TCA

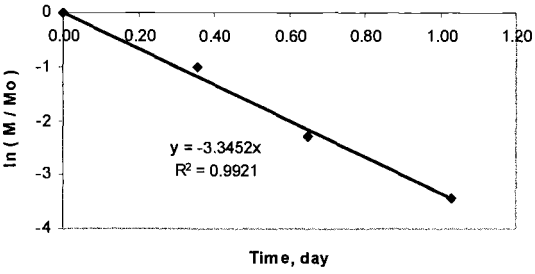

e) The 5th addition of 1,1,1-TCA

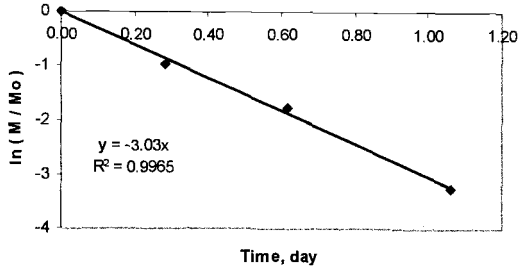

Figure D.2 1,1,1-TCA transformation rate data plotted on a semi-logarithmic scale.

The values of the pseudo first-order rate coefficient (P) from each graph in Figure D.2 are then plotted against time, as shown in Table D.1 and Figure D.3. The exponential regression line in the graph is obtained from Microsoft Excel 2000. The slope and the power of the exponential regression line will provide the values of the pseudo first-order rate parameter ($k_{max}X_0/K_s$) and cell decay rate (b), respectively, as following:

$$P = \frac{k_{\max} X_0}{K_s}\left(\frac{V_\ell}{V_\ell + H_{CC}V_g}\right)e^{-bt} \qquad \text{(D.8)}$$

Cell decay rate (b) = Power of the exponential regression line

= 0.22 day^{-1}

Pseudo first-order rate parameter ($k_{max}X_0/K_s$) = $\dfrac{\text{Slope of the exponential regression line}}{\left(\dfrac{V_l}{V_l + H_{cc}V_g}\right)}$

$$= \frac{5.4817}{\left(\dfrac{0.75}{0.75 + (0.55)(0.82)}\right)}$$

= 8.77 day^{-1}

Table D.1 The values of the pseudo first-order rate coefficient (P) and time.

Starting Day	Time (day)	P (day^{-1})
30.49	0	5.77
31.17	0.68	4.68
31.80	1.31	3.98
32.48	1.99	3.34
33.51	3.02	3.03

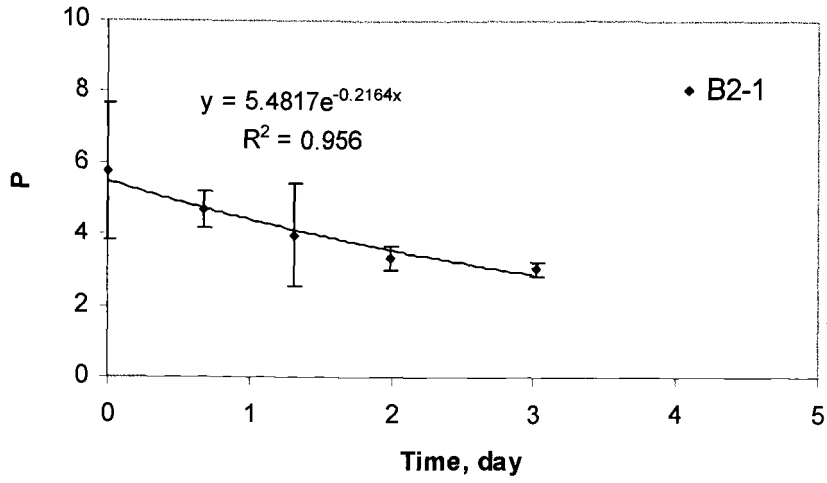

Figure D.3 The decrease in pseudo-first-order rate coefficient (P) as a function.

APPENDIX E
THE KINEITC EXPERIMENT OF BUTANE AND 1,1,1-TCA

E.1 DERIVATION OF MONOD KINEITCS

The rates of butane utilization and 1,1,1-TCA transformation were described by Monod kinetics. The experiments were designed to avoid competitive inhibition. The effects of product toxicity and reducing power limitation were also assumed to be negligible. The kinetic rate was described by equation E.1 relating the transformation rate to each concentration in aqueous phase.

$$\frac{\partial M}{\partial t} = -\frac{k_{\max} X C_l}{K_s + C_l} \cdot V_l \qquad \text{(E.1)}$$

where,

M	=	Total mass of butane or 1,1,1-TCA at time t, mg
C_l	=	Butane or 1,1,1-TCA concentration in aqueous phase, mg/L
K_s	=	Half-saturation constant for butane or 1,1,1-TCA, mg/L
k_{max}	=	Maximum specific rate of butane or 1,1,1-TCA, mg/mg-day
X	=	Active microbial concentration, mg/L
t	=	Time, day

The mass balance on butane or 1,1,1-TCA in the microcosms can be written as

$$M = C_l V_l + C_g V_g \qquad \text{(E.2)}$$

where,

C_g	=	Butane or 1,1,1-TCA concentration in gas phase, mg/L
V_l	=	Liquid volume, L
V_g	=	Gas volume, L

The equilibrium two-phase (air and liquid) partitioning was assumed based on Henry's Law. The dimensionless Henry partition coefficient (H_{cc}) was used to describe the distribution of 1,1,1-TCA between phases. Equation E.2 was rearranged and expressed in terms of the aqueous concentration.

$$C_l = \frac{M}{V_l + H_{cc}V_g} \tag{E.3}$$

E.1.1 Pseudo first-order model

For the relatively low aqueous concentration (assuming $C_l << K_s$), the transformation rate (equation E.1) was simplified to follow a pseudo first order model.

$$\frac{\partial M}{\partial t} = -\frac{k_{max}XC_l}{K_s} \cdot V_l \tag{E.4}$$

Substituting equation E.3 into E.4,

$$\frac{\partial M}{\partial t} = -\frac{k_{max}X}{K_s}\left(\frac{M}{V_l + H_{cc}V_g}\right) \cdot V_l$$

$$= -\frac{k_{max}XM}{K_s}\left(\frac{V_l}{V_l + H_{cc}V_g}\right)$$

Letting $P = \frac{k_{max}X}{K_s}\left(\frac{V_l}{V_l + H_{cc}V_g}\right)$,

$$\frac{\partial M}{\partial t} = -PM \tag{E.5}$$

Integrating equation E.5,

$$\int_{M_0}^{M} \frac{\partial M}{M} = -P \int_{0}^{t} \partial t$$

$$\ln \frac{M}{M_0} = -Pt \qquad \text{(E.6)}$$

where,

M_0 = Initial total mass of butane or 1,1,1-TCA, mg

Equation E.6 represents the linear equation y = mx + b, allowing the y-axis to be ln M/M_0, and the x-axis to be time. The regression line of the experimental data plotted in the graph should follow this linear equation, providing a P value from the slope of the regression line.

E.1.2 Zero-order model

For the relatively high aqueous concentration (assuming $C_l >> K_s$), the transformation rate (equation E.1) was simplified to follow a zero-order model.

$$\frac{\partial M}{\partial t} = -k_{max} X V_l \qquad \text{(E.7)}$$

Integrating equation E.7,

$$\int_{M_0}^{M} \partial M = -k_{max} X V_l \int_{0}^{t} \partial t$$

$$M_t - M_0 = -k_{max} X V_l t$$

$$M_t = M_0 - k_{max} X V_l t \qquad \text{(E.8)}$$

Similar to the pseudo first-order model, equation E.8 can symbolize y = b+mx. The experimental data in high aqueous concentration will be plotted against time. The value of $k_{max}XV_l$ will be obtained from the slope of the regression line.

Since the value of P, V_l, V_g, H_{cc}, and $k_{max}XV_l$ (from the zero-order model) were known, K_s can be solved. The following is the example, showing how these values are determined.

E.2 EXAMPLE OF CALCULATION

Figure E.1 presents the experimental data of butane obtained from the kinetic experiment in microcosm BR3-2. The data at high concentration tend to follow zero-order kinetics and the data at low concentration seem to follow first-order kinetics. The data at high concentration are plotted against time, as shown in Figure E.2. The slope of the linear regression presents the value of $k_{max}XV_l$ as illustrated in equation E.8.

$k_{max}XV_l$ = Slope of the linear regression line

= 0.18

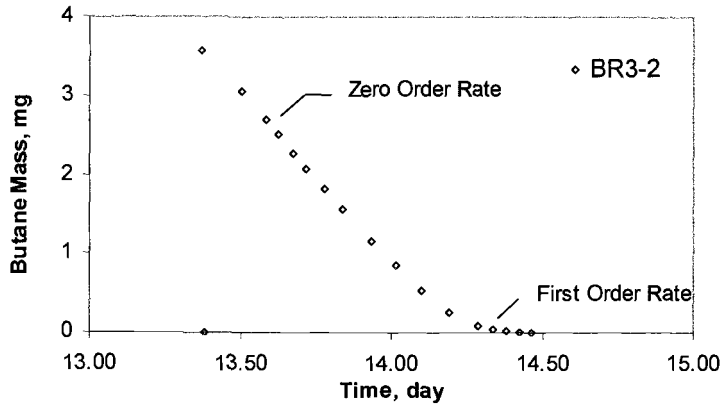

Figure E.1 Experimental data for the kinetic experiment conducted in microcosm BR3-2.

Figure E.3 presents the data at low concentration plotted on a logarithmic scale. The slope of the linear regression line presents the pseudo first-order rate coefficient (P), the combination term of kinetic parameters and biomass as illustrated in equation E.5.

Pseudo first-order rate coefficient (P) = Slope of the linear regression line

= 0.73

Dividing $k_{max} XV_l$ by P

$$\frac{k_{max} XV_l}{P} = \frac{k_{max} XV_l}{\frac{k_{max} X}{K_s}\left(\frac{V_l}{V_l + H_{cc}V_g}\right)}$$

$$= K_s(V_l + H_{cc}V_g)$$

So

$$K_s = \frac{\frac{k_{max} XV_l}{P}}{(V_l + H_{cc}V_g)}$$

$$= \frac{\frac{0.18}{0.7299}}{0.1 + (38.05)(0.57)}$$

$$= 0.011 \text{ mg/L}$$

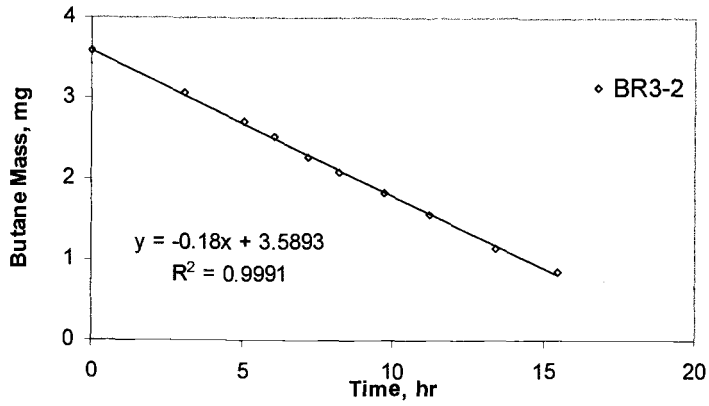

Figure E.2 Experimental data at high concentration plotted against time to test for zero-order kinetics.

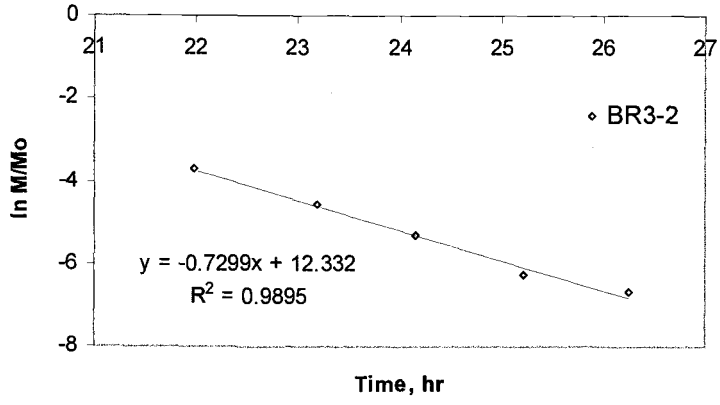

Figure E.3 Experimental data at low concentration plotted on a logarithmic scale to test for first-order kinetics.

APPENDIX F
MODEL DEVELOPMENT

F.1 BUTANE UTILIZATION AND 1,1,1-TCA TRANSFORMATION

The rates of butane utilization and 1,1,1-TCA transformations were described by Monod kinetics that relates the transformation rate to each concentration in aqueous phase. To simplify the kinetics expressions, the experiments were designed to avoid the effects of competitive inhibition. The effect of reducing power limitation was also assumed to be negligible. The rates of butane utilization and 1,1,1-TCA transformations were described by equations F.1 and F.2, respectively.

$$\frac{dM_{But}}{dt} = -\frac{k_{\max,But} X C_{l,But}}{K_{s,But} + C_{l,But}} \cdot V_l \qquad \text{(F.1)}$$

$$\frac{dM_{TCA}}{dt} = -\frac{k_{\max,TCA} X C_{l,TCA}}{K_{s,TCA} + C_{l,TCA}} \cdot V_l \qquad \text{(F.2)}$$

where,

M_{But}	=	Total mass of butane, mg
M_{TCA}	=	Total mass of 1,1,1-TCA, mg
$C_{l,But}$	=	Butane concentration in liquid phase, mg/L
$C_{l,TCA}$	=	1,1,1-TCA concentration in liquid phase, mg/L
$k_{max,But}$	=	Maximum specific rate of butane, mg/mg-day
$k_{max,TCA}$	=	Maximum specific rate of butane or 1,1,1-TCA, mg/mg-day
$K_{s,But}$	=	Half-saturation constant for butane, mg/L
$K_{s,TCA}$	=	Half-saturation constant for butane or 1,1,1-TCA, mg/L
X	=	Active microbial concentration, mg/L

t = Time, day

The mass balance on butane and 1,1,1-TCA in the microcosms can be written as equations F.3 and F.4, respectively.

$$M_{But} = C_{l,But}V_l + C_{g,But}V_g \quad \text{(F.3)}$$

$$M_{TCA} = C_{l,TCA}V_l + C_{g,TCA}V_g \quad \text{(F.4)}$$

where,

$C_{g,But}$ = Butane concentration in gas phase, mg/L

$C_{g,TCA}$ = 1,1,1-TCA concentration in gas phase, mg/L

V_g = Gas volume, L

V_l = Liquid volume, L

Since the experiments were conducted for long periods of time, equilibrium two-phase (air and liquid) partitioning was assumed based on Henry's Law. The dimensionless Henry partition coefficient (H_{cc}) was used to describe the distribution of butane and 1,1,1-TCA between phases. Equations F.3 and F.4 were rearranged and expressed in terms of the aqueous concentration of butane and 1,1,1-TCA, respectively.

$$C_{l,But} = \frac{M_{But}}{V_l + H_{cc,But}V_g} \quad \text{(F.5)}$$

$$C_{l,TCA} = \frac{M_{TCA}}{V_l + H_{cc,TCA}V_g} \quad \text{(F.6)}$$

Substituting equations F.5 and F.6 and F.6 into F.1 and F.2, respectively,

$$\frac{dM_{But}}{dt} = -\frac{k_{\max,But}X}{K_{s,But} + \left(\frac{M_{But}}{V_\ell + H_{cc,But}V_g}\right)}\left(\frac{M_{But}}{V_\ell + H_{cc,But}V_g}\right)\cdot V_l \qquad \text{(F.7)}$$

$$\frac{dM_{TCA}}{dt} = -\frac{k_{\max,TCA}X}{K_{s,TCA} + \left(\frac{M_{TCA}}{V_\ell + H_{cc,TCA}V_g}\right)}\left(\frac{M_{TCA}}{V_\ell + H_{cc,TCA}V_g}\right)\cdot V_l \qquad \text{(F.8)}$$

F.2 MICROBIAL GROWTH

Similar to the rate of butane utilization and 1,1,1-TCA transformation, Monod kinetics was also used to express the rate of microbial growth as a function of growth consumption and cell decay:

$$\frac{dX}{dt} = \mu X = Y\frac{dM_{But}}{V_l dt} - bX \qquad \text{(F.9)}$$

where,

μ	=	Net specific cellular growth rate, day^{-1}
Y	=	Cellular yield of butane, mg cell/ mg butane
b	=	Cell decay rate, day^{-1}

Substituting equation F.7 into F.9,

$$\frac{dX}{dt} = Y\frac{k_{\max,But}X}{K_{s,But} + \left(\frac{M_{But}}{V_\ell + H_{cc,But}V_g}\right)}\left(\frac{M_{But}}{V_\ell + H_{cc,But}V_g}\right) - bX \qquad \text{(F.10)}$$

Since the transformation product toxicity is another factor that effects cell decay, it was also incorporated into the model. The effect of transformation product toxicity on cell activity is quantified in terms of the transformation capacity (T_c), representing it as a constant defined by the amount of 1,1,1-TCA compound degraded divided by the amount of cell inactivated. The transformation capacity term (T_c) was incorporated into equation F.9 to include the effect of transformation product toxicity on cell activity.

$$\frac{dX}{dt} = Y\frac{dM_{But}}{V_l dt} - \frac{1}{T_c}\frac{dM_{TCA}}{V_l dt} - bX \qquad \text{(F.11)}$$

where,

T_c = Transformation capacity for 1,1,1-TCA, mg TCA / mg cells

Substituting equations F.7 and F.8 into F.11,

$$\frac{dX}{dt} = Y\frac{k_{\max,But}X}{K_{s,But} + \left(\frac{M_{But}}{V_\ell + H_{cc,But}V_g}\right)}\left(\frac{M_{But}}{V_\ell + H_{cc,But}V_g}\right) - \frac{1}{T_c}\frac{-k_{\max,TCA}X}{K_{s,TCA} + \left(\frac{M_{TCA}}{V_\ell + H_{cc,TCA}V_g}\right)}\left(\frac{M_{TCA}}{V_\ell + H_{cc,TCA}V_g}\right) - bX \qquad \text{(F.12)}$$

To develop the model, the values of all parameters were introduced into the above equations. The differential equations F.7, F.8, and F.10 or F.12 were solved in STELLA®. Numerical integration in time was performed in STELLA® using a fourth-order Runge-Kutta method. Map, diagram and equations for model simulation in STELLA® are shown in Figures F.1, F.2 and F.3, respectively.

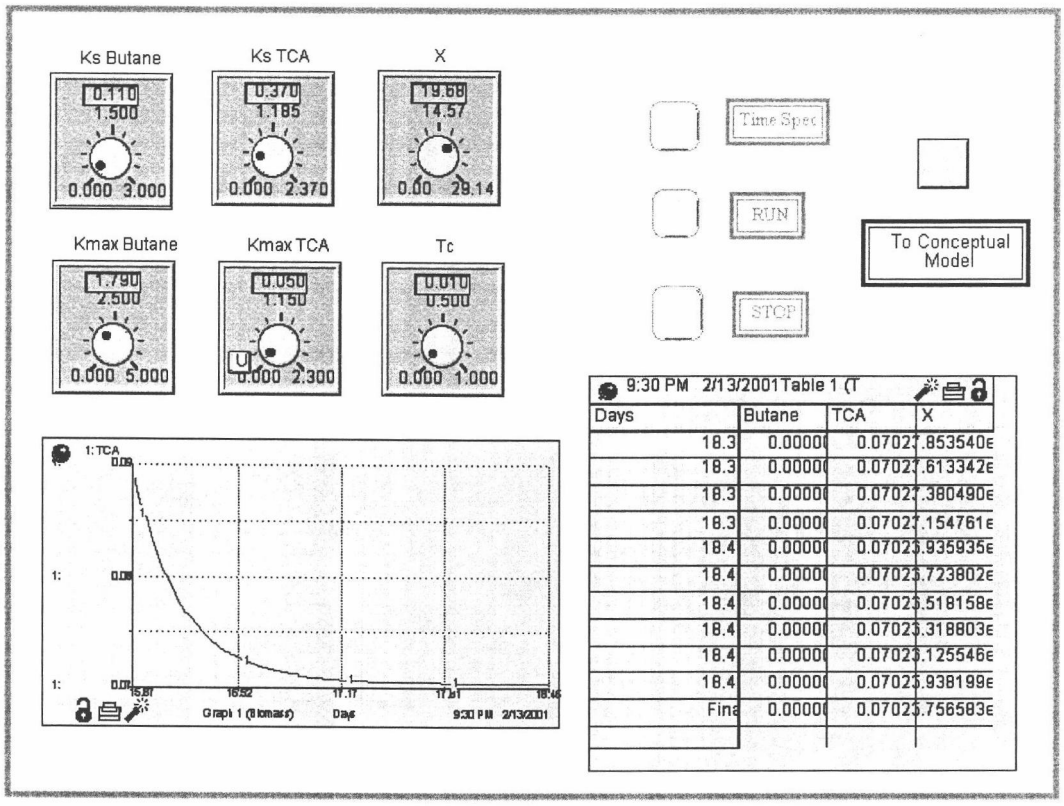

Figure F.1 Map for model simulation in STELLA®.

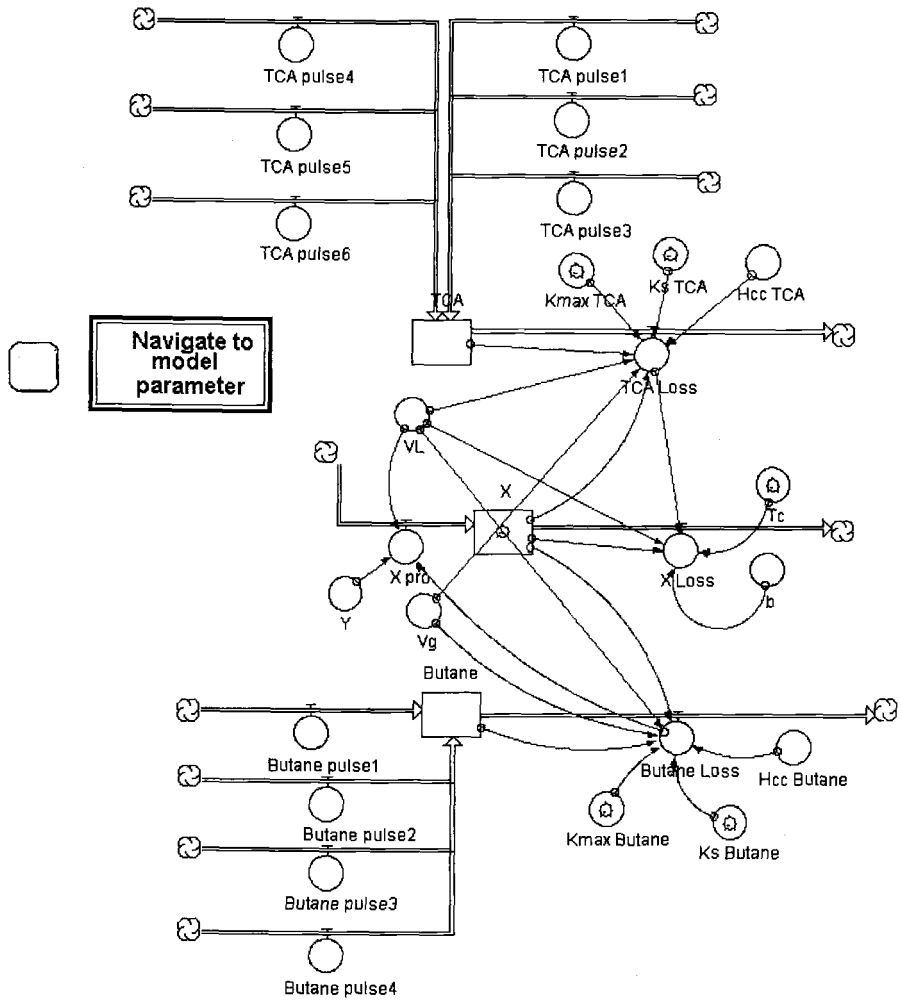

Figure F.2 Diagram for model simulation in STELLA®.

Butane(t) = Butane(t - dt) + (Butane_pulse1 + Butane_pulse2 + Butane_pulse3 + Butane_pulse4 - Butane_Loss) * dt

INIT Butane = 0

Butane_pulse1 = pulse (0,4.25, 0)

Butane_pulse2 = pulse (0, 13.38,0)

Butane_pulse3 = pulse (0,5.11,0)

Butane_pulse4 = pulse(0,6.27,0)

Butane_Loss = (Kmax_Butane * X * VL * (Butane / (VL + Vg * Hcc_Butane))) / (Ks_Butane + (Butane / (VL + Vg * Hcc_Butane)))

TCA(t) = TCA(t - dt) + (TCA_pulse1 + TCA_pulse2 + TCA_pulse3 + TCA_pulse4 + TCA_pulse5 + TCA_pulse6 - TCA_Loss) * dt

INIT TCA = 0.089

TCA_pulse1 = pulse (0,15.87,0)

TCA_pulse2 = pulse (0,8.8,0)

TCA_pulse3 = pulse (0,11.79,0)

TCA_pulse4 = pulse (0,5.34,0)

TCA_pulse5 = pulse (0,6.98,0)

TCA_pulse6 = pulse (0,9.0,0)

TCA_Loss = (Kmax_TCA * X * VL * (TCA / (VL + Vg * Hcc_TCA))) / (Ks_TCA + (TCA / (VL + Vg * Hcc_TCA)))

Figure F.3 Equations for model simulation in STELLA®.

X(t) = X(t - dt) + (X_pro - X_Loss) * dt

INIT X = 19.68

X_pro = Y * Butane_Loss / VL

X_Loss = (b * X) + (TCA_Loss / (VL * Tc))

b = 0.15

Hcc_Butane = 38.05

Hcc_TCA = 0.548

Kmax_Butane = 1.79

Kmax_TCA = 0.5

Ks_Butane = 0.11

Ks_TCA = 0.37

Tc = 0.01

Vg = 0.057

VL = 0.1

Y = 0.7

Figure F.3, Continued.

APPENDIX G

LABORATORY DATA

G.1 CULTURE DEVELOPMENT FOR BIOAUGMENTATION STUDIES

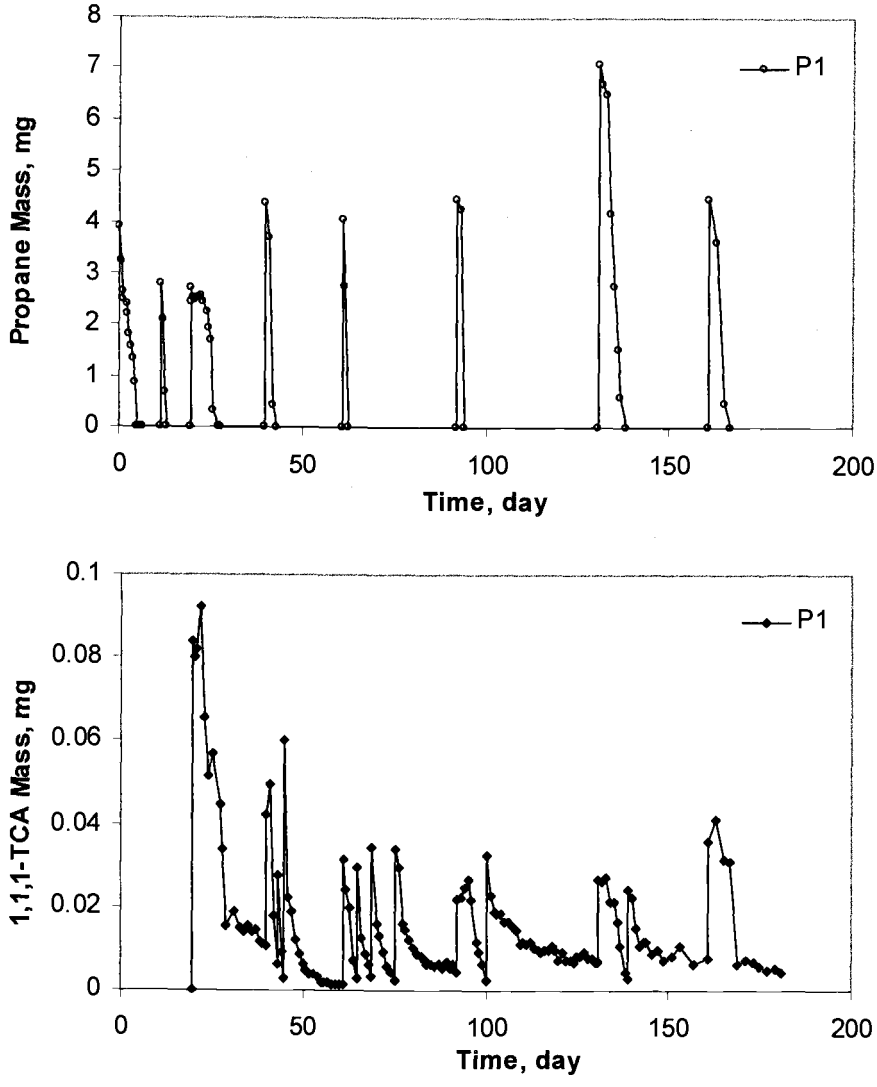

Figure G.1 Propane utilization and 1,1,1-TCA transformation achieved in indigenous microcosm P1.

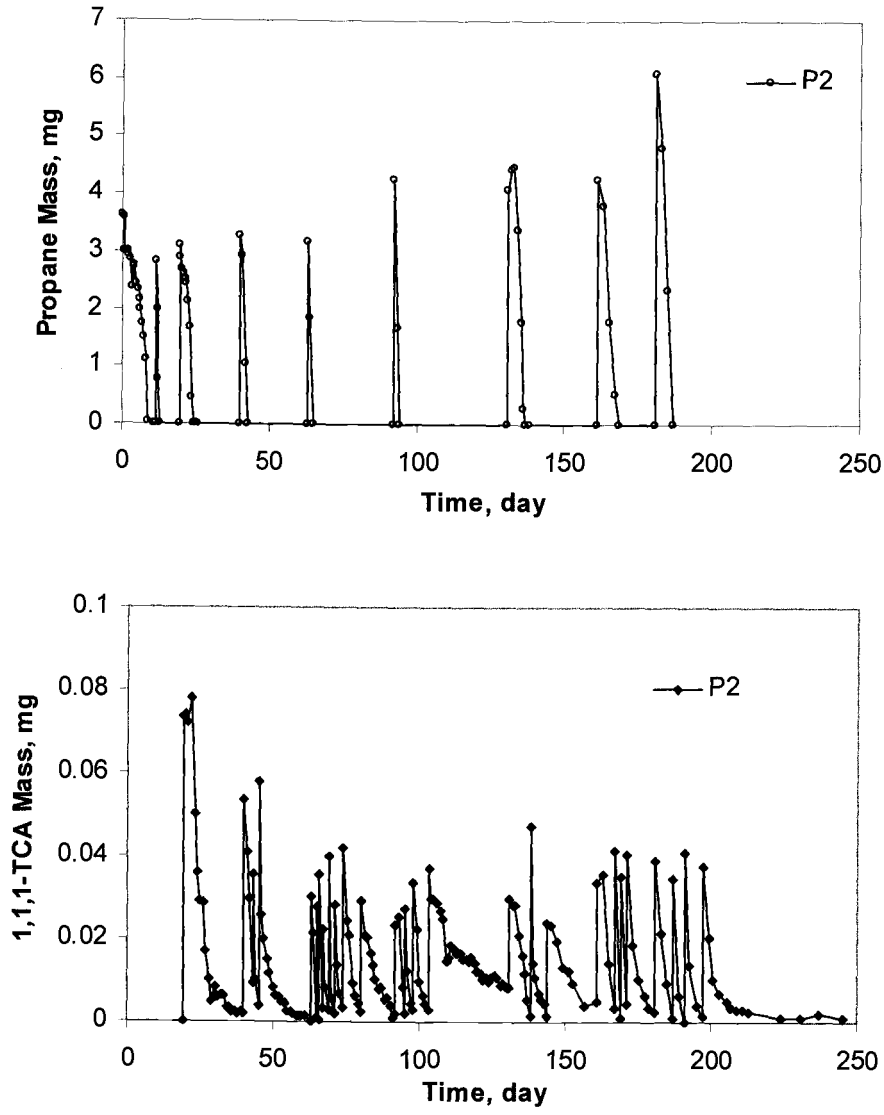

Figure G.2 Propane utilization and 1,1,1-TCA transformation achieved in bioaugmented microcosm P2.

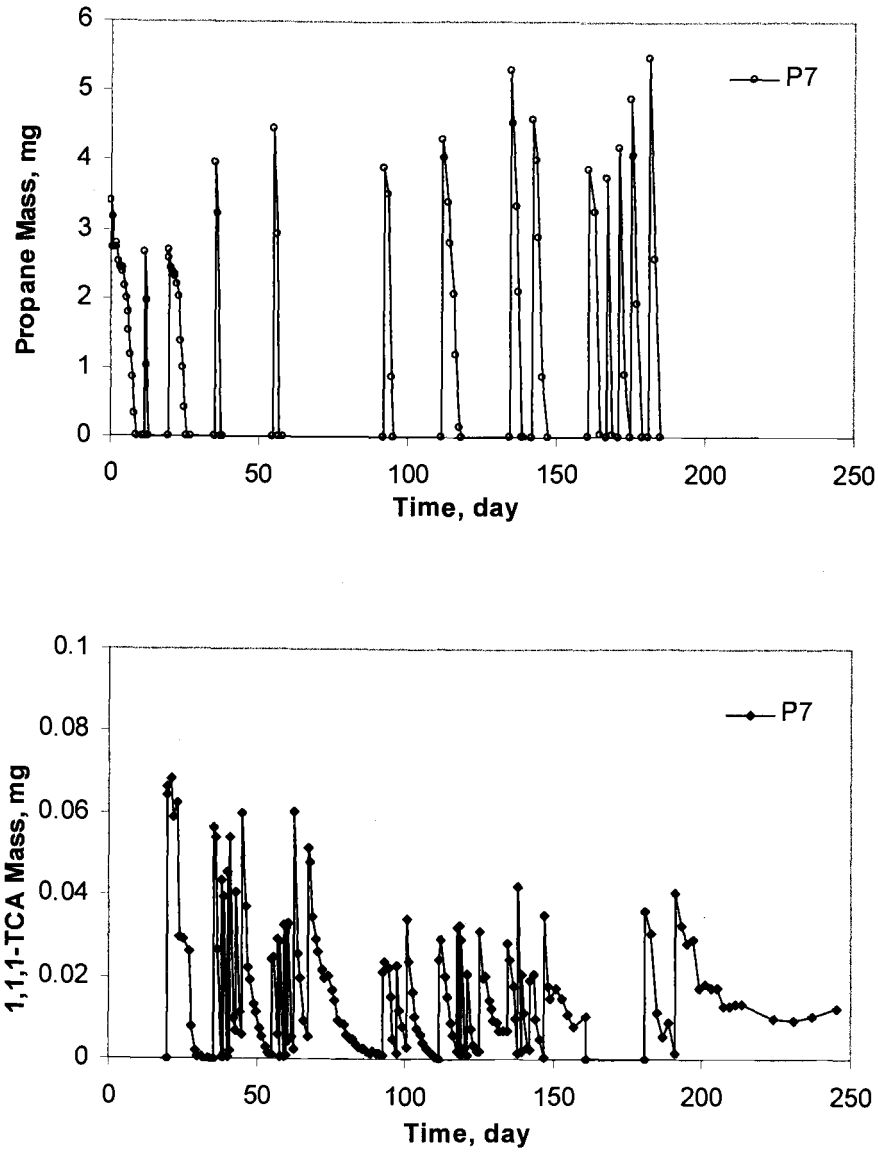

Figure G.3 Propane utilization and 1,1,1-TCA transformation achieved in bioaugmented microcosm P7.

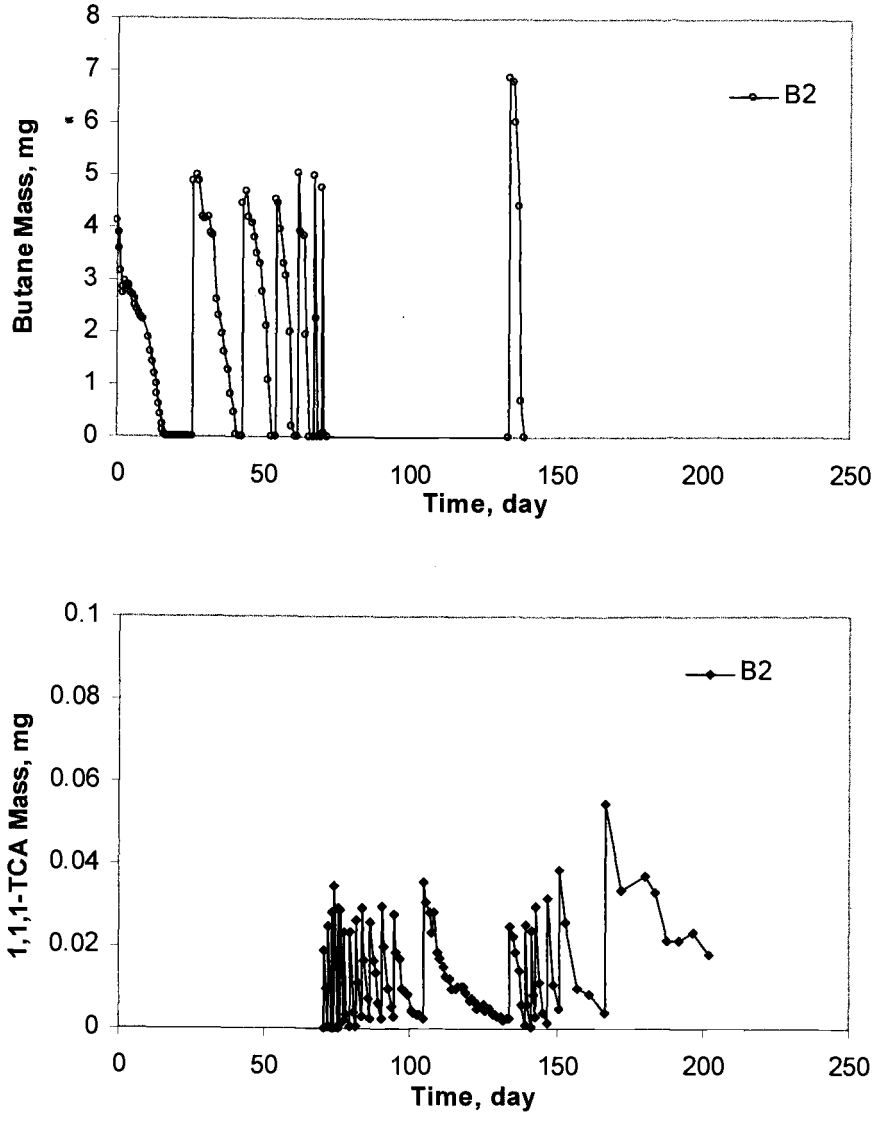

Figure G.4 Butane utilization and 1,1,1-TCA transformation achieved in bioaugmented microcosm B2.

G.2 MICROCOSM STUDIES WITH GROUNDWATER AND SOIL FROM MICROCOSM B6

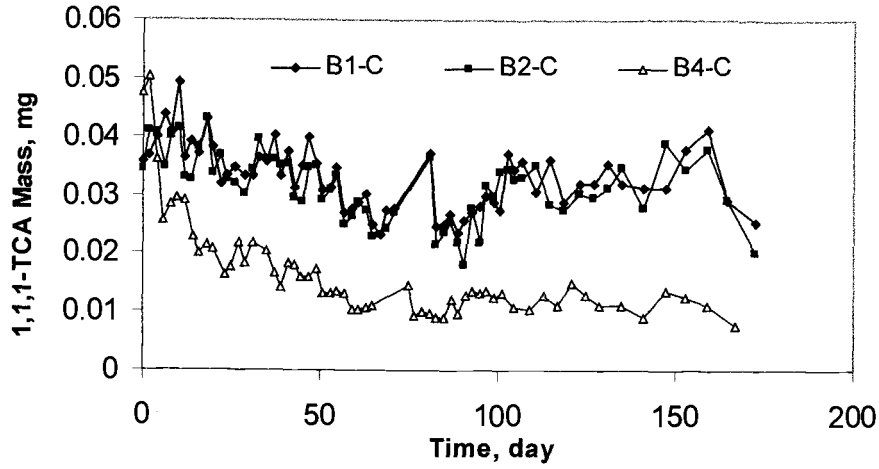

Figure G.5 Control bottles of the B1, B2 and B4 microcosm sets.

Table G.1 The values of the pseudo-first-order rate coefficient (P) and time obtained from the 1,1,1-TCA transformation rate measurement for microcosm B2-1

a) During day 30 – 35

Starting Day	Time (day)	P (day^{-1})
30.49	0	5.77
31.17	0.68	4.68
31.80	1.31	3.98
32.48	1.99	3.34
33.51	3.02	3.03

b) During day 38-45

Starting Day	Time (day)	P (day^{-1})
38.30	0	10.41
39.95	1.65	2.62
44.01	5.71	3.12

Table G.2 The values of the pseudo-first-order rate coefficient (P) and time obtained from the 1,1,1-TCA transformation rate measurement for microcosm B2-2

a) During day 30 - 35

Starting Day	Time (day)	P (day^{-1})
30.49	0	6.14
31.17	0.68	6.17
31.80	1.31	5.19
32.48	1.99	4.07
33.12	2.64	3.50

b) During day 38-45

Starting Day	Time (day)	P (day^{-1})
38.30	0	10.75
39.95	1.65	1.48
44.01	5.71	2.93

Table G.3 The values of the pseudo-first-order rate coefficient (P) and time obtained from the 1,1,1-TCA transformation rate measurement for microcosm B2-3

a) During day 30 - 35

Starting Day	Time (day)	P (day^{-1})
30.49	0	5.33
31.17	0.68	4.34
31.80	1.31	3.40
32.48	1.99	296
33.51	3.02	2.63

Table G.3, Continued

b) During day 38-45

Starting Day	Time (day)	P (day^{-1})
38.52	0	6.85
39.95	1.42	1.87
44.01	5.49	1.70

Table G.4 The values of the pseudo-first-order rate coefficient (P) and time obtained from the 1,1,1-TCA transformation rate measurement for microcosm B4-1

a) During day 30 - 35

Starting Day	Time (day)	P (day^{-1})
30.81	0	4.54
31.48	0.68	3.14
32.48	1.67	2.42
33.51	2.70	2.08

b) During day 38-45

Starting Day	Time (day)	P (day^{-1})
38.52	0	6.56
39.95	1.42	1.83
44.01	5.49	1.57

Table G.5 The values of the pseudo-first-order rate coefficient (P) and time obtained from the 1,1,1-TCA transformation rate measurement for microcosm B4-2

a) During day 30 - 35

Starting Day	Time (day)	P (day^{-1})
31.17	0	2.11
32.48	1.31	1.62

b) During day 38-45

Starting Day	Time (day)	P (day^{-1})
39.74	0	1.3
42.29	1.42	0.12

Table G.6 The values of the pseudo-first-order rate coefficient (P) and time obtained from the 1,1,1-TCA transformation rate measurement for microcosm B4-3

a) During day 30 - 35

Starting Day	Time (day)	P (day^{-1})
30.81	0	3.25
31.48	0.68	2.67
32.48	1.67	2.41
33.51	2.70	2.10

b) During day 38-45

Starting Day	Time (day)	P (day^{-1})
38.52	0	4.57
39.95	1.42	0.77
44.01	5.49	0.61

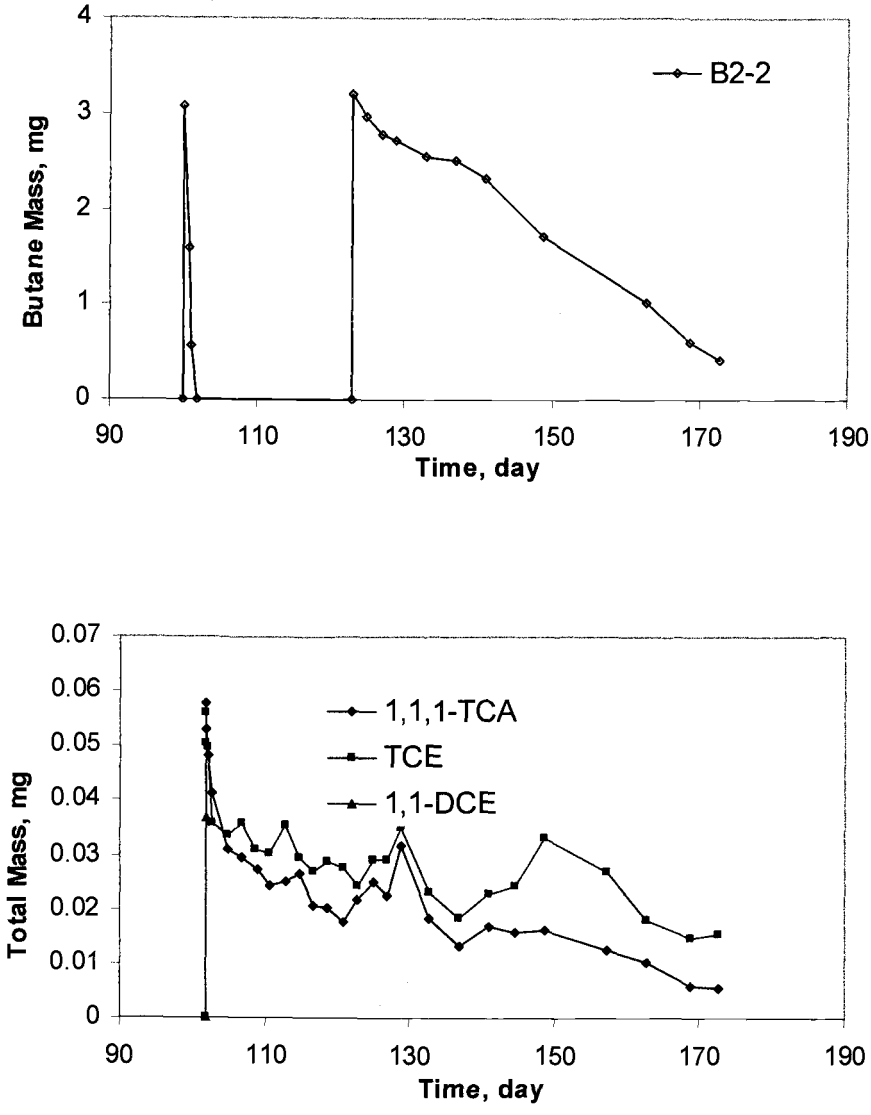

Figure G.6 Butane utilization and chlorinated compound transformation achieved in slurry-inoculated microcosm B2-2

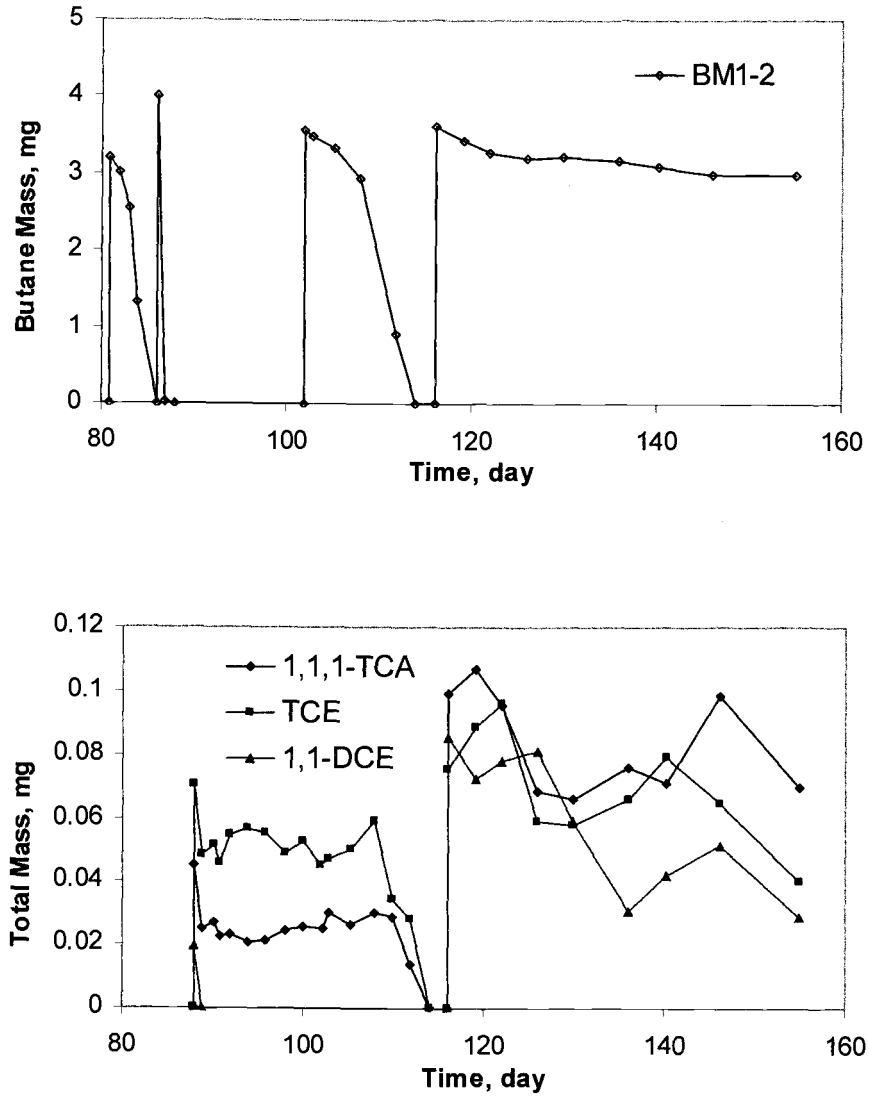

Figure G.7 Butane utilization and chlorinated compound transformation achieved in the media-culture inoculated microcosm BM1-2

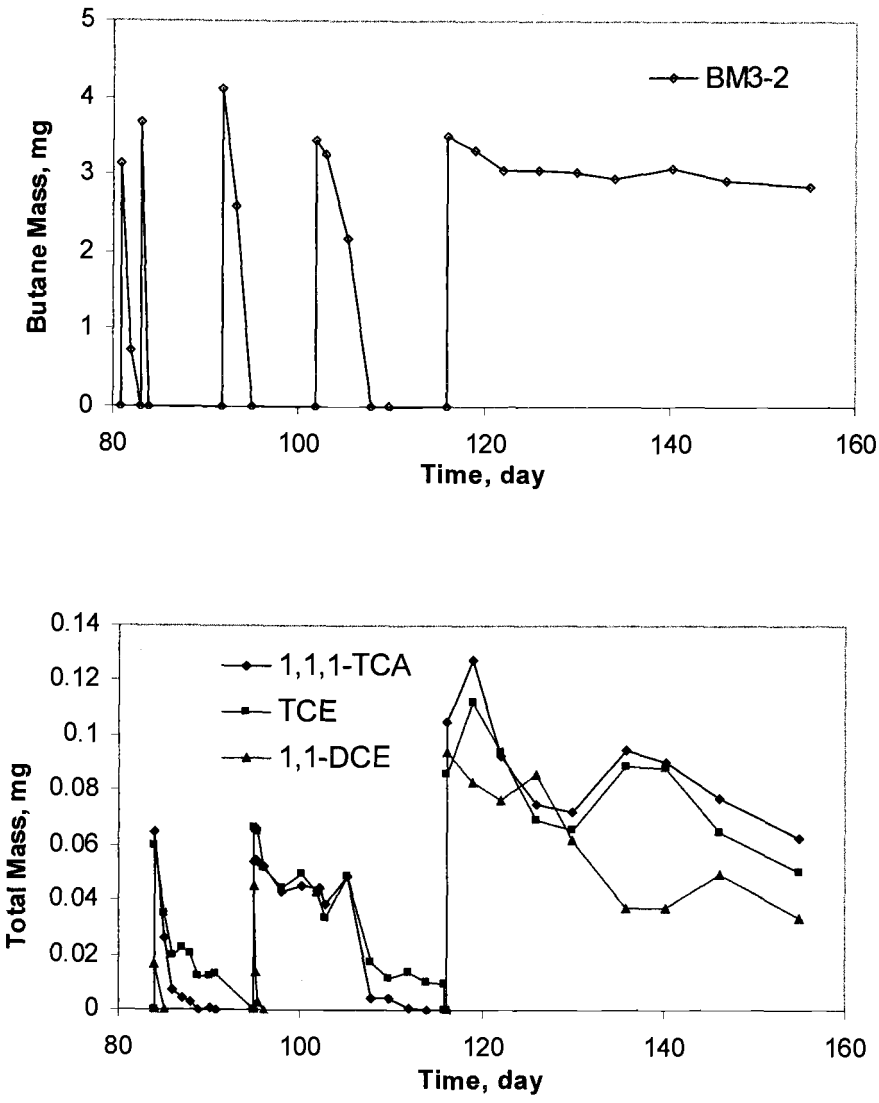

Figure G.8 Butane utilization and chlorinated compound transformation achieved in the media-culture inoculated microcosm BM3-2

G.3 MICROCOSM STUDIES WITH FROZEN BUTANE-UTILIZING CULTURE

Table G.7 The values of pseudo-first-order rate coefficient (P) and time obtained from the 1,1,1-TCA transformation rate measurement in microcosm BR2-2

Starting Day	Time (day)	P (day^{-1})
28.28	0	2.7
29.26	0.98	2.02
30.29	2.01	1.79
31.35	3.08	1.56
32.70	4.43	1.15

Table G.8 The values of pseudo-first-order rate coefficient (P) and time obtained from the 1,1,1-TCA transformation rate measurement in microcosm BR2-3

Starting Day	Time (day)	P (day^{-1})
28	0	3.46
28.54	0.54	3.14
29.26	1.26	2.37
30.10	2.10	2.37
30.97	2.97	1.95
32.26	4.26	1.74

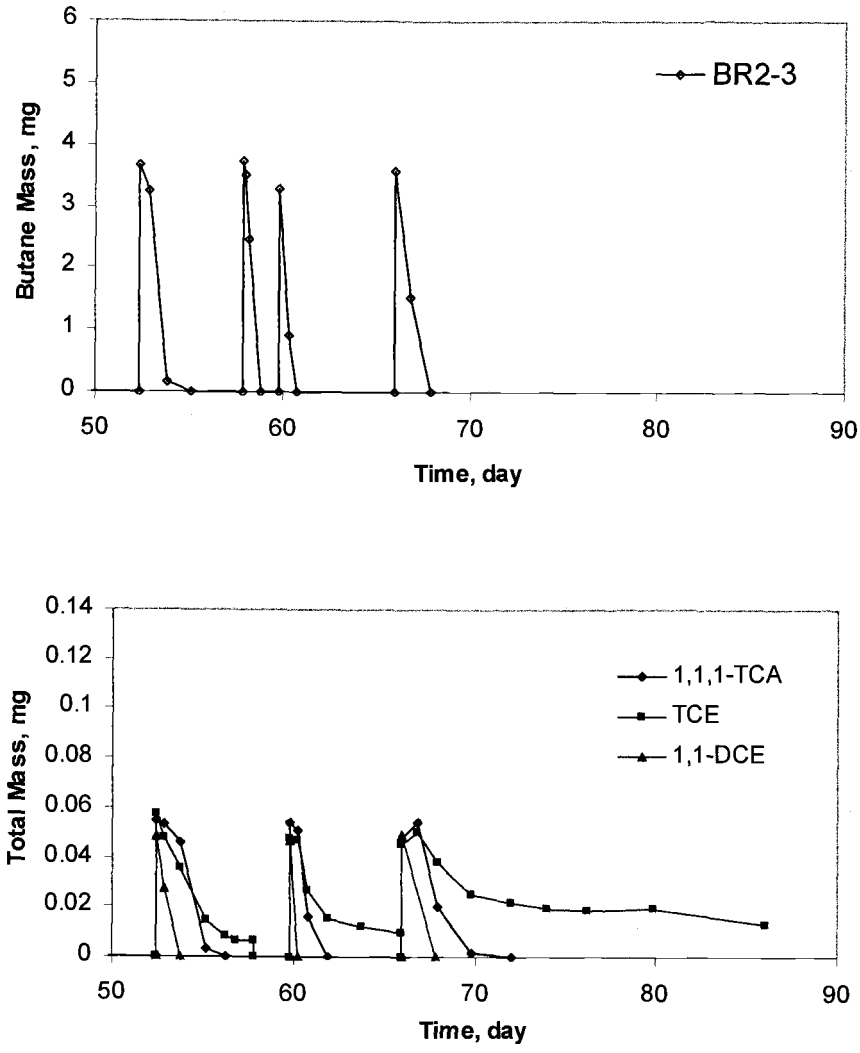

Figure G.9 Butane utilization and chlorinated compound transformation achieved in the media-culture inoculated microcosm BR2-3

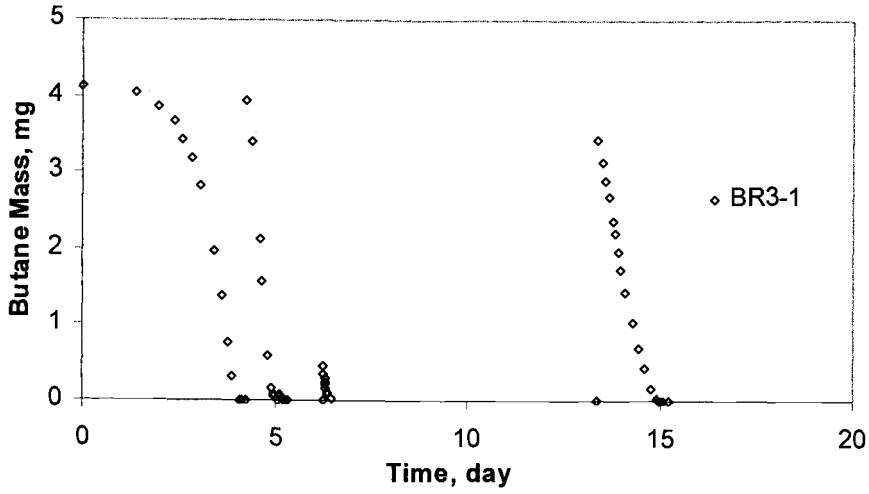

Figure G.10 Overall results from the butane kinetic experiments conducted in the bioaugmented microcosm, BR3-1

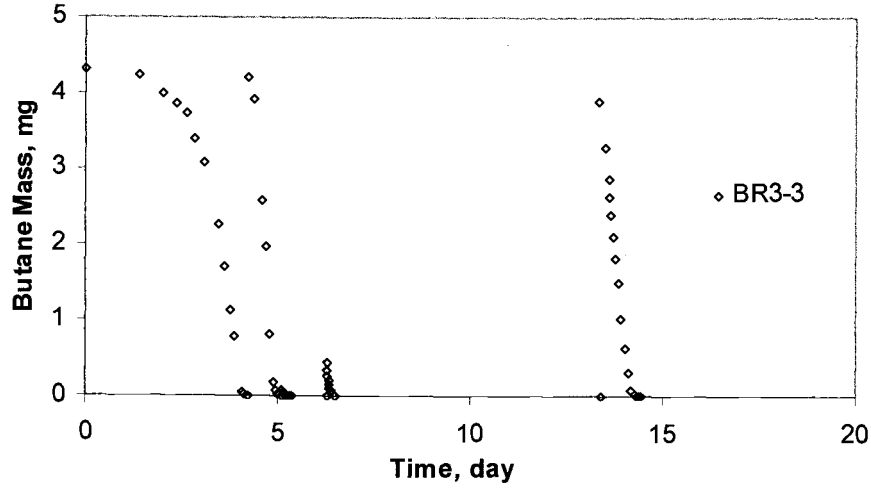

Figure G.11 Overall results from the butane kinetic experiments conducted in the bioaugmented microcosm, BR3-3

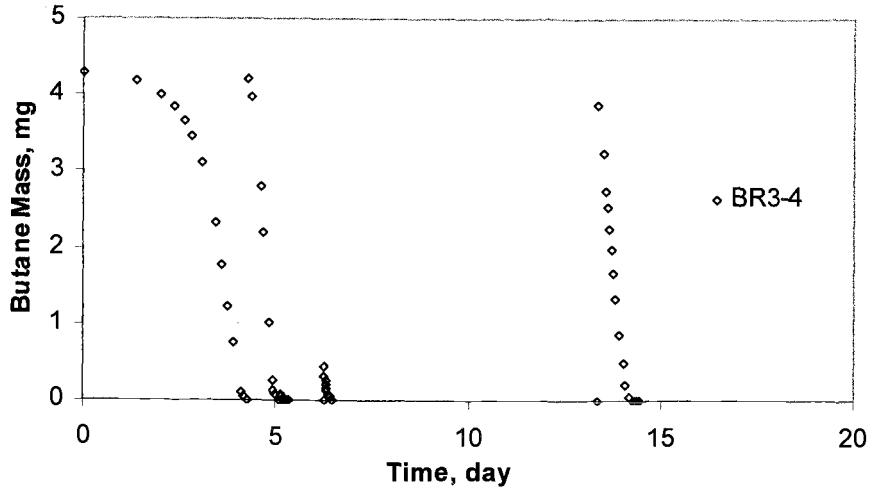

Figure G.12 Overall results from the butane kinetic experiments conducted in the bioaugmented microcosm, BR3-4

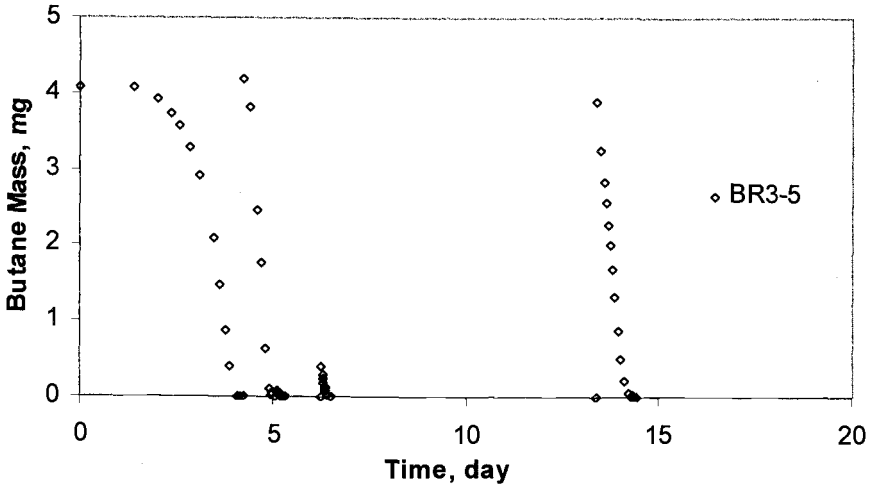

Figure G.13 Overall results from the butane kinetic experiments conducted in the bioaugmented microcosm, BR3-5

Table G.9 The results from the butane kinetic experiments conducted in the BR3 microcosm set

a) The fourth addition of butane

Microcosm	First-order kinetics		Zero-order kinetics		K_s (mg/L)
	Slope	$k_{max}*X/K_s$ (day^{-1})	Slope	$k_{max}*X$ (mg/L-day)	
BR3-1	0.64	14.57	0.17	1.74	0.119
BR3-2	0.81	18.45	0.19	1.92	0.104
BR3-3	0.90	20.43	0.22	2.23	0.109
BR3-4	0.87	19.81	0.22	2.17	0.11
BR3-5	0.84	19.06	0.23	2.28	0.12

b) The fifth addition of butane

Microcosm	First-order kinetics		Zero-order kinetics		K_s (mg/L)
	Slope	$k_{max}*X/K_s$ (day^{-1})	Slope	$k_{max}*X$ (mg/L-day)	
BR3-1	0.64	14.57	0.11	1.11	0.077
BR3-2	0.81	18.45	0.18	1.8	0.109
BR3-3	0.90	20.43	0.21	2.14	0.102
BR3-4	0.87	19.81	0.23	2.29	0.113
BR3-5	0.84	19.06	0.23	2.31	0.132

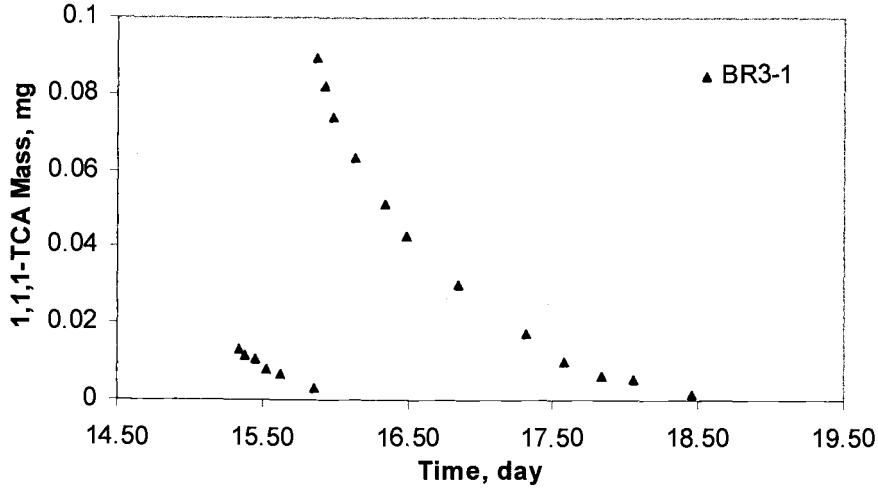

Figure G.14 Overall results from the 1,1,1-TCA kinetic experiments conducted in the bioaugmented microcosm, BR3-1

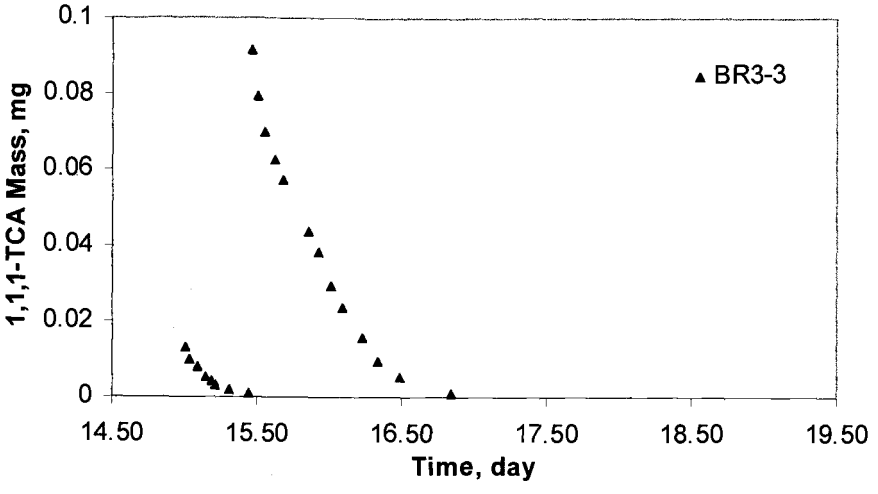

Figure G.15 Overall results from the 1,1,1-TCA kinetic experiments conducted in the bioaugmented microcosm, BR3-3

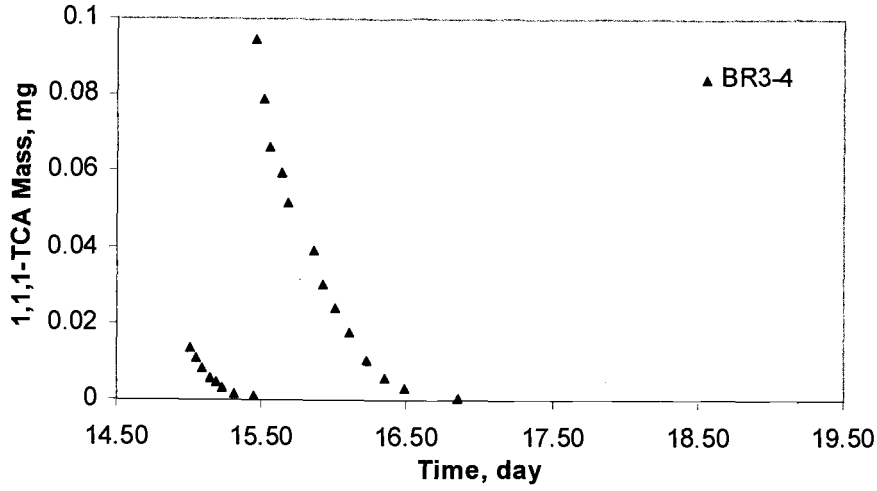

Figure G.16 Overall results from the 1,1,1-TCA kinetic experiments conducted in the bioaugmented microcosm, BR3-4

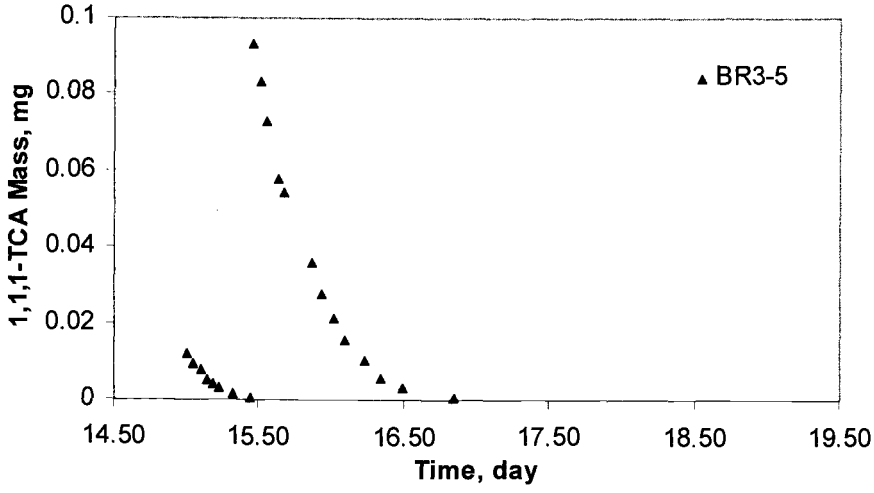

Figure G.17 Overall results from the 1,1,1-TCA kinetic experiments conducted in the bioaugmented microcosm, BR3-5

Table G.10 The results from the 1,1,1-TCA kinetic experiments conducted in the BR3 microcosm set

Microcosm	First-order kinetics		Zero-order kinetics		
	Slope	$k_{max}*X/K_s$ (day^{-1})	Slope	$k_{max}*X$ (mg/L-day)	K_s (mg/L)
BR3-1	0.06	0.08	0.0033	0.033	0.400
BR3-2	0.139	0.18	0.0081	0.081	0.443
BR3-3	0.15	0.19	0.0063	0.063	0.324
BR3-4	0.17	0.23	0.0076	0.076	0.335
BR3-5	0.17	0.23	0.0078	0.078	0.345

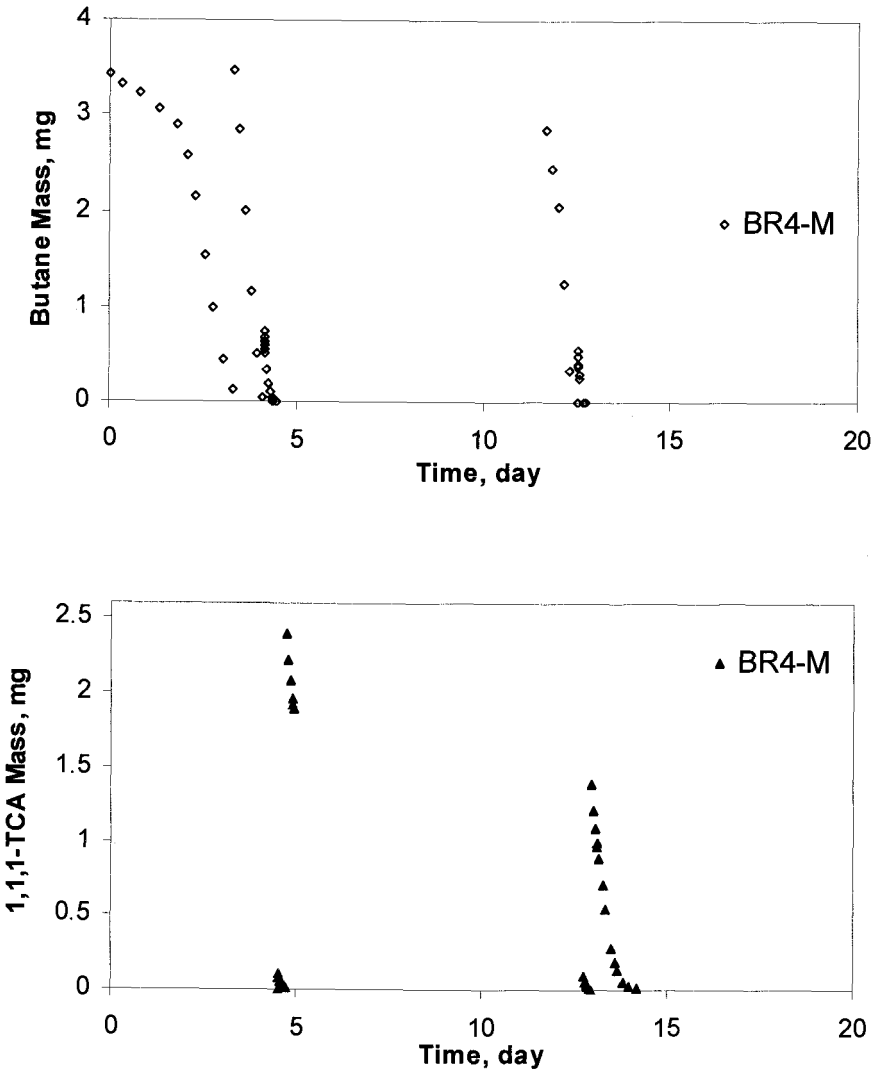

Figure G.18 Overall results from the butane and 1,1,1-TCA kinetic experiments conducted in bioaugmented microcosm BR4-M

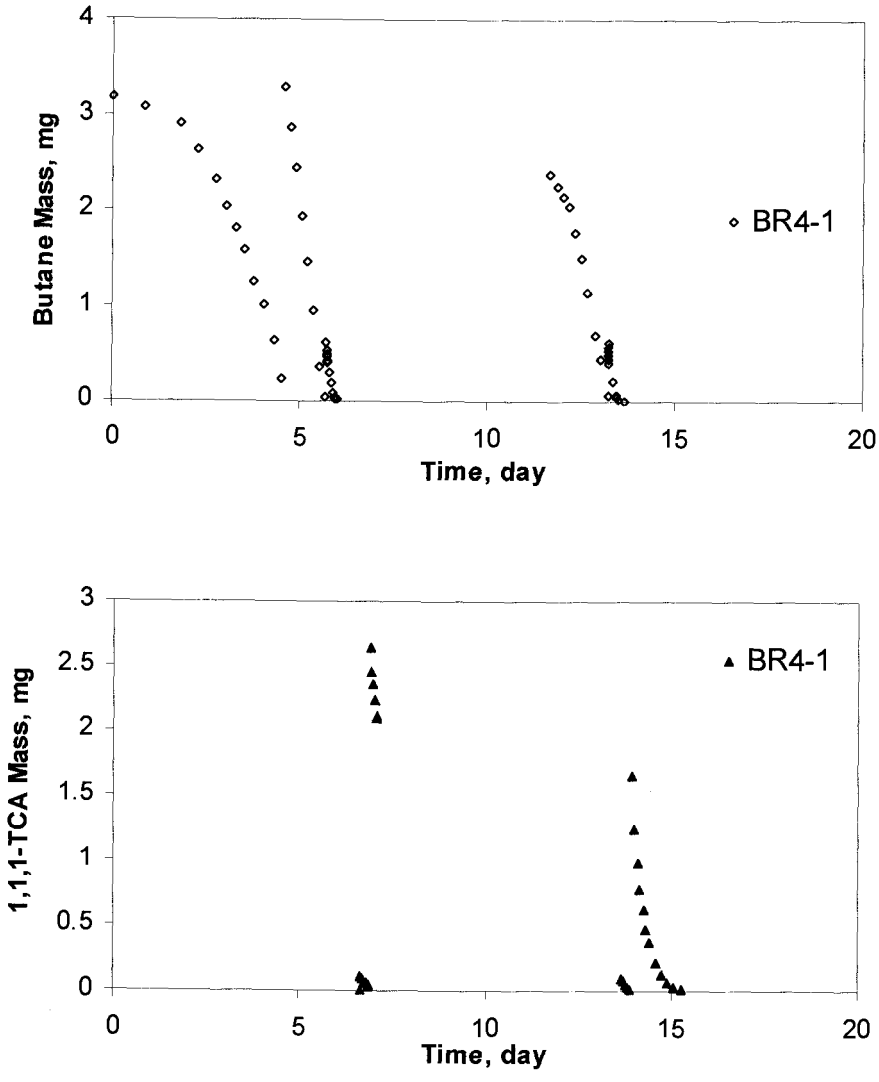

Figure G.19 Overall results from the butane and 1,1,1-TCA kinetic experiments conducted in bioaugmented microcosm BR4-1

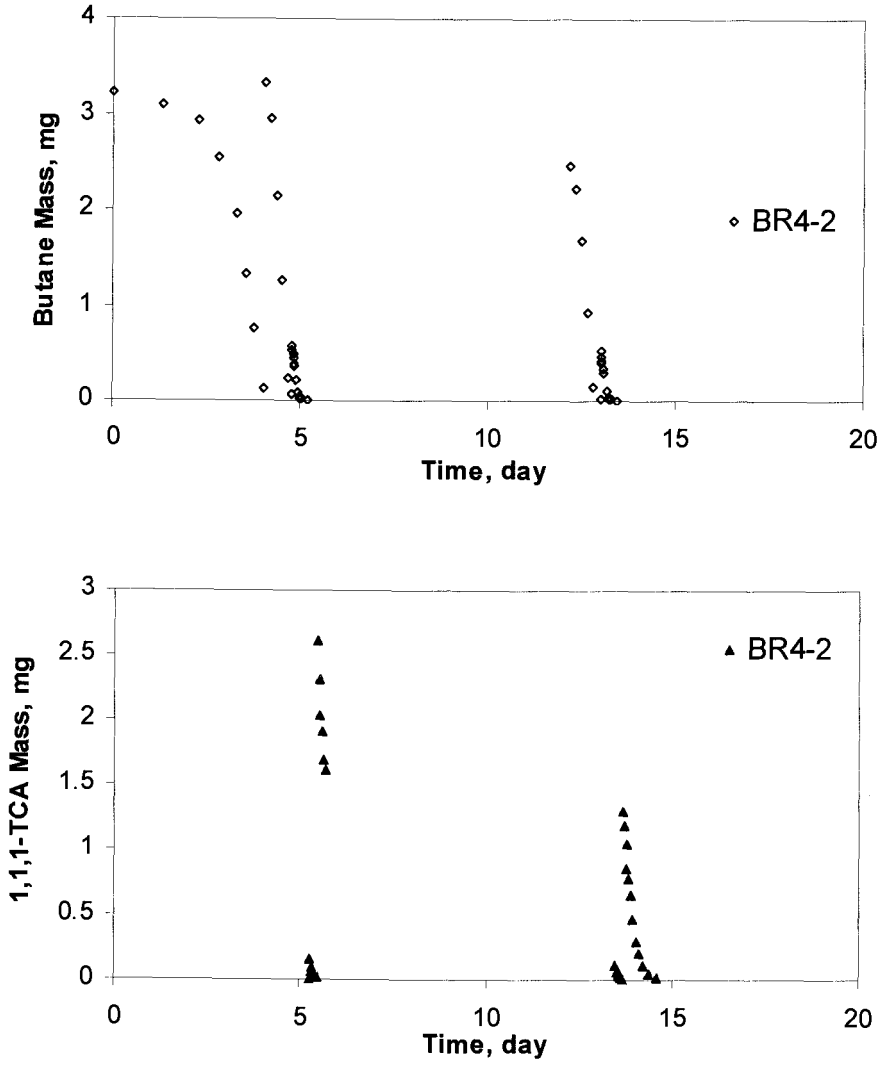

Figure G.20 Overall results from the butane and 1,1,1-TCA kinetic experiments conducted in bioaugmented microcosm BR4-2

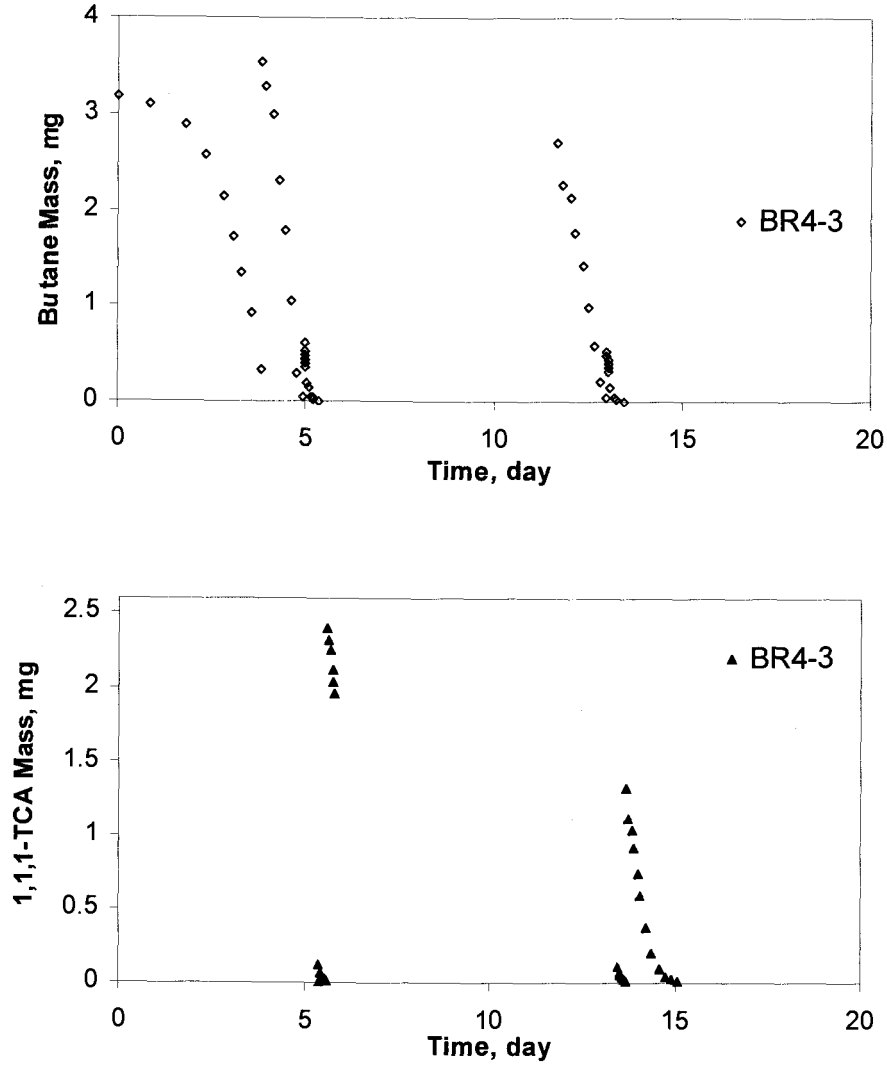

Figure G.21 Overall results from the butane and 1,1,1-TCA kinetic experiments conducted in bioaugmented microcosm BR4-3

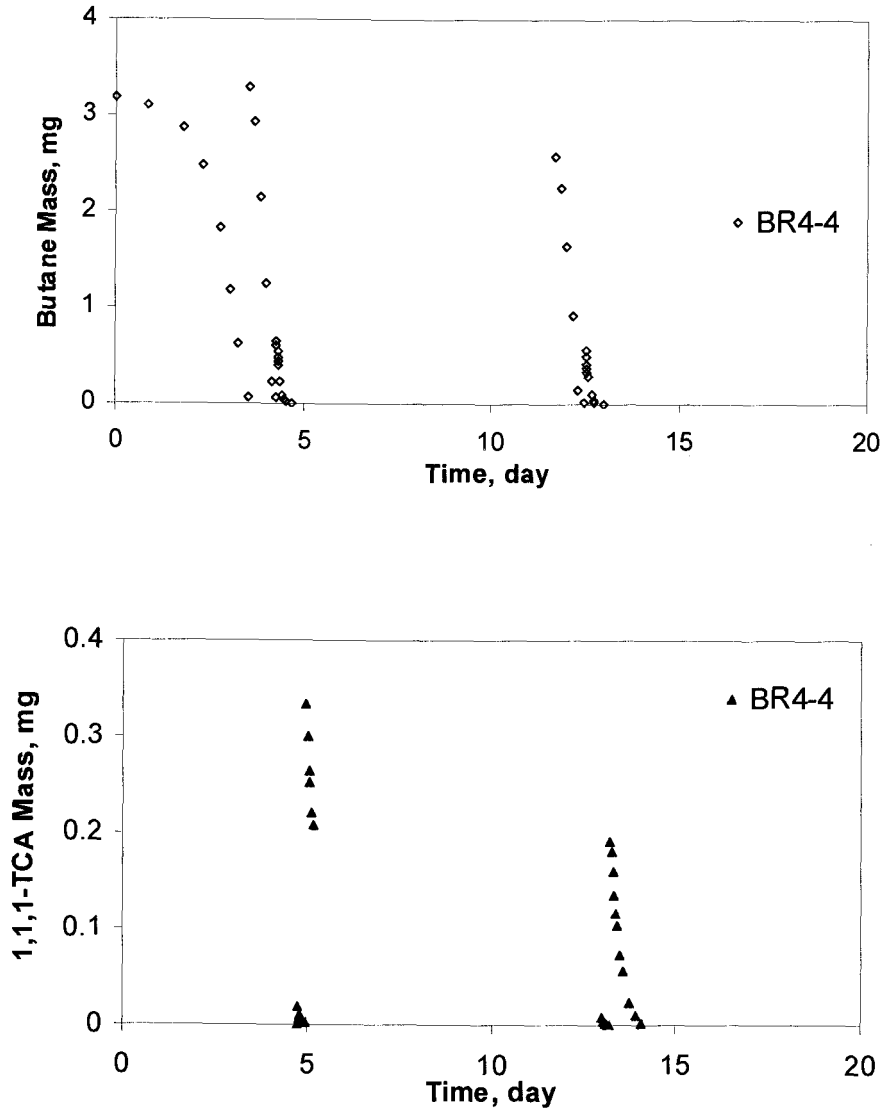

Figure G.22 Overall results from the butane and 1,1,1-TCA kinetic experiments conducted in bioaugmented microcosm BR4-4

Table G.11 The results from the butane kinetic experiments conducted in the BR4 microcosm set

a) The third addition of butane

Microcosm	First-order kinetics		Zero-order kinetics		K_s (mg/L)
	Slope	$k_{max}*X/K_s$ (day^{-1})	Slope	$k_{max}*X$ (mg/L-day)	
BR4-M	2.08	47.08	0.28	2.85	0.061
BR4-1	1	22.6	0.21	2.14	0.095
BR4-2	1.08	24.42	0.26	2.65	0.108
BR4-3	0.95	21.50	0.28	2.78	0.129
BR4-4	1.04	23.67	0.3	3	0.127
BR4-5	1.04	23.64	0.27	2.68	0.113

b) The fifth addition of butane

Microcosm	First-order kinetics		Zero-order kinetics		K_s (mg/L)
	Slope	$k_{max}*X/K_s$ (day^{-1})	Slope	$k_{max}*X$ (mg/L-day)	
BR4-M	1.68	38.06	0.27	2.67	0.071
BR4-1	1.01	22.80	0.24	2.40	0.105
BR4-2	0.94	21.30	0.2	1.99	0.093
BR4-3	0.96	21.77	0.25	2.47	0.116
BR4-4	0.92	20.96	0.25	2.45	0.117
BR4-5	1.1	24.91	0.25	2.49	0.100

Table G.12 The results from the 1,1,1-TCA kinetic experiments conducted in the BR4 microcosm set

a) The first and second additions of 1,1,1-TCA

Microcosm	First-order kinetics		Zero-order kinetics		
	Slope	$k_{max}*X/K_s$ (day^{-1})	Slope	$k_{max}*X$ (mg/L-day)	K_s (mg/L)
BR4-M	0.36	0.48	0.0146	0.146	0.306
BR4-1	0.25	0.33	0.0172	0.172	0.519
BR4-2	0.51	0.67	0.0321	0.321	0.480
BR4-3	0.39	0.51	0.0132	0.132	0.259
BR4-4	0.46	0.61	0.0281	0.281	0.464
BR4-5	0.53	0.7	0.0298	0.298	0.427

b) The third and fourth additions of 1,1,1-TCA

Microcosm	First-order kinetics		Zero-order kinetics		
	Slope	$k_{max}*X/K_s$ (day^{-1})	Slope	$k_{max}*X$ (mg/L-day)	K_s (mg/L)
BR4-M	0.53	0.7	0.0144	0.144	0.206
BR4-1	0.35	0.46	0.0167	0.167	0.365
BR4-2	0.53	0.70	0.0185	0.185	0.263
BR4-3	0.39	0.52	0.0096	0.096	0.186
BR4-4	0.54	0.71	0.0205	0.205	0.289
BR4-5	0.58	0.76	0.0209	0.209	0.276

Table G.13 Parameters for model simulations in Figures G.23

Parameters	T_c = 0.01 mg TCA /mg cells		T_c = 0.1 mg TCA /mg cells		T_c = 0.2 mg TCA /mg cells	
	The 1st addition of TCA	The 2nd addition of TCA	The 1st addition of TCA	The 2nd addition of TCA	The 1st addition of TCA	The 2nd addition of TCA
Starting day	15.33	15.87	15.33	15.87	15.33	15.87
Ending day	15.87	18.46	15.87	18.46	15.87	18.46
X_0, mg/L	30.51 [a]	19.68 [a]	30.51 [a]	27.20 [a]	30.51 [a]	27.67 [a]
Y, mg/mg	0.7	0.7	0.7	0.7	0.7	0.7
b, day^{-1}	0.15	0.15	0.15	0.15	0.15	0.15
$K_{s,But}$, mg/L	0.11	0.11	0.11	0.11	0.11	0.11
$k_{max,But}$, mg/mg-day	1.79	1.79	1.79	1.79	1.79	1.79
$K_{s,TCA}$, mg/L	0.37	0.37	0.37	0.37	0.37	0.37
$k_{max,TCA}$, mg/mg-day	0.05	0.05	0.05	0.05	0.05	0.05
T_c, mg/mg	0.01	0.01	0.1	0.1	0.2	0.2
V_L, L	0.1	0.1	0.1	0.1	0.1	0.1
V_g, L	0.057	0.057	0.057	0.057	0.057	0.057
$H_{cc,But}$, mg-L/mg-L	38.05	38.05	38.05	38.05	38.05	38.05
$H_{cc,TCA}$, mg-L/mg-L	0.55	0.55	0.55	0.55	0.55	0.55

Note a = Obtained from the previous simulation

Table G.14 Parameters for model simulations in Figure G.24

Parameters	T_c = 0.01 mg TCA /mg cells		T_c = 0.1 mg TCA /mg cells		T_c = 0.2 mg TCA /mg cells	
	The 1st addition of TCA	The 2nd addition of TCA	The 1st addition of TCA	The 2nd addition of TCA	The 1st addition of TCA	The 2nd addition of TCA
Starting day	15.01	15.47	15.01	15.47	15.01	15.47
Ending day	15.47	16.86	15.47	16.86	15.47	16.86
X_0, mg/L	33.55[a]	18.40[a]	33.55[a]	25.58[a]	33.55[a]	29.06[a]
Y, mg/mg	0.7	0.7	0.7	0.7	0.7	0.7
b, day^{-1}	0.15	0.15	0.15	0.15	0.15	0.15
$K_{s,But}$, mg/L	0.11	0.11	0.11	0.11	0.11	0.11
$k_{max,But}$, mg/mg-day	1.74	1.74	1.74	1.74	1.74	1.74
$K_{s,TCA}$, mg/L	0.37	0.37	0.37	0.37	0.37	0.37
$k_{max,TCA}$, mg/mg-day	0.12	0.12	0.12	0.12	0.12	0.12
T_c, mg/mg	0.01	0.01	0.1	0.1	0.2	0.2
V_L, L	0.1	0.1	0.1	0.1	0.1	0.1
V_g, L	0.057	0.057	0.057	0.057	0.057	0.057
$H_{cc,But}$, mg-L/mg-L	38.05	38.05	38.05	38.05	38.05	38.05
$H_{cc,TCA}$, mg-L/mg-L	0.55	0.55	0.55	0.55	0.55	0.55

Note a = Obtained from the previous simulation

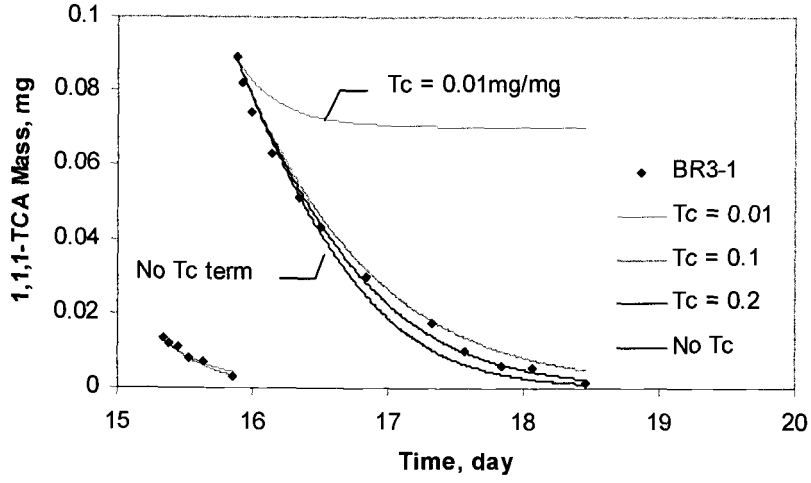

Section	Biomass (X) at starting of model simulation (mg/L)			
	$T_c = 0.01$	$T_c = 0.1$	$T_c = 0.2$	No T_c term
E	30.51	30.51	30.51	30.51
F	19.68	27.20	27.67	28.14

Figure G.23 Simulations of 1,1,1-TCA transformation for microcosm BR3-1 over a range transformation capacities

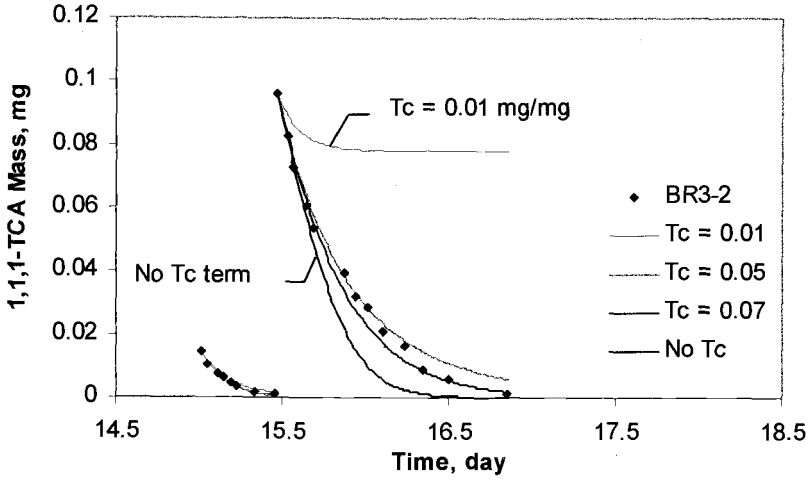

Section	Biomass (X) at starting of model simulation, mg/L			
	$T_c = 0.01$	$T_c = 0.05$	$T_c = 0.07$	No T_c term
E	33.55	33.55	33.55	33.55
F	18.40	25.58	29.06	31.31

Figure G.24 Simulations of 1,1,1-TCA transformation for microcosm BR3-2 over a range transformation capacities

Table G.15 Parameters for model simulations in Figure G.25

Parameters	T_c = 0.01 mg TCA /mg cells		T_c = 0.1 mg TCA /mg cells		T_c = 0.2 mg TCA /mg cells	
	The 1st addition of TCA	The 2nd addition of TCA	The 1st addition of TCA	The 2nd addition of TCA	The 1st addition of TCA	The 2nd addition of TCA
Starting day	15	15.46	15	15.46	15	15.46
Ending day	15.46	16.84	15.46	16.84	15.46	16.84
X_0, mg/L	33.56[a]	21.85[a]	33.56[a]	30.24[a]	33.56[a]	31.21[a]
Y, mg/mg	0.7	0.7	0.7	0.7	0.7	0.7
b, day^{-1}	0.15	0.15	0.15	0.15	0.15	0.15
$K_{s,But}$, mg/L	0.11	0.11	0.11	0.11	0.11	0.11
$k_{max,But}$, mg/mg-day	1.76	1.76	1.76	1.76	1.76	1.76
$K_{s,TCA}$, mg/L	0.37	0.37	0.37	0.37	0.37	0.37
$k_{max,TCA}$, mg/mg-day	0.11	0.11	0.11	0.11	0.11	0.11
T_c, mg/mg	0.01	0.01	0.1	0.1	0.2	0.2
V_L, L	0.1	0.1	0.1	0.1	0.1	0.1
V_g, L	0.057	0.057	0.057	0.057	0.057	0.057
$H_{cc,But}$, mg-L/mg-L	38.05	38.05	38.05	38.05	38.05	38.05
$H_{cc,TCA}$, mg-L/mg-L	0.55	0.55	0.55	0.55	0.55	0.55

Note a = Obtained from the previous simulation

Table G.16 Parameters for model simulations in Figure G.26

Parameters	T_c = 0.01 mg TCA /mg cells		T_c = 0.1 mg TCA /mg cells		T_c = 0.2 mg TCA /mg cells	
	The 1st addition of TCA	The 2nd addition of TCA	The 1st addition of TCA	The 2nd addition of TCA	The 1st addition of TCA	The 2nd addition of TCA
Starting day	15	15.46	15	15.46	15	15.46
Ending day	15.46	16.85	15.46	16.85	15.46	16.85
X_0, mg/L	37.17[a]	23.71[a]	37.17[a]	33.53[a]	37.17[a]	34.11[a]
Y, mg/mg	0.7	0.7	0.7	0.7	0.7	0.7
b, day^{-1}	0.14	0.14	0.14	0.14	0.14	0.14
$K_{s,But}$, mg/L	0.11	0.11	0.11	0.11	0.11	0.11
$k_{max,But}$, mg/mg-day	1.73	1.73	1.73	1.73	1.73	1.73
$K_{s,TCA}$, mg/L	0.37	0.37	0.37	0.37	0.37	0.37
$k_{max,TCA}$, mg/mg-day	0.09	0.09	0.09	0.09	0.09	0.09
T_c, mg/mg	0.01	0.01	0.1	0.1	0.2	0.2
V_L, L	0.1	0.1	0.1	0.1	0.1	0.1
V_g, L	0.057	0.057	0.057	0.057	0.057	0.057
$H_{cc,But}$, mg-L/mg-L	38.05	38.05	38.05	38.05	38.05	38.05
$H_{cc,TCA}$, mg-L/mg-L	0.55	0.55	0.55	0.55	0.55	0.55

Note a = Obtained from the previous simulation

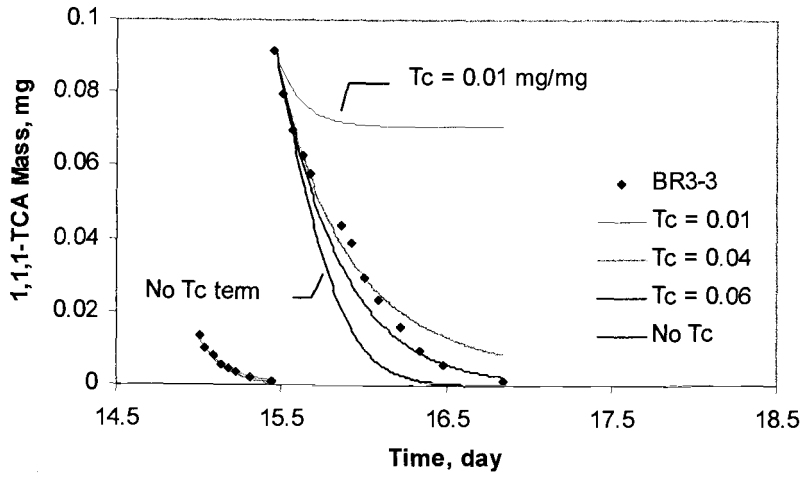

Section	Biomass (X) at starting of model simulation, mg/L			
	$T_c = 0.01$	$T_c = 0.04$	$T_c = 0.06$	No T_c term
E	35.56	35.56	35.56	35.56
F	21.85	30.24	31.21	33.19

Figure G.25 Simulations of 1,1,1-TCA transformation for microcosm BR3-3 over a range transformation capacities

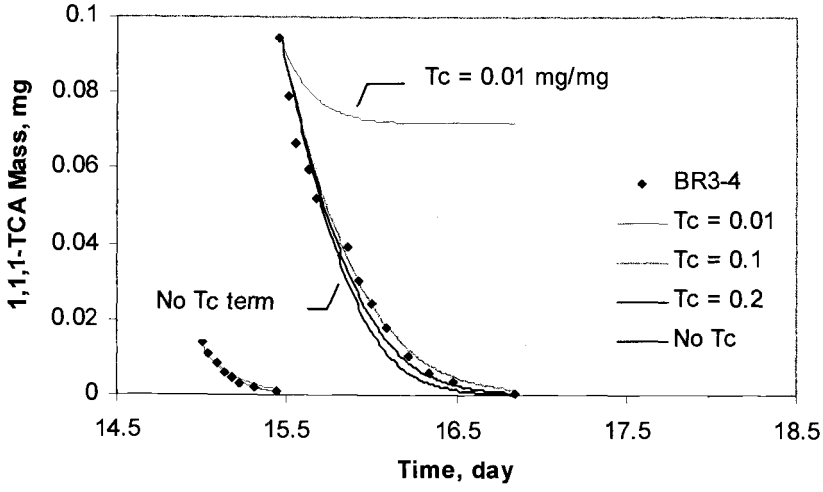

Section	Biomass (X) at starting of model simulation, mg/L			
	$T_c = 0.01$	$T_c = 0.1$	$T_c = 0.2$	No T_c term
E	37.17	37.17	37.17	37.17
F	23.71	33.53	34.11	34.69

Figure G.26 Simulations of 1,1,1-TCA transformation for microcosm BR3-4 over a range transformation capacities

Table G.17 Parameters for model simulations in Figure G.27

Parameters	The 1st addition of butane	The 2nd addition of butane	The 3rd addition of butane	The 1st addition of TCA	The 2nd addition of TCA	The 4th addition of butane	The 5th addition of butane	The 3rd addition of TCA	The 4th addition of TCA
Starting day	0	4.55	5.71	6.67	6.89	11.67	13.23	13.68	13.92
Ending day	4.55	5.71	6.67	6.89	7.1	13.23	13.68	13.92	15.26
X_0, mg/L	0.45	18.29[a]	36.21[a]	35.14[a]	34[a]	16.6[a]	27.15[a]	29.4[a]	28.36[a]
Y, mg/mg	0.7	0.7	0.7	0.7	0.7	0.7	0.7	0.7	0.7
b, day^{-1}	0.15	0.15	0.15	0.15	0.15	0.15	0.15	0.15	0.15
$K_{s,But}$, mg/L	0.11	0.11	0.11	0.11	0.11	0.11	0.11	0.11	0.11
$k_{max,But}$, mg/mg-day	1.58	1.58	1.58	1.58	1.58	1.58	1.58	1.58	1.58
$K_{s,TCA}$, mg/L	0.37	0.37	0.37	0.37	0.37	0.37	0.37	0.37	0.37
$k_{max,TCA}$, mg/mg-day	-[b]	-[b]	-[b]	0.1	0.1	0.1	0.1	0.1	0.1
T_c, mg/mg	-[b]	-[b]	-[b]	-[b]	-[b]	-[b]	-[b]	-[b]	-[b]
V_L, L	0.1	0.1	0.1	0.1	0.1	0.1	0.1	0.1	0.1
V_g, L	0.057	0.057	0.057	0.057	0.057	0.057	0.057	0.057	0.057
$H_{cc,But}$, mg-L/mg-L	38.05	38.05	38.05	38.05	38.05	38.05	38.05	38.05	38.05
$H_{cc,TCA}$, mg-L/mg-L	0.55	0.55	0.55	0.55	0.55	0.55	0.55	0.55	0.55

Note a = Obtained from the previous simulation
b = Not used in the simulation

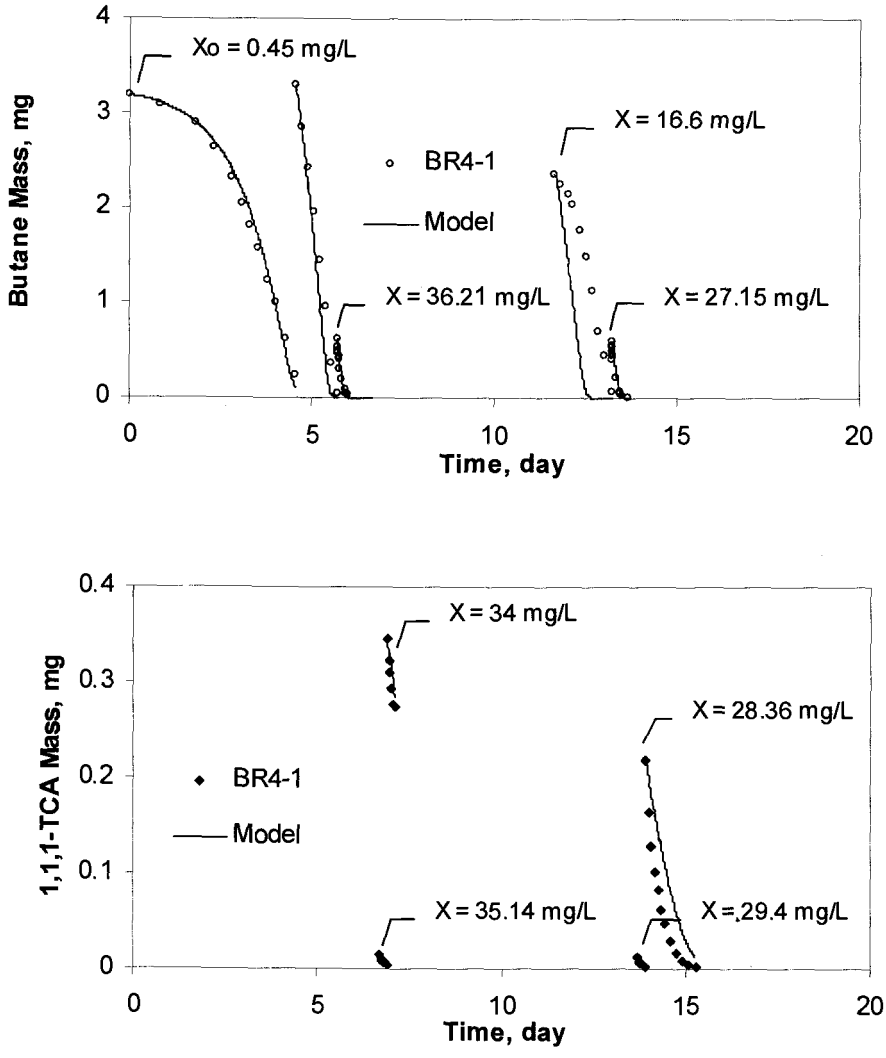

Figure G.27 Simulations of butane utilization and 1,1,1-TCA transformation for microcosm BR4-1 without the term for transformation capacity

Table G.18 Parameters for model simulations in Figure G.28

Parameters	The 1st addition of butane	The 2nd addition of butane	The 3rd addition of butane	The 1st addition of TCA	The 2nd addition of TCA	The 4th addition of butane	The 5th addition of butane	The 3rd addition of TCA	The 4th addition of TCA
Starting day	0	4.05	4.8	5.24	5.47	12.17	13.02	13.47	13.68
Ending day	4.05	4.8	5.24	5.47	5.68	13.02	13.47	13.68	14.58
X_0, mg/L	0.45	18.64[a]	36.4[a]	37.89[a]	36.6[a]	13.4[a]	26.93[a]	28.69[a]	27.8[a]
Y, mg/mg	0.7	0.7	0.7	0.7	0.7	0.7	0.7	0.7	0.7
b, day^{-1}	0.15	0.15	0.15	0.15	0.15	0.15	0.15	0.15	0.15
$K_{s,But}$, mg/L	0.11	0.11	0.11	0.11	0.11	0.11	0.11	0.11	0.11
$k_{max,But}$, mg/mg-day	1.74	1.74	1.74	1.74	1.74	1.74	1.74	1.74	1.74
$K_{s,TCA}$, mg/L	0.37	0.37	0.37	0.37	0.37	0.37	0.37	0.37	0.37
$k_{max,TCA}$, mg/mg-day	-[b]	-[b]	-[b]	0.19	0.19	0.19	0.19	0.19	0.19
T_c, mg/mg	-[b]	-[b]	-[b]	-[b]	-[b]	-[b]	-[b]	-[b]	-[b]
V_L, L	0.1	0.1	0.1	0.1	0.1	0.1	0.1	0.1	0.1
V_g, L	0.057	0.057	0.057	0.057	0.057	0.057	0.057	0.057	0.057
$H_{cc,But}$, mg-L/mg-L	38.05	38.05	38.05	38.05	38.05	38.05	38.05	38.05	38.05
$H_{cc,TCA}$, mg-L/mg-L	0.55	0.55	0.55	0.55	0.55	0.55	0.55	0.55	0.55

Note a = Obtained from the previous simulation
b = Not used in the simulation

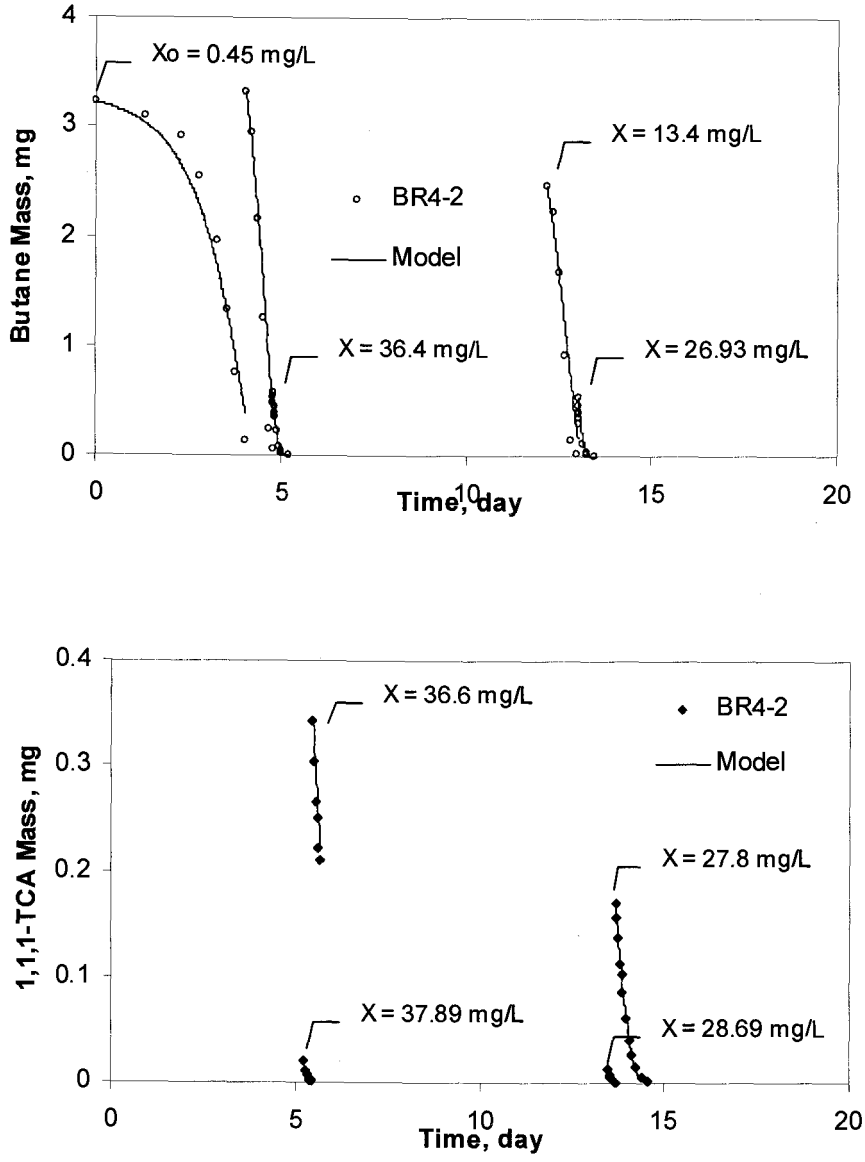

Figure G.28 Simulations of butane utilization and 1,1,1-TCA transformation for microcosm BR4-2 without the term for transformation capacity.

Table G.19 Parameters for model simulations in Figure G.29

Parameters	The 1st addition of butane	The 2nd addition of butane	The 3rd addition of butane	The 1st addition of TCA	The 2nd addition of TCA	The 4th addition of butane	The 5th addition of butane	The 3rd addition of TCA	The 4th addition of TCA
Starting day	0	3.8	4.96	5.39	5.64	11.67	13.01	13.47	13.68
Ending day	3.8	4.96	5.39	5.64	5.83	13.01	13.47	13.68	15.08
X_0, mg/L	0.45	16.22[a]	36.07[a]	37.8[a]	36.41[a]	14.74[a]	28.67[a]	30.25[a]	29.31[a]
Y, mg/mg	0.7	0.7	0.7	0.7	0.7	0.7	0.7	0.7	0.7
b, day^{-1}	0.15	0.15	0.15	0.15	0.15	0.15	0.15	0.15	0.15
$K_{s,But}$, mg/L	0.11	0.11	0.11	0.11	0.11	0.11	0.11	0.11	0.11
$k_{max,But}$, mg/mg-day	1.74	1.74	1.74	1.74	1.74	1.74	1.74	1.74	1.74
$K_{s,TCA}$, mg/L	0.37	0.37	0.37	0.37	0.37	0.37	0.37	0.37	0.37
$k_{max,TCA}$, mg/mg-day	-[b]	-[b]	-[b]	0.14	0.14	0.14	0.14	0.14	0.14
T_c, mg/mg	-[b]	-[b]	-[b]	-[b]	-[b]	-[b]	-[b]	-[b]	-[b]
V_L, L	0.1	0.1	0.1	0.1	0.1	0.1	0.1	0.1	0.1
V_g, L	0.057	0.057	0.057	0.057	0.057	0.057	0.057	0.057	0.057
$H_{cc,But}$, mg-L/mg-L	38.05	38.05	38.05	38.05	38.05	38.05	38.05	38.05	38.05
$H_{cc,TCA}$, mg-L/mg-L	0.55	0.55	0.55	0.55	0.55	0.55	0.55	0.55	0.55

Note a = Obtained from the previous simulation
b = Not used in the simulation

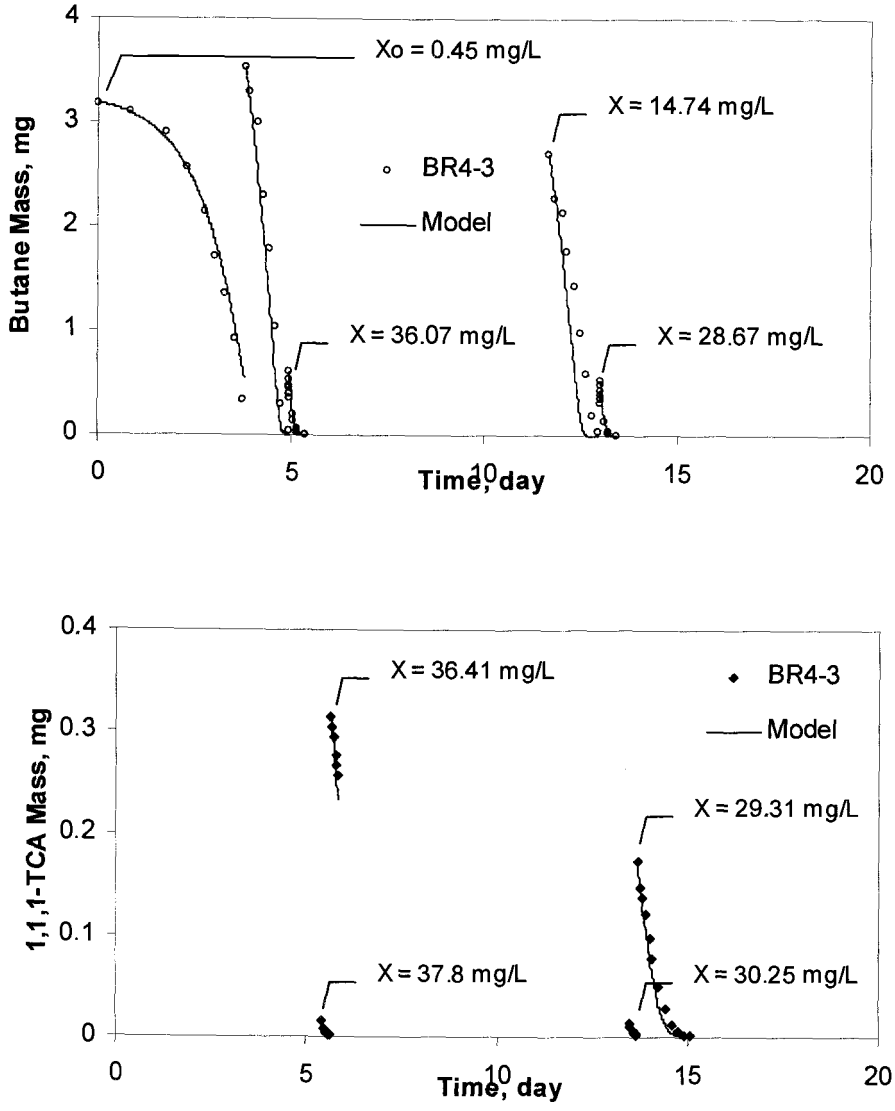

Figure G.29 Simulations of butane utilization and 1,1,1-TCA transformation for microcosm BR4-3 without the term for transformation capacity

Table G.20 Parameters for model simulations in Figure G.30

Parameters	The 1st addition of butane	The 2nd addition of butane	The 3rd addition of butane	The 1st addition of TCA	The 2nd addition of TCA	The 4th addition of butane	The 5th addition of butane	The 3rd addition of TCA	The 4th addition of TCA
Starting day	0	3.54	4.34	4.74	4.96	11.42	12.52	12.97	13.17
Ending day	3.54	4.34	4.74	4.96	5.17	12.52	12.97	13.17	14.07
X_0, mg/L	0.45	18.15[a]	37.9[a]	39.45[a]	38.17[a]	14.48[a]	29.99[a]	31.86[a]	30.92[a]
Y, mg/mg	0.7	0.7	0.7	0.7	0.7	0.7	0.7	0.7	0.7
b, day^{-1}	0.15	0.15	0.15	0.15	0.15	0.15	0.15	0.15	0.15
$K_{s,But}$, mg/L	0.11	0.11	0.11	0.11	0.11	0.11	0.11	0.11	0.11
$k_{max,But}$, mg/mg-day	1.93	1.93	1.93	1.93	1.93	1.93	1.93	1.93	1.93
$K_{s,TCA}$, mg/L	0.37	0.37	0.37	0.37	0.37	0.37	0.37	0.37	0.37
$k_{max,TCA}$, mg/mg-day	-[b]	-[b]	-[b]	0.16	0.16	0.16	0.16	0.16	0.16
T_c, mg/mg	-[b]	-[b]	-[b]	-[b]	-[b]	-[b]	-[b]	-[b]	-[b]
V_L, L	0.1	0.1	0.1	0.1	0.1	0.1	0.1	0.1	0.1
V_g, L	0.057	0.057	0.057	0.057	0.057	0.057	0.057	0.057	0.057
$H_{cc,But}$, mg-L/mg-L	38.05	38.05	38.05	38.05	38.05	38.05	38.05	38.05	38.05
$H_{cc,TCA}$, mg-L/mg-L	0.55	0.55	0.55	0.55	0.55	0.55	0.55	0.55	0.55

Note a = Obtained from the previous simulation
b = Not used in the simulation

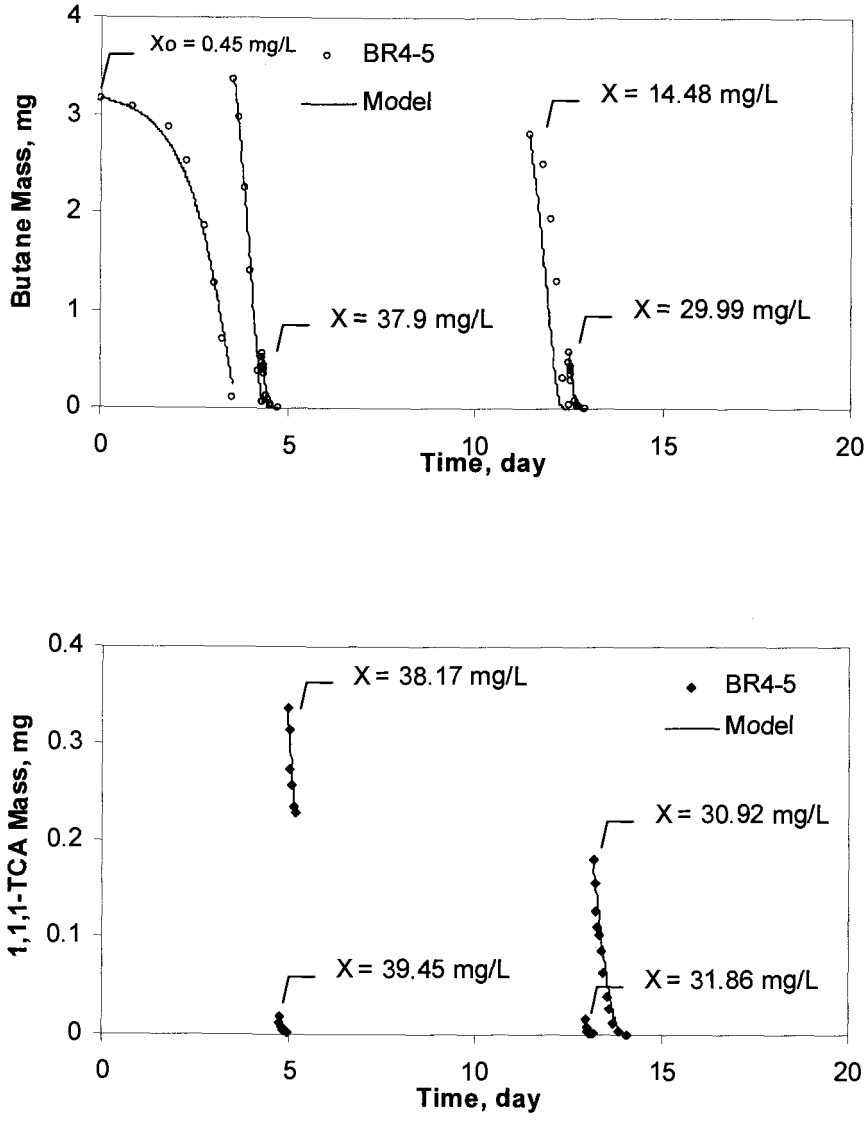

Figure G.30 Simulations of butane utilization and 1,1,1-TCA transformation for microcosm BR4-5 without the term for transformation capacity

Table G.21 Parameters for model simulations in Figure G.31

a) T_c = 0.1 mg TCA/mg cells

Parameters	The 1st addition of TCA	The 2nd addition of TCA	The 4th addition of butane	The 5th addition of butane	The 3rd addition of TCA	The 4th addition of TCA
Starting day	4.5	4.73	11.67	12.53	12.75	12.98
Ending day	4.73	4.97	12.53	12.75	12.98	14.17
X_0, mg/L	43.92[a]	41.2[a]	11.63[a]	28.66[a]	31.41[a]	29.48[a]
Y, mg/mg	0.7	0.7	0.7	0.7	0.7	0.7
b, day^{-1}	0.15	0.15	0.15	0.15	0.15	0.15
$K_{s,But}$, mg/L	0.11	0.11	0.11	0.11	0.11	0.11
$k_{max,But}$, mg/mg-day	2.2	2.2	2.2	2.2	2.2	2.2
$K_{s,TCA}$, mg/L	0.37	0.37	0.37	0.37	0.37	0.37
$k_{max,TCA}$, mg/mg-day	0.11	0.11	0.11	0.11	0.11	0.11
T_c, mg/mg	0.1	0.1	0.1	0.1	0.1	0.1
V_L, L	0.1	0.1	0.1	0.1	0.1	0.1
V_g, L	0.057	0.057	0.057	0.057	0.057	0.057
$H_{cc,But}$, mg-L/mg-L	38.05	38.05	38.05	38.05	38.05	38.05
$H_{cc,TCA}$, mg-L/mg-L	0.55	0.55	0.55	0.55	0.55	0.55

Note a = Obtained from the previous simulation

Table G.21, Continued

b) T_c = 0.2 mg TCA/mg cells

Parameters	The 1st addition of TCA	The 2nd addition of TCA	The 4th addition of butane	The 5th addition of butane	The 3rd addition of TCA	The 4th addition of TCA
Starting day	4.5	4.73	11.67	12.53	12.75	12.98
Ending day	4.73	4.97	12.53	12.75	12.98	14.17
X_0, mg/L	43.92[a]	41.81[a]	13.2[a]	30.21[a]	32.92[a]	31.36[a]
Y, mg/mg	0.7	0.7	0.7	0.7	0.7	0.7
b, day^{-1}	0.15	0.15	0.15	0.15	0.15	0.15
$K_{s,But}$, mg/L	0.11	0.11	0.11	0.11	0.11	0.11
$k_{max,But}$, mg/mg-day	2.2	2.2	2.2	2.2	2.2	2.2
$K_{s,TCA}$, mg/L	0.37	0.37	0.37	0.37	0.37	0.37
$k_{max,TCA}$, mg/mg-day	0.11	0.11	0.11	0.11	0.11	0.11
T_c, mg/mg	0.2	0.2	0.2	0.2	0.2	0.2
V_L, L	0.1	0.1	0.1	0.1	0.1	0.1
V_g, L	0.057	0.057	0.057	0.057	0.057	0.057
$H_{cc,But}$, mg-L/mg-L	38.05	38.05	38.05	38.05	38.05	38.05
$H_{cc,TCA}$, mg-L/mg-L	0.55	0.55	0.55	0.55	0.55	0.55

Note a = Obtained from the previous simulation

Table G.21, Continued

c) T_c = 0.3 mg TCA/mg cells

Parameters	The 1st addition of TCA	The 2nd addition of TCA	The 4th addition of butane	The 5th addition of butane	The 3rd addition of TCA	The 4th addition of TCA
Starting day	4.5	4.73	11.67	12.53	12.75	12.98
Ending day	4.73	4.97	12.53	12.75	12.98	14.17
X_0, mg/L	43.92[a]	42.02[a]	13.77[a]	30.71[a]	33.41[a]	31.98[a]
Y, mg/mg	0.7	0.7	0.7	0.7	0.7	0.7
b, day^{-1}	0.15	0.15	0.15	0.15	0.15	0.15
$K_{s,But}$, mg/L	0.11	0.11	0.11	0.11	0.11	0.11
$k_{max,But}$, mg/mg-day	2.2	2.2	2.2	2.2	2.2	2.2
$K_{s,TCA}$, mg/L	0.37	0.37	0.37	0.37	0.37	0.37
$k_{max,TCA}$, mg/mg-day	0.11	0.11	0.11	0.11	0.11	0.11
T_c, mg/mg	0.3	0.3	0.3	0.3	0.3	0.3
V_L, L	0.1	0.1	0.1	0.1	0.1	0.1
V_g, L	0.057	0.057	0.057	0.057	0.057	0.057
$H_{cc,But}$, mg-L/mg-L	38.05	38.05	38.05	38.05	38.05	38.05
$H_{cc,TCA}$, mg-L/mg-L	0.55	0.55	0.55	0.55	0.55	0.55

Note a = Obtained from the previous simulation

a) The first addition of 1,1,1-TCA on day 4

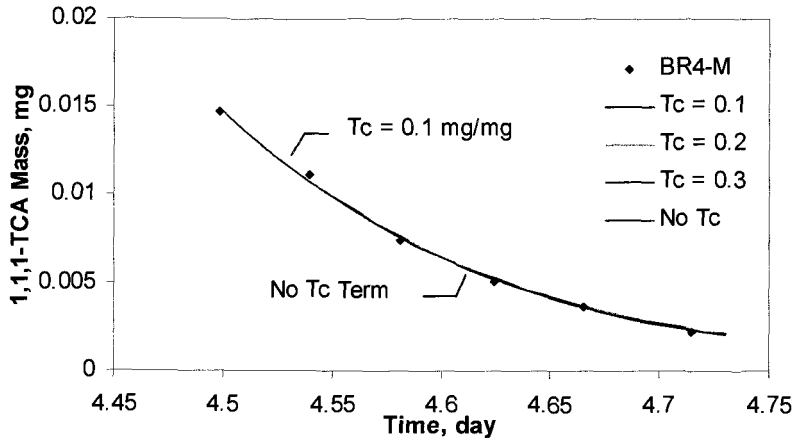

Biomass (X) at starting of model simulation (mg/L)			
$T_c = 0.1$	$T_c = 0.2$	$T_c = 0.3$	No T_c term
43.92	43.92	43.92	43.92

b) The second addition of 1,1,1-TCA on day 4

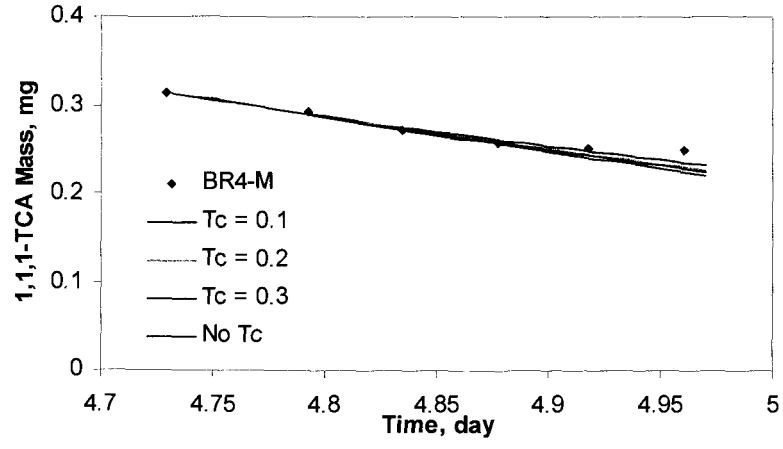

Biomass (X) at starting of model simulation (mg/L)			
$T_c = 0.1$	$T_c = 0.2$	$T_c = 0.3$	No T_c term
41.20	41.81	42.02	42.43

Figure G.31 Simulations of butane utilization and 1,1,1-TCA transformation for microcosm BR4-M over a range transformation capacities

c) The fourth addition of butane on day 11

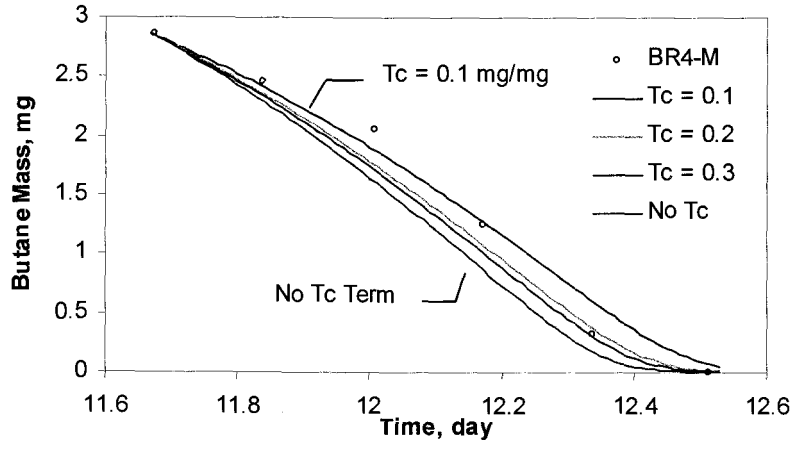

Biomass (X) at starting of model simulation (mg/L)			
$T_c = 0.1$	$T_c = 0.2$	$T_c = 0.3$	No T_c term
11.63	13.20	13.77	14.98

d) The fifth addition of butane on day 12

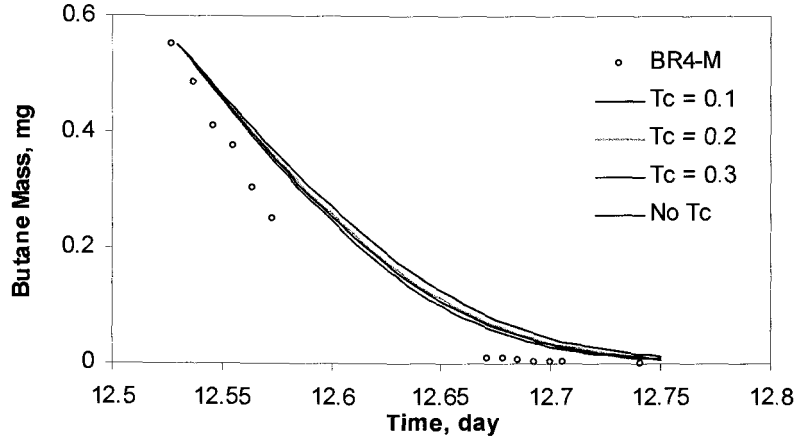

Biomass (X) at starting of model simulation (mg/L)			
$T_c = 0.1$	$T_c = 0.2$	$T_c = 0.3$	No T_c term
28.66	30.21	30.71	31.74

Figure G.31, Continued

e) The third addition of 1,1,1-TCA on day 12

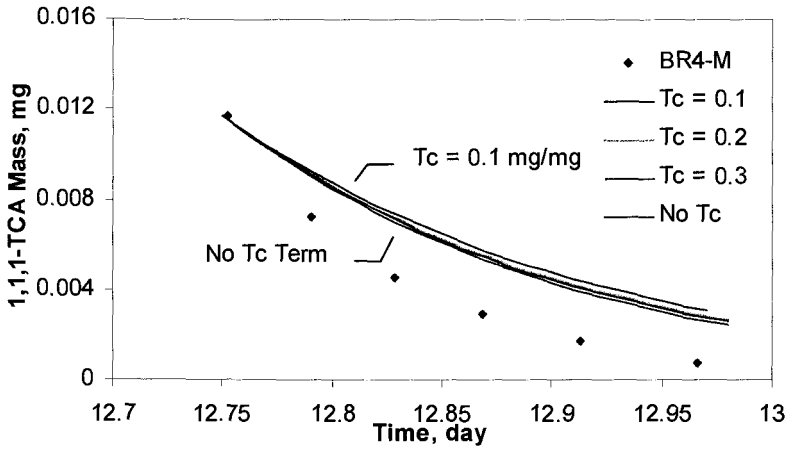

Biomass (X) at starting of model simulation (mg/L)			
$T_c = 0.1$	$T_c = 0.2$	$T_c = 0.3$	No T_c term
31.41	32.92	33.41	34.42

f) The fourth addition of 1,1,1-TCA on day 12

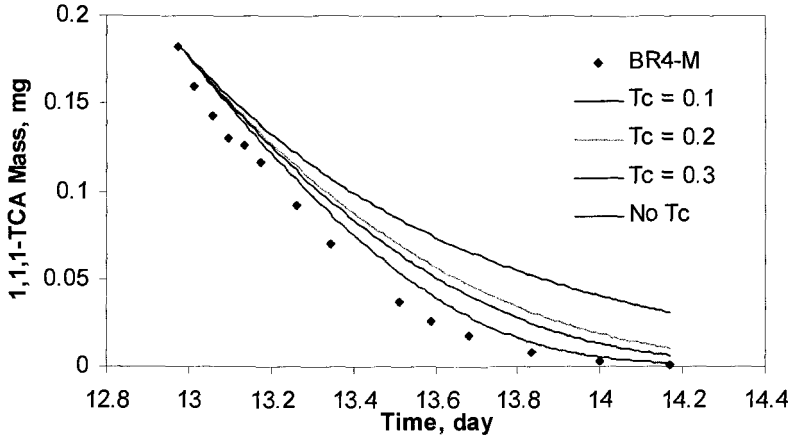

Biomass (X) at starting of model simulation (mg/L)			
$T_c = 0.1$	$T_c = 0.2$	$T_c = 0.3$	No T_c term
29.48	31.36	31.98	33.25

Figure G.31, Continued

Table G.22 Parameters for model simulations in Figure G.32

a) T_c = 0.1 mg TCA/mg cells

Parameters	The 1st addition of TCA	The 2nd addition of TCA	The 4th addition of butane	The 5th addition of butane	The 3rd addition of TCA	The 4th addition of TCA
Starting day	6.67	6.89	11.67	13.23	13.68	13.92
Ending day	6.89	7.1	13.23	13.68	13.92	15.26
X_0, mg/L	35.4[a]	32.97[a]	13.42[a]	24.8[a]	27.2[a]	25.47[a]
Y, mg/mg	0.7	0.7	0.7	0.7	0.7	0.7
b, day^{-1}	0.15	0.15	0.15	0.15	0.15	0.15
$K_{s,But}$, mg/L	0.11	0.11	0.11	0.11	0.11	0.11
$k_{max,But}$, mg/mg-day	1.58	1.58	1.58	1.58	1.58	1.58
$K_{s,TCA}$, mg/L	0.37	0.37	0.37	0.37	0.37	0.37
$k_{max,TCA}$, mg/mg-day	0.1	0.1	0.1	0.1	0.1	0.1
T_c, mg/mg	0.1	0.1	0.1	0.1	0.1	0.1
V_L, L	0.1	0.1	0.1	0.1	0.1	0.1
V_g, L	0.057	0.057	0.057	0.057	0.057	0.057
$H_{cc,But}$, mg-L/mg-L	38.05	38.05	38.05	38.05	38.05	38.05
$H_{cc,TCA}$, mg-L/mg-L	0.55	0.55	0.55	0.55	0.55	0.55

Note a = Obtained from the previous simulation

Table G.22, Continued

b) T_c = 0.2 mg TCA/mg cells

Parameters	The 1st addition of TCA	The 2nd addition of TCA	The 4th addition of butane	The 5th addition of butane	The 3rd addition of TCA	The 4th addition of TCA
Starting day	6.67	6.89	11.67	13.23	13.68	13.92
Ending day	6.89	7.1	13.23	13.68	13.92	15.26
X_0, mg/L	35.4[a]	33.48[a]	14.92[a]	25.90[a]	28.23[a]	26.45[a]
Y, mg/mg	0.7	0.7	0.7	0.7	0.7	0.7
b, day^{-1}	0.15	0.15	0.15	0.15	0.15	0.15
$K_{s,But}$, mg/L	0.11	0.11	0.11	0.11	0.11	0.11
$k_{max,But}$, mg/mg-day	1.58	1.58	1.58	1.58	1.58	1.58
$K_{s,TCA}$, mg/L	0.37	0.37	0.37	0.37	0.37	0.37
$k_{max,TCA}$, mg/mg-day	0.1	0.1	0.1	0.1	0.1	0.1
T_c, mg/mg	0.2	0.2	0.2	0.2	0.2	0.2
V_L, L	0.1	0.1	0.1	0.1	0.1	0.1
V_g, L	0.057	0.057	0.057	0.057	0.057	0.057
$H_{cc,But}$, mg-L/mg-L	38.05	38.05	38.05	38.05	38.05	38.05
$H_{cc,TCA}$, mg-L/mg-L	0.55	0.55	0.55	0.55	0.55	0.55

Note a = Obtained from the previous simulation

Table G.22, Continued

c) T_c = 0.3 mg TCA/mg cells

Parameters	The 1st addition of TCA	The 2nd addition of TCA	The 4th addition of butane	The 5th addition of butane	The 3rd addition of TCA	The 4th addition of TCA
Starting day	6.67	6.89	11.67	13.23	13.68	13.92
Ending day	6.89	7.1	13.23	13.68	13.92	15.26
X_0, mg/L	35.4[a]	33.65[a]	15.46[a]	26.30[a]	28.61[a]	27.33[a]
Y, mg/mg	0.7	0.7	0.7	0.7	0.7	0.7
b, day^{-1}	0.15	0.15	0.15	0.15	0.15	0.15
$K_{s,But}$, mg/L	0.11	0.11	0.11	0.11	0.11	0.11
$k_{max,But}$, mg/mg-day	1.58	1.58	1.58	1.58	1.58	1.58
$K_{s,TCA}$, mg/L	0.37	0.37	0.37	0.37	0.37	0.37
$k_{max,TCA}$, mg/mg-day	0.1	0.1	0.1	0.1	0.1	0.1
T_c, mg/mg	0.3	0.3	0.3	0.3	0.3	0.3
V_L, L	0.1	0.1	0.1	0.1	0.1	0.1
V_g, L	0.057	0.057	0.057	0.057	0.057	0.057
$H_{cc,But}$, mg-L/mg-L	38.05	38.05	38.05	38.05	38.05	38.05
$H_{cc,TCA}$, mg-L/mg-L	0.55	0.55	0.55	0.55	0.55	0.55

Note a = Obtained from the previous simulation

a) The first addition of 1,1,1-TCA on day 6

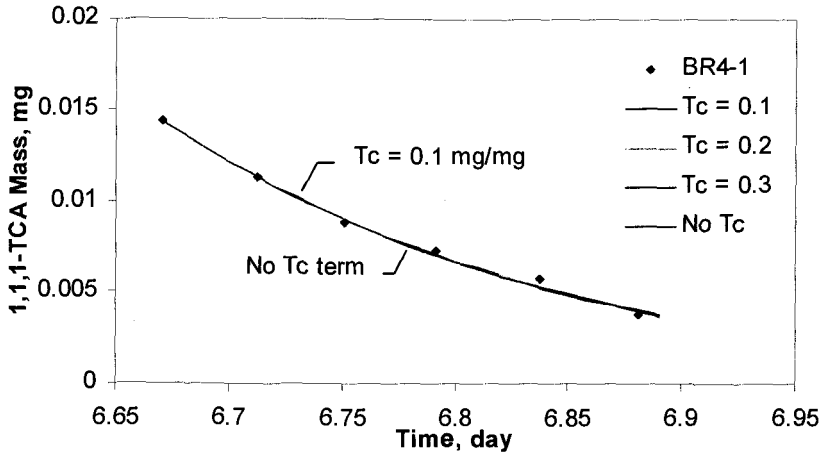

Biomass (X) at starting of model simulation (mg/L)			
$T_c = 0.1$	$T_c = 0.2$	$T_c = 0.3$	No T_c term
35.4	35.4	35.4	35.4

b) The second addition of 1,1,1-TCA on day 6

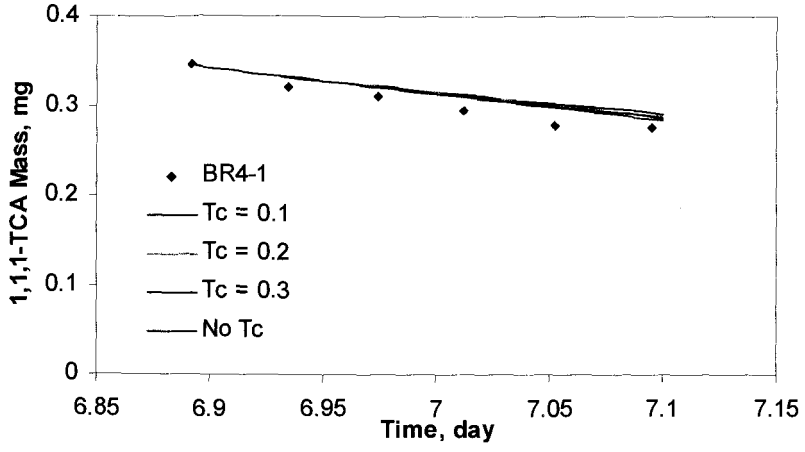

Biomass (X) at starting of model simulation (mg/L)			
$T_c = 0.1$	$T_c = 0.2$	$T_c = 0.3$	No T_c term
32.97	33.48	33.65	34

Figure G.32 Simulations of butane utilization and 1,1,1-TCA transformation for microcosm BR4-1 over a range transformation capacities

c) The fourth addition of butane on day 11

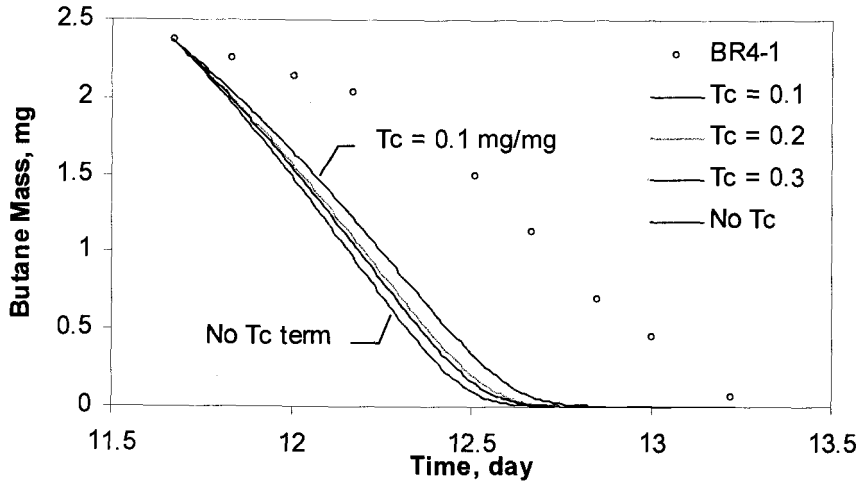

Biomass (X) at starting of model simulation (mg/L)			
$T_c = 0.1$	$T_c = 0.2$	$T_c = 0.3$	No T_c term
13.42	14.92	15.46	16.60

d) The fifth addition of butane on day 13

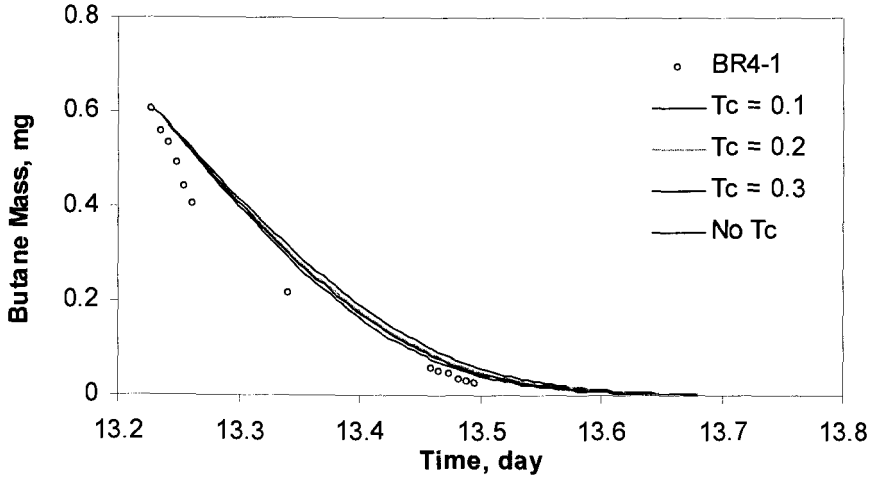

Biomass (X) at starting of model simulation (mg/L)			
$T_c = 0.1$	$T_c = 0.2$	$T_c = 0.3$	No T_c term
24.80	25.90	26.30	27.15

Figure G.32, Continued

e) The third addition of 1,1,1-TCA on day 13

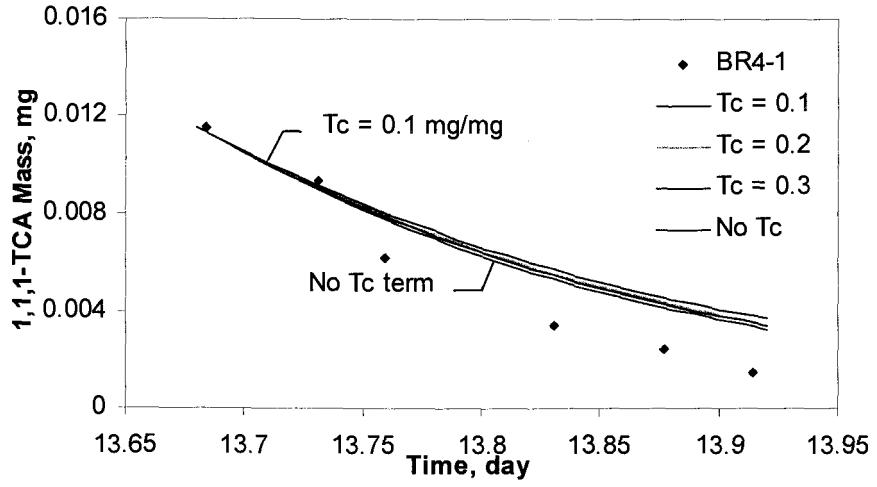

Biomass (X) at starting of model simulation (mg/L)			
$T_c = 0.1$	$T_c = 0.2$	$T_c = 0.3$	No T_c term
27.2	28.23	28.61	29.40

f) The fourth addition of 1,1,1-TCA on day 13

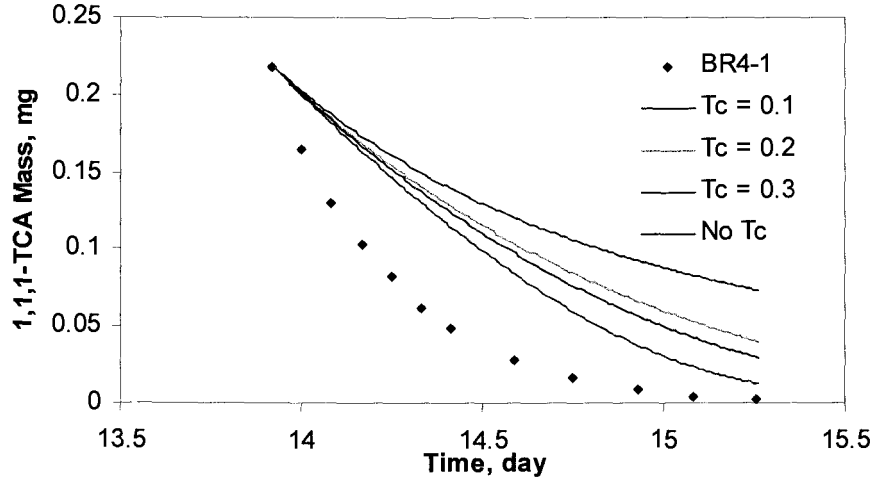

Biomass (X) at starting of model simulation (mg/L)			
$T_c = 0.1$	$T_c = 0.2$	$T_c = 0.3$	No T_c term
25.47	26.84	27.33	28.36

Figure G.32, Continued

Table G.23 Parameters for model simulations in Figure G.33

a) T_c = 0.1 mg TCA/mg cells

Parameters	The 1st addition of TCA	The 2nd addition of TCA	The 4th addition of butane	The 5th addition of butane	The 3rd addition of TCA	The 4th addition of TCA
Starting day	5.24	5.47	12.17	13.02	13.47	13.68
Ending day	5.47	5.68	13.02	13.47	13.68	14.58
X_0, mg/L	37.89[a]	34.75[a]	9.06[a]	19.44[a]	21.67[a]	19.98[a]
Y, mg/mg	0.7	0.7	0.7	0.7	0.7	0.7
b, day^{-1}	0.15	0.15	0.15	0.15	0.15	0.15
$K_{s,But}$, mg/L	0.11	0.11	0.11	0.11	0.11	0.11
$k_{max,But}$, mg/mg-day	1.74	1.74	1.74	1.74	1.74	1.74
$K_{s,TCA}$, mg/L	0.37	0.37	0.37	0.37	0.37	0.37
$k_{max,TCA}$, mg/mg-day	0.19	0.19	0.19	0.19	0.19	0.19
T_c, mg/mg	0.1	0.1	0.1	0.1	0.1	0.1
V_L, L	0.1	0.1	0.1	0.1	0.1	0.1
V_g, L	0.057	0.057	0.057	0.057	0.057	0.057
$H_{cc,But}$, mg-L/mg-L	38.05	38.05	38.05	38.05	38.05	38.05
$H_{cc,TCA}$, mg-L/mg-L	0.55	0.55	0.55	0.55	0.55	0.55

Note a = Obtained from the previous simulation

Table G.23, Continued

b) T_c = 0.2 mg TCA/mg cells

Parameters	The 1st addition of TCA	The 2nd addition of TCA	The 4th addition of butane	The 5th addition of butane	The 3rd addition of TCA	The 4th addition of TCA
Starting day	5.24	5.47	12.17	13.02	13.47	13.68
Ending day	5.47	5.68	13.02	13.47	13.68	14.58
X_0, mg/L	37.89[a]	35.67[a]	11.01[a]	23.09[a]	25.10[a]	23.78[a]
Y, mg/mg	0.7	0.7	0.7	0.7	0.7	0.7
b, day^{-1}	0.15	0.15	0.15	0.15	0.15	0.15
$K_{s,But}$, mg/L	0.11	0.11	0.11	0.11	0.11	0.11
$k_{max,But}$, mg/mg-day	1.74	1.74	1.74	1.74	1.74	1.74
$K_{s,TCA}$, mg/L	0.37	0.37	0.37	0.37	0.37	0.37
$k_{max,TCA}$, mg/mg-day	0.19	0.19	0.19	0.19	0.19	0.19
T_c, mg/mg	0.2	0.2	0.2	0.2	0.2	0.2
V_L, L	0.1	0.1	0.1	0.1	0.1	0.1
V_g, L	0.057	0.057	0.057	0.057	0.057	0.057
$H_{cc,But}$, mg-L/mg-L	38.05	38.05	38.05	38.05	38.05	38.05
$H_{cc,TCA}$, mg-L/mg-L	0.55	0.55	0.55	0.55	0.55	0.55

Note a = Obtained from the previous simulation

Table G.23, Continued

c) T_c = 0.3 mg TCA/mg cells

Parameters	The 1st addition of TCA	The 2nd addition of TCA	The 4th addition of butane	The 5th addition of butane	The 3rd addition of TCA	The 4th addition of TCA
Starting day	5.24	5.47	12.17	13.02	13.47	13.68
Ending day	5.47	5.68	13.02	13.47	13.68	14.58
X_0, mg/L	37.89[a]	35.89[a]	11.76[a]	24.39[a]	26.31[a]	25.12[a]
Y, mg/mg	0.7	0.7	0.7	0.7	0.7	0.7
b, day^{-1}	0.15	0.15	0.15	0.15	0.15	0.15
$K_{s,But}$, mg/L	0.11	0.11	0.11	0.11	0.11	0.11
$k_{max,But}$, mg/mg-day	1.74	1.74	1.74	1.74	1.74	1.74
$K_{s,TCA}$, mg/L	0.37	0.37	0.37	0.37	0.37	0.37
$k_{max,TCA}$, mg/mg-day	0.19	0.19	0.19	0.19	0.19	0.19
T_c, mg/mg	0.3	0.3	0.3	0.3	0.3	0.3
V_L, L	0.1	0.1	0.1	0.1	0.1	0.1
V_g, L	0.057	0.057	0.057	0.057	0.057	0.057
$H_{cc,But}$, mg-L/mg-L	38.05	38.05	38.05	38.05	38.05	38.05
$H_{cc,TCA}$, mg-L/mg-L	0.55	0.55	0.55	0.55	0.55	0.55

Note a = Obtained from the previous simulation

a) The first addition of 1,1,1-TCA on day 5

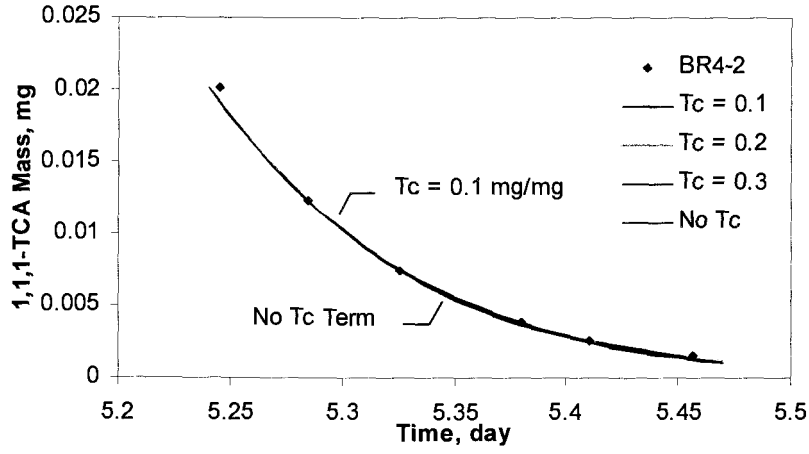

Biomass (X) at starting of model simulation (mg/L)			
$T_c = 0.1$	$T_c = 0.2$	$T_c = 0.3$	No T_c term
37.89	37.89	37.89	37.89

b) The second addition of 1,1,1-TCA on day 5

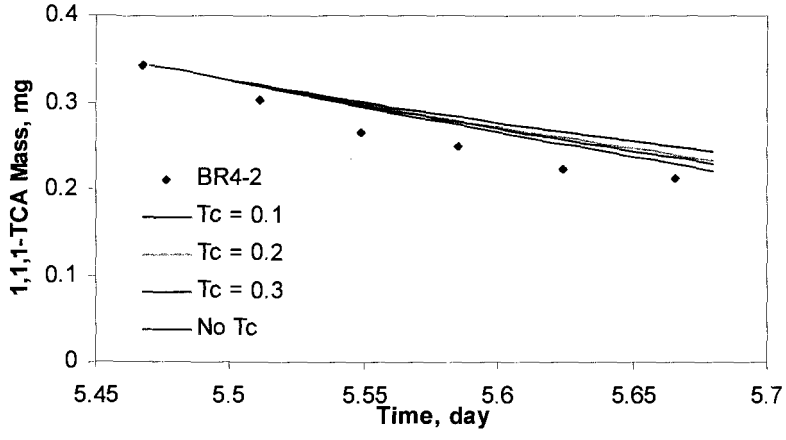

Biomass (X) at starting of model simulation (mg/L)			
$T_c = 0.1$	$T_c = 0.2$	$T_c = 0.3$	No T_c term
34.75	35.67	35.89	36.60

Figure G.33 Simulations of butane utilization and 1,1,1-TCA transformation for microcosm BR4-2 over a range transformation capacities

c) The fourth addition of butane on day 12

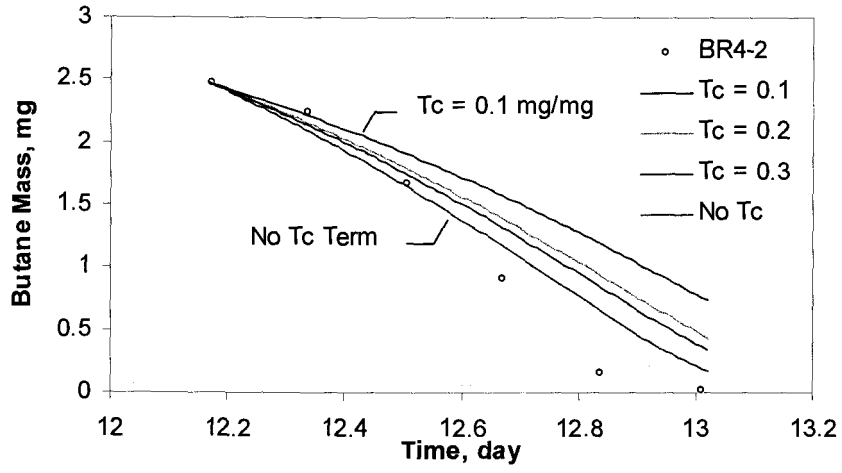

Biomass (X) at starting of model simulation (mg/L)			
$T_c = 0.1$	$T_c = 0.2$	$T_c = 0.3$	No T_c term
9.06	11.01	11.76	13.40

d) The fifth addition of butane on day 13

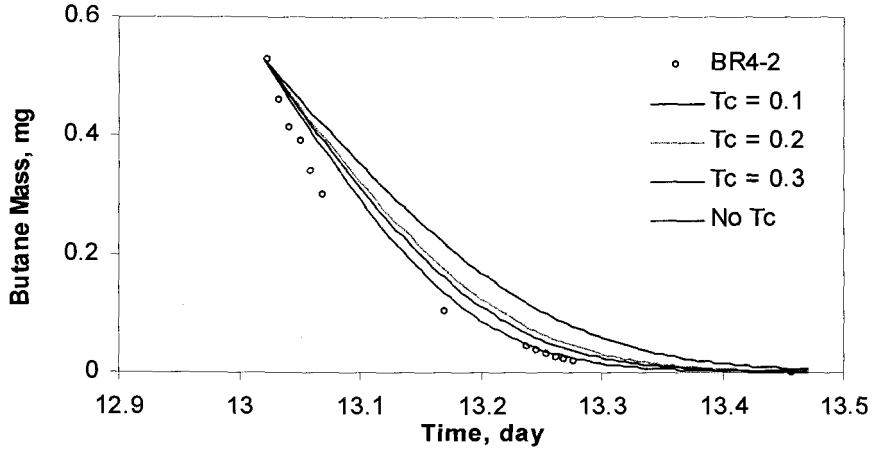

Biomass (X) at starting of model simulation (mg/L)			
$T_c = 0.1$	$T_c = 0.2$	$T_c = 0.3$	No T_c term
19.44	23.09	24.39	26.93

Figure G.33, Continued

e) The third addition of 1,1,1-TCA on day 13

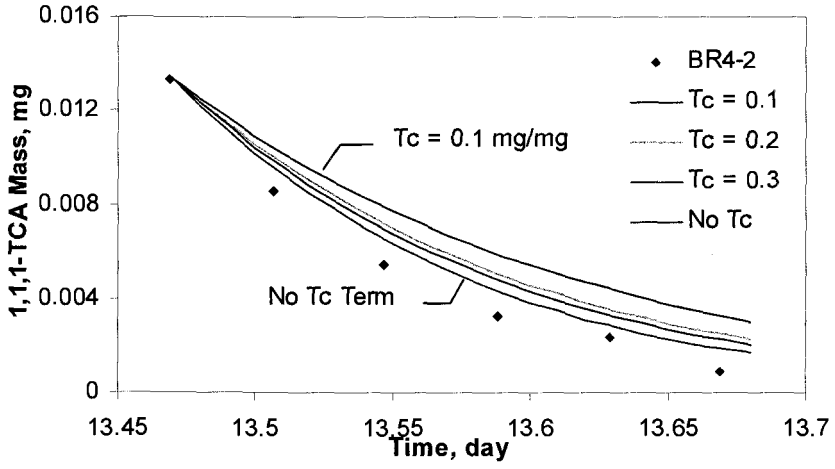

Biomass (X) at starting of model simulation (mg/L)			
$T_c = 0.1$	$T_c = 0.2$	$T_c = 0.3$	No T_c term
21.67	25.10	26.31	28.69

f) The fourth addition of 1,1,1-TCA on day 13

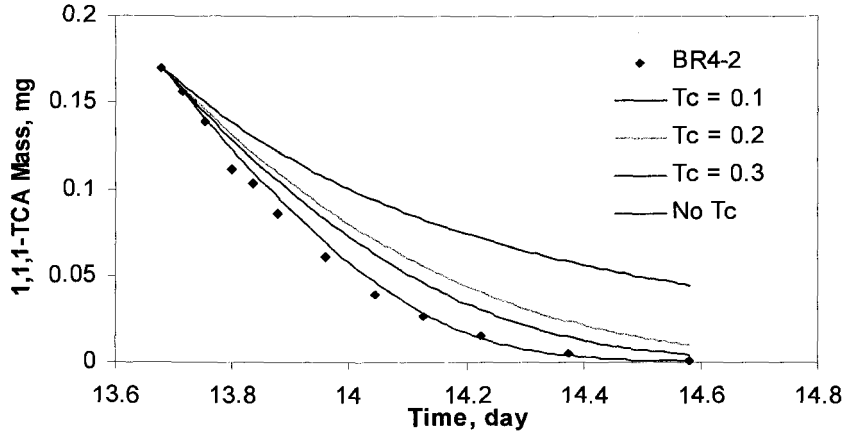

Biomass (X) at starting of model simulation (mg/L)			
$T_c = 0.1$	$T_c = 0.2$	$T_c = 0.3$	No T_c term
19.98	23.78	25.12	27.8

Figure G.33, Continued

Table G.24 Parameters for model simulations in Figure G.34

a) T_c = 0.1 mg TCA/mg cells

Parameters	The 1st addition of TCA	The 2nd addition of TCA	The 4th addition of butane	The 5th addition of butane	The 3rd addition of TCA	The 4th addition of TCA
Starting day	5.64	11.67	13.01	13.47	13.68	5.64
Ending day	5.83	13.01	13.47	13.68	15.08	5.83
X_0, mg/L	37.8 [a]	34.94[a]	11.28[a]	26.10[a]	27.85[a]	25.96[a]
Y, mg/mg	0.7	0.7	0.7	0.7	0.7	0.7
b, day^{-1}	0.15	0.15	0.15	0.15	0.15	0.15
$K_{s,But}$, mg/L	0.11	0.11	0.11	0.11	0.11	0.11
$k_{max,But}$, mg/mg-day	1.74	1.74	1.74	1.74	1.74	1.74
$K_{s,TCA}$, mg/L	0.37	0.37	0.37	0.37	0.37	0.37
$k_{max,TCA}$, mg/mg-day	0.14	0.14	0.14	0.14	0.14	0.14
T_c, mg/mg	0.1	0.1	0.1	0.1	0.1	0.1
V_L, L	0.1	0.1	0.1	0.1	0.1	0.1
V_g, L	0.057	0.057	0.057	0.057	0.057	0.057
$H_{cc,But}$, mg-L/mg-L	38.05	38.05	38.05	38.05	38.05	38.05
$H_{cc,TCA}$, mg-L/mg-L	0.55	0.55	0.55	0.55	0.55	0.55

Note a = Obtained from the previous simulation

Table G.24, Continued

b) T_c = 0.2 mg TCA/mg cells

Parameters	The 1st addition of TCA	The 2nd addition of TCA	The 4th addition of butane	The 5th addition of butane	The 3rd addition of TCA	The 4th addition of TCA
Starting day	5.64	11.67	13.01	13.47	13.68	5.64
Ending day	5.83	13.01	13.47	13.68	15.08	5.83
X_0, mg/L	37.8 [a]	35.67[a]	12.89[a]	27.28[a]	28.95[a]	27.52[a]
Y, mg/mg	0.7	0.7	0.7	0.7	0.7	0.7
b, day^{-1}	0.15	0.15	0.15	0.15	0.15	0.15
$K_{s,But}$, mg/L	0.11	0.11	0.11	0.11	0.11	0.11
$k_{max,But}$, mg/mg-day	1.74	1.74	1.74	1.74	1.74	1.74
$K_{s,TCA}$, mg/L	0.37	0.37	0.37	0.37	0.37	0.37
$k_{max,TCA}$, mg/mg-day	0.14	0.14	0.14	0.14	0.14	0.14
T_c, mg/mg	0.2	0.2	0.2	0.2	0.2	0.2
V_L, L	0.1	0.1	0.1	0.1	0.1	0.1
V_g, L	0.057	0.057	0.057	0.057	0.057	0.057
$H_{cc,But}$, mg-L/mg-L	38.05	38.05	38.05	38.05	38.05	38.05
$H_{cc,TCA}$, mg-L/mg-L	0.55	0.55	0.55	0.55	0.55	0.55

Note a = Obtained from the previous simulation

Table G.24, Continued

c) T_c = 0.3 mg TCA/mg cells

Parameters	The 1st addition of TCA	The 2nd addition of TCA	The 4th addition of butane	The 5th addition of butane	The 3rd addition of TCA	The 4th addition of TCA
Starting day	5.64	11.67	13.01	13.47	13.68	5.64
Ending day	5.83	13.01	13.47	13.68	15.08	5.83
X_0, mg/L	37.8 [a]	35.92[a]	13.48[a]	27.72[a]	29.36[a]	28.09[a]
Y, mg/mg	0.7	0.7	0.7	0.7	0.7	0.7
b, day^{-1}	0.15	0.15	0.15	0.15	0.15	0.15
$K_{s,But}$, mg/L	0.11	0.11	0.11	0.11	0.11	0.11
$k_{max,But}$, mg/mg-day	1.74	1.74	1.74	1.74	1.74	1.74
$K_{s,TCA}$, mg/L	0.37	0.37	0.37	0.37	0.37	0.37
$k_{max,TCA}$, mg/mg-day	0.14	0.14	0.14	0.14	0.14	0.14
T_c, mg/mg	0.3	0.3	0.3	0.3	0.3	0.3
V_L, L	0.1	0.1	0.1	0.1	0.1	0.1
V_g, L	0.057	0.057	0.057	0.057	0.057	0.057
$H_{cc,But}$, mg-L/mg-L	38.05	38.05	38.05	38.05	38.05	38.05
$H_{cc,TCA}$, mg-L/mg-L	0.55	0.55	0.55	0.55	0.55	0.55

Note a = Obtained from the previous simulation

a) The first addition of 1,1,1-TCA on day 5

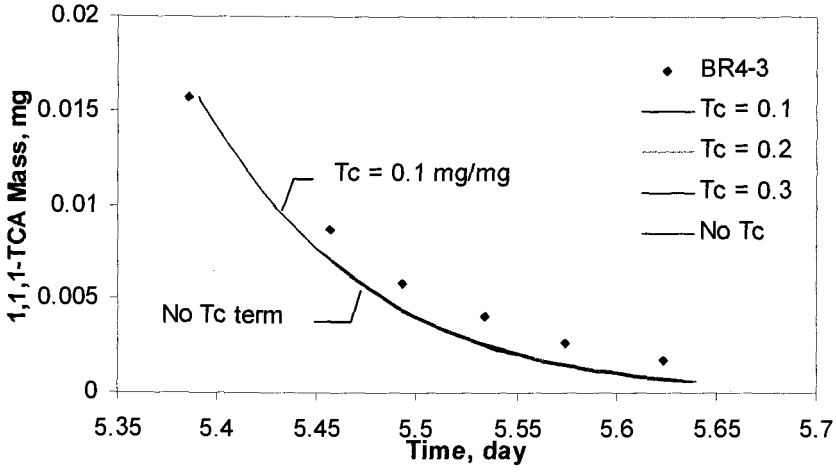

Biomass (X) at starting of model simulation (mg/L)			
$T_c = 0.1$	$T_c = 0.2$	$T_c = 0.3$	No T_c term
37.80	37.80	37.80	37.80

b) The second addition of 1,1,1-TCA on day 5

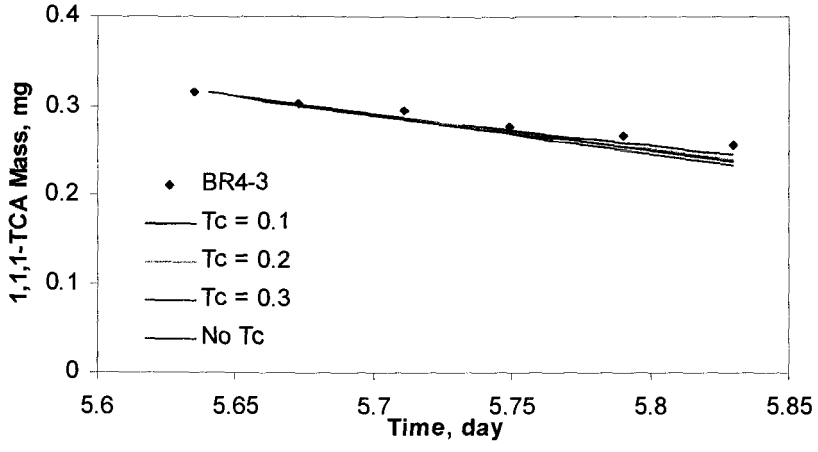

Biomass (X) at starting of model simulation (mg/L)			
$T_c = 0.1$	$T_c = 0.2$	$T_c = 0.3$	No T_c term
34.94	35.67	35.92	36.41

Figure G.34 Simulations of butane utilization and 1,1,1-TCA transformation for microcosm BR4-3 over a range transformation capacities

c) The fourth addition of butane on day 11

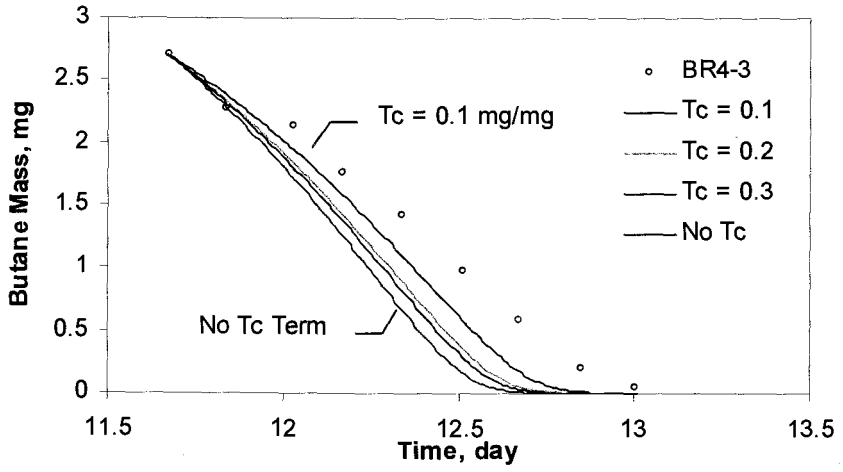

Biomass (X) at starting of model simulation (mg/L)			
$T_c = 0.1$	$T_c = 0.2$	$T_c = 0.3$	No T_c term
11.28	12.89	13.48	14.74

d) The fifth addition of butane on day 13

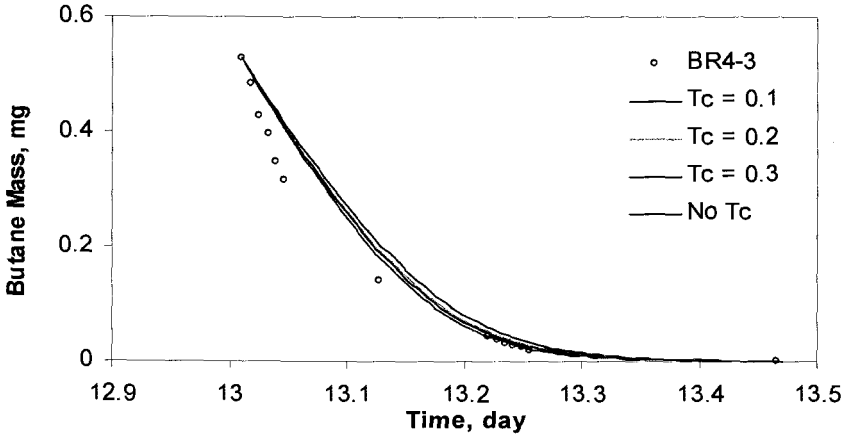

Biomass (X) at starting of model simulation (mg/L)			
$T_c = 0.1$	$T_c = 0.2$	$T_c = 0.3$	No T_c term
26.10	27.28	27.72	28.67

Figure G.34, Continued

e) The third addition of 1,1,1-TCA on day 13

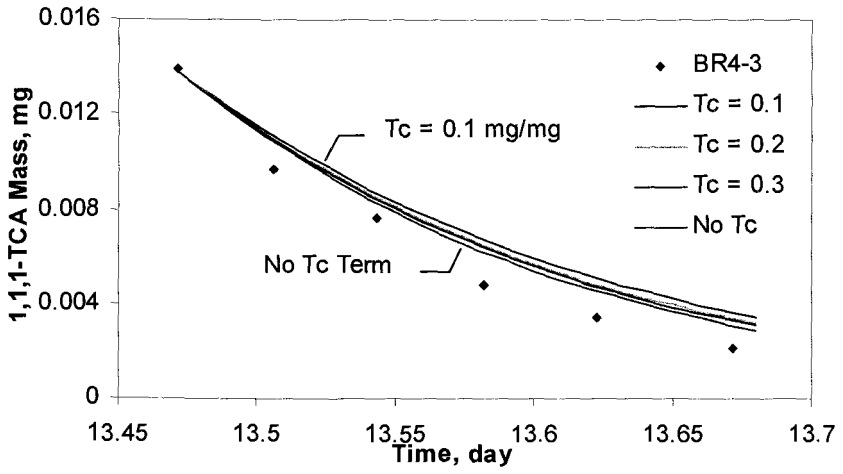

Biomass (X) at starting of model simulation (mg/L)			
$T_c = 0.1$	$T_c = 0.2$	$T_c = 0.3$	No T_c term
27.85	28.95	29.36	30.25

f) The fourth addition of 1,1,1-TCA on day 13

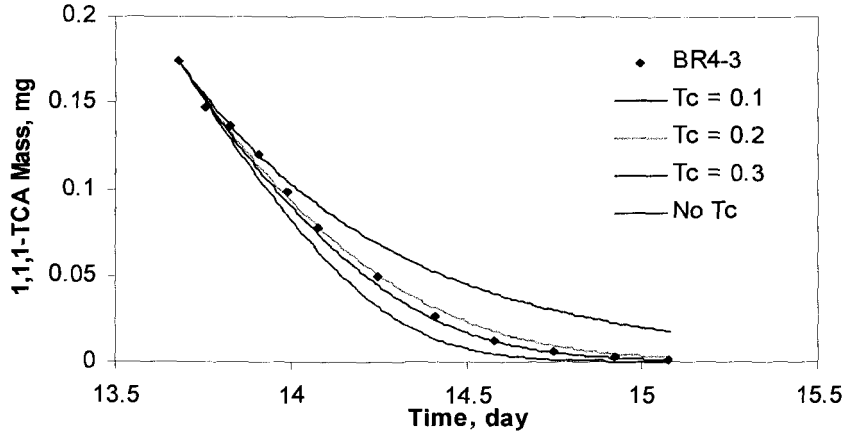

Biomass (X) at starting of model simulation (mg/L)			
$T_c = 0.1$	$T_c = 0.2$	$T_c = 0.3$	No T_c term
25.96	27.52	28.09	29.31

Figure G.34, Continued

Table G.25 Parameters for model simulations in Figure G.35

a) T_c = 0.1 mg TCA/mg cells

Parameters	The 1st addition of TCA	The 2nd addition of TCA	The 4th addition of butane	The 5th addition of butane	The 3rd addition of TCA	The 4th addition of TCA
Starting day	4.74	4.96	11.67	12.52	13.01	13.21
Ending day	4.96	5.17	12.52	13.01	13.21	14.07
X_0, mg/L	39.83[a]	36.89[a]	9.61[a]	22.57[a]	24.69[a]	23.34[a]
Y, mg/mg	0.7	0.7	0.7	0.7	0.7	0.7
b, day^{-1}	0.15	0.15	0.15	0.15	0.15	0.15
$K_{s,But}$, mg/L	0.11	0.11	0.11	0.11	0.11	0.11
$k_{max,But}$, mg/mg-day	1.95	1.95	1.95	1.95	1.95	1.95
$K_{s,TCA}$, mg/L	0.37	0.37	0.37	0.37	0.37	0.37
$k_{max,TCA}$, mg/mg-day	0.16	0.16	0.16	0.16	0.16	0.16
T_c, mg/mg	0.1	0.1	0.1	0.1	0.1	0.1
V_L, L	0.1	0.1	0.1	0.1	0.1	0.1
V_g, L	0.057	0.057	0.057	0.057	0.057	0.057
$H_{cc,But}$, mg-L/mg-L	38.05	38.05	38.05	38.05	38.05	38.05
$H_{cc,TCA}$, mg-L/mg-L	0.55	0.55	0.55	0.55	0.55	0.55

Note a = Obtained from the previous simulation

Table G.25, Continued

b) T_c = 0.2 mg TCA/mg cells

Parameters	The 1st addition of TCA	The 2nd addition of TCA	The 4th addition of butane	The 5th addition of butane	The 3rd addition of TCA	The 4th addition of TCA
Starting day	4.74	4.96	11.67	12.52	13.01	13.21
Ending day	4.96	5.17	12.52	13.01	13.21	14.07
X_0, mg/L	39.83[a]	37.71[a]	11.64[a]	26.13[a]	27.99[a]	26.84[a]
Y, mg/mg	0.7	0.7	0.7	0.7	0.7	0.7
b, day^{-1}	0.15	0.15	0.15	0.15	0.15	0.15
$K_{s,But}$, mg/L	0.11	0.11	0.11	0.11	0.11	0.11
$k_{max,But}$, mg/mg-day	1.95	1.95	1.95	1.95	1.95	1.95
$K_{s,TCA}$, mg/L	0.37	0.37	0.37	0.37	0.37	0.37
$k_{max,TCA}$, mg/mg-day	0.16	0.16	0.16	0.16	0.16	0.16
T_c, mg/mg	0.2	0.2	0.2	0.2	0.2	0.2
V_L, L	0.1	0.1	0.1	0.1	0.1	0.1
V_g, L	0.057	0.057	0.057	0.057	0.057	0.057
$H_{cc,But}$, mg-L/mg-L	38.05	38.05	38.05	38.05	38.05	38.05
$H_{cc,TCA}$, mg-L/mg-L	0.55	0.55	0.55	0.55	0.55	0.55

Note a = Obtained from the previous simulation

Table G.25, Continued

c) T_c = 0.3 mg TCA/mg cells

Parameters	The 1st addition of TCA	The 2nd addition of TCA	The 4th addition of butane	The 5th addition of butane	The 3rd addition of TCA	The 4th addition of TCA
Starting day	4.74	4.96	11.67	12.52	13.01	13.21
Ending day	4.96	5.17	12.52	13.01	13.21	14.07
X_0, mg/L	39.83[a]	37.71[a]	12.41[a]	27.23[a]	29.01[a]	27.93[a]
Y, mg/mg	0.7	0.7	0.7	0.7	0.7	0.7
b, day^{-1}	0.15	0.15	0.15	0.15	0.15	0.15
$K_{s,But}$, mg/L	0.11	0.11	0.11	0.11	0.11	0.11
$k_{max,But}$, mg/mg-day	1.95	1.95	1.95	1.95	1.95	1.95
$K_{s,TCA}$, mg/L	0.37	0.37	0.37	0.37	0.37	0.37
$k_{max,TCA}$, mg/mg-day	0.16	0.16	0.16	0.16	0.16	0.16
T_c, mg/mg	0.3	0.3	0.3	0.3	0.3	0.3
V_L, L	0.1	0.1	0.1	0.1	0.1	0.1
V_g, L	0.057	0.057	0.057	0.057	0.057	0.057
$H_{cc,But}$, mg-L/mg-L	38.05	38.05	38.05	38.05	38.05	38.05
$H_{cc,TCA}$, mg-L/mg-L	0.55	0.55	0.55	0.55	0.55	0.55

Note a = Obtained from the previous simulation

a) The first addition of 1,1,1-TCA on day 4

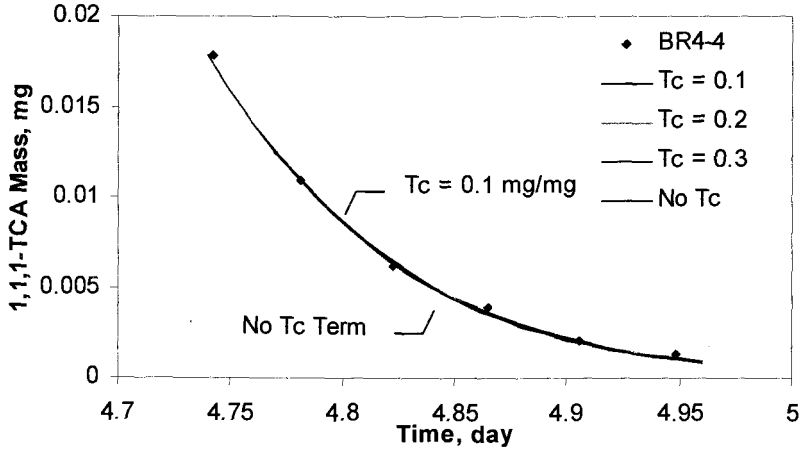

Biomass (X) at starting of model simulation (mg/L)			
$T_c = 0.1$	$T_c = 0.2$	$T_c = 0.3$	No T_c term
39.83	39.83	39.83	39.83

b) The second addition of 1,1,1-TCA on day 4

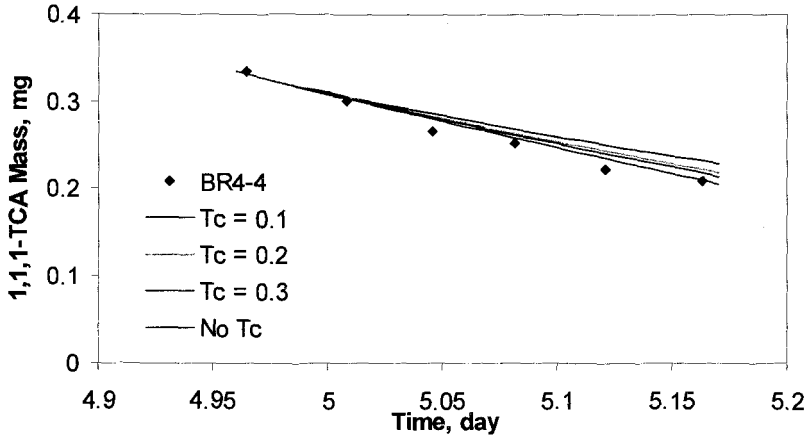

Biomass (X) at starting of model simulation (mg/L)			
$T_c = 0.1$	$T_c = 0.2$	$T_c = 0.3$	No T_c term
36.89	37.71	37.99	38.54

Figure G.35 Simulations of butane utilization and 1,1,1-TCA transformation for microcosm BR4-4 over a range transformation capacities

c) The fourth addition of butane on day 11

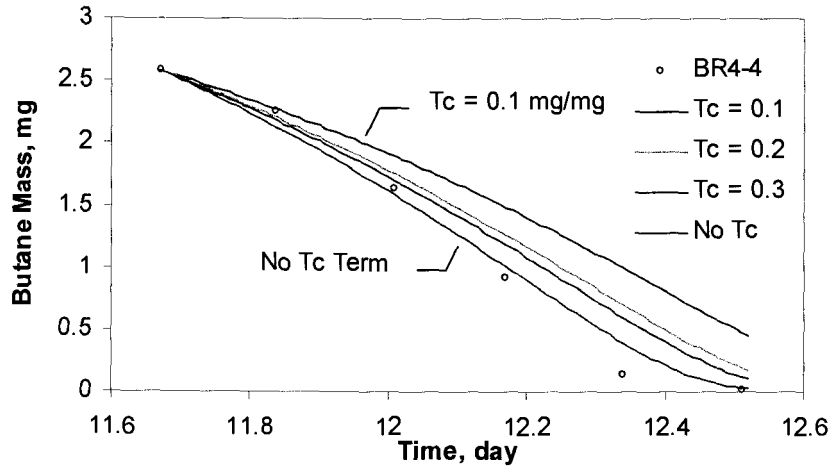

Biomass (X) at starting of model simulation (mg/L)			
$T_c = 0.1$	$T_c = 0.2$	$T_c = 0.3$	No T_c term
9.61	11.64	12.41	14.09

d) The fifth addition of butane on day 12

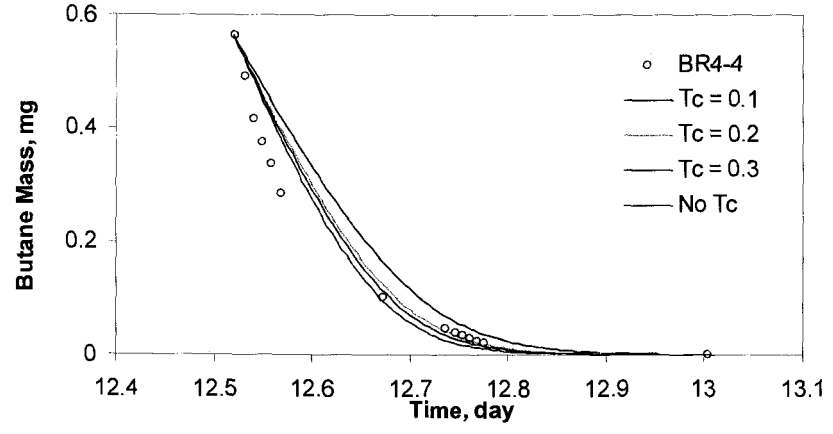

Biomass (X) at starting of model simulation (mg/L)			
$T_c = 0.1$	$T_c = 0.2$	$T_c = 0.3$	No T_c term
22.57	26.13	27.23	29.14

Figure G.35, Continued

e) The third addition of 1,1,1-TCA on day 13

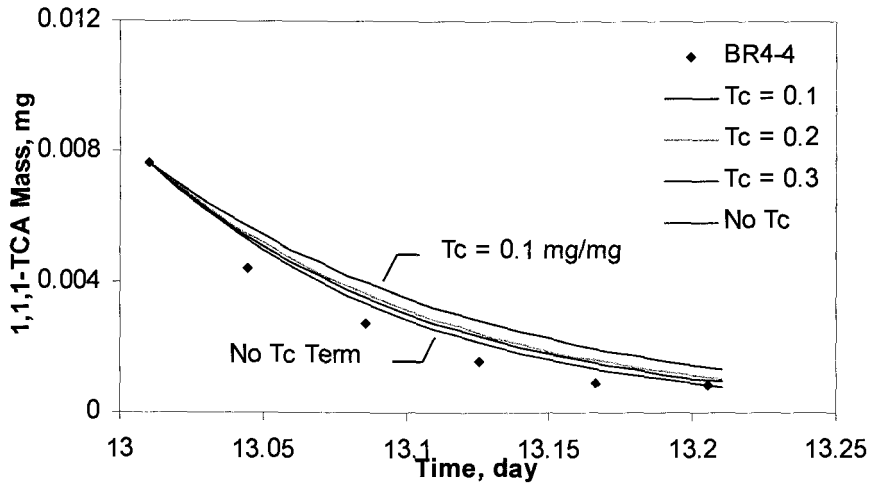

Biomass (X) at starting of model simulation (mg/L)			
$T_c = 0.1$	$T_c = 0.2$	$T_c = 0.3$	No T_c term
24.69	27.99	29.01	30.79

f) The fourth addition of 1,1,1-TCA on day 13

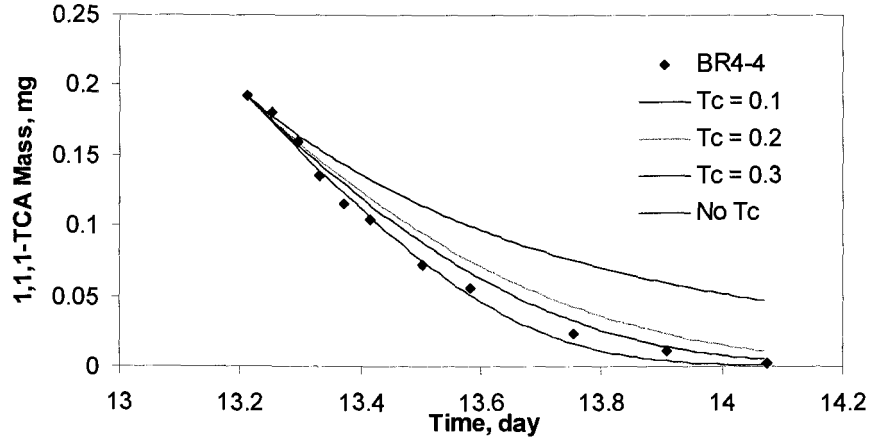

Biomass (X) at starting of model simulation (mg/L)			
$T_c = 0.1$	$T_c = 0.2$	$T_c = 0.3$	No T_c term
23.34	26.84	27.93	29.88

Figure G.35, Continued

Table G.26 Parameters for model simulations in Figures G.36 and G.37

Parameters	Figure G.36	Figure G.37
Starting day	0	25.02
Ending day	33	41.02
X_0, mg/L	0.5	23.87[a]
Y, mg/mg	0.7	0.7
b, day^{-1}	0.15	0.15
$K_{s,But}$, mg/L	0.11	0.11
$k_{max,But}$, mg/mg-day	2.2	2.2
$K_{s,TCA}$, mg/L	0.37	0.37
$k_{max,TCA}$, mg/mg-day	-[b]	0.15
T_c, mg/mg	-[b]	-[b]
V_L, L	0.075	0.075
V_g, L	0.082	0.082
$H_{cc,But}$, mg-L/mg-L	38.05	38.05
$H_{cc,TCA}$, mg-L/mg-L	0.55	0.55

Note a = Obtained from the previous simulation
b = Not used in the simulation

Table G.27 Parameters for model simulations in Figure G.38

Parameters	T_c = 0.1 mg TCA/mg cells	T_c = 0.2 mg TCA/mg cells	T_c = 0.4 mg TCA/mg cells
Starting day	25.02	25.02	25.02
Ending day	41.02	41.02	41.02
X_0, mg/L	23.87[a]	23.87[a]	23.87[a]
Y, mg/mg	0.7	0.7	0.7
b, day^{-1}	0.15	0.15	0.15
$K_{s,But}$, mg/L	0.11	0.11	0.11
$k_{max,But}$, mg/mg-day	2.2	2.2	2.2
$K_{s,TCA}$, mg/L	0.37	0.37	0.37
$k_{max,TCA}$, mg/mg-day	0.15	0.15	0.15
T_c, mg/mg	0.1	0.2	0.4
V_L, L	0.075	0.075	0.075
V_g, L	0.082	0.082	0.082
$H_{cc,But}$, mg-L/mg-L	38.05	38.05	38.05
$H_{cc,TCA}$, mg-L/mg-L	0.55	0.55	0.55

Note a = Obtained from the previous simulation

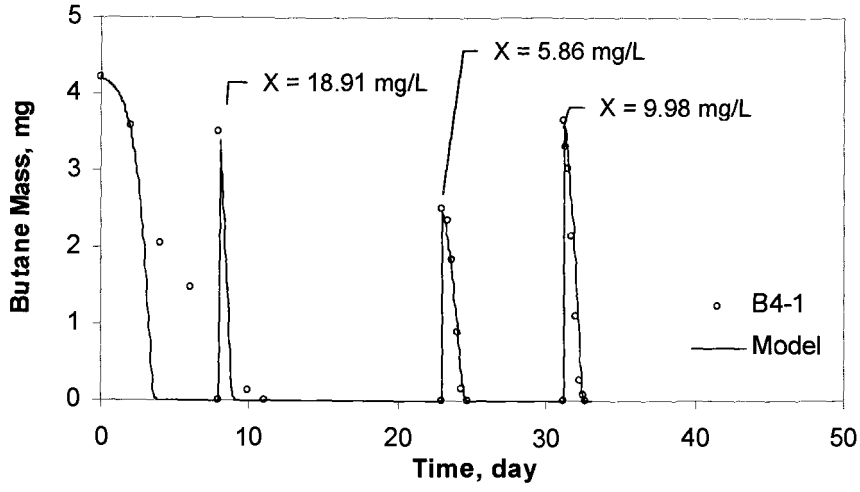

Figure G.36 Simulations of butane utilization for microcosm B4-1without the term for transformation capacity

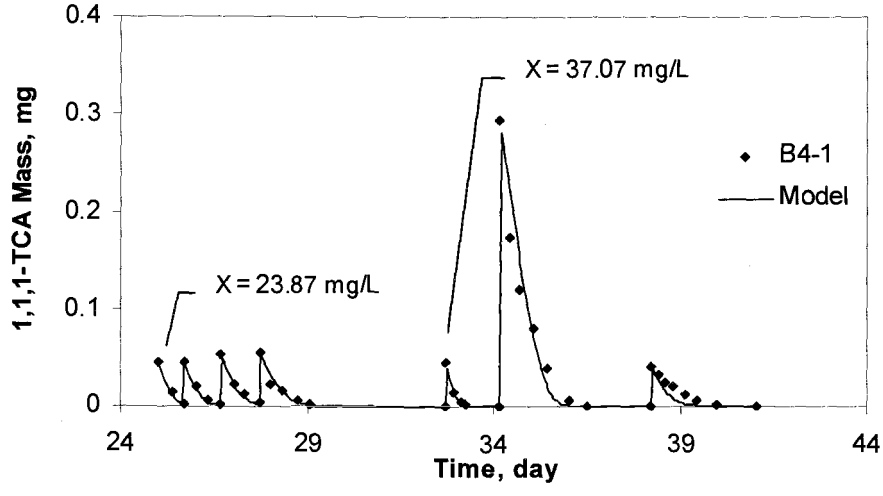

Figure G.37 Simulations of 1,1,1-TCA transformation for microcosm B4-1 without the term for transformation capacity

a) 1,1,1-TCA transformation from day 25 to 30

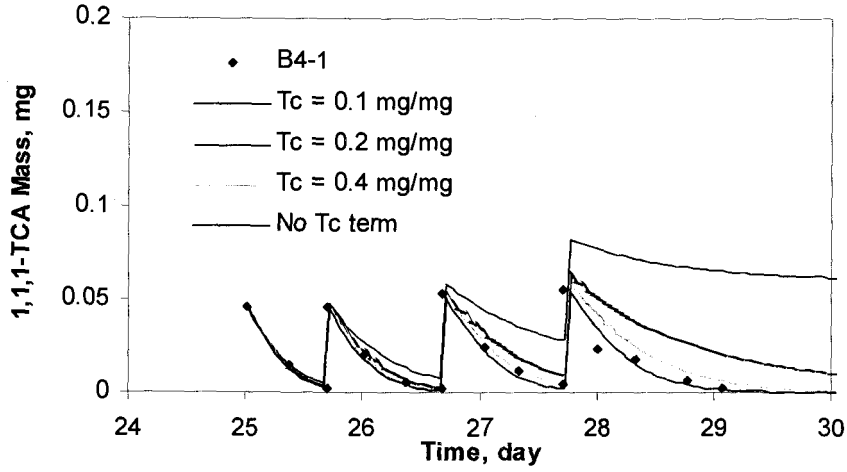

Biomass (X) at starting of model simulation (mg/L)			
$T_c = 0.1$	$T_c = 0.2$	$T_c = 0.4$	No T_c term
23.87	23.87	23.87	23.87

b) Butane utilization from day 31 to 33

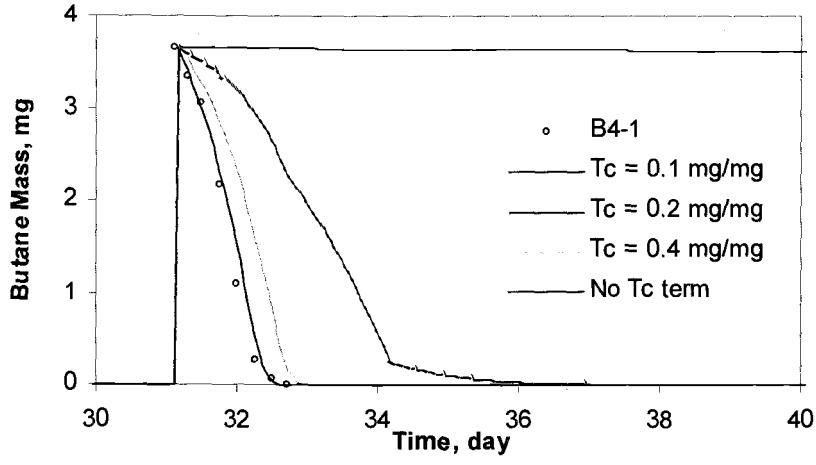

Biomass (X) at starting of model simulation (mg/L)			
$T_c = 0.1$	$T_c = 0.2$	$T_c = 0.4$	No T_c term
0.11	2.59	6.30	10.02

Figure G.38 Simulations of butane utilization and 1,1,1-TCA transformation for microcosm B4-1 over a range transformation capacities

c) 1,1,1-TCA transformation from day 33 to 41

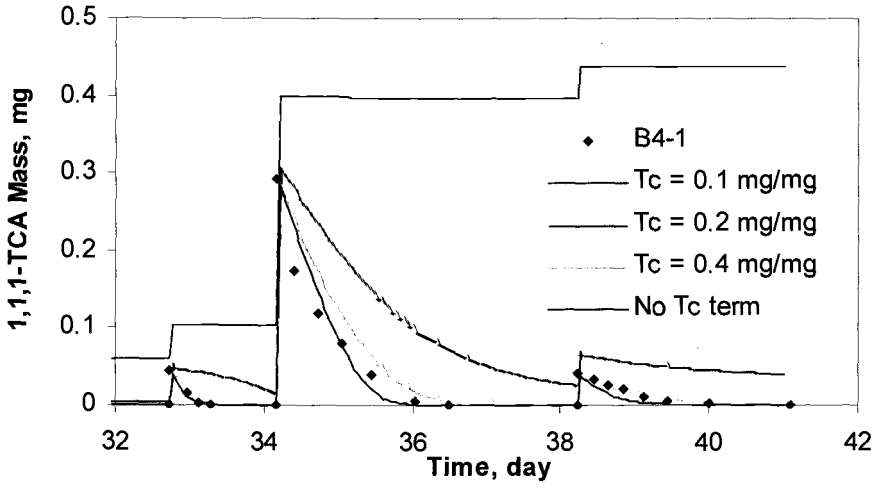

Biomass (X) at starting of model simulation (mg/L)			
$T_c = 0.1$	$T_c = 0.2$	$T_c = 0.4$	No T_c term
0.19	14.8	34.37	37.07

Figure G.38, Continued

Table G.28 Parameters for model simulations in Figures G.39 and G.40

Parameters	Figure G.39	Figure G.40
Starting day	0	25.38
Ending day	34	91.03
X_0, mg/L	0.5	23.35 [a]
Y, mg/mg	0.7	0.7
b, day^{-1}	0.15	0.15
$K_{s,But}$, mg/L	0.11	0.11
$k_{max,But}$, mg/mg-day	2.2	2.2
$K_{s,TCA}$, mg/L	0.37	0.37
$k_{max,TCA}$, mg/mg-day	- [b]	0.10
T_c, mg/mg	- [b]	- [b]
V_L, L	0.075	0.075
V_g, L	0.082	0.082
$H_{cc,But}$, mg-L/mg-L	38.05	38.05
$H_{cc,TCA}$, mg-L/mg-L	0.55	0.55

Note a = Obtained from the previous simulation
b = Not used in the simulation

Table G.29 Parameters for model simulations in Figure G.41

Parameters	T_c = 0.1 mg TCA/mg cells	T_c = 0.2 mg TCA/mg cells	T_c = 0.4 mg TCA/mg cells
Starting day	25.38	25.38	25.38
Ending day	91.03	91.03	91.03
X_0, mg/L	23.35 [a]	23.35 [a]	23.35 [a]
Y, mg/mg	0.7	0.7	0.7
b, day^{-1}	0.15	0.15	0.15
$K_{s,But}$, mg/L	0.11	0.11	0.11
$k_{max,But}$, mg/mg-day	2.2	2.2	2.2
$K_{s,TCA}$, mg/L	0.37	0.37	0.37
$k_{max,TCA}$, mg/mg-day	0.10	0.10	0.10
T_c, mg/mg	0.1	0.2	0.4
V_L, L	0.075	0.075	0.075
V_g, L	0.082	0.082	0.082
$H_{cc,But}$, mg-L/mg-L	38.05	38.05	38.05
$H_{cc,TCA}$, mg-L/mg-L	0.55	0.55	0.55

Note a = Obtained from the previous simulation

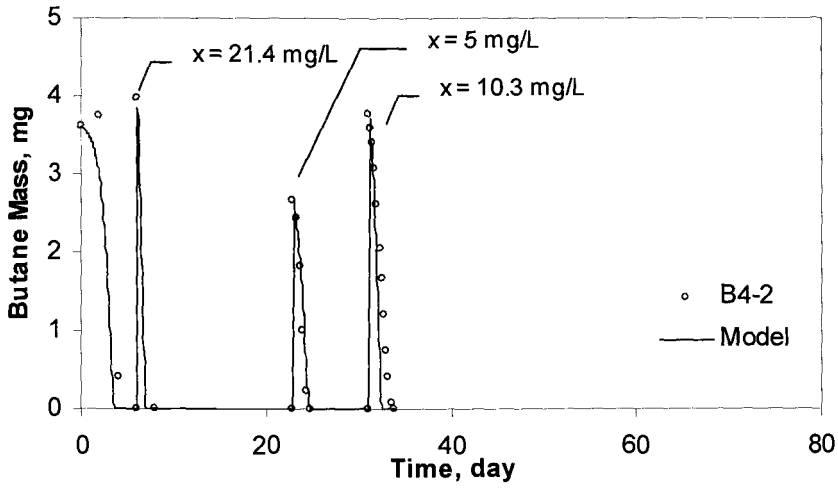

Figure G.39 Simulations of butane utilization for microcosm B4-2without the term for transformation capacity

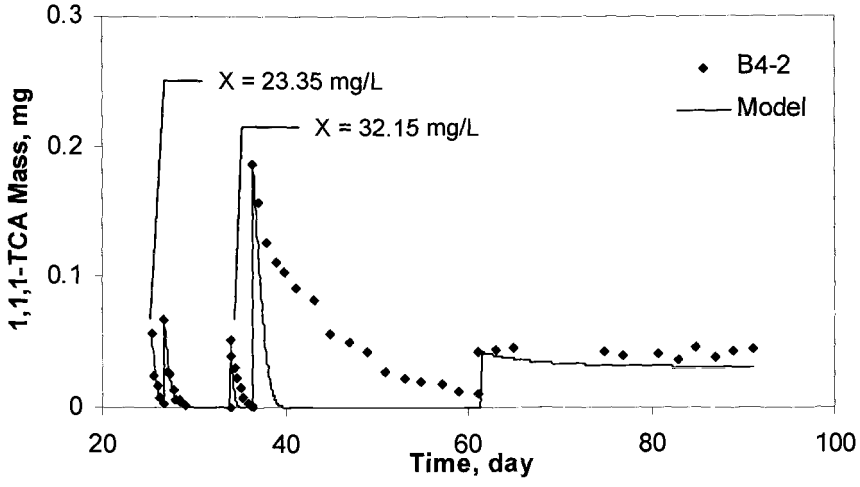

Figure G.40 Simulations of 1,1,1-TCA transformation for microcosm B4-2 without the term for transformation capacity

a) 1,1,1-TCA transformation from day 25 to 32

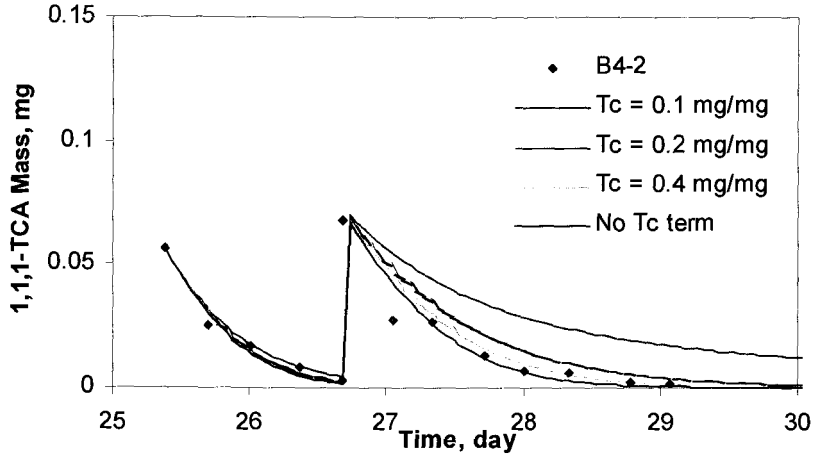

Biomass (X) at starting of model simulation (mg/L)			
$T_c = 0.1$	$T_c = 0.2$	$T_c = 0.4$	No T_c term
23.35	23.35	23.35	23.35

b) Butane utilization from day 31 to 34

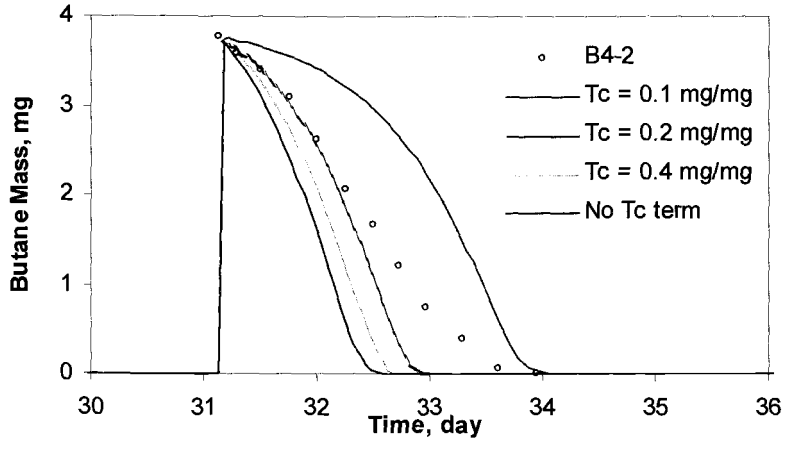

Biomass (X) at starting of model simulation (mg/L)			
$T_c = 0.1$	$T_c = 0.2$	$T_c = 0.4$	No T_c term
1.66	5.77	8.08	10.33

Figure G.41 Simulations of butane utilization and 1,1,1-TCA transformation for microcosm B4-2 over a range transformation capacities

c) 1,1,1-TCA transformation from day 33 to 43

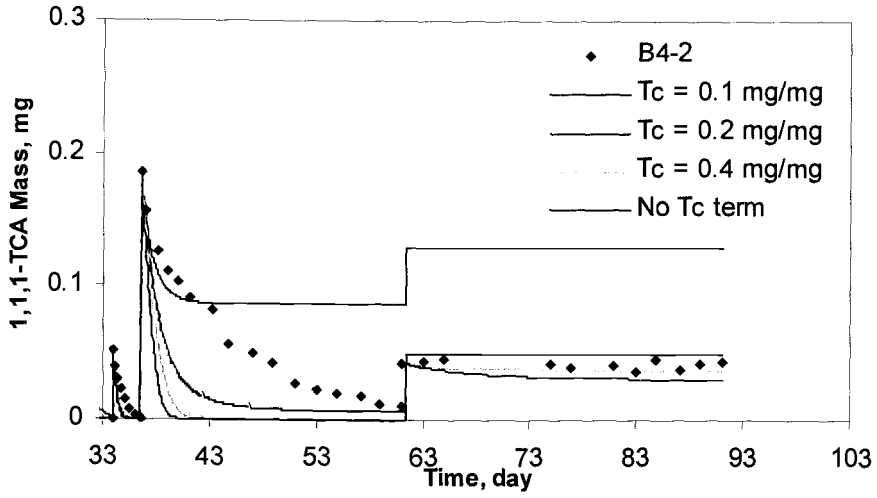

Biomass (X) at starting of model simulation (mg/L)			
$T_c = 0.1$	$T_c = 0.2$	$T_c = 0.4$	No T_c term
29.86	30.21	31.08	33.98

Figure G.41, Continued

Table G.30 Parameters for model simulations in Figure G.42

Parameter	The 1st addition of butane	The 2nd addition of butane	The 3rd addition of butane	The 4th addition of butane	The 5th addition of butane	The 1st addition of TCA	The 2nd addition of TCA
Starting day	0	9.12	10.98	11.2	20.06	26.49	31.54
Ending day	9.12	10.98	11.2	20.06	26.49	31.54	95
X_0, mg/L	0.006[c]	21.59[a]	38.45[a]	37.78[a]	0.2[c]	18.79[a]	8.81[a]
Y, mg/mg	0.7	0.7	0.7	0.7	0.7	0.7	0.7
b, day^{-1}	0.15	0.15	0.15	0.15	0.15	0.15	0.15
$K_{s,But}$, mg/L	0.11	0.11	0.11	0.11	0.11	0.11	0.11
$k_{max,But}$, mg/mg-day	1.76	1.76	1.76	1.76	1.76	1.76	1.76
$K_{s,TCA}$, mg/L	0.37	0.37	0.37	0.37	0.37	0.37	0.37
$k_{max,TCA}$, mg/mg-day	-[b]	-[b]	-[b]	-[b]	-[b]	0.09	0.09
T_c, mg/mg	-[b]	-[b]	-[b]	-[b]	-[b]	-[b]	-[b]
V_L, L	0.1	0.1	0.1	0.1	0.1	0.1	0.1
V_g, L	0.057	0.057	0.057	0.057	0.057	0.057	0.057
$H_{cc,But}$, mg-L/mg-L	38.05	38.05	38.05	38.05	38.05	38.05	38.05
$H_{cc,TCA}$, mg-L/mg-L	0.55	0.55	0.55	0.55	0.55	0.55	0.55

Note a = Obtained from the previous simulation
b = Not used in the simulation
c = Obtained from the variation

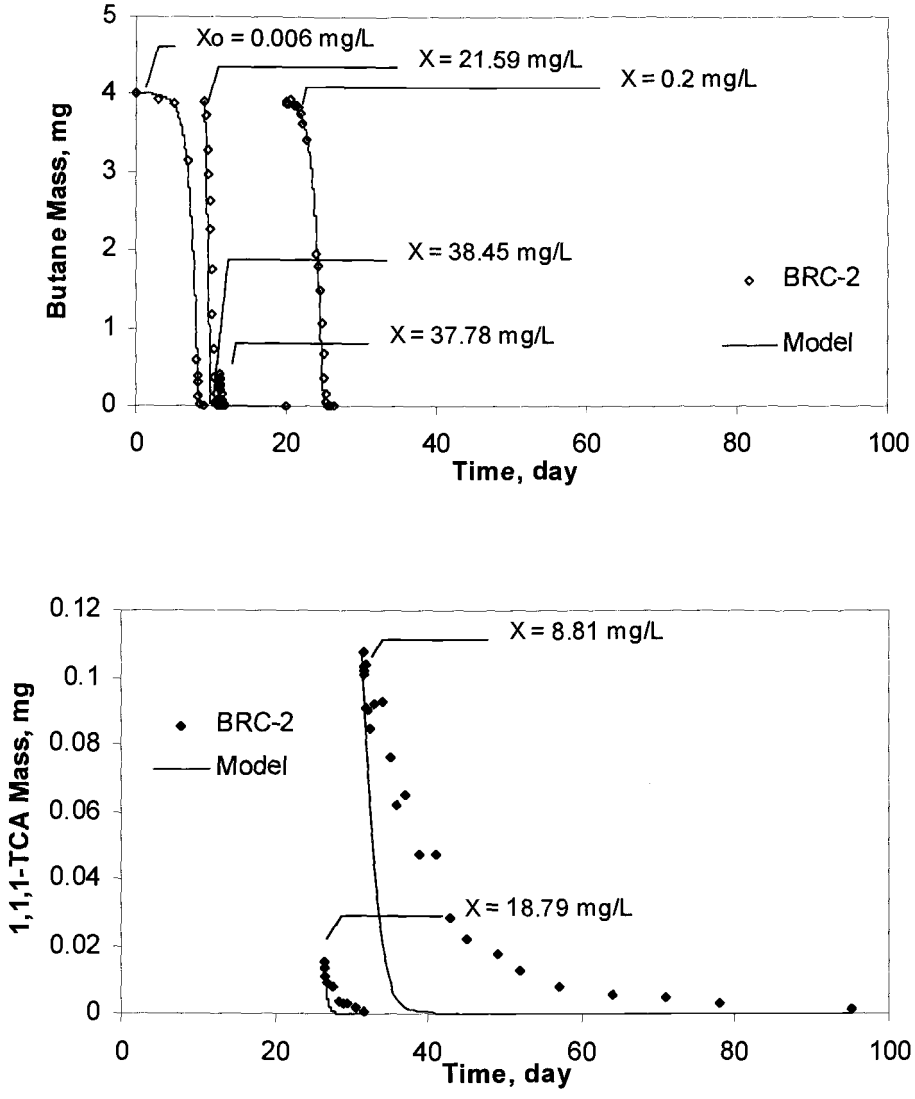

Figure G.42 Simulations of butane utilization and 1,1,1-TCA transformation for microcosm BRC-2 without the term for transformation capacity

Table G.31 Parameters for model simulations in Figure G.43

Parameter	The 1st addition of butane	The 2nd addition of butane	The 3rd addition of butane	The 4th addition of butane	The 5th addition of butane	The 1st addition of TCA	The 2nd addition of TCA
Starting day	0	10.98	12.94	13.25	20.06	25.06	32.85
Ending day	10.98	12.94	13.25	20.06	25.06	32.85	95.3
X_0, mg/L	0.001[c]	22.07[a]	37.31[a]	36.21[a]	1[c]	19.56[a]	6.08[a]
Y, mg/mg	0.7	0.7	0.7	0.7	0.7	0.7	0.7
b, day^{-1}	0.15	0.15	0.15	0.15	0.15	0.15	0.15
$K_{s,But}$, mg/L	0.11	0.11	0.11	0.11	0.11	0.11	0.11
$k_{max,But}$, mg/mg-day	1.76	1.76	1.76	1.76	1.76	1.76	1.76
$K_{s,TCA}$, mg/L	0.37	0.37	0.37	0.37	0.37	0.37	0.37
$k_{max,TCA}$, mg/mg-day	-[b]	-[b]	-[b]	-[b]	-[b]	0.09	0.09
T_c, mg/mg	-[b]	-[b]	-[b]	-[b]	-[b]	-[b]	-[b]
V_L, L	0.1	0.1	0.1	0.1	0.1	0.1	0.1
V_g, L	0.057	0.057	0.057	0.057	0.057	0.057	0.057
$H_{cc,But}$, mg-L/mg-L	38.05	38.05	38.05	38.05	38.05	38.05	38.05
$H_{cc,TCA}$, mg-L/mg-L	0.55	0.55	0.55	0.55	0.55	0.55	0.55

Note a = Obtained from the previous simulation
b = Not used in the simulation
c = Obtained from the variation

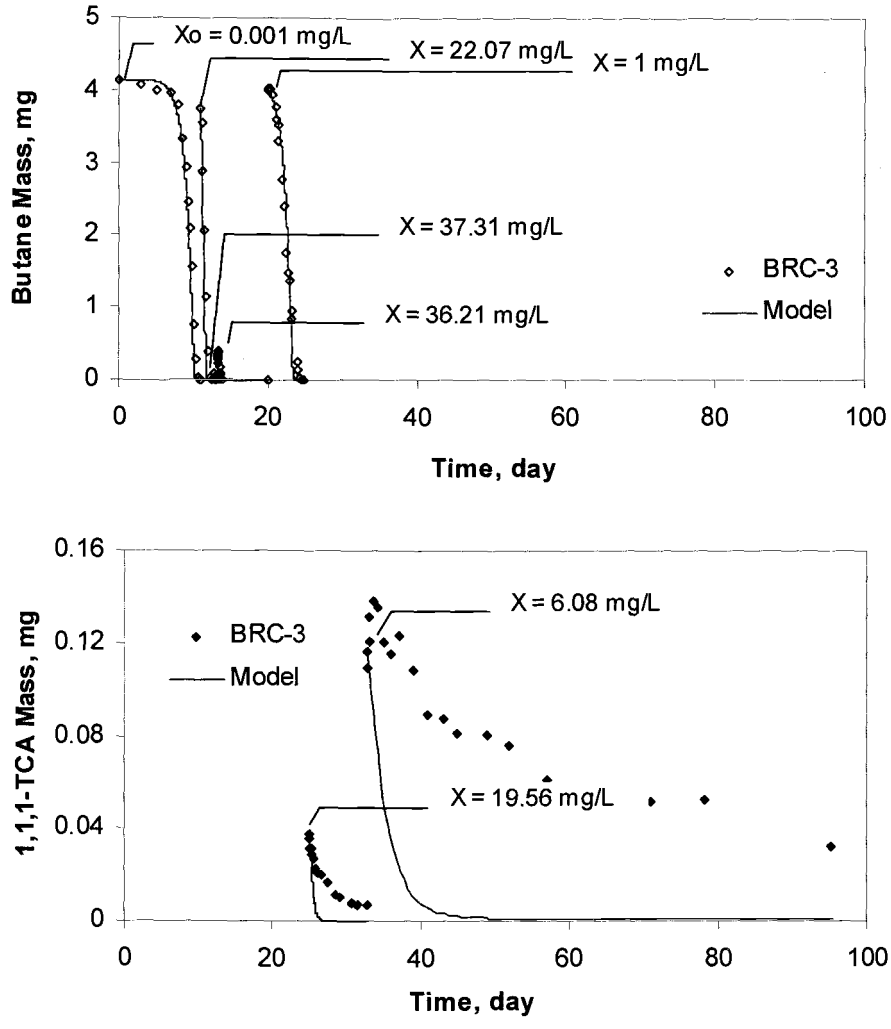

Figure G.43 Simulations of butane utilization and 1,1,1-TCA transformation for microcosm BRC-3 without the term for transformation capacity

Table G.32 Parameters for model simulations in Figure G.44

Parameter	The 1st addition of butane	The 2nd addition of butane	The 3rd addition of butane	The 4th addition of butane	The 5th addition of butane	The 1st addition of TCA	The 2nd addition of TCA
Starting day	0	9.12	10.2	10.98	20.06	31.54	38.05
Ending day	9.12	10.2	10.98	20.06	31.54	38.05	95.1
X_0, mg/L	0.004[c]	23.91[a]	44.33[a]	39.94[a]	0.001[c]	19.26[a]	7.25[a]
Y, mg/mg	0.7	0.7	0.7	0.7	0.7	0.7	0.7
b, day^{-1}	0.15	0.15	0.15	0.15	0.15	0.15	0.15
$K_{s,But}$, mg/L	0.11	0.11	0.11	0.11	0.11	0.11	0.11
$k_{max,But}$, mg/mg-day	1.76	1.76	1.76	1.76	1.76	1.76	1.76
$K_{s,TCA}$, mg/L	0.37	0.37	0.37	0.37	0.37	0.37	0.37
$k_{max,TCA}$, mg/mg-day	-[b]	-[b]	-[b]	-[b]	-[b]	0.09	0.09
T_c, mg/mg	-[b]	-[b]	-[b]	-[b]	-[b]	-[b]	-[b]
V_L, L	0.1	0.1	0.1	0.1	0.1	0.1	0.1
V_g, L	0.057	0.057	0.057	0.057	0.057	0.057	0.057
$H_{cc,But}$, mg-L/mg-L	38.05	38.05	38.05	38.05	38.05	38.05	38.05
$H_{cc,TCA}$, mg-L/mg-L	0.55	0.55	0.55	0.55	0.55	0.55	0.55

Note a = Obtained from the previous simulation
b = Not used in the simulation
c = Obtained from the variation

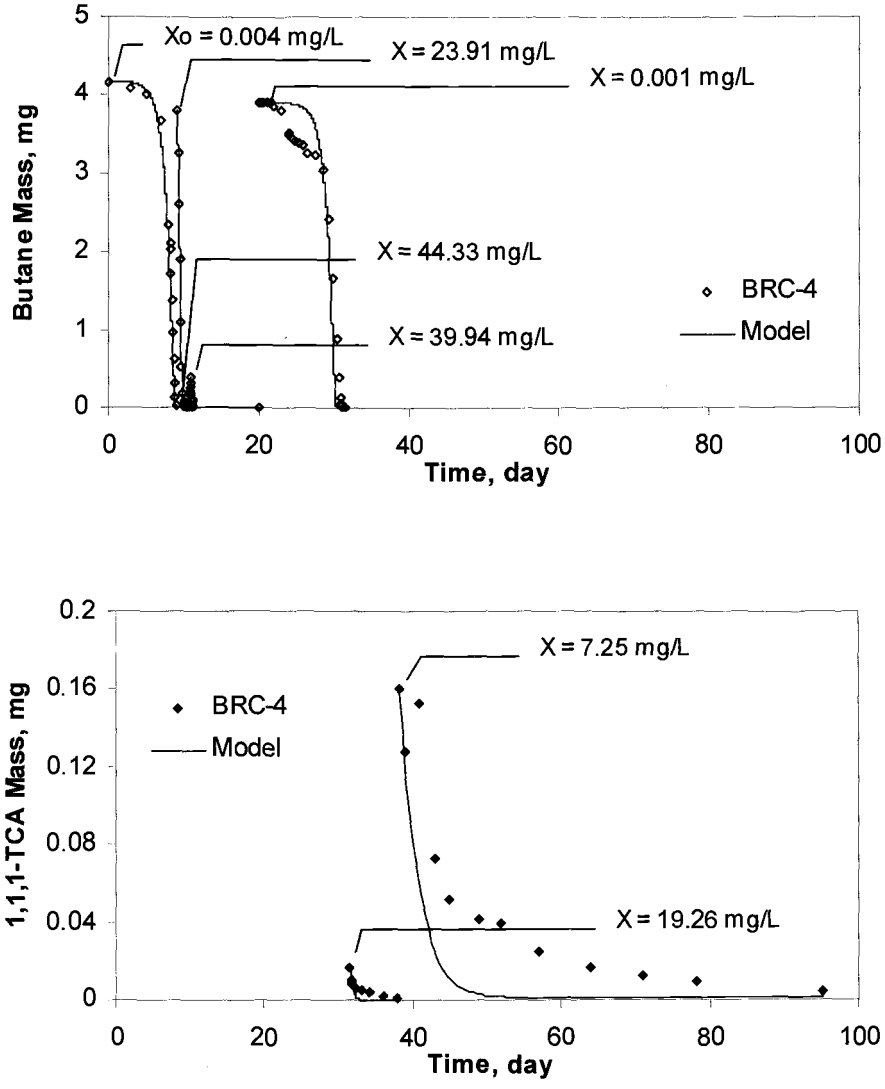

Figure G.44 Simulations of butane utilization and 1,1,1-TCA transformation for microcosm BRC-4 without the term for transformation capacity

Table G.33 Parameters for model simulations in Figure G.45

Parameter	The 1st addition of butane	The 2nd addition of butane	The 3rd addition of butane	The 4th addition of butane	The 5th addition of butane	The 1st addition of TCA
Starting day	0	9.13	12.95	14.98	20.07	25.06
Ending day	9.13	12.95	14.98	20.07	25.06	95.1
X_0, mg/L	0.005[c]	21.08[a]	27.19[a]	20.58[a]	0.7[c]	19.17[a]
Y, mg/mg	0.7	0.7	0.7	0.7	0.7	0.7
b, day^{-1}	0.15	0.15	0.15	0.15	0.15	0.15
$K_{s,But}$, mg/L	0.11	0.11	0.11	0.11	0.11	0.11
$k_{max,But}$, mg/mg-day	1.76	1.76	1.76	1.76	1.76	1.76
$K_{s,TCA}$, mg/L	0.37	0.37	0.37	0.37	0.37	0.37
$k_{max,TCA}$, mg/mg-day	-[b]	-[b]	-[b]	-[b]	-[b]	0.09
T_c, mg/mg	-[b]	-[b]	-[b]	-[b]	-[b]	-[b]
V_L, L	0.1	0.1	0.1	0.1	0.1	0.1
V_g, L	0.057	0.057	0.057	0.057	0.057	0.057
$H_{cc,But}$, mg-L/mg-L	38.05	38.05	38.05	38.05	38.05	38.05
$H_{cc,TCA}$, mg-L/mg-L	0.55	0.55	0.55	0.55	0.55	0.55

Note a = Obtained from the previous simulation
b = Not used in the simulation
c = Obtained from the variation

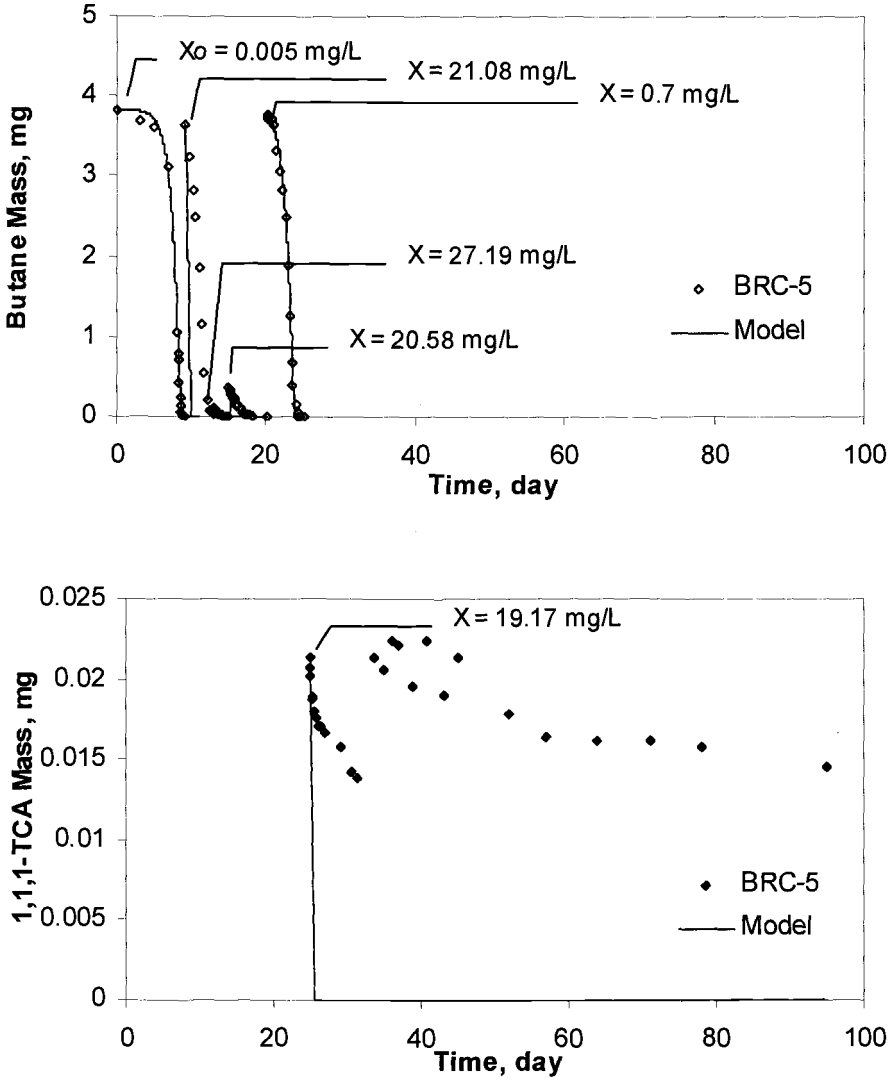

Figure G.45 Simulations of butane utilization and 1,1,1-TCA transformation for microcosm BRC-5 without the term for transformation capacity

Table G.34 Parameters for model simulations in Figures G.46

Parameters	T_c = 0.01 mg TCA /mg cells		T_c = 0.3 mg TCA /mg cells		T_c = 0.4 mg TCA /mg cells	
	The 1st addition of TCA	The 2nd addition of TCA	The 1st addition of TCA	The 2nd addition of TCA	The 1st addition of TCA	The 2nd addition of TCA
Starting day	26.49	31.54	26.49	31.54	26.49	31.54
Ending day	31.54	95	31.54	95	31.54	95
X_0, mg/L	18.79[a]	0.16[a]	18.79[a]	8.46[a]	18.79[a]	8.55[a]
Y, mg/mg	0.7	0.7	0.7	0.7	0.7	0.7
b, day^{-1}	0.15	0.15	0.15	0.15	0.15	0.15
$K_{s,But}$, mg/L	0.11	0.11	0.11	0.11	0.11	0.11
$k_{max,But}$, mg/mg-day	1.76	1.76	1.76	1.76	1.76	1.76
$K_{s,TCA}$, mg/L	0.37	0.37	0.37	0.37	0.37	0.37
$k_{max,TCA}$, mg/mg-day	0.09	0.09	0.09	0.09	0.09	0.09
T_c, mg/mg	0.01	0.01	0.3	0.3	0.4	0.4
V_L, L	0.1	0.1	0.1	0.1	0.1	0.1
V_g, L	0.057	0.057	0.057	0.057	0.057	0.057
$H_{cc,But}$, mg-L/mg-L	38.05	38.05	38.05	38.05	38.05	38.05
$H_{cc,TCA}$, mg-L/mg-L	0.55	0.55	0.55	0.55	0.55	0.55

Note a = Obtained from the previous simulation

Section F: The first addition of 1,1,1-TCA on day 26

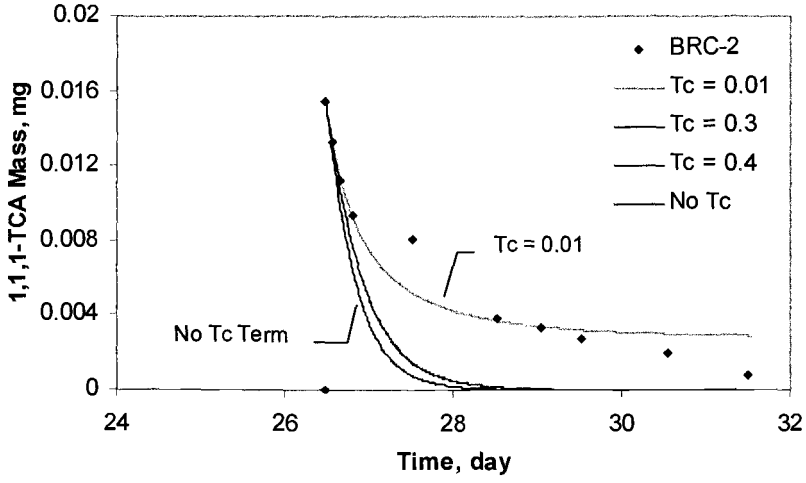

Biomass (X) at starting of model simulation (mg/L)			
$T_c = 0.01$	$T_c = 0.3$	$T_c = 0.4$	No T_c term
18.79	18.79	18.79	18.79

Section G: The second addition of 1,1,1-TCA on day 31

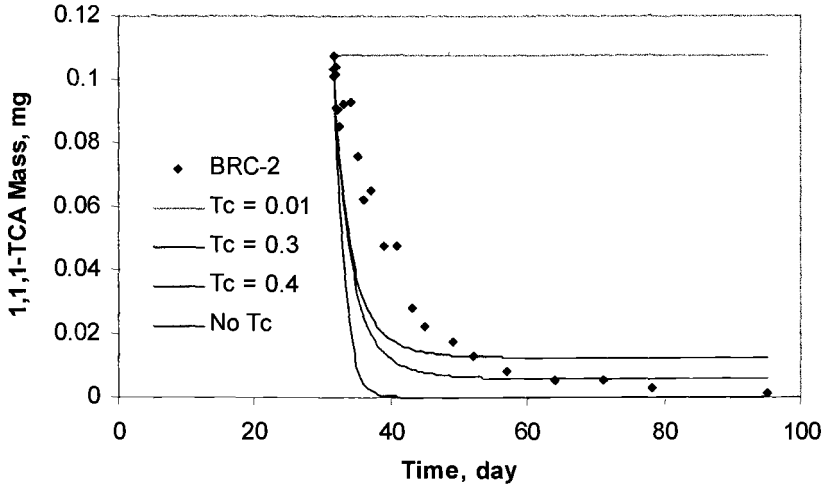

Biomass (X) at starting of model simulation (mg/L)			
$T_c = 0.01$	$T_c = 0.3$	$T_c = 0.4$	No T_c term
0.16	8.46	8.55	8.81

Figure G.46 Simulations of 1,1,1-TCA transformation for microcosm BRC-2 over a range of transformation capacities

Table G.35 Parameters for model simulations in Figures G.47

Parameters	T_c = 0.01 mg TCA /mg cells		T_c = 0.3 mg TCA /mg cells		T_c = 0.4 mg TCA /mg cells	
	The 1st addition of TCA	The 2nd addition of TCA	The 1st addition of TCA	The 2nd addition of TCA	The 1st addition of TCA	The 2nd addition of TCA
Starting day	25.06	32.85	25.06	32.85	25.06	32.85
Ending day	32.85	95.3	32.85	95.3	32.85	95.3
X_0, mg/L	19.56 [a]	$1.43*10^{-10}$ [a]	19.56 [a]	5.24 [a]	19.56 [a]	8.46 [a]
Y, mg/mg	0.7	0.7	0.7	0.7	0.7	0.7
b, day^{-1}	0.15	0.15	0.15	0.15	0.15	0.15
$K_{s,But}$, mg/L	0.11	0.11	0.11	0.11	0.11	0.11
$k_{max,But}$, mg/mg-day	1.76	1.76	1.76	1.76	1.76	1.76
$K_{s,TCA}$, mg/L	0.37	0.37	0.37	0.37	0.37	0.37
$k_{max,TCA}$, mg/mg-day	0.09	0.09	0.09	0.09	0.09	0.09
T_c, mg/mg	0.01	0.01	0.3	0.3	0.4	0.4
V_L, L	0.1	0.1	0.1	0.1	0.1	0.1
V_g, L	0.057	0.057	0.057	0.057	0.057	0.057
$H_{cc,But}$, mg-L/mg-L	38.05	38.05	38.05	38.05	38.05	38.05
$H_{cc,TCA}$, mg-L/mg-L	0.55	0.55	0.55	0.55	0.55	0.55

Note a = Obtained from the previous simulation

Section F: The first addition of 1,1,1-TCA on day 25

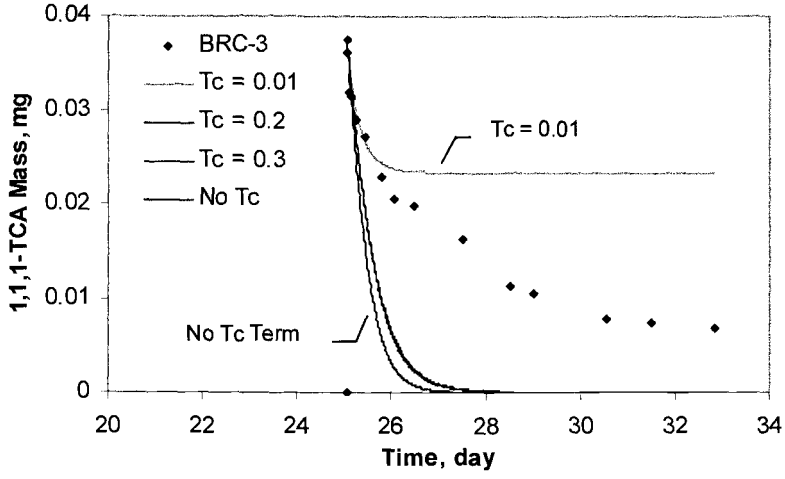

Biomass (X) at starting of model simulation (mg/L)			
$T_c = 0.01$	$T_c = 0.2$	$T_c = 0.3$	No T_c term
19.56	19.56	19.56	19.56

Section G: The second addition of 1,1,1-TCA on day 32

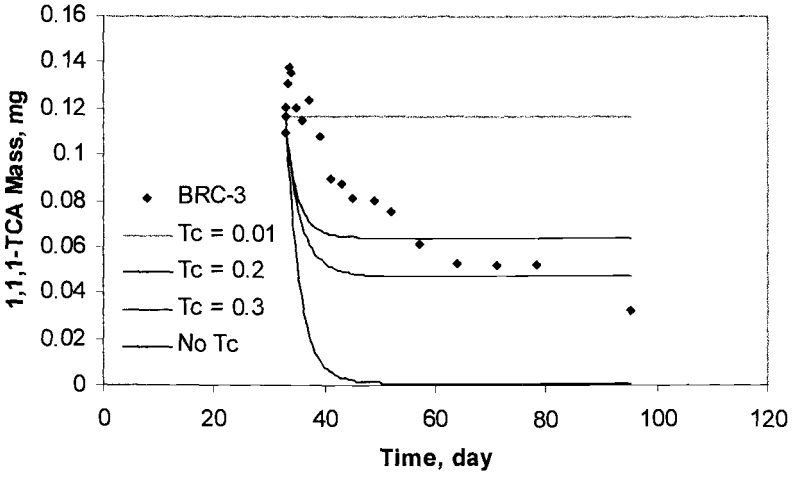

Biomass (X) at starting of model simulation (mg/L)			
$T_c = 0.01$	$T_c = 0.2$	$T_c = 0.3$	No T_c term
$1.43*10^{-10}$	5.24	5.52	6.08

Figure G.47 Simulations of 1,1,1-TCA transformation for microcosm BRC-3 over a range of transformation capacities

Table G.36 Parameters for model simulations in Figures G.48

Parameters	T_c = 0.01 mg TCA /mg cells		T_c = 0.3 mg TCA /mg cells		T_c = 0.4 mg TCA /mg cells	
	The 1st addition of TCA	The 2nd addition of TCA	The 1st addition of TCA	The 2nd addition of TCA	The 1st addition of TCA	The 2nd addition of TCA
Starting day	31.54	38.05	31.54	38.05	31.54	38.05
Ending day	38.05	95.1	38.05	95.1	38.05	95.1
X_0, mg/L	19.26[a]	0.04[a]	19.26[a]	7.11[a]	19.26[a]	7.14[a]
Y, mg/mg	0.7	0.7	0.7	0.7	0.7	0.7
b, day^{-1}	0.15	0.15	0.15	0.15	0.15	0.15
$K_{s,But}$, mg/L	0.11	0.11	0.11	0.11	0.11	0.11
$k_{max,But}$, mg/mg-day	1.76	1.76	1.76	1.76	1.76	1.76
$K_{s,TCA}$, mg/L	0.37	0.37	0.37	0.37	0.37	0.37
$k_{max,TCA}$, mg/mg-day	0.09	0.09	0.09	0.09	0.09	0.09
T_c, mg/mg	0.01	0.01	0.3	0.3	0.4	0.4
V_L, L	0.1	0.1	0.1	0.1	0.1	0.1
V_g, L	0.057	0.057	0.057	0.057	0.057	0.057
$H_{cc,But}$, mg-L/mg-L	38.05	38.05	38.05	38.05	38.05	38.05
$H_{cc,TCA}$, mg-L/mg-L	0.55	0.55	0.55	0.55	0.55	0.55

Note a = Obtained from the previous simulation

Section F: The first addition of 1,1,1-TCA on day 31

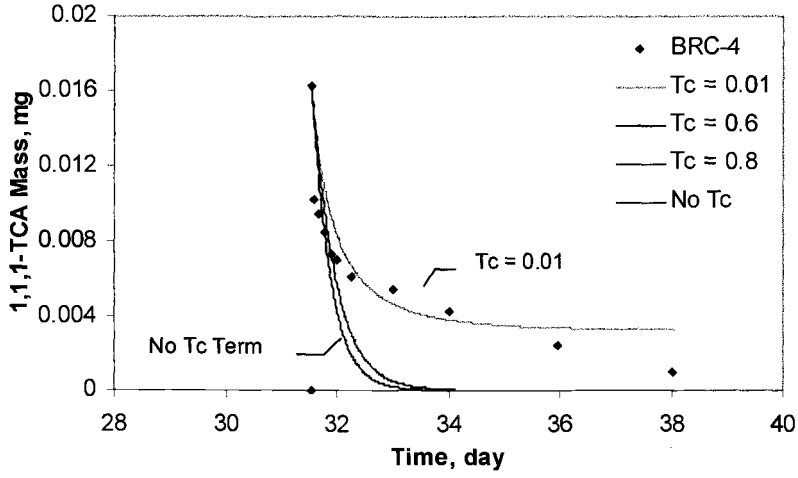

Biomass (X) at starting of model simulation (mg/L)			
$T_c = 0.01$	$T_c = 0.6$	$T_c = 0.8$	No T_c term
19.26	19.26	19.26	19.26

Section G: The second addition of 1,1,1-TCA on day 38

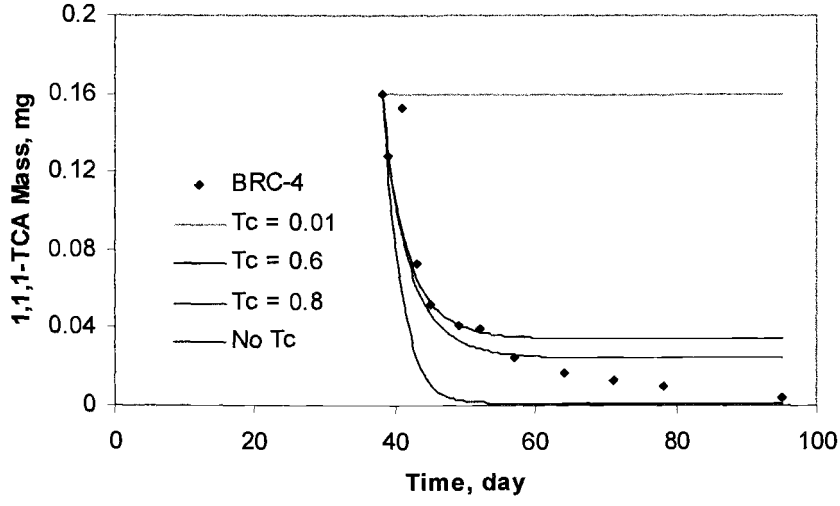

Biomass (X) at starting of model simulation (mg/L)			
$T_c = 0.01$	$T_c = 0.6$	$T_c = 0.8$	No T_c term
0.04	7.11	7.14	7.25

Figure G.48: Simulations of 1,1,1-TCA transformation for microcosm BRC-4 over a range of transformation capacities

Table G.37 Parameters for model simulations in Figures G.49

Parameters	b= 0.15 day^{-1}		b= 0.2 day^{-1}		b= 0.3 day^{-1}		b= 1.3 day^{-1}	
	The 1st addition of TCA	The 2nd addition of TCA	The 1st addition of TCA	The 2nd addition of TCA	The 1st addition of TCA	The 2nd addition of TCA	The 1st addition of TCA	The 2nd addition of TCA
Starting day	26.49	31.54	26.49	31.54	26.49	31.54	26.49	31.54
Ending day	31.54	95	31.54	95	31.54	95	31.54	95
X_0, mg/L	18.79[a]	8.55[a]	18.79[a]	6.64[a]	18.79[a]	4.00[a]	18.79[a]	0.024[a]
Y, mg/mg	0.7	0.7	0.7	0.7	0.7	0.7	0.7	0.7
b, day^{-1}	0.15	0.15	0.2	0.2	0.3	0.3	1.3	1.3
$K_{s,But}$, mg/L	0.11	0.11	0.11	0.11	0.11	0.11	0.11	0.11
$k_{max,But}$, mg/mg-day	1.76	1.76	1.76	1.76	1.76	1.76	1.76	1.76
$K_{s,TCA}$, mg/L	0.37	0.37	0.37	0.37	0.37	0.37	0.37	0.37
$k_{max,TCA}$, mg/mg-day	0.09	0.09	0.09	0.09	0.09	0.09	0.09	0.09
T_c, mg/mg	0.4	0.4	0.4	0.4	0.4	0.4	0.4	0.4
V_L, L	0.1	0.1	0.1	0.1	0.1	0.1	0.1	0.1
V_g, L	0.057	0.057	0.057	0.057	0.057	0.057	0.057	0.057
$H_{cc,But}$, mg-L/mg-L	38.05	38.05	38.05	38.05	38.05	38.05	38.05	38.05
$H_{cc,TCA}$, mg-L/mg-L	0.55	0.55	0.55	0.55	0.55	0.55	0.55	0.55

Note a = Obtained from the previous simulation

Section F: The first addition of 1,1,1-TCA on day 26

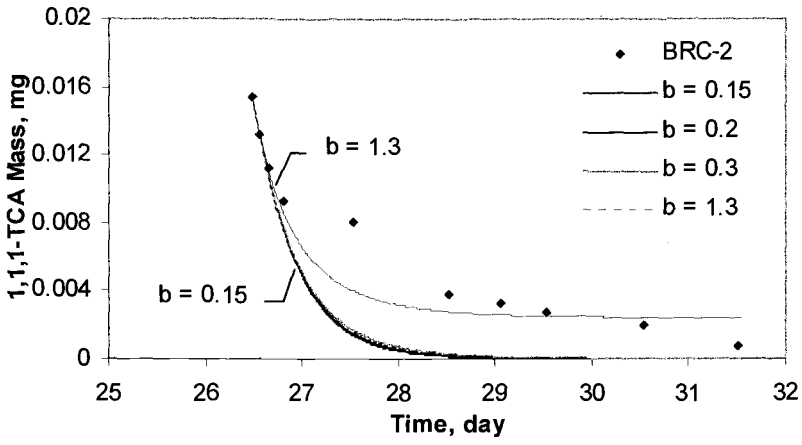

Biomass (X) at starting of model simulation (mg/L)			
b = 0.15	b = 0.2	b = 0.3	b = 1.3
18.79	18.79	18.79	18.79

Section G: The second addition of 1,1,1-TCA on day 31

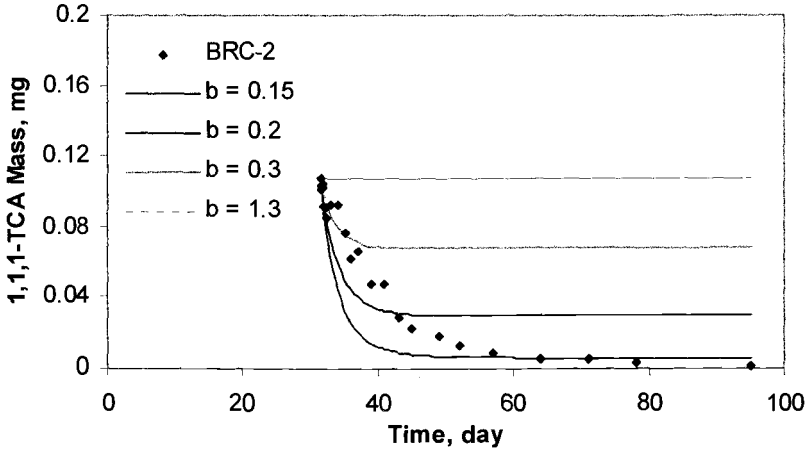

Biomass (X) at starting of model simulation (mg/L)			
b = 0.15	b = 0.2	b = 0.3	b = 1.3
8.55	6.64	4.00	0.024

Figure G.49: Simulations of 1,1,1-TCA transformation for microcosm BRC-2 over a range of decay rates

Table G.38 Parameters for model simulations in Figures G.50

Parameters	b= 0.15 day^{-1}		b= 0.2 day^{-1}		b= 0.3 day^{-1}		b= 1.2 day^{-1}	
	The 1st addition of TCA	The 2nd addition of TCA	The 1st addition of TCA	The 2nd addition of TCA	The 1st addition of TCA	The 2nd addition of TCA	The 1st addition of TCA	The 2nd addition of TCA
Starting day	25.06	32.85	25.06	32.85	25.06	32.85	25.06	32.85
Ending day	32.85	95.3	32.85	95.3	32.85	95.3	32.85	95.3
X_0, mg/L	19.56[a]	5.52[a]	19.56[a]	3.73[a]	19.56[a]	1.69[a]	19.56[a]	0.001[a]
Y, mg/mg	0.7	0.7	0.7	0.7	0.7	0.7	0.7	0.7
b, day^{-1}	0.15	0.15	0.2	0.2	0.3	0.3	1.2	1.2
$K_{s,But}$, mg/L	0.11	0.11	0.11	0.11	0.11	0.11	0.11	0.11
$k_{max,But}$, mg/mg-day	1.76	1.76	1.76	1.76	1.76	1.76	1.76	1.76
$K_{s,TCA}$, mg/L	0.37	0.37	0.37	0.37	0.37	0.37	0.37	0.37
$k_{max,TCA}$, mg/mg-day	0.09	0.09	0.09	0.09	0.09	0.09	0.09	0.09
T_c, mg/mg	0.3	0.3	0.3	0.3	0.3	0.3	0.3	0.3
V_L, L	0.1	0.1	0.1	0.1	0.1	0.1	0.1	0.1
V_g, L	0.057	0.057	0.057	0.057	0.057	0.057	0.057	0.057
$H_{cc,But}$, mg-L/mg-L	38.05	38.05	38.05	38.05	38.05	38.05	38.05	38.05
$H_{cc,TCA}$, mg-L/mg-L	0.55	0.55	0.55	0.55	0.55	0.55	0.55	0.55

Note a = Obtained from the previous simulation

Section F: The first addition of 1,1,1-TCA on day 25

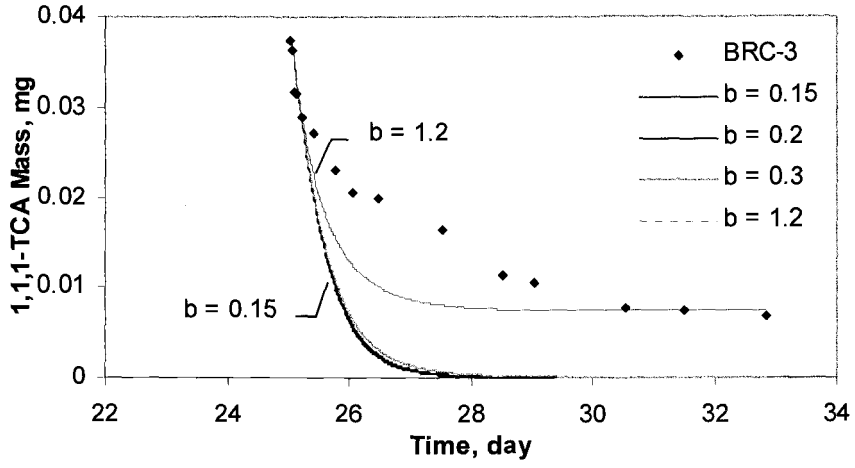

Biomass (X) at starting of model simulation (mg/L)			
b = 0.15	b = 0.2	b = 0.3	b = 1.2
19.56	19.56	19.56	19.56

Section G: The second addition of 1,1,1-TCA on day 32

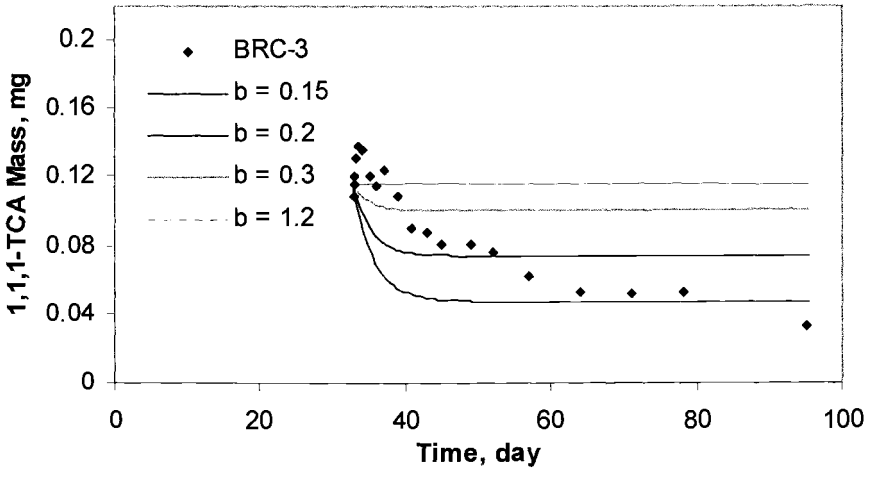

Biomass (X) at starting of model simulation (mg/L)			
b = 0.15	b = 0.2	b = 0.3	b = 1.2
5.52	3.73	1.69	0.001

Figure G.50: Simulations of 1,1,1-TCA transformation for microcosm BRC-3 over a range of decay rates

Table G.39 Parameters for model simulations in Figures G.51

Parameters	b= 0.15 day^{-1}		b= 0.2 day^{-1}		b= 0.3 day^{-1}		b= 1.5 day^{-1}	
	The 1st addition of TCA	The 2nd addition of TCA	The 1st addition of TCA	The 2nd addition of TCA	The 1st addition of TCA	The 2nd addition of TCA	The 1st addition of TCA	The 2nd addition of TCA
Starting day	31.54	38.05	31.54	38.05	31.54	38.05	31.54	38.05
Ending day	38.05	95.1	38.05	95.1	38.05	95.1	38.05	95.1
X_0, mg/L	19.26[a]	7.11[a]	19.26[a]	5.13[a]	19.26[a]	2.67[a]	19.26[a]	0.001[a]
Y, mg/mg	0.7	0.7	0.7	0.7	0.7	0.7	0.7	0.7
b, day^{-1}	0.15	0.15	0.2	0.2	0.3	0.3	1.5	1.5
$K_{s,But}$, mg/L	0.11	0.11	0.11	0.11	0.11	0.11	0.11	0.11
$k_{max,But}$, mg/mg-day	1.76	1.76	1.76	1.76	1.76	1.76	1.76	1.76
$K_{s,TCA}$, mg/L	0.37	0.37	0.37	0.37	0.37	0.37	0.37	0.37
$k_{max,TCA}$, mg/mg-day	0.09	0.09	0.09	0.09	0.09	0.09	0.09	0.09
T_c, mg/mg	0.6	0.6	0.6	0.6	0.6	0.6	0.6	0.6
V_L, L	0.1	0.1	0.1	0.1	0.1	0.1	0.1	0.1
V_g, L	0.057	0.057	0.057	0.057	0.057	0.057	0.057	0.057
$H_{cc,But}$, mg-L/mg-L	38.05	38.05	38.05	38.05	38.05	38.05	38.05	38.05
$H_{cc,TCA}$, mg-L/mg-L	0.55	0.55	0.55	0.55	0.55	0.55	0.55	0.55

Note a = Obtained from the previous simulation

Section F: The first addition of 1,1,1-TCA on day 31

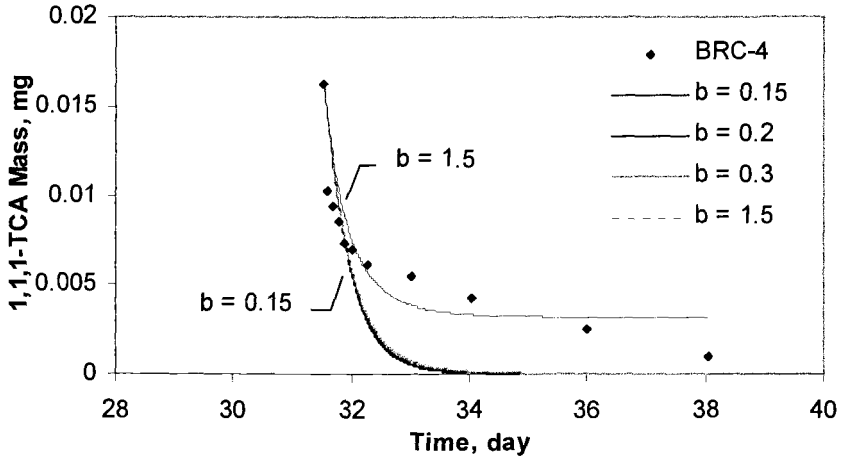

Biomass (X) at starting of model simulation (mg/L)			
b = 0.15	b = 0.2	b = 0.3	b = 1.5
19.26	19.26	19.26	19.26

Section G: The second addition of 1,1,1-TCA on day 38

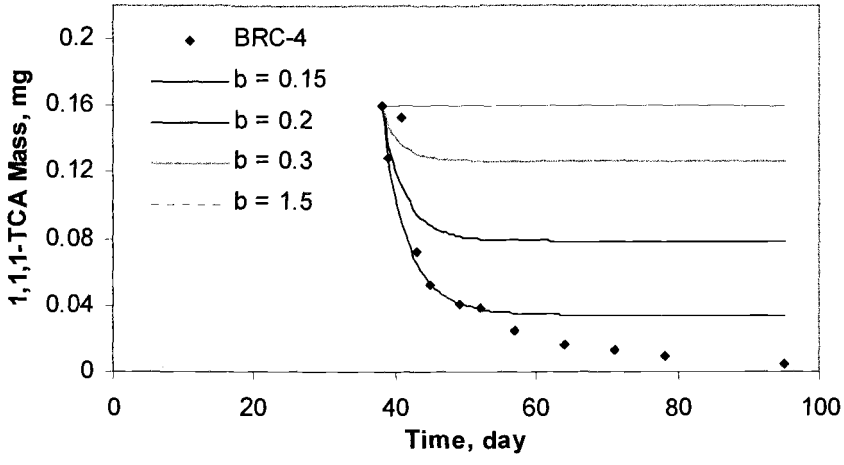

Biomass (X) at starting of model simulation (mg/L)			
b = 0.15	b = 0.2	b = 0.3	b = 1.5
7.11	5.13	2.67	0.001

Figure G.51: Simulations of 1,1,1-TCA transformation for microcosm BRC-4 over a range of decay rates

Table G.40 Parameters for model simulations in Figures G.52

Parameters	k_{max} = 0.02 mg/mg-day		k_{max} = 0.05 mg/mg-day		k_{max} = 0.09 mg/mg-day		k_{max} = 0.12 mg/mg-day	
	The 1st addition of TCA	The 2nd addition of TCA	The 1st addition of TCA	The 2nd addition of TCA	The 1st addition of TCA	The 2nd addition of TCA	The 1st addition of TCA	The 2nd addition of TCA
Starting day	26.49	31.54	26.49	31.54	26.49	31.54	26.49	31.54
Ending day	31.54	95	31.54	95	31.54	95	31.54	95
X_0, mg/L	18.79[a]	8.54[a]	18.79[a]	8.53[a]	18.79[a]	8.55[a]	18.79[a]	8.55[a]
Y, mg/mg	0.7	0.7	0.7	0.7	0.7	0.7	0.7	0.7
b, day^{-1}	0.15	0.15	0.2	0.2	0.3	0.3	1.5	1.5
$K_{s,But}$, mg/L	0.11	0.11	0.11	0.11	0.11	0.11	0.11	0.11
$k_{max,But}$, mg/mg-day	1.76	1.76	1.76	1.76	1.76	1.76	1.76	1.76
$K_{s,TCA}$, mg/L	0.37	0.37	0.37	0.37	0.37	0.37	0.37	0.37
$k_{max,TCA}$, mg/mg-day	0.09	0.09	0.09	0.09	0.09	0.09	0.09	0.09
T_c, mg/mg	0.4	0.4	0.4	0.4	0.4	0.4	0.4	0.4
V_L, L	0.1	0.1	0.1	0.1	0.1	0.1	0.1	0.1
V_g, L	0.057	0.057	0.057	0.057	0.057	0.057	0.057	0.057
$H_{cc,But}$, mg-L/mg-L	38.05	38.05	38.05	38.05	38.05	38.05	38.05	38.05
$H_{cc,TCA}$, mg-L/mg-L	0.55	0.55	0.55	0.55	0.55	0.55	0.55	0.55

Note a = Obtained from the previous simulation

Section F: The first addition of 1,1,1-TCA on day 26

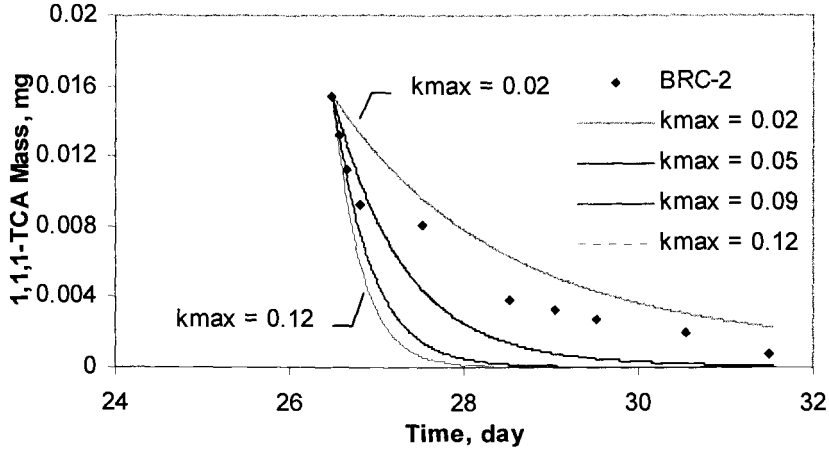

Biomass (X) at starting of model simulation (mg/L)			
$k_{max,TCA}$ = 0.02	$k_{max,TCA}$ = 0.05	$k_{max,TCA}$ = 0.09	$k_{max,TCA}$ = 0.12
18.79	18.79	18.79	18.79

Section G: The second addition of 1,1,1-TCA on day 31

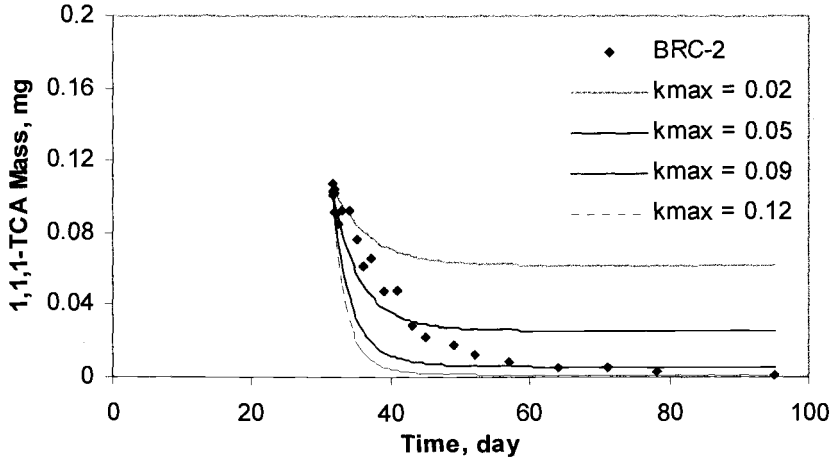

Biomass (X) at starting of model simulation (mg/L)			
$k_{max,TCA}$ = 0.02	$k_{max,TCA}$ = 0.05	$k_{max,TCA}$ = 0.09	$k_{max,TCA}$ = 0.12
8.54	8.53	8.55	8.55

Figure G.52 Simulations of 1,1,1-TCA transformation for microcosm BRC-2 over a range of 1,1,1-TCA maximum specific rates

Table G.41 Parameters for model simulations in Figures G.53

Parameters	k_{max} = 0.02 mg/mg-day		k_{max} = 0.05 mg/mg-day		k_{max} = 0.09 mg/mg-day		k_{max} = 0.12 mg/mg-day	
	The 1st addition of TCA	The 2nd addition of TCA	The 1st addition of TCA	The 2nd addition of TCA	The 1st addition of TCA	The 2nd addition of TCA	The 1st addition of TCA	The 2nd addition of TCA
Starting day	31.54	38.05	31.54	38.05	31.54	38.05	31.54	38.05
Ending day	38.05	95.1	38.05	95.1	38.05	95.1	38.05	95.1
X_0, mg/L	19.26[a]	7.11[a]	19.26[a]	5.13[a]	19.26[a]	2.67[a]	19.26[a]	0.001[a]
Y, mg/mg	0.7	0.7	0.7	0.7	0.7	0.7	0.7	0.7
b, day^{-1}	0.15	0.15	0.2	0.2	0.3	0.3	1.5	1.5
$K_{s,But}$, mg/L	0.11	0.11	0.11	0.11	0.11	0.11	0.11	0.11
$k_{max,But}$, mg/mg-day	1.76	1.76	1.76	1.76	1.76	1.76	1.76	1.76
$K_{s,TCA}$, mg/L	0.37	0.37	0.37	0.37	0.37	0.37	0.37	0.37
$k_{max,TCA}$, mg/mg-day	0.09	0.09	0.09	0.09	0.09	0.09	0.09	0.09
T_c, mg/mg	0.6	0.6	0.6	0.6	0.6	0.6	0.6	0.6
V_L, L	0.1	0.1	0.1	0.1	0.1	0.1	0.1	0.1
V_g, L	0.057	0.057	0.057	0.057	0.057	0.057	0.057	0.057
$H_{cc,But}$, mg-L/mg-L	38.05	38.05	38.05	38.05	38.05	38.05	38.05	38.05
$H_{cc,TCA}$, mg-L/mg-L	0.55	0.55	0.55	0.55	0.55	0.55	0.55	0.55

Note a = Obtained from the previous simulation

Section F: The first addition of 1,1,1-TCA on day 25

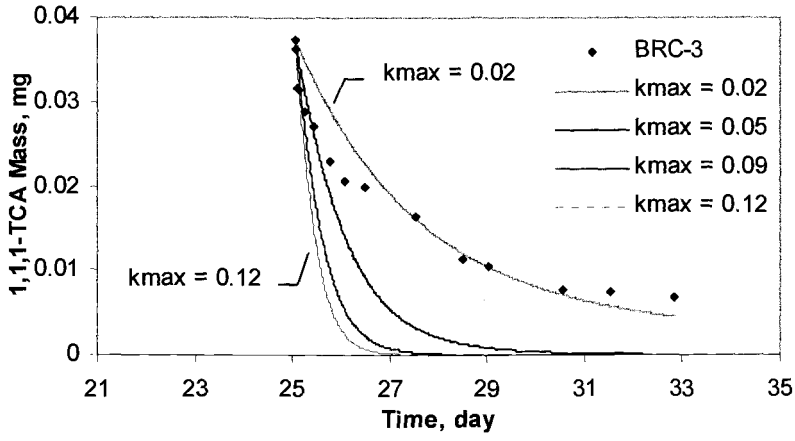

Biomass (X) at starting of model simulation (mg/L)			
$k_{max,TCA}$ = 0.02	$k_{max,TCA}$ = 0.05	$k_{max,TCA}$ = 0.09	$k_{max,TCA}$ = 0.12
19.56	19.56	19.56	19.56

Section G: The second addition of 1,1,1-TCA on day 32

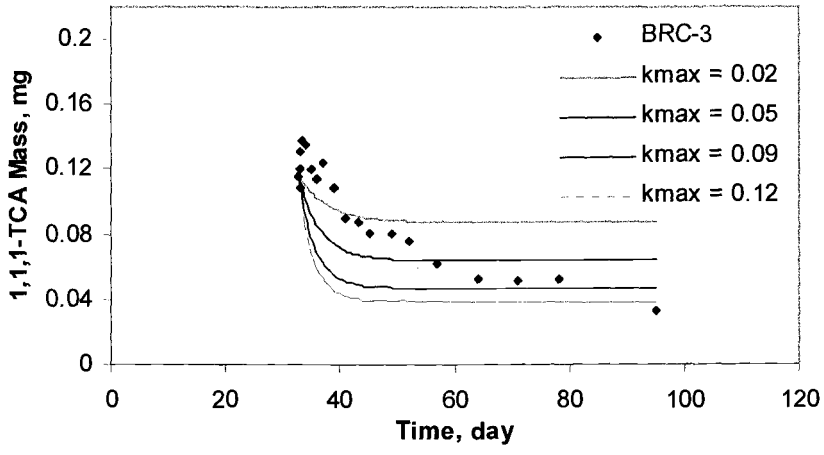

Biomass (X) at starting of model simulation (mg/L)			
$k_{max,TCA}$ = 0.02	$k_{max,TCA}$ = 0.05	$k_{max,TCA}$ = 0.09	$k_{max,TCA}$ = 0.12
5.42	5.47	5.52	5.53

Figure G.53 Simulations of 1,1,1-TCA transformation for microcosm BRC-3 over a range of 1,1,1-TCA maximum specific rates

Table G.42 Parameters for model simulations in Figures G.54

Parameters	k_{max} = 0.02 mg/mg-day		k_{max} = 0.05 mg/mg-day		k_{max} = 0.09 mg/mg-day		k_{max} = 0.12 mg/mg-day	
	The 1st addition of TCA	The 2nd addition of TCA	The 1st addition of TCA	The 2nd addition of TCA	The 1st addition of TCA	The 2nd addition of TCA	The 1st addition of TCA	The 2nd addition of TCA
Starting day	31.54	38.05	31.54	38.05	31.54	38.05	31.54	38.05
Ending day	38.05	95.1	38.05	95.1	38.05	95.1	38.05	95.1
X_0, mg/L	19.26[a]	7.11[a]	19.26[a]	5.13[a]	19.26[a]	2.67[a]	19.26[a]	0.001[a]
Y, mg/mg	0.7	0.7	0.7	0.7	0.7	0.7	0.7	0.7
b, day^{-1}	0.15	0.15	0.2	0.2	0.3	0.3	1.5	1.5
$K_{s,But}$, mg/L	0.11	0.11	0.11	0.11	0.11	0.11	0.11	0.11
$k_{max,But}$, mg/mg-day	1.76	1.76	1.76	1.76	1.76	1.76	1.76	1.76
$K_{s,TCA}$, mg/L	0.37	0.37	0.37	0.37	0.37	0.37	0.37	0.37
$k_{max,TCA}$, mg/mg-day	0.09	0.09	0.09	0.09	0.09	0.09	0.09	0.09
T_c, mg/mg	0.6	0.6	0.6	0.6	0.6	0.6	0.6	0.6
V_L, L	0.1	0.1	0.1	0.1	0.1	0.1	0.1	0.1
V_g, L	0.057	0.057	0.057	0.057	0.057	0.057	0.057	0.057
$H_{cc,But}$, mg-L/mg-L	38.05	38.05	38.05	38.05	38.05	38.05	38.05	38.05
$H_{cc,TCA}$, mg-L/mg-L	0.55	0.55	0.55	0.55	0.55	0.55	0.55	0.55

Note a = Obtained from the previous simulation

Section F: The first addition of 1,1,1-TCA on day 31

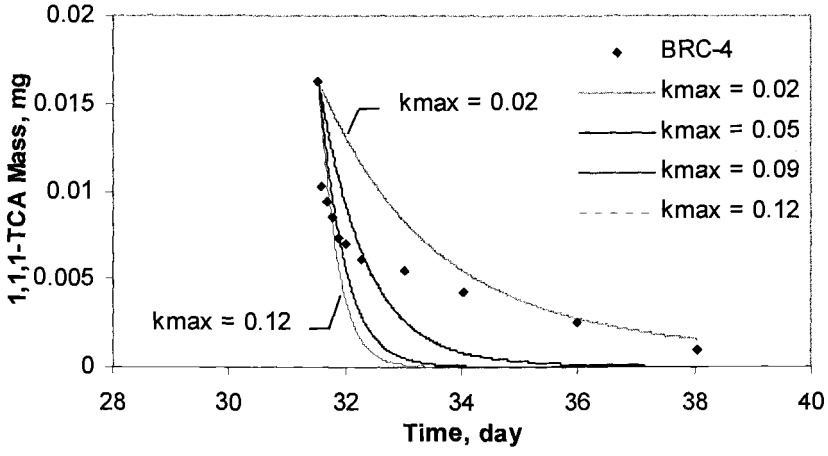

Biomass (X) at starting of model simulation (mg/L)			
$k_{max,TCA}$ = 0.02	$k_{max,TCA}$ = 0.05	$k_{max,TCA}$ = 0.09	$k_{max,TCA}$ = 0.12
19.26	19.26	19.26	19.26

Section G: The second addition of 1,1,1-TCA on day 38

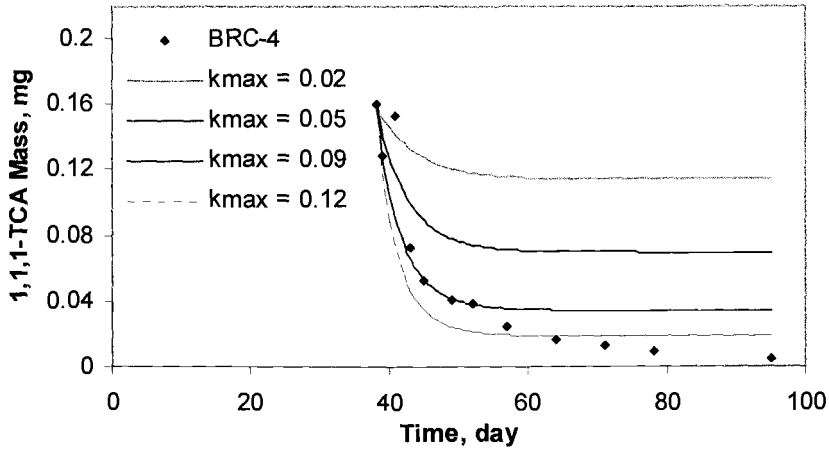

Biomass (X) at starting of model simulation (mg/L)			
$k_{max,TCA}$ = 0.02	$k_{max,TCA}$ = 0.05	$k_{max,TCA}$ = 0.09	$k_{max,TCA}$ = 0.12
7.09	7.10	7.11	7.11

Figure G.54 Simulations of 1,1,1-TCA transformation for microcosm BRC-4 over a range of 1,1,1-TCA maximum specific rates

Table G.43 Parameters for model simulations in Figures G.55

Parameters	k_{max} = 0.02 mg/mg-day		k_{max} = 0.05 mg/mg-day		k_{max} = 0.09 mg/mg-day		k_{max} = 0.12 mg/mg-day	
	The 1st addition of TCA	The 2nd addition of TCA	The 1st addition of TCA	The 2nd addition of TCA	The 1st addition of TCA	The 2nd addition of TCA	The 1st addition of TCA	The 2nd addition of TCA
Starting day	26.49	31.54	26.49	31.54	26.49	31.54	26.49	31.54
Ending day	31.54	95	31.54	95	31.54	95	31.54	95
X_0, mg/L	18.79[a]	8.55[a]	18.79[a]	6.64[a]	18.79[a]	4.00[a]	18.79[a]	0.024[a]
Y, mg/mg	0.7	0.7	0.7	0.7	0.7	0.7	0.7	0.7
b, day^{-1}	0.15	0.15	0.2	0.2	0.3	0.3	1.5	1.5
$K_{s,But}$, mg/L	0.11	0.11	0.11	0.11	0.11	0.11	0.11	0.11
$k_{max,But}$, mg/mg-day	1.76	1.76	1.76	1.76	1.76	1.76	1.76	1.76
$K_{s,TCA}$, mg/L	0.37	0.37	0.37	0.37	0.37	0.37	0.37	0.37
$k_{max,TCA}$, mg/mg-day	0.09	0.09	0.09	0.09	0.09	0.09	0.09	0.09
T_c, mg/mg	0.4	0.4	0.4	0.4	0.4	0.4	0.4	0.4
V_L, L	0.1	0.1	0.1	0.1	0.1	0.1	0.1	0.1
V_g, L	0.057	0.057	0.057	0.057	0.057	0.057	0.057	0.057
$H_{cc,But}$, mg-L/mg-L	38.05	38.05	38.05	38.05	38.05	38.05	38.05	38.05
$H_{cc,TCA}$, mg-L/mg-L	0.55	0.55	0.55	0.55	0.55	0.55	0.55	0.55

Note a = Obtained from the previous simulation

Section F: The first addition of 1,1,1-TCA on day 26

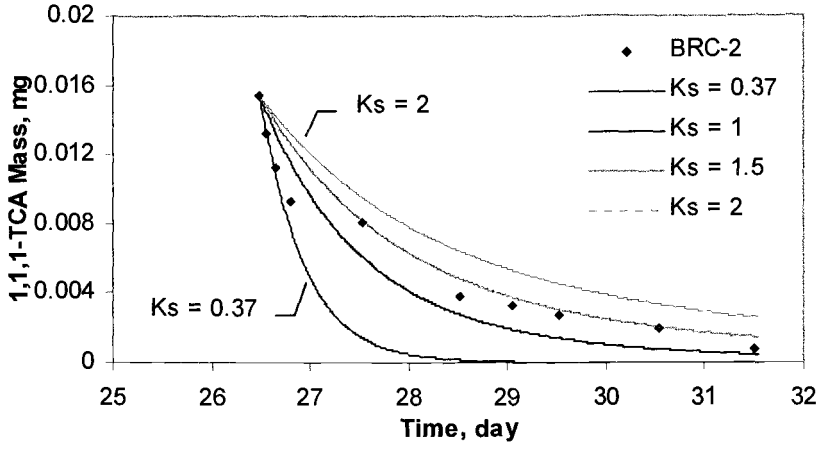

Biomass (X) at starting of model simulation (mg/L)			
$K_{s,TCA}$ = 0.37	$K_{s,TCA}$ = 1	$K_{s,TCA}$ = 1.5	$K_{s,TCA}$ = 2
18.79	18.79	18.79	18.79

Section G: The second addition of 1,1,1-TCA on day 31

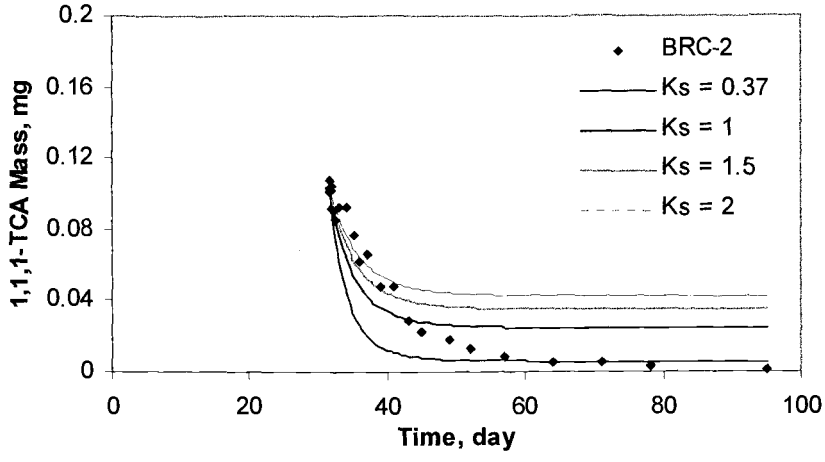

Biomass (X) at starting of model simulation (mg/L)			
$K_{s,TCA}$ = 0.37	$K_{s,TCA}$ = 1	$K_{s,TCA}$ = 1.5	$K_{s,TCA}$ = 2
8.55	8.53	8.54	8.55

Figure G.55 Simulations of 1,1,1-TCA transformation for microcosm BRC-2 over a range of 1,1,1-TCA half-saturation constants

Table G.44 Parameters for model simulations in Figures G.56

Parameters	k_{max} = 0.02 mg/mg-day		k_{max} = 0.05 mg/mg-day		k_{max} = 0.09 mg/mg-day		k_{max} = 0.12 mg/mg-day	
	The 1st addition of TCA	The 2nd addition of TCA	The 1st addition of TCA	The 2nd addition of TCA	The 1st addition of TCA	The 2nd addition of TCA	The 1st addition of TCA	The 2nd addition of TCA
Starting day	31.54	38.05	31.54	38.05	31.54	38.05	31.54	38.05
Ending day	38.05	95.1	38.05	95.1	38.05	95.1	38.05	95.1
X_0, mg/L	19.26[a]	7.11[a]	19.26[a]	5.13[a]	19.26[a]	2.67[a]	19.26[a]	0.001[a]
Y, mg/mg	0.7	0.7	0.7	0.7	0.7	0.7	0.7	0.7
b, day^{-1}	0.15	0.15	0.2	0.2	0.3	0.3	1.5	1.5
$K_{s,But}$, mg/L	0.11	0.11	0.11	0.11	0.11	0.11	0.11	0.11
$k_{max,But}$, mg/mg-day	1.76	1.76	1.76	1.76	1.76	1.76	1.76	1.76
$K_{s,TCA}$, mg/L	0.37	0.37	0.37	0.37	0.37	0.37	0.37	0.37
$k_{max,TCA}$, mg/mg-day	0.09	0.09	0.09	0.09	0.09	0.09	0.09	0.09
T_c, mg/mg	0.6	0.6	0.6	0.6	0.6	0.6	0.6	0.6
V_L, L	0.1	0.1	0.1	0.1	0.1	0.1	0.1	0.1
V_g, L	0.057	0.057	0.057	0.057	0.057	0.057	0.057	0.057
$H_{cc,But}$, mg-L/mg-L	38.05	38.05	38.05	38.05	38.05	38.05	38.05	38.05
$H_{cc,TCA}$, mg-L/mg-L	0.55	0.55	0.55	0.55	0.55	0.55	0.55	0.55

Note a = Obtained from the previous simulation

Section F: The first addition of 1,1,1-TCA on day 25

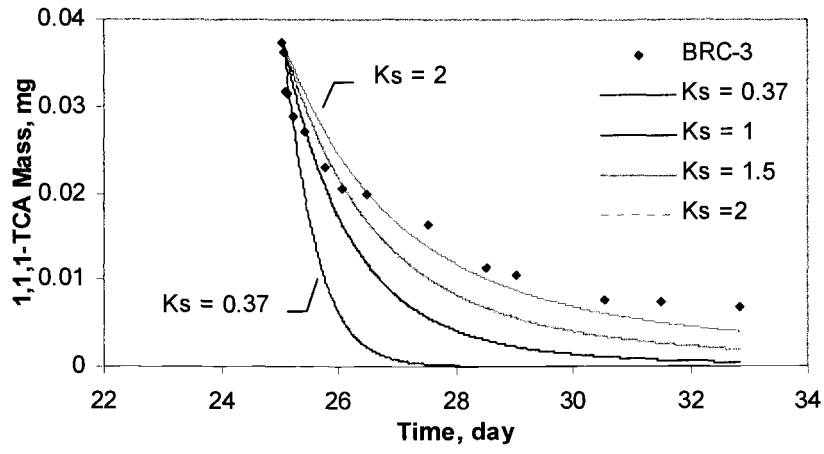

Biomass (X) at starting of model simulation (mg/L)			
$K_{s,TCA}$ = 0.37	$K_{s,TCA}$ = 1	$K_{s,TCA}$ = 1.5	$K_{s,TCA}$ = 2
19.56	19.56	19.56	19.56

Section G: The second addition of 1,1,1-TCA on day 32

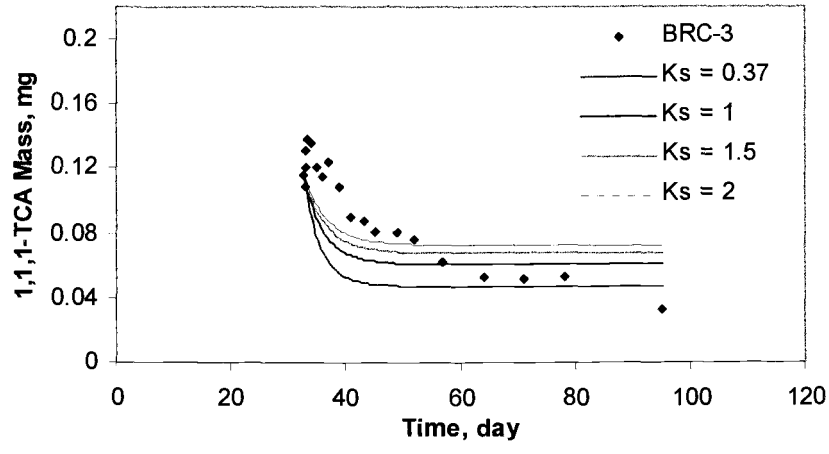

Biomass (X) at starting of model simulation (mg/L)			
$K_{s,TCA}$ = 0.37	$K_{s,TCA}$ = 1	$K_{s,TCA}$ = 1.5	$K_{s,TCA}$ = 2
5.52	5.45	5.43	5.44

Figure G.56 Simulations of 1,1,1-TCA transformation for microcosm BRC-3 over a range of 1,1,1-TCA half-saturation constants

Table G.45 Parameters for model simulations in Figures G.57

Parameters	k_{max} = 0.02 mg/mg-day		k_{max} = 0.05 mg/mg-day		k_{max} = 0.09 mg/mg-day		k_{max} = 0.12 mg/mg-day	
	The 1st addition of TCA	The 2nd addition of TCA	The 1st addition of TCA	The 2nd addition of TCA	The 1st addition of TCA	The 2nd addition of TCA	The 1st addition of TCA	The 2nd addition of TCA
Starting day	31.54	38.05	31.54	38.05	31.54	38.05	31.54	38.05
Ending day	38.05	95.1	38.05	95.1	38.05	95.1	38.05	95.1
X_0, mg/L	19.26[a]	7.11[a]	19.26[a]	5.13[a]	19.26[a]	2.67[a]	19.26[a]	0.001[a]
Y, mg/mg	0.7	0.7	0.7	0.7	0.7	0.7	0.7	0.7
b, day^{-1}	0.15	0.15	0.2	0.2	0.3	0.3	1.5	1.5
$K_{s,But}$, mg/L	0.11	0.11	0.11	0.11	0.11	0.11	0.11	0.11
$k_{max,But}$, mg/mg-day	1.76	1.76	1.76	1.76	1.76	1.76	1.76	1.76
$K_{s,TCA}$, mg/L	0.37	0.37	0.37	0.37	0.37	0.37	0.37	0.37
$k_{max,TCA}$, mg/mg-day	0.09	0.09	0.09	0.09	0.09	0.09	0.09	0.09
T_c, mg/mg	0.6	0.6	0.6	0.6	0.6	0.6	0.6	0.6
V_L, L	0.1	0.1	0.1	0.1	0.1	0.1	0.1	0.1
V_g, L	0.057	0.057	0.057	0.057	0.057	0.057	0.057	0.057
$H_{cc,But}$, mg-L/mg-L	38.05	38.05	38.05	38.05	38.05	38.05	38.05	38.05
$H_{cc,TCA}$, mg-L/mg-L	0.55	0.55	0.55	0.55	0.55	0.55	0.55	0.55

Note a = Obtained from the previous simulation

Section F: The first addition of 1,1,1-TCA on day 31

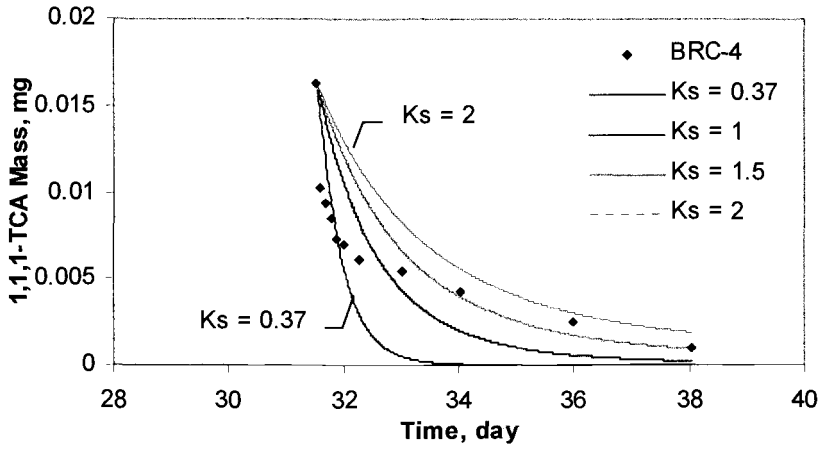

Biomass (X) at starting of model simulation (mg/L)			
$K_{s,TCA}$ = 0.37	$K_{s,TCA}$ = 1	$K_{s,TCA}$ = 1.5	$K_{s,TCA}$ = 2
19.26	19.26	19.26	19.26

Section G: The second addition of 1,1,1-TCA on day 38

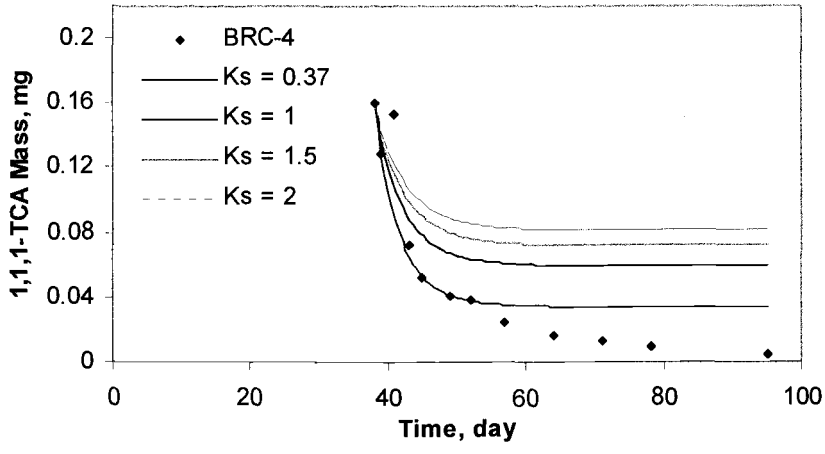

Biomass (X) at starting of model simulation (mg/L)			
$K_{s,TCA}$ = 0.37	$K_{s,TCA}$ = 1	$K_{s,TCA}$ = 1.5	$K_{s,TCA}$ = 2
7.11	7.09	7.09	7.09

Figure G.57 Simulations of 1,1,1-TCA transformation for microcosm BRC-4 over a range of 1,1,1-TCA half-saturation constants